NATIONAL COOPERATIVE HIGHWAY RESEARCH PROGRAM

NCHRP Report 439

Superelevation Distribution Methods and Transition Designs

Transportation Research Board
National Research Council

NATIONAL COOPERATIVE HIGHWAY RESEARCH PROGRAM

Report 439

Superelevation Distribution Methods and Transition Designs

JAMES A. BONNESON
Texas Transportation Institute
Texas A&M University
College Station, TX

Subject Areas

Highway and Facility Design

Research Sponsored by the American Association of State Highway and Transportation Officials in Cooperation with the Federal Highway Administration

TRANSPORTATION RESEARCH BOARD
NATIONAL RESEARCH COUNCIL

NATIONAL ACADEMY PRESS
Washington, D.C. 2000

NATIONAL COOPERATIVE HIGHWAY RESEARCH PROGRAM

Systematic, well-designed research provides the most effective approach to the solution of many problems facing highway administrators and engineers. Often, highway problems are of local interest and can best be studied by highway departments individually or in cooperation with their state universities and others. However, the accelerating growth of highway transportation develops increasingly complex problems of wide interest to highway authorities. These problems are best studied through a coordinated program of cooperative research.

In recognition of these needs, the highway administrators of the American Association of State Highway and Transportation Officials initiated in 1962 an objective national highway research program employing modern scientific techniques. This program is supported on a continuing basis by funds from participating member states of the Association and it receives the full cooperation and support of the Federal Highway Administration, United States Department of Transportation.

The Transportation Research Board of the National Research Council was requested by the Association to administer the research program because of the Board's recognized objectivity and understanding of modern research practices. The Board is uniquely suited for this purpose as it maintains an extensive committee structure from which authorities on any highway transportation subject may be drawn; it possesses avenues of communications and cooperation with federal, state and local governmental agencies, universities, and industry; its relationship to the National Research Council is an insurance of objectivity; it maintains a full-time research correlation staff of specialists in highway transportation matters to bring the findings of research directly to those who are in a position to use them.

The program is developed on the basis of research needs identified by chief administrators of the highway and transportation departments and by committees of AASHTO. Each year, specific areas of research needs to be included in the program are proposed to the National Research Council and the Board by the American Association of State Highway and Transportation Officials. Research projects to fulfill these needs are defined by the Board, and qualified research agencies are selected from those that have submitted proposals. Administration and surveillance of research contracts are the responsibilities of the National Research Council and the Transportation Research Board.

The needs for highway research are many, and the National Cooperative Highway Research Program can make significant contributions to the solution of highway transportation problems of mutual concern to many responsible groups. The program, however, is intended to complement rather than to substitute for or duplicate other highway research programs.

Note: The Transportation Research Board, the National Research Council, the Federal Highway Administration, the American Association of State Highway and Transportation Officials, and the individual states participating in the National Cooperative Highway Research Program do not endorse products or manufacturers. Trade or manufacturers' names appear herein solely because they are considered essential to the object of this report.

NCHRP REPORT 439

Project C15-16A FY'97

ISSN 0077-5614

ISBN 0-309-06623-9

Library of Congress Control Number 00-130563

Price $43.00

NOTICE

The project that is the subject of this report was a part of the National Cooperative Highway Research Program conducted by the Transportation Research Board with the approval of the Governing Board of the National Research Council. Such approval reflects the Governing Board's judgment that the program concerned is of national importance and appropriate with respect to both the purposes and resources of the National Research Council.

The members of the technical committee selected to monitor this project and to review this report were chosen for recognized scholarly competence and with due consideration for the balance of disciplines appropriate to the project. The opinions and conclusions expressed or implied are those of the research agency that performed the research, and, while they have been accepted as appropriate by the technical committee, they are not necessarily those of the Transportation Research Board, the National Research Council, the American Association of State Highway and Transportation Officials, or the Federal Highway Administration, U.S. Department of Transportation.

Each report is reviewed and accepted for publication by the technical committee according to procedures established and monitored by the Transportation Research Board Executive Committee and the Governing Board of the National Research Council.

Published reports of the

NATIONAL COOPERATIVE HIGHWAY RESEARCH PROGRAM

are available from:

Transportation Research Board
National Research Council
2101 Constitution Avenue, N.W.
Washington, D.C. 20418

and can be ordered through the Internet at:

http://www4.nationalacademies.org/trb/homepage.nsf

Printed in the United States of America

FOREWORD

By Staff
Transportation Research Board

This report evaluates and recommends revisions to the horizontal curve guidance presented in the 1994 AASHTO publication, *A Policy on Geometric Design of Highways and Streets*. The two principal design elements evaluated were the use of superelevation and the transition from a tangent to a curve, though all elements of a curve were considered in the analysis. Geometric designers will gain a greater understanding of the physics involved in negotiating a curve and the procedures for designing them by reading this report.

Chapter III of the 1994 AASHTO publication, *A Policy on Geometric Design of Highways and Streets* (referred to herein as the *Green Book*) contains information on superelevation design procedures for the full spectrum of highway conditions, including rural highways and high-speed urban streets, low-speed urban streets, turning roadways, and intersection curves. These design procedures include distribution of both the superelevation rate (e) and the side friction factor (f) as well as the design of superelevation transitions. These procedures are based on limited empirical data from the 1930s and 1940s.

Five methods are discussed in the *Green Book* for distributing the superelevation rate and side friction factor, but there is limited understanding of the operational characteristics of these different methods. The current use of multiple methods by different agencies produces inconsistent designs. Different agencies have also adopted different methods of transitioning from a tangent, crowned cross section to the superelevated cross section used on a horizontal curve.

This report comprises the results of NCHRP Projects 15-16 and 15-16A, conducted by the University of Nebraska at Lincoln and the Texas Transportation Institute at Texas A&M University, respectively. Two contracts were needed because the principal investigator changed employment. Following a thorough literature review and survey of the domestic and international practice, the researchers collected data at 55 curves in 8 states to quantify the relationship among side friction demand, speed, curve radius, and superelevation rate. Simulation was then used to evaluate the effect of alternative transition designs on vehicle lane position and control. Recommendations for the *Green Book* were then developed to make the design of curves easier and more consistent throughout the United States.

This report describes the research approach used, recommends new approaches to curve design, and presents the justification for these approaches. It also includes recommendations for future research.

CONTENTS

AUTHOR ACKNOWLEDGMENTS

The research reported herein was performed under NCHRP Project 15-16 by the Texas Transportation Institute (TTI). Dr. James A. Bonneson served as principal investigator and, as such, was responsible for overall project coordination. Dr. Bonneson was assisted in the research by Dr. Patrick T. McCoy with the Department of Civil Engineering at the University of Nebraska-Lincoln, Dr. Daniel B. Fambro with TTI, and Mr. Roger P. Bligh with TTI. The TTI staff members who made significant contributions to the research include Mr. Ramon Labrador and Mr. Karl Passetti.

The following individuals and their respective state and local highway agencies were very helpful during the data collection task: Mr. Kirk Barnes, Texas Department of Transportation, Bryan District, Bryan, Texas; Mr. Rick Berry, Traffic Engineering Division, City of Mesquite, Texas; Mr. Larry W. Cervenka, Transportation Department, City of Garland, Texas; Mr. Mike Cynecki, Street Transportation Department, City of Phoenix, Arizona; Mr. David G. Gerard, Transportation Division, City of Austin, Texas; Mr. Larry E. Jackson, Texas Department of Transportation, Austin District, Austin, Texas; Mr. Terry H. Otterness, Highway Division, Arizona Department of Transportation; and Mr. M. Srinivasan, Development Services Department, City of Plano, Texas. These individuals identified candidate data collection sites and also provided geometric and traffic volume data for these sites. The research team is grateful to each of these individuals and their respective agencies.

Several individuals provided data and information collected for previous research projects. These individuals include Dr. Raymond Krammes, Federal Highway Administration, Washington, D.C.; Mr. Jon Collins, Kimley-Horn & Associates, Inc., San Diego, California; Mr. C. Brian Shamburger, Parsons Transportation Group, Fort Worth, Texas; Mr. Brian A. Moen, Parsons Transportation Group, Dallas, Texas; and Dr. Kay Fitzpatrick, TTI, College Station, Texas. The research team appreciates the assistance provided by these individuals in reassembling the original data and facilitating its interpretation.

Finally, the research team would like to acknowledge the engineers who participated in the focus group assembled for this research project. These individuals include Mr. James O. Brewer, State Road Office, Kansas Department of Transportation; Mr. Charles Goessel, Quality Management Services, New Jersey Department of Transportation; Mr. Terry G. McCoy, Texas Department of Transportation; Mr. A.D. Perkins, Design Quality Assurance Bureau, New York State Department of Transportation; Mr. George Sloop, State Road Office, Kansas Department of Transportation; Mr. Steve Walker, Design Bureau, Alabama Department of Transportation; and Mr. Rick Wilder, Design Quality Assurance Bureau, New York State Department of Transportation. Their thoughtful advice and comment on the candidate design guidance are greatly appreciated.

SUPERELEVATION DISTRIBUTION METHODS AND TRANSITION DESIGNS

SUMMARY

The objective of this research was to evaluate and recommend revisions to the horizontal curve design guidelines presented in the 1994 AASHTO publication *A Policy on Geometric Design of Highways and Streets* (referred to herein as the *Green Book*). The guidelines of interest were those related to (1) superelevation distribution and (2) transition design. The full spectrum of highway conditions was considered including all rural highways and high-speed urban streets, low-speed urban streets, and turning roadways.

The evaluation was based on a review of current practice, a review of the research literature, and an analysis of alternative guidelines and design control values. Initially, the design policies of 6 international transportation agencies and the design manuals of 27 state departments of transportation (DOTs) were reviewed. The objective of this review was to synthesize the horizontal curve design controls used by these agencies and to compare them to the controls recommended in the *Green Book*.

The analysis of alternative guidelines and design control values required developing and calibrating several theoretical models. Models of side friction demand, curve speed, vehicle dynamics on a horizontal curve, and lateral motion in the transition section were developed for this research.

These models were calibrated using field data gathered at 55 horizontal curve study sites. The data collected included driver speed and headway at each site as well as measurement of the site's radius, superelevation rate, and grade. Eight states were represented in the database, which contained more than 8,100 valid speed observations.

The results of the evaluation led to several conclusions. These conclusions formed the basis for the recommended revisions to the *Green Book*. The conclusions are listed first, followed by the recommended revisions. The following conclusions have been reached as a result of this research:

1. Drivers slow on sharp horizontal curves. The magnitude of their speed reduction reflects a compromise between a desire for a comfortable level of lateral acceleration and a desire to minimize travel time. From a curve design standpoint, designers should avoid curves that are so sharp that they promote a significant speed reduction (more than 15 km/h). However, for the design of minimum radius

curves, a nominal speed reduction of 3 to 5 km/h was found to provide an acceptable compromise between driver comfort and travel time.

2. Drivers have similar side friction demands when traveling on street and highway curves. Thus, the use of separate side friction factors for the design of curves on low- and high-speed urban streets does not appear justified.
3. Significant roadway downgrade depletes the friction supply available for cornering. This depletion results from the use of a portion of the friction supply to provide the necessary braking force required to maintain speed on the downgrade. The reduction in side friction supply reduces the margin of safety for vehicles traveling on downgrade horizontal curves. The reduction in margin of safety is particularly significant for heavy trucks because of their greater weight and higher peak side friction demands.
4. Superelevation Distribution Method 5, in combination with the use of multiple maximum superelevation rates, does not promote design consistency. Method 5 can yield different superelevation rates for the same speed and radius depending on the designer's choice of maximum superelevation rate.
5. A kinematic analysis of a vehicle's lateral motion within the transition section indicates that proper design of this section can minimize or eliminate lateral shift. This shift manifests itself as a "drift" within the traffic lane; however, it is actually the result of unbalanced lateral accelerations acting on the vehicle as it travels through the transition. An outward shift is particularly troublesome because it requires a corrective steering action by the driver that precipitates a "critical" path radius that is sharper than that of the curve. A critical radius is associated with a peak side friction demand exceeding that intended by the designer.
6. For tangent-to-curve transition designs, many agencies are not maintaining a minimum superelevation runoff length equal to 2.0 s travel time at the design speed. Rather, these agencies are using controls that dictate runoff length on the basis of a maximum relative gradient or a maximum rate of pavement rotation. This finding and the results from a kinematic analysis of vehicle motion indicate that adherence to the "travel time" control is not essential in tangent-to-curve transition design because it does not appear to improve motorist comfort or safety.
7. The *Green Book* does not explicitly address the topic of road surface drainage in the transition section. The warping of the roadway in this section can pose several drainage problems. This warping can result in there being inadequate longitudinal or lateral slope for drainage purposes that can result in a significant reduction in the friction supply. Inadequate drainage in the transition section is particularly hazardous because additional friction demands are placed on the tire-pavement interface during curve entry.
8. A review of the literature on the safety and operational benefits of spiral curve transitions indicates that these benefits are small and can only be realized under certain limited conditions. These marginal benefits are likely to be one reason so many state DOTs (estimated to exceed 70 percent) do not require the use of spirals.
9. There is evidence that spiral curve transition length has an effect on curve operations and safety. Several international agencies have adopted controls that define both a maximum and a minimum spiral length. Excessively long spirals mislead drivers about the sharpness of the impending curve. Excessively short spirals result in relatively large levels of peak lateral acceleration. A kinematic analysis of vehicle motion indicates that lateral shift in the lane can be minimized when the spiral length is equal to the driver's steering time.

This research led to the formulation of several recommended revisions to the 1994 edition of the *Green Book*. These recommendations are fully described in Chapter 3.

They are also more formally presented in Appendix E as recommended revisions to the *Green Book*. The recommendations made in this report are focused on design controls; however, there are also some recommendations regarding horizontal curve design guidance. These recommendations include the following:

1. **Curve Design Speed.** The term "curve design speed" is recommended for use in horizontal curve design. This term is defined as the expected 95th percentile speed of freely flowing passenger cars on the curve. For design applications, curve design speed is equal to the 95th percentile approach speed less the selected curve speed reduction. This speed reduction ranges from 0 km/h for the flattest curves to 5 km/h for the sharpest curves.
2. **Maximum Design Side Friction Factors.** It is recommended that a single set of side friction factors be used for all facility types. The recommended factors represent the 95th percentile side friction demand based on an acceptable speed reduction of 3 to 5 km/h. These factors yield minimum radii that are very similar to those currently recommended in the *Green Book*.
3. **Minimum Radius with Normal Cross Slope.** A simpler and more direct means of determining the minimum-radius-with-normal-cross-slope is recommended; the resulting radii are very similar to those currently recommended in the *Green Book*. This radius is defined using a limiting level of side friction for the outside traffic lane, relative to the curve direction.
4. **Superelevation Distribution for Rural Highways and High-Speed Urban Streets.** To achieve consistency in curve design, a superelevation distribution method is recommended that provides a unique relationship among design speed, radius, and superelevation rate. This distribution accommodates all of the current maximum superelevation rates used by state DOTs. It yields design superelevation rates that are similar to those currently recommended in the *Green Book*, especially for maximum rates in the range of 6 to 10 percent. The recommended distribution simplifies the presentation of the design superelevation rates by reducing the number of tables to two (there are currently five tables) and reconfiguring them to provide a range of radii for selected superelevation rates.
5. **Superelevation Transition Design.** It is recommended that the superelevation runoff and tangent runout design controls provided in Chapter 3 be used for all facility types. These controls are applicable to low- and high-speed facilities in urban and rural areas. The main benefit derived from implementation of this recommendation is consistency in design.
6. **Minimum Length of Superelevation Runoff.** It is recommended that the minimum length of runoff for the tangent-to-curve transition be based solely on the maximum relative gradient control. In this regard, it is recommended that adherence to a minimum length equal to 2.0 s travel time be eliminated. This deletion will yield shorter runoff lengths when the superelevation rate is low or the design speed is high. This change will improve pavement drainage and produce a smooth pavement edge without compromising safety or operations.
7. **Portion of Runoff Located Prior to the Curve.** The kinematic analysis of lateral motion indicated that the portion of the superelevation runoff located prior to the curve can influence the magnitude of lateral shift within the lane. The portion that minimizes this shift varies from 0.70 to 0.90 (i.e., 70 to 90 percent) and depends on speed and the number of lanes in the transition section. It is recommended that this control be specified for each alignment and consistently used on each curve of the alignment but that its value be selected at the onset of the project based on the design speed and number of lanes in the cross section.

8. **Limiting Superelevation Rates.** The kinematic analysis of lateral motion indicated that larger superelevation rates are sometimes associated with excessive lateral shift. Specifically, rates in excess of 8, 10, 11, and 11 percent for 95th percentile approach speeds of 30, 40, 50, and 60 km/h, respectively, are likely associated with shifts in excess of 1.0 m. The magnitude of shift for speeds of 70 km/h and above are not likely to be excessive provided that the superelevation rate is 12 percent or less. It is recommended that these limiting rates be included in the *Green Book* with the instruction that they not be exceeded without some consideration given to widening the width of the traveled way.
9. **Minimum Transition Grades.** It is recommended the *Green Book* provide guidance on the relationship between grade in the transition section and pavement drainage. Preliminary guidance is provided in Chapter 3. This guidance indicates the need for a minimum profile grade of 0.5 percent in the transition section. It also indicates the need for a minimum edge of pavement grade of 0.2 percent (0.5 percent for curbed streets).
10. **Spiral Curve Transition Design.** It is recommended that the spiral curve transition design controls provided in Chapter 3 be used for all facility types. These controls are applicable to low- and high-speed facilities in urban and rural areas. The main benefit derived from implementation of this recommendation is consistency in design.
11. **Guidance on the Use of a Spiral Curve Transition.** It is recommended that the *Green Book* continue to recognize the use of spiral curve transitions. However, it is also recommended that additional guidance be provided on the conditions where a spiral is likely to offer a tangible benefit, relative to the tangent-to-curve design. This guidance would be intended for those agencies that currently use spirals and would not be presented as a "warranting" condition.
12. **Maximum Radius for Use of a Spiral Curve Transition.** Present evidence indicates that spiral curve transitions may offer a safety benefit for the sharpest curves. In this regard, it is recommended that spirals be considered when the centripetal acceleration associated with the horizontal curve ($= V^2/R$) exceeds 1.3 m/s^2.
13. **Minimum, Maximum, and Desirable Length of Spiral Curve Transition.** As noted previously, there is considerable evidence that spiral curve transition length can have an effect on operations and safety. Several international agencies have adopted controls that define both a maximum and a minimum spiral length. Therefore, it is recommended that the minimum, maximum, and desirable spiral curve length controls described in Chapter 3 be included in the *Green Book* to help designers select a safe and comfortable spiral length.

Finally, the material in Appendix E presents the recommended design guidelines and design controls in a format that is consistent with the presentation in the *Green Book*. This material is offered to the AASHTO Task Force on Geometric Design for consideration and possible inclusion in the next update of the *Green Book*.

CHAPTER 1

INTRODUCTION AND RESEARCH APPROACH

PROBLEM STATEMENT

Chapter III of the 1994 AASHTO publication *A Policy on Geometric Design of Highways and Streets* (*1*) (referred to herein as the *Green Book*) contains information on a range of geometric design elements. These elements are broadly categorized as sight distance, horizontal alignment, and vertical alignment. Within the category of horizontal alignment, the *Green Book* identifies two design elements that have a significant effect on alignment design, these elements are (1) distribution of the superelevation rate and side friction factor over the range of candidate curve radii and (2) transition section design.

Five methods for distributing superelevation and side friction are discussed in the *Green Book*. Intuitive arguments are offered regarding the relative merits of each method; however, there is limited quantitative understanding of their operational characteristics. As a result, there has been some variation among highway design agencies regarding which method is most appropriate for various design conditions. This variability has reduced the consistency of horizontal alignment design procedures within and among states.

Transition section design includes the geometric elements associated with the roadway segment in the vicinity of the horizontal curve's beginning and ending points. Specifically, these are the elements that describe (1) the cross slope transition from a normal crown section to a fully superelevated section and (2) the alignment transition curvature between the tangent and horizontal curve. As with the method of superelevation distribution, state and local agencies have adopted a variety of transition design procedures that do not yield consistent designs within and among states.

In addition to their inconsistent application, there is some concern that the roadway design and construction practices, vehicle and driver characteristics, and pavement surface properties that underlie these procedures are outdated. In fact, many of the characteristics and properties used to define existing control values are based on limited empirical data from the 1930s and 1940s. As a result, state highway officials concluded that a substantial research effort was needed to update or revise the guidelines for superelevation distribution and transition design for the purpose of ensuring the consistent design and safe operation of all newly constructed streets and highways.

RESEARCH OBJECTIVE

The objective of this research was to evaluate and recommend updates or revisions to the *Green Book* guidelines for (1) distributing the superelevation rate and side friction factor and (2) designing transition sections for horizontal curves. The updates or revisions were to be based on quantitative evidence obtained from field observations, simulations, theoretic considerations, or any combination of these three sources. The recommended guidelines were to be documented in a final report and presented in a form suitable for insertion into the *Green Book*.

SCOPE OF STUDY

The focus of this study is on the design controls recommended in the *Green Book* for the design of horizontal curves in urban or rural areas on new alignments or those undergoing major reconstruction. The full spectrum of highway conditions was considered including all rural highways and high-speed urban streets, low-speed urban streets, and turning roadways.

The design controls considered in this research represent those applicable to the design of the horizontal alignment. The components of the horizontal alignment include (1) horizontal curve, (2) superelevation transition, (3) alignment transition, and (4) tangent. Particular emphasis was placed on controls related to the first three components and their associated design elements.

With regard to the alignment transition design element, three types of alignment designs were considered: (1) tangent-to-curve transition, (2) spiral curve transition, and (3) compound curve transition. The term "tangent-to-curve" is used herein to refer to the situation where compound or spiral curvature is not used in the transition. Thus, in the tangent-to-curve design, the tangent section of the alignment intersects directly with the horizontal curve. Of the three transition types considered, compound curve transitions were given the least emphasis because a survey of practitioners indicated that they are rarely used for transition design.

A wide range of horizontal curve design controls were considered for this research. These controls were categorized as basic or element-specific. Basic design controls are those having a broad impact on most aspects of the alignment

design and include the design speed and maximum design side friction factor. Element-specific controls are those used to limit the size, orientation, or arrangement of specific design elements. These controls include maximum superelevation rate, minimum length of superelevation runoff, minimum spiral curve length, and so forth.

Several curve design control values were evaluated and, where appropriate, updated to reflect current driver and vehicle characteristics as well as pavement surface properties. The characteristics of both passenger cars and heavy trucks were considered in the evaluation and reflected in all updated control values. The effect of roadway grade was also considered in the evaluation.

The evaluation of existing and alternative design controls emphasized the quantification of their effect on vehicle operations. Aberrant operating conditions were identified and safety implications discussed. The investigation of a control's safety effect (in terms of crash frequency) was based on a synthesis of published research. This approach was undertaken due to limited project resources and consideration of the subtle effect of many controls on crash potential.

The guidelines developed in this research are intended for new construction and major reconstruction of streets, highways, and turning roadways in urban and rural areas. They are not developed explicitly for application in "3R" (i.e., resurfacing, restoration, or rehabilitation) or minor reconstruction projects. In this regard, construction costs were not explicitly considered in the development of the guidelines. However, if used for 3R or minor reconstruction projects, they would provide the same level of safety and efficiency as would be realized for new construction.

RESEARCH APPROACH

The research approach was divided into two phases and eight tasks. Phase I of the research comprises the first four tasks; Phase II comprises the last four tasks. The tasks identified for this project were as follows:

- Task 1—Review *Green Book* Guidelines and Compare to International Practice
- Task 2—Determine Current Domestic Practice
- Task 3—Develop Revisions to the Work Plan
- Task 4—Prepare Interim Report and Revised Work Plan
- Task 5—Assess Superelevation Distribution Methods
- Task 6—Assess Superelevation Transition Designs
- Task 7—Develop Recommended Design Guidelines and *Green Book* Modifications
- Task 8—Prepare Final Report

During the first task, the highway design policies of several international transportation agencies and organizations were reviewed. The objective of this review was to synthesize the horizontal curve design controls used by these agencies and compare them to the controls recommended in the *Green Book.* The guidelines for six international agencies were reviewed in this manner (*2, 3, 4, 5, 6, 7*); these agencies represent the following countries: Australia, Canada, France, Germany, Sweden, and the United Kingdom (U.K.).

During the second task, a survey of engineers with city, county, and state transportation agencies was conducted. The objective of the survey was to gather information on the standards and policies currently being used for horizontal curve design. The distribution included engineers with all 50 state DOTs, 21 city transportation departments, and 19 county highway agencies. Of the 90 questionnaires sent out, 44 completed questionnaires (49 percent) were returned. These responses represented 35 state DOTs, four cities, and five counties.

During the third task, the work plan for the remaining tasks was amplified and updated using the findings from the first two tasks. It was proposed that field data were needed describing the relationship among side friction demand, speed, curve radius, and superelevation rate. These data were needed for the accurate evaluation of existing superelevation distribution methods and the possible development of an alternative distribution method.

During the fifth task, field data were gathered at 55 horizontal curve study sites. These data included the measurement of a representative sample of driver speeds and headways at each site as well as measurement of the site's radius, superelevation rate, and grade. Eight states were represented in the database, which contained more than 8,100 valid speed observations. These data were used to compute each vehicle's side friction demand and to evaluate the factors that affect the magnitude of this demand. The results of this evaluation were used to develop a means of distributing side friction demand and superelevation rate over a range of radii.

During the sixth task, published data and simulation were used to evaluate the effect of alternative transition designs on vehicle lane position and control. Specifically, a kinematic model was developed and calibrated; it was then used to evaluate the effect of transition design length and location on vehicle position within the lane. A wide range of control values were considered for this investigation.

The seventh task folded the findings of the previous tasks into a series of recommended guidelines for horizontal curve design. These guidelines were presented in a format and sequence that complemented that used in the *Green Book.* The report documenting these recommended guidelines and suggested modifications to the *Green Book* is included in Appendix E.

The final report was developed in the eighth task. This report documented the research findings, the recommended controls and associated criteria, and the suggestions for future research.

CHAPTER 2

FINDINGS

INTRODUCTION

This chapter presents a summary of the major findings of this research. These findings represent investigations into a wide range of issues related to horizontal alignment design. To organize the investigation, the horizontal alignment was divided into four components: (1) horizontal curve, (2) superelevation transition, (3) alignment transition, and (4) tangent. The first component consists of two design elements: curve radius and superelevation rate. The second and third components consist of several design elements associated with the road section near the terminus (i.e., beginning or end) of a horizontal curve. The design guidance associated with the first three components was the focus of this research.

The topics of horizontal curve design, superelevation transition design, and alignment transition design are described in separate sections of this chapter. Each section begins with a review of the guidance provided in the *Green Book* and a summary of current practice. Then, issues and implications of this guidance are explored in the context of misconceptions, possible deviations from intended application, or need for update to reflect current conditions. Emphasis is placed on the design elements associated with each component and the design controls used to size these elements.

Before describing the three horizontal alignment components, a section of terminology is included. The concepts and definitions introduced in this section are intended to provide some context and perspective on the relationship between design controls and the design process. They are also intended to ensure the reader's understanding of the terminology used in this report.

TERMINOLOGY

Hierarchy of Roadway Design

A review of the *Green Book* discussion of horizontal alignment design issues and guidelines indicated that a hierarchical arrangement of terms is used to describe a roadway in terms of its function and design. This hierarchy of descriptors is not formally defined in the *Green Book* and, in some instances, is loosely applied within it. However, the following framework has been established as representative of the hierarchy of roadway design terms used in the *Green Book*:

Descriptor	*Examples*
Functional Classification	Rural Principal Arterial
Movement Type	Through or Turning
Design Features	Horizontal Alignment, Vertical Alignment
Design Components	Horizontal Curve, Tangent, Alignment Transition
Design Elements	Superelevation Rate, Radius, Cross Slope
Design Controls	Maximum Superelevation Rate, Minimum Grade
Design Values	Design Superelevation Rate, Design Grade

Many of the descriptors listed in the framework are formally used in the *Green Book*. However, two of these descriptors, Movement Type and Design Features, are recognized but used more informally. The Movement Type descriptor is used to differentiate between through and turning roadways. Turning roadways are connecting roadways serving traffic turning between two intersecting through roadways (i.e., intersection curves and interchange ramps).

The Design Features descriptor is used to identify the various major parts of a roadway design. Design features would include the horizontal alignment, vertical alignment, cross section, intersections, drainage, lighting, and so forth. Each design feature consists of various design components. In turn, each design component is composed of one or more design elements. For example, the horizontal alignment design components include the horizontal curve, superelevation transition section, alignment transition section, and tangent. Continuing the example, the horizontal curve has superelevation rate and curve radius as design elements.

Design Controls can be categorized as one of two types: basic and element-specific. At the basic level, design controls constitute direct inputs to the design process. Basic design controls are frequently determined from (or in conjunction with) the roadway functional classification and movement type. In general, most of the basic design controls and associated criteria are described in Chapter II of the *Green Book*. Examples of basic design controls include design speed, facility type, and side friction factor.

At the element-specific level, design controls define limiting design values for a range of permissible values. In general,

element-specific design controls are determined from the basic design controls, defined parametrically, or they are computed from selected combinations of controls. These controls may be used individually or in combination to limit the size, orientation, or arrangement of the corresponding element. Element-specific controls are generally described in *Green Book* Chapters III through X. Examples of element-specific controls include the maximum superelevation rate, minimum cross slope, and minimum radius.

Design controls are intended to be used to constrain the dimensions of critical roadway design elements. The limiting value associated with a control is denoted as a design criterion. The quantity selected for a design element (i.e., the design value) should equal or exceed the design criterion.

Theoretic Considerations

When a vehicle moves in a circular path, it undergoes a centripetal acceleration that acts toward the center of curvature. This acceleration is sustained by the friction between the tire and pavement and, if the road is superelevated, by a component of gravity. Lateral acceleration represents the portion of centripetal acceleration that is sustained by friction. The general relationship between these accelerations is as follows:

$$a_f = a_r - a_e \tag{1}$$

where:

a_f = acceleration sustained by friction (or lateral acceleration) (= $g f_D$), m/s^2;
a_r = centripetal acceleration (= v^2/R), m/s^2;
a_e = acceleration sustained by superelevation (= $ge/100$), m/s^2;
e = superelevation rate, percent;
f_D = side friction demand factor;
v = vehicle speed, m/s;
g = gravitational acceleration (= 9.807 m/s^2); and
R = radius of curve, m.

The formulas provided in the definition of each acceleration term can be combined with Equation 1 to obtain a more commonly found equation relating side friction demand, superelevation rate, speed, and radius. The form of this equation is as follows:

$$f_D = \frac{v^2}{gR} - \frac{e}{100} \tag{2}$$

The side friction demanded by a driver is directly related to the amount of lateral acceleration experienced when the driver chooses to travel at speed v on a curve of radius R and superelevation rate e. The essence of horizontal curve design is to provide a radius and superelevation rate that combine to yield a safe and comfortable lateral acceleration for a reasonably large percentage of drivers.

Facility Types

One of the basic design controls for horizontal alignment design is Facility Type. The *Green Book* describes horizontal alignment design guidelines for three facility types. Collectively, these three facility types embrace all possible combinations of functional classification, movement type, and design speed. The following facility types are recognized by the *Green Book*:

1. All Rural Highways and High-Speed Urban Streets (RHS),
2. Low-Speed Urban Streets (LS), and
3. Turning Roadways (TR).

The acronyms listed with each facility type have been coined for this report.

The "speed" referred to in the facility-type names is the design speed. Facilities with a design speed of 60 km/h or less are referred to as low-speed facilities. Facilities with a design speed of 80 km/h or more are referred to as high-speed facilities. The intermediate design speed of 70 km/h can be considered as either low or high speed, depending on other conditions along the roadway.

Turning roadways are connecting roadways serving traffic turning between two intersecting through roadways. Turning roadways include an exit terminal, a central section, and an entrance terminal—all of which can include one or more curves. Turning roadways can be further categorized as either interchange ramps or intersection curves. Interchange ramps have horizontal alignments that (1) have a loop or a diamond configuration and (2) may include tangent sections, as needed, to minimize the right-of-way requirements. In contrast, intersection curves have alignments that have a diamond configuration and generally consist only of curves. Finally, turning roadways have design speeds of 20 km/h or more and, at intersections, are associated with a channelizing island.

The *Green Book* Chapters III, IX and X contain guidance for turning roadways. The material in Chapter III (*1*, p. 192–200) and Chapter IX (*1*, 690–695, 726–739) is directed primarily toward low-speed (and in some cases intermediate-speed) intersection curves. High-speed intersection curves (e.g., free-right turn lanes at rural intersections) are not explicitly addressed in Chapters III and IX. The material in Chapter X (*1*, 918–924) is directed toward low- and high-speed interchange ramps.

The three facility types were not explicitly recognized in the AASHTO policy documents until the 1984 *Green Book* (*8*). This document was the first to combine the urban and rural design guidelines into one document. The 1994 *Green Book* maintains these three facility types; moreover, it is the

first AASHTO policy document to formally introduce the three facility types and refer to them as "types of highway facilities" (*1*, p. 146).

CONTROLS FOR HORIZONTAL CURVE DESIGN

This section presents the findings from a critical review of the horizontal curve design guidelines provided in the *Green Book* (*1*). These guidelines are described primarily in Chapter III of the *Green Book* with some additional guidance being provided in the facility-specific chapters that follow. This review includes a synthesis of *Green Book* guidance, a summary of state DOT practice, and a discussion of some problematic design issues related to horizontal curve design.

Review of Horizontal Curve Design Controls

The design controls applicable to horizontal curve design are listed in Table 1. The element-specific controls that are listed are intended to provide an appropriate combination of superelevation and radius for the specified roadway function and design speed. As the table indicates, many of the element-specific controls are defined by the basic controls.

Maximum Design Side Friction Factors

One of the most fundamental controls related to horizontal curve design is the maximum design side friction factor (referred to as the "side friction factor" in the *Green Book*). The adjectives "maximum" and "design" are added for this report to precisely define this factor as a design control. The term "maximum" is added for consistency with the terminology used for most other design controls (e.g., minimum radius, maximum superelevation rate). The term "design" is added to distinguish this friction factor from other side friction factors (e.g., side friction demand factor or side friction supply factor). The maximum design side friction factors recommended by the *Green Book* are shown in Figure 1.

The maximum design side friction factors described in the *Green Book* were based on the identification of the side friction demand level considered acceptable by a majority of motorists. For highway curves, field studies were based on identifying side friction levels that were deemed (by the study participants) to be at the upper limits of comfort. For intersection curves, studies were based on identifying the side friction demand for the 95th percentile driver; no direct measurement of comfort was made. Numerous "friction" studies of these two types were conducted during the period between 1920 and 1952. These studies were synthesized by the *Green Book* authors and used to define the maximum design side friction factors shown in Figure 1.

Minimum Cross Slope

In contrast to other curve design controls, the guidance provided on minimum cross slope is primarily located in Chapter IV of the *Green Book*. This chapter emphasizes the need for a minimum cross slope to facilitate road surface drainage. This guidance is synthesized in Table 2 for high-type pavement. For example, when there are two lanes in the subject direction of travel, the inside lane cross slope should range from 1.5 to 2.0 percent and the outside lane cross slope should range from 2.0 to 3.0 percent.

As indicated by Table 2, the *Green Book* authors recommend the use of a minimum cross slope of 1.5 to 2.0 percent for the inside (or only) traffic lane. For multilane facilities, the minimum slope increases slightly for each additional lane to facilitate drainage to the right side of the roadway. It should be noted that the *Green Book* authors indicate that cross

TABLE 1 Design controls for horizontal curve design

Descriptor	Control Type	No.	Name	Basis
Class & Type		1	Functional Classification (urban..., rural...)	Specified
		2	Movement Type (through, turning)	Specified
Design Control	Basic	3	Design Speed	Specified
		4	Facility Type (RHS, LS, & TR)[1]	Based on 1, 2 & 3
		5	Maximum Design Side Friction Factor	Based on 1, 2 & 3
	Element-Specific	6	Minimum Cross Slope	Based on 1& drainage
		7	Maximum Superelevation Rate	Based on 4 & climate
		8	Method of Distributing e and f	Based on 4
		9	Minimum Radius at Maximum Superelevation	Based on 3, 5 & 7
		10	Minimum Radius With Normal Cross Section	Based on 3, 6 & 8

[1] RHS: All rural highways and high-speed urban streets; LS: Low-speed urban streets; TR: Turning roadways.

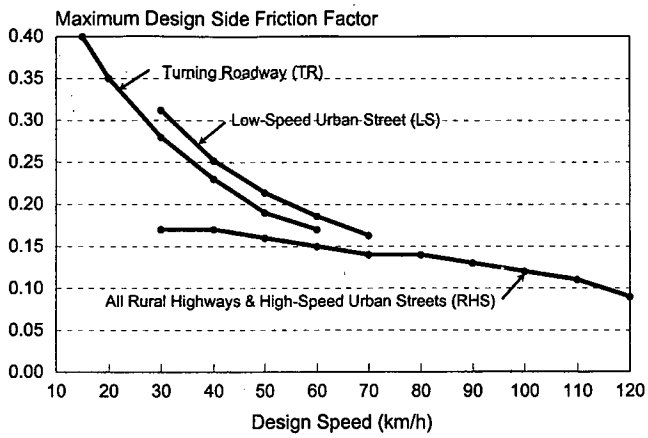

Figure 1. Comparison of the maximum design side friction factors for the three facility types.

slopes up to 2.0 percent are "barely perceptible" by the driver with regard to the effect of cross slope on steering effort.

The *Green Book* authors indicate that pavements of lower quality, as might be found on low-volume county roads, may need more cross slope than that shown in Table 2 (perhaps as much as 6 percent). This need stems from the greater likelihood of excessive settlement and deformation of the cross section associated with these facilities.

Maximum Superelevation Rate

Through Roadways. The *Green Book* describes a rationale for limiting the superelevation rate for RHS and LS facility curves based on climatic conditions, terrain, area type (i.e., urban, rural), and the frequency of slow-moving vehicles. Engineers in northern states, where ice and snow occur, typically use a lower maximum superelevation rate than southern states. Engineers in urban areas typically use lower maximum superelevation rates on low-speed streets to minimize the impact of the curve on adjacent property drainage or access. Table 3 synthesizes the guidance provided in the *Green Book* on the possible maximum superelevation rate (or rates) that are applicable to horizontal curve design.

Design policy documents published by AASHTO before 1984 encouraged the use of only one maximum superelevation rate in a state or region. Specifically, the 1954 AASHTO Policy (*9*, p. 132) stated "For actual design in a State or region only one of the above maximum rates will apply, although there is no inhibition against the use of more than one, say for different road systems." This guidance has been revised in recent editions of the *Green Book*. A statement in the 1994 edition encourages the use of multiple maximum rates. This statement reads: "Consideration of these factors jointly leads to the conclusion that no single maximum superelevation rate is universally applicable and that a range of rates must be used." (*1*, p. 151).

Turning Roadways. The *Green Book* separately describes the maximum superelevation rate control separately for intersection curves and for interchange ramps. Maximum rates for high-speed interchange ramps are discussed in Chapter X. The discussion in Chapter X recommends the use of *Green Book* Tables III-7 through III-11 (i.e., the superelevation distribution tables for RHS facilities) for high-speed interchange ramps. This recommendation implies that maximum superelevation rates of 4, 6, 8, 10, and 12 percent are acceptable for these ramps.

The material in Chapters III and IX is presented in the context of "low-speed intersection curves." However, references in Chapter X indicate that the materials in Chapters III and IX are also applicable to low-speed interchange ramps. Hence, it appears that the material in Chapters III and IX is applicable to all low-speed TR facilities.

Guidance on the selection of a maximum superelevation rate for low-speed TR facilities is provided in *Green Book* Tables III-16 and IX-12. The recommended ranges of maximum rates obtained from the latter table are shown in the last row of Table 4.

A maximum superelevation rate of 10 percent is implied by Table IX-12 for low-speed turning roadways. However, discussion associated with this table indicates that this value is illustrative and that "any other maximum rate can be used." (*1*, p. 729). In contrast, guidance on a previous page states the following:

> "The general factors that control the maximum rates of superelevation for open highway conditions . . . also apply to intersections. Maximum superelevation rates up to 12% may be used where climatic conditions are favorable. However, at intersections the maximum superelevation rate for curves is 10% except that a maximum rate of 8% generally should be used where snow and icing conditions prevail." (1, p. 726).

TABLE 2 Minimum cross slopes for high-type pavement[1]

No. Lanes in the Subject Travel Direction	Lane Location		
1	Only		
2	Inside	Outside	
3	Inside	Middle	Outside
Minimum Cross Slopes[2] (%):	1.5 - 2.0	2.0 - 3.0	2.5 - 4.0

[1] The slopes reported are based on an interpretation of the discussion in the *Green Book* (*1*, p. 330-332).
[2] An additional 0.5 percent can be added in areas of intense rainfall.

TABLE 3 Maximum superelevation rates for RHS and LS facilities

Max. Superelevation Rate, e_{max} (%)	Facility Type		Snow and Ice Conditions
	RHS	LS	
4[1]	OK	OK	If significant
6	OK	OK	If significant
8	OK	--	If frequent enough to be a factor
10	OK	--	If infrequent
12	OK	--	If it never occurs

[1] 4% is applicable to urban streets only, based on the footnote in *Green Book* Table III-7 (*1*, p. 167).

This guidance is interpreted to mean that 12 percent rates may be used on RHS facilities but that 10 percent is the largest maximum rate for low-speed turning roadways. Maximum rates of 4, 6, and 8 percent can also be used for these facilities.

The *Green Book* authors define a "minimum" maximum superelevation rate in Table III-16. This min.-max. rate is listed in row 3 of Table 4. They recognize that this rate is truly a "maximum" but that it represents the "minimum" value in a range of possible maximums. They state that larger maximum rates could be used on any curve designed with the minimum radius shown in row 4 of Table 4. Their rationale is that any extra superelevation (beyond the min.-max. rate) would allow drivers "to drive the curves a little faster or drive them more comfortably because of less friction." (*1*, p. 194).

Superelevation and Side Friction Distribution Method

The *Green Book* describes five methods for determining the amount of superelevation and side friction that is needed for a given design speed and design curve radius. Of these five methods, the *Green Book* recommends only two for design applications (i.e., Methods 2 and 5). Three of the methods are unique and different (i.e., Methods 1, 2, and 3). Method 4 is a variation of Method 3 and Method 5 is synthesized as a compromise between Methods 1 and 4. The five distribution methods are illustrated in Figure 2. The operational objective underlying the derivation of each method is described in the following paragraphs.

RHS Facilities. Distribution Method 5 is used for RHS facilities. The intent of Method 5 is to emphasize superelevation and to limit the use of maximum side friction to only the sharpest curve radius. This emphasis on superelevation is intended to favor the tendency of some drivers to travel at or near the design speed along curves of intermediate radius. This method provides sufficient superelevation to counteract most of the centripetal acceleration experienced by drivers on intermediate to flat curves. Tables III-7 through III-11 in the *Green Book* identify the recommended design superelevation rates for a given design speed and radius based on Method 5. Table III-9 is reproduced in Figure 3 to illustrate the type of guidance provided in these tables.

LS Facilities. Distribution Method 2 is used for LS facilities. The objective of this method is to use side friction to the maximum extent possible with little or no use of superelevation. This method is appropriate for urban design because it minimizes the disruption to adjacent property access and drainage caused by superelevated cross sections. It also minimizes the amount of negative side friction that occurs when traffic congestion or control devices slow turning vehicles to very low speeds.

The *Green Book* does not provide a table of design superelevation rates for LS facilities (as it does for RHS facilities); instead, it provides Figure III-18. This figure is reproduced here as Figure 4. It should be noted that the design speed range for low-speed urban streets was expanded for the 1994 *Green Book* to include the 70-km/h design speed; this modification is reflected in Figure 4.

TABLE 4 Maximum superelevation rates for low-speed TR facilities

Table[1]	Design Speed (km/h):	15	20	30	40	50	60	70
III-16	Max. Design Side Friction Factor:	0.40	0.35	0.28	0.23	0.19	0.17	not id.
III-16	Minimum Superelevation Rate[2] (%):	0	0	2	4	6	8	not id.
III-16	Minimum Curve Radius (m):	7	10	25	50	80	115	not id.
IX-12	Range of Max. Superelevation Rates:	not id.[3]	2 - 10	2 - 10	4 - 10	6 - 10	8 - 10	9 - 10

[1] *Green Book* (*1*) table from which the data shown were obtained.
[2] "Minimum Superelevation Rate" is the term used in the *Green Book*; it is actually the smallest recommended *maximum* rate.
[3] "not id.": Values not identified in the corresponding *Green Book* table.

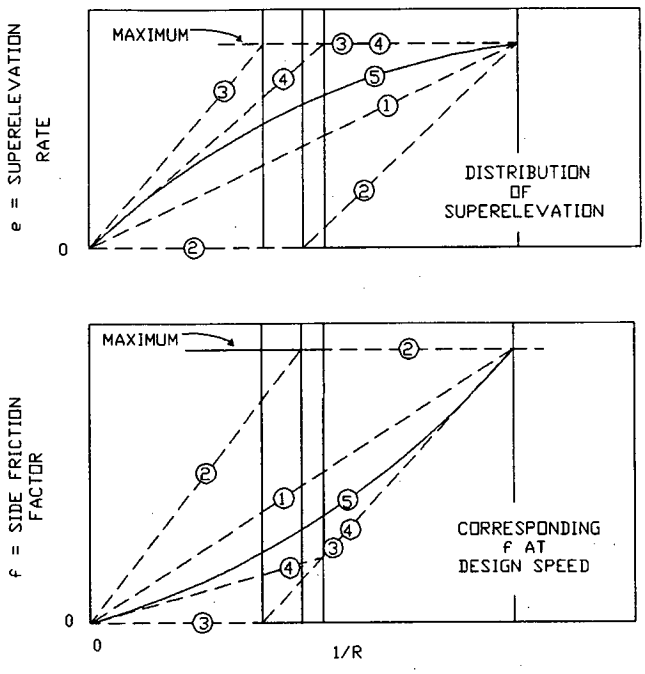

Figure 2. Methods of distributing superelevation and side friction.

The trends in Figure 4 are based on Equation 2 and the maximum design side friction factors for low-speed urban streets (shown in Figure 1). Superelevation rate is selected for a given combination of speed and radius (radii are shown as labels on each trend line shown). For a given speed, radii larger than those associated with a cross slope rate of −1.5 to −2.0 percent (i.e., a rate equal to the normal cross slope rate) can be used without superelevation.

Turning Roadways. The method of superelevation distribution for TR facilities is not explicitly defined in the *Green Book* in terms of one of the five methods previously discussed. However, guidance is provided in Chapters III, IX, and X. The guidance provided in Chapters III and IX relates to low-speed intersection curves. That provided in Chapter X relates to interchange ramps. The discussion in Chapter X indicates that design superelevation rates defined for RHS facilities (i.e., distribution Method 5) would also apply to those interchange ramps with a design speed greater than 60 km/h. This discussion also indicates that the guidance provided for low-speed intersection curves is also applicable to low-speed interchange ramps.

Guidelines on the design superelevation rate for low-speed intersection curves and interchange ramps (i.e., low-speed TR facilities) are provided in *Green Book* Chapter IX (i.e., Table IX-12). These guidelines are in the form of a range of superelevation rates for each radius and design speed combination. Hence, they are much more flexible than those provided for RHS and LS facilities. The information provided in Table IX-12 is reproduced in Table 5.

An examination of the upper and lower rates provided for each radius-speed combination in Table 5 indicates that there is some correlation between these rates and two of the five distribution methods. Specifically, the lower superelevation rate of each range for a given design speed appears to follow distribution Method 2 whereas the upper rate of each range appears to follow distribution Method 1. This latter method does not emphasize either superelevation or side friction; rather, it applies each quantity in amounts that are directly proportional to the inverse of the curve radius.

Distribution Methods Used by Highway Agencies. A comprehensive examination of state DOT design procedures was conducted for this research. This examination explored DOT interpretations of and extensions to the *Green Book* guidance. It consisted of a review of 27 state DOT design manuals, a survey of engineers with 35 state DOTs, and a review of guideline documents published by 6 foreign countries. One objective of this examination was to identify the method of superelevation distribution used by state DOTs.

Almost all of the state DOTs surveyed were found to use the distribution methods described in the *Green Book.* In fact, with one exception, the choice of Method 5 for RHS facilities and interchange ramps is unanimous among the DOTs. The exception is the California DOT. It provides one table that includes all of its maximum superelevation rates (i.e., 8, 10, and 12 percent). This table provides a range of radii for each integer value of the design superelevation rate; there is no explicit sensitivity to design speed. The design superelevation rates range from 2 to 12 percent. The relationship between radii and superelevation rate roughly follows that provided in the *Green Book* Table III-11 (e_{max} = 12 percent) for a design speed of 80 km/h. Hence, the California distribution generally provides less superelevation than would be recommended by the *Green Book* for design speeds in excess of 80 km/h.

Four of the six international guidelines reviewed for this research were found to provide a continuous mathematical relationship among superelevation, radius, and design speed (or an equivalent table or figure). The mathematical relationships recommended in four of these guidelines are compared in Figure 5 with that recommended in the *Green Book* for a 70-km/h design speed. The line labeled "e = 100 $v^2/(gR)$" in this figure represents the amount of superelevation needed to match the centripetal acceleration associated with travel on a curved path; as such, this line represents a theoretical upper bound on superelevation rate.

The trends shown in Figure 5 indicate that there is a wide range of guidance being provided by international agencies. Of course, some of the differences are due to the use of different maximum design side friction factors. In general, all of the distribution methods tend to emphasize the use of superelevation.

	V_d= 30 km/h			V_d= 40 km/h			V_d= 50 km/h			V_d= 60 km/h			V_d= 70 km/h			V_d= 80 km/h			V_d= 90 km/h			V_d= 100 km/h			V_d= 110 km/h			V_d= 120 km/h		
		L (m)			L (m)			L (m)			L (m)			L (m)			L (m)			L (m)			L (m)			L (m)			L (m)	
R	e	2	4	e	2	4	e	2	4	e	2	4	e	2	4	e	2	4	e	2	4	e	2	4	e	2	4	e	2	4
(m)	(%)	Lns	Lns	(%)	Lns	Lns	(%)	Lns	Lns	(%)	Lns	Lns	(%)	Lns	Lns	(%)	Lns	Lns	(%)	Lns	Lns	(%)	Lns	Lns	(%)	Lns	Lns	(%)	Lns	Lns
7000	NC	0	0	NC	0	0	NC	0	0	NC	0	0	NC	0	0	NC	0	0	NC	0	0	NC	0	0	NC	0	0	NC	0	0
5000	NC	0	0	NC	0	0	NC	0	0	NC	0	0	NC	0	0	NC	0	0	NC	0	0	NC	0	0	NC	0	0	NC	0	0
3000	NC	0	0	NC	0	0	NC	0	0	NC	0	0	NC	0	0	NC	0	0	NC	0	0	RC	56	84	2.1	61	92	2.4	67	101
2500	NC	0	0	NC	0	0	NC	0	0	NC	0	0	NC	0	0	NC	0	0	RC	50	75	2.1	56	84	2.4	61	92	2.9	67	101
2000	NC	0	0	NC	0	0	NC	0	0	NC	0	0	NC	0	0	RC	44	66	2.2	50	75	2.6	56	84	3.0	61	92	3.5	67	101
1500	NC	0	0	NC	0	0	NC	0	0	NC	0	0	RC	39	59	2.4	44	66	2.8	50	75	3.4	56	84	3.9	61	92	4.6	67	101
1400	NC	0	0	NC	0	0	NC	0	0	RC	33	50	2.1	39	59	2.5	44	66	3.0	50	75	3.6	56	84	4.1	61	92	4.9	67	101
1300	NC	0	0	NC	0	0	NC	0	0	RC	33	50	2.2	39	59	2.7	44	66	3.2	50	75	3.8	56	84	4.4	61	92	5.2	67	101
1200	NC	0	0	NC	0	0	NC	0	0	RC	33	50	2.4	39	59	2.9	44	66	3.4	50	75	4.1	56	84	4.7	61	92	5.6	67	101
1000	NC	0	0	NC	0	0	RC	28	42	2.2	33	50	2.8	39	59	3.4	44	66	4.0	50	75	4.8	56	84	5.5	61	92	6.5	67	101
900	NC	0	0	NC	0	0	RC	28	42	2.4	33	50	3.1	39	59	3.7	44	66	4.4	50	75	5.2	56	84	6.0	61	92	7.1	67	101
800	NC	0	0	NC	0	0	RC	28	42	2.7	33	50	3.4	39	59	4.1	44	66	4.8	50	75	5.7	56	84	6.5	61	92	7.6	68	103
700	NC	0	0	RC	22	33	2.2	28	42	3.0	33	50	3.8	39	59	4.5	44	66	5.3	50	75	6.3	56	84	7.2	62	93	8.0	72	108
600	NC	0	0	RC	22	33	2.6	28	42	3.4	33	50	4.3	39	59	5.1	44	66	6.0	50	75	6.9	56	84	7.7	66	99	R_{min} = 655		
500	NC	0	0	2.2	22	33	3.0	28	42	3.9	33	50	4.9	39	59	5.8	44	66	6.7	51	76	7.6	61	91	8.0	69	103			
400	RC	17	26	2.7	22	33	3.6	28	42	4.7	33	50	5.7	39	59	6.6	48	71	7.5	57	85	8.0	64	96	R_{min} = 500					
300	2.1	17	26	3.4	22	33	4.5	28	42	5.6	34	51	6.7	44	66	7.6	55	82	R_{min} = 305			R_{min} = 395								
250	2.5	17	26	4.0	22	33	5.1	28	42	6.2	37	56	7.3	48	72	7.9	57	85												
200	3.0	17	26	4.6	24	36	5.8	31	47	7.0	42	63	7.9	52	78	R_{min} = 230														
175	3.4	17	26	5.0	26	39	6.2	33	50	7.4	44	67	8.0	52	79															
150	3.8	18	27	5.4	28	42	6.7	36	54	7.8	47	70	R_{min} = 175																	
140	4.0	19	29	5.6	29	43	6.9	37	56	7.9	47	71																		
130	4.2	20	30	5.8	30	45	7.1	38	58	8.0	48	72																		
120	4.4	21	32	6.0	31	46	7.3	39	59	R_{min} = 125																				
110	4.7	23	34	6.3	32	49	7.6	41	62																					
100	4.9	23	35	6.5	33	50	7.8	42	63																					
90	5.2	25	37	6.9	36	53	7.9	43	64																					
80	5.5	26	40	7.2	37	56	8.0	43	65																					
70	5.9	28	42	7.5	39	58	R_{min} = 80																							
60	6.4	31	46	7.8	40	60																								
50	6.9	33	50	8.0	41	62																								
40	7.5	36	54	R_{min} = 50																										
30	8.0	38	57																											
	R_{min} = 30																													

e_{max} = **8.0%**
R = radius of curve
V = assumed design speed
e = rate of superelevation
L = minimum length of runoff (does not include tangent runout)
NC = normal crown section
RC = remove adverse crown, superelevate at normal crown slope

Note: Lengths rounded in multiples of 10 m permit simpler calculations.

Figure 3. Design superelevation table for RHS facilities (1).

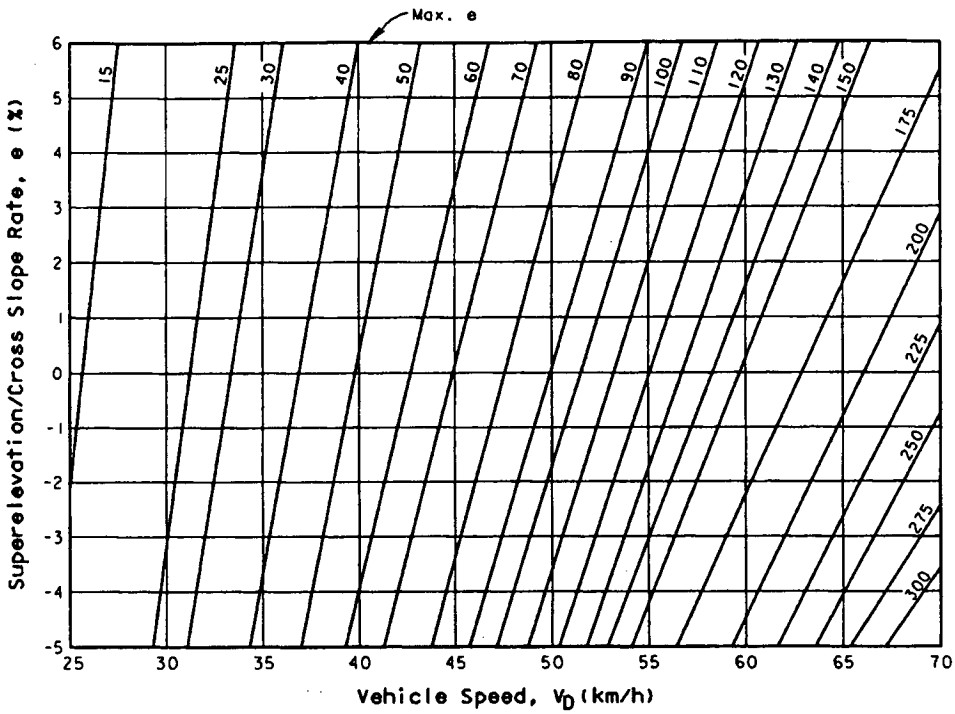

Figure 4. Design superelevation figure for LS facilities (1).

The German, French, and U.K. distribution methods are represented by linear (or very nearly so) relationships between superelevation rate and curvature. This trend is in sharp contrast to the asymmetric parabolic distribution used in the *Green Book*. The obvious advantage of a linear relationship is the simplicity of computation relative to the parabola.

Like RHS facilities, the distribution methods described in the *Green Book* for LS and TR facilities are also frequently used by the state DOTs. Four of the state DOTs surveyed deviated from the Method 2 distribution for LS facilities. The relationship between superelevation and curvature used by each of these DOTs, as well as *Green Book* Method 2, are shown in Figure 6. *Green Book* Method 5 and the method recommended by ITE Technical Council Committee 5-5 (*10*) are also shown for reference.

The trend lines shown in Figure 6 indicate that the California and Ohio DOTs have made the greatest deviation from Method 2. In contrast, the Montana and New York DOTs have made much smaller changes. All of the deviations provide more superelevation for the same radius than would be

TABLE 5 Design superelevation table for TR facilities[1]

Radius (m)	Design Speed (km/h)					
	20	30	40	50	60	70
15	**2 - 10%**	---	---	---	---	---
25	2 - 7	**2 - 10%**	---	---	---	---
50	2 - 5	2 - 8	**4 - 10%**	---	---	---
70	2 - 4	2 - 6	3 - 8	**6 - 10%**	---	---
100	2 - 3	2 - 4	3 - 6	5 - 9	**8 - 10%**	---
150	2 - 3	2 - 3	3 - 5	4 - 7	6 - 9	**9 - 10%**
200	2	2 - 3	2 - 4	3 - 5	5 - 7	7 - 9
300	2	2 - 3	2 - 3	3 - 4	4 - 5	5 - 6
500	2	2	2	2 - 3	3 - 4	4 - 5
700	2	2	2	2	2 - 3	3 - 4
1,000	2	2	2	2	2	2 - 3

[1] Values in bold represent the range of maximum superelevation rates for a given design speed.

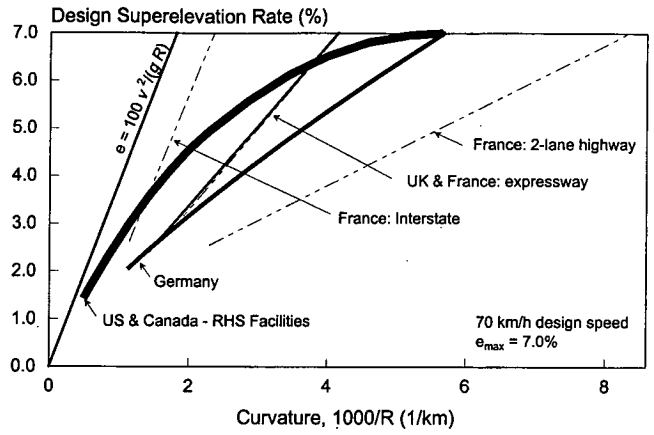

Figure 5. Superelevation distribution methods recommended by several international agencies for high-speed facilities.

provided by Method 2 but less than that provided by Method 5. It should be noted that the Ohio DOT distribution is very consistent with Method 1 (i.e., an equal distribution between superelevation rate and side friction).

Methods for Presenting Superelevation Rate Guidance. Almost all of the state DOTs surveyed were found to use a table to define the relationship among superelevation rate, radius, and design speed for RHS facilities. The table format is generally consistent with that used in the *Green Book* (i.e., Tables III-7 through III-11). However, the California and Montana DOTs have revised this format to present a *range* of radii applicable to *integer* values of the superelevation rate. The motivation for adopting this approach is likely based on (1) a desire to improve design consistency, (2) a realistic recognition of the practical limits of superelevation constructability, and (3) recognition of the negligible operational difference between a fractional superelevation rate and its integer equivalent (e.g., between 4.5 and 5.0 percent). An example of the superelevation distribution table provided in the Montana DOT design manual is shown in Figure 7.

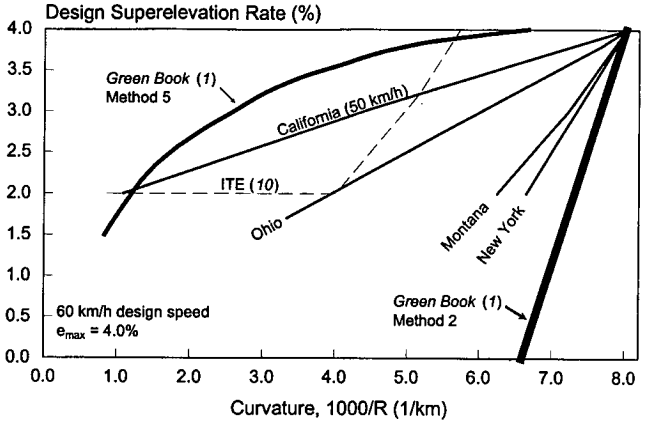

Figure 6. Superelevation distribution methods used by various agencies for LS facilities.

For LS facilities, about 40 percent of the DOTs surveyed chose to present the relationship among design superelevation rate, design speed, and radius using a table rather than the figure provided in the *Green Book* (i.e., Figure III-18). Many of these DOTs configured the table format to be consistent with the tables provided in the *Green Book* for RHS facilities (i.e., Tables III-7 through III-11).

Issues Related to Horizontal Curve Design

This section describes three issues inherently related to horizontal curve design and its associated controls: design consistency, deceleration as a result of speed reduction, and curve versus path radius. The discussion in this section provides a context for the recommended horizontal curve design controls described in the next chapter.

Impact of Green Book Controls on Design Consistency

Design consistency relates to the uniformity of the roadway alignment and its associated design element dimensions in terms of their collective ability to indicate to the driver a safe and reasonable speed. The design-speed concept used in the *Green Book* is intended to promote this consistency.

There are several measures that can be used to assess a design's consistency. One measure of design consistency is the uniformity of operating speeds along the alignment. Another measure is the uniformity of the driving workload (as measured by the amount of driving information presented relative to the available processing time). Design elements that are inconsistent with driver expectancy increase the processing time and thus, the driver workload. Logically, there is an inherent relationship between design consistency and motorist safety, with "consistent" designs being associated with lower crash potential.

A major drawback of superelevation distribution Method 5, as it is applied in the *Green Book*, is that its use can lead to a violation in design consistency. This violation stems from the availability of significantly different superelevation rates for the same curve radius. The violation occurs when different maximum superelevation rates are used on nearby facilities and drivers traveling among these facilities encounter different superelevation rates (and corresponding side friction demands) for curves of similar radius.

It is believed that the original intent of Method 5 was that *one* maximum superelevation rate (and corresponding design superelevation table) would be used for all RHS facilities within a region of similar climate and topography. Through this application, a driver would learn to expect the same amount of superelevation (and side friction demand) when

e (%)	V = 90 km/h			V = 100 km/h			V = 110 km/h		
	R (m)	Trans. Length		R (m)	Trans. Length		R (m)	Trans. Length	
		L (m)	TR (m)		L (m)	TR (m)		L (m)	TR (m)
NC	R > 2965	0	0	R ≥ 3625	0	0	R ≥ 4180	0	0
2	2965 > R ≥ 2185	50	50.00	3625 > R ≥2675	60	60.00	4180 > R ≥ 3095	65	65.00
3	2185 > R ≥ 1400	50	33.33	2675 > R ≥ 1750	60	40.00	3095 > R ≥ 2000	65	43.33
4	1400 > R ≥ 1000	50	25.00	1750 > R ≥ 1250	60	30.00	2000 > R ≥ 1465	65	32.50
5	1000 > R ≥770	50	20.00	1250 > R ≥ 950	60	24.00	1465 > R ≥ 1140	65	26.00
6	770 > R ≥ 600	50	16.67	950 > R ≥ 750	60	20.00	1140 > R ≥ 900	65	21.67
7	600 > R ≥ 465	60	17.14	750 > R ≥ 590	60	17.14	900 > R ≥ 735	65	18.57
8	465 > R ≥ 305	65	16.25	590 > R ≥ 395	70	17.50	735 > R ≥ 505	75	18.57
	R_{min} = 305 m			R_{min} = 395 m			R_{min} = 505 m		

Key:

R = radius of curve, m
V = design speed, km/h
e = superelevation rate, %
L = minimum length of superelevation runoff (from adverse slope removed to full super)
TR = tangent runout from NC to adverse slope removed
NC = normal crown

e_{max} = 8 %

Figure 7. Example design superelevation rate table from the Montana DOT design manual.

driving on a curve of given radius, regardless of where in the region it was encountered.

Current practice is not fully consistent with the perceived original intent of Method 5. In particular, the state DOTs of many bordering states have tended to be more dissimilar (than similar) in their adoption of appropriate maximum superelevation rates. The magnitude of this diversity was demonstrated by Hayward (*11*) who identified the maximum superelevation rates used by several states. He found that while Illinois and Indiana had maximum rates of 8 percent, the state to their immediate southeast, Kentucky, had a maximum rate of 10 percent. He also found that the states of California and Texas allowed maximum rates to vary from 8 to 12 percent within their borders. Similar trends were confirmed during the examination of state DOT design manuals conducted for this research.

Hayward (*11*) noted that the use of different maximum superelevation rates within a region results in inconsistent horizontal curve designs. Specifically, he noted that the use of different maximum superelevation rates yields a situation where one curve radius-superelevation rate combination can have any number of possible design speeds. This problem is demonstrated in Table 6 for a range of radii and superelevation rates (the speeds shown in this table were "soft-converted" by Hayward from their English equivalents).

To illustrate the consistency problem suggested by Table 6, consider a curve with a radius of 218 m and a design speed of 55 km/h (or 56 km/h). The values in Table 6 indicate that

TABLE 6 Range of possible design speeds for a curve with a known superelevation and radius

Actual Superelevation (%)	Radius (meters)	Possible Design Speed (km/h)			
		e_{max} = 6%	e_{max} = 8%	e_{max} = 10%	e_{max} = 12%
5	582	89	79	72	69
	218	56	47	45	43
	175	50	43	42	40
6	582	113	89	80	77
	218	72	55	48	47
	175	64	48	45	43
8	582	--	121	98	92
	218	--	79	63	56
	175	--	68	55	51

Source: Hayward (*11*).

superelevation rates ranging from 5 to 8 percent can be used for this speed and radius, depending on the choice of maximum superelevation rate. Clearly, this is a wide range of superelevation rates. The differences in side friction demand associated with the rates in this range would likely be detectable by the driver.

Krammes et al. (*12*) have also noted the adverse effect of multiple maximum rates on design consistency. They examined the relationship between superelevation rate and radius for 138 two-lane, rural highway curves in five states. The results of this examination revealed that the collective use of several maximum rates (and Method 5) resulted in there being no correlation between the radius and superelevation rate on these 138 curves. Based on their findings, Krammes et al. argue that this type of inconsistent design practice "complicates the driver's task of selecting the appropriate speed on curves" and has led to an increase in driver workload. As a result, they recommended the nationwide adoption of a single, maximum superelevation rate.

In summary, *Green Book* Tables III-7 through III-11 define *one* superelevation rate for a given design speed, radius, and maximum superelevation rate. The current use of multiple maximum rates indirectly provides designers with a *range* of acceptable superelevation rates by allowing them to consider several tables. Although the provision of a range of rates has obvious benefit in terms of design flexibility, a consequence of this provision is reduced design consistency.

Effect of Speed Reduction on Margin of Safety

Field studies of driver speed on horizontal curves were conducted for this research. An analysis of the data (documented in Appendix A) indicated that drivers tend to reduce their speed prior to and through the initial portion of sharp horizontal curves. This speed reduction was often found to be accompanied by a small increase in side friction demand (as computed using Equation 2). Logically, an increase in friction demand reduces the margin of safety (i.e., the difference between side friction demand and supply) drivers have while traveling along the curve.

The margin of safety drivers have is also affected by any change in side friction supply. The deceleration associated with a speed reduction "consumes" a portion of the friction supply and, thereby, reduces that available for cornering. In summary, the margin of safety is reduced on sharp curves because (1) drivers tend to increase their friction demand and (2) their deceleration reduces friction supply.

Theoretic models of friction supply and demand were developed for this research. These models were based on a dynamic analysis of forces acting on the vehicle traveling at a given speed while on a curve of given geometry. The model of friction supply was developed to include a sensitivity to the effect of vehicle deceleration during curve entry. The side friction demand and supply models were used together to compute the margin of safety for both passenger cars and trucks. Details of these models and their application are provided in Appendix C.

Figures 8 and 9 illustrate the effect of speed, grade, and braking on the margin of safety for passenger cars and trucks, respectively. In each figure, two scenarios are represented: one scenario represents a downgrade condition where the driver will likely brake to achieve a nominal speed reduction; the second scenario represents an upgrade condition where it is assumed that the driver will use the available engine power to maintain speed (i.e., no speed reduction). Both of these scenarios represent realistic, albeit worst-case, combinations of traction/braking and grade. Finally, it should be noted that the friction supply and demand were computed for the critical travel path radius on a curve designed with the minimum radius for design. This critical path radius was estimated to be 87 percent (= 1/1.15) of the minimum radius for design.

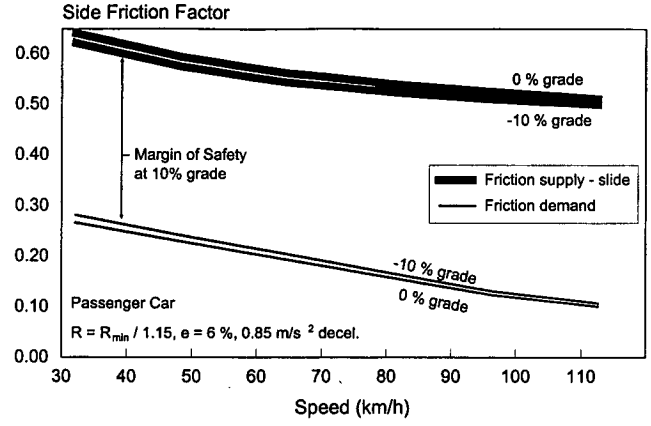

a. Speed reduction of 3 km/h.

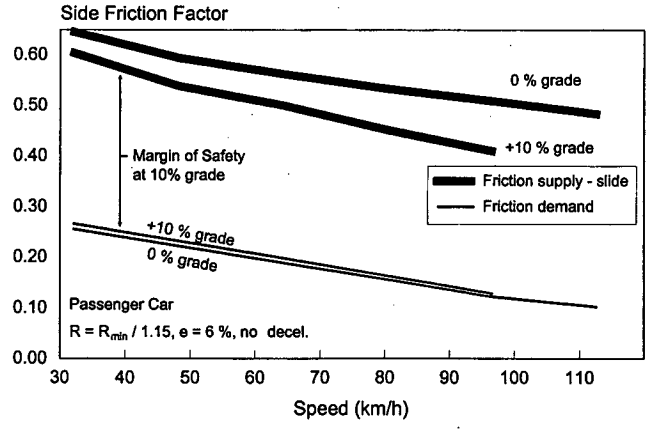

b. No speed reduction.

Figure 8. Effect of speed reduction on passenger car margin of safety against slide failure.

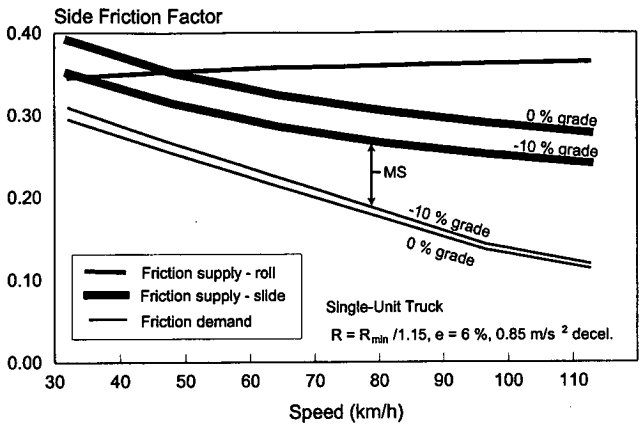

a. Speed reduction of 3 km/h.

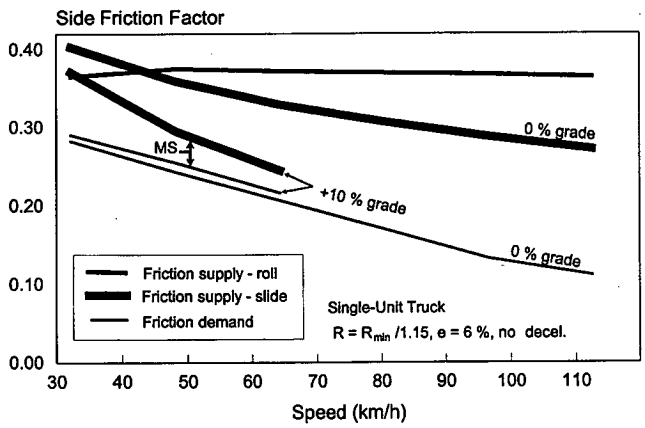

b. No speed reduction.

Figure 9. Effect of speed reduction on truck margin of safety against slide or roll failure.

The passenger car side friction supply shown in Figure 8 is based on the slide failure condition. The truck friction supply shown in Figure 9 is based on both the slide and the roll failure conditions. The roll failure friction supply for the passenger car is not shown in Figure 8 because it is significantly greater than that for slide failure. Hence, slide failure is the dominant failure mode for passenger cars on curves.

The trends in Figures 8 and 9 indicate that friction demand and supply (for slide failure) both decrease with increasing speed. This trend tends to yield a margin of safety that is relatively constant over the range of speeds. Also, the trends indicate that both up and downgrades yield an increase in side friction demand and a decrease side friction supply. *The result is a significant decrease in the margin of safety resulting from roadway grade.*

Examination of the trends in Figure 9 indicates that slide failure will occur before roll failure for trucks except on the slower speed curves. The friction supply for the 10 percent upgrade condition in Figure 9b does not extend beyond 65 km/h because the truck engine has insufficient power to maintain higher speeds on this grade.

A comparison of the trends shown in 8 and 9 indicates that *trucks are provided significantly less margin of safety than passenger cars on sharp curves.* This trend is partly due to a larger friction demand associated with trucks. This friction demand represents the largest demand in any one truck tire—an amount that can vary as a result of differences in tire properties, suspensions, and loading. Trucks are also associated with larger tractive and braking friction demands because of their greater weight.

Also shown in each figure are trend lines reflecting the level (no grade) condition. Comparison of these lines in Figures 8a and 8b (or 9a and 9b) indicates that deceleration as a result of braking reduces the side friction supply and is associated with an increase in the side friction demand. *Together, these changes result in a significant reduction in margin of safety as a result of braking* (about 17 percent and 35 percent for cars and trucks, respectively).

In summary, drivers tend to slow on sharp horizontal curves. When these curves are located on significant grades (up or down), both cars and trucks have a lower margin of safety than they would on a level roadway. Sharp curves on downgrades are of greater concern because (1) most drivers will be compelled to brake to maintain a safe speed and (2) most drivers are also likely to brake an added amount to reduce speed during curve entry. These two events combine to significantly reduce the margin of safety for most vehicles. Finally, the reduction in margin of safety because of grade, braking, or both tends to be more critical for trucks than cars because a significant portion of the friction supply is effectively used to slow (or propel) the heavier truck.

Effect of Lateral Shift on the Travel Path Radius

It has been observed by Emmerson (*13*) that vehicles shift laterally inward, relative to the traffic lane, while cornering. This shift results in the vehicle tracking a larger radius than that of the lane. The benefit of a larger radius is a corresponding reduction in side friction demand. Emmerson offered the following equation for computing the effective increase in curve radius as a result of a lateral shift within the lane:

$$dr = \frac{y_{max}}{1 - \cos(0.5\, I_c)} \qquad (3)$$

where:

dr = increase in lane radius, m;
y_{max} = maximum lateral shift of vehicle, m; and
I_c = curve deflection angle, rad.

Based on observation of several vehicles, Emmerson offered a value of 0.9 m for the lateral shift of most vehicles.

Examination of Equation 3 indicates that the value of *dr* increases rapidly with decreasing curve deflection angle. Typical values of *dr* are shown in Table 7. To illustrate the use of the values in this table, consider a two-lane highway curve with a radius of 1,000 m and a deflection angle of 10 degrees. A lateral shift of 0.9 m on this curve produces a travel path radius of 1,234 m (= 1,000 + 234). This increase in radius reduces the corresponding side friction demand by as much as 20 percent.

The data reported by Emmerson (*13*) were re-examined for this research and some additional analysis was conducted to determine the range of curve radii and deflection angles most affected by lateral shift. This analysis was conducted using Equations 2 and 3 and the curve speed model described in Appendix A. This model was used to compute curve speed as a function of radius. The effect of shift was examined in the context of the decrease in side friction demand resulting from an increase in path radius. The results of this analysis indicated that curves with a large radius or a large deflection angle were not associated with a significant reduction in friction demand as a result of lateral shift.

Further examination of the effect of lateral shift on side friction demand indicated that the effect of radius and angle could be combined using their product—curve length. This examination led to the generalization that curve lengths in excess of 140 m were not associated with a significant reduction in friction demand. Specifically, it was determined that the increase in radius associated with lateral shift on curves 140 m or more in length was not sufficient to produce more than a 0.02 decrease in side friction demand. The relationship between this limiting curve length, curve radius, and deflection angle is shown in Figure 10.

The trend lines shown in Figure 10 reflect the relationship between radius and deflection angle for specified curve lengths. Based on the previous discussion, combinations of deflection angle and radius that intersect above or to the right of the line corresponding to a length of 140 m will not be significantly affected by lateral shift. A survey of 3,304 horizontal curves on two-lane highways conducted by Glennon et al. (*14*) suggests that less than 25 percent of all curves have lengths shorter than 140 m. Hence, a large majority of curves are not likely to be affected by the lateral shift effect.

The *Green Book* (*1*, p. 224) recommends that curve length in meters should exceed three times the design speed in km/h (i.e., slightly more than 10 s travel time). Thus, a design speed of 30 km/h corresponds to a minimum curve length of 90 m. A curve length of 140 m is slightly shorter than the 150 m length associated with a 50 km/h design speed. These two

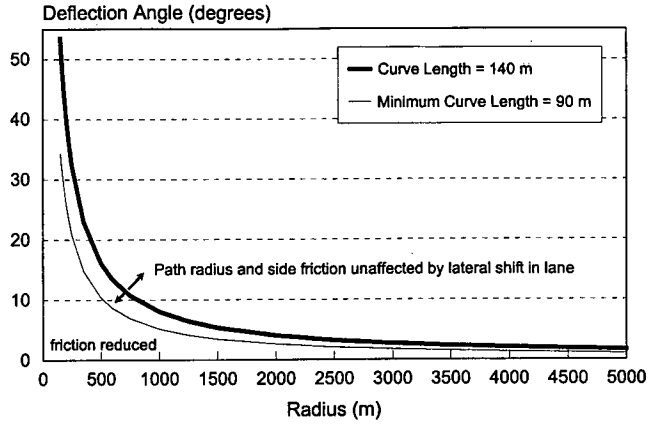

Figure 10. Radii and deflection angles that do and do not significantly affect side friction demand.

lengths are represented in Figure 10 by the two trend lines shown. Combinations of radius and deflection angle intersecting above or to the right of either line satisfies the minimum curve length control for the corresponding design speed. This finding, combined with that noted in the preceding paragraph, suggests that the beneficial effect of lateral shift would only be attained on curves with design speeds of 30, 40, or 50 km/h.

CONTROLS FOR SUPERELEVATION TRANSITION DESIGN

This section presents the findings from a critical review of the guidelines provided in the *Green Book* for designing the superelevation transition section. This section of roadway is located at the beginning and end of the horizontal curve and serves to transition the roadway from a normal crown section to a fully superelevated cross section. The guidelines for superelevation transition design are described primarily in Chapter III of the *Green Book* with some additional guidance provided in Chapters IX and X. The review of these guidelines includes a synthesis of *Green Book* guidance, a summary of state DOT practice, and a discussion of some problematic issues related to transition design.

Review of Superelevation Transition Design Controls

The superelevation transition section is composed of the superelevation runoff section and the tangent runout section.

TABLE 7 Increase in lane radius due to a lateral shift in lane position

	Curve Deflection Angle (degrees)											
Increase in Radius (m)	1	2	3	4	5	6	7	8	9	10	15	20
	23,634	5,907	2,624	1,475	943	654	480	367	290	234	103	57

The length of each of these components is individually calculated and combined to yield the minimum superelevation transition section length. The following equation quantifies this relationship:

$$L_{st} = L_r + L_t \quad (4)$$

where:

L_{st} = minimum length of superelevation transition, m;
L_r = minimum length of superelevation runoff, m; and
L_t = minimum length of tangent runout, m.

The purpose of the superelevation transition section is to provide a gradual transition between the normal cross slope on the tangent and the superelevated cross slope on the curve. The tangent runout section is used to rotate the cross section from a point where it has a normal cross slope to one where the adverse cross slope in the outside lane is removed. The superelevation runoff section is used to rotate the cross section from a point where adverse cross slope is removed to a point where the superelevation rate is fully attained.

This section describes the design controls and values that apply to superelevation transition design. This design component has several controls associated with it to reflect the many elements associated with its design. The controls applicable to superelevation transition design vary with functional classification, movement type, and design speed. The applicable design controls for this design element are listed in Table 8.

The discussion in the *Green Book* regarding the controls listed in Table 8 is not consistent among the three facility types. Specifically, the portion-of-runoff-prior-to-curve and the minimum-length-of-tangent-runout controls are not explicitly discussed for LS and TR facilities. These two controls are only discussed in sections of the *Green Book* that apply to RHS facilities. It is not clear whether this discussion also applies to LS and TR facilities.

For turning roadways, the *Green Book* (*1*, p. 729, 923) indicates many of the controls identified for RHS facilities are applicable to turning roadways. The *Green Book* discussion related to LS facilities offers no guidance in this regard.

Minimum Length of Superelevation Runoff

Three controls are recommended in the *Green Book* for computing the minimum length of superelevation runoff. They are coined the "gradient," "travel time," and "comfort" controls for the purposes of this report. The first two controls are used to define runoff length for RHS facilities. The comfort control is used for LS facilities. The gradient control is used for TR facilities.

The gradient control provides for a maximum grade differential between the axis of rotation and the edge of traveled way. The *Green Book* indicates that this control is intended to provide acceptable "appearance and comfort" (*1*, p. 177). The travel time control provides for a minimum 2.0 s travel time through the runoff section. The *Green Book* indicates that this control is considered for purposes of "general appearance and to avoid undesirably abrupt edge-of-pavement profiles" (*1*, p. 177). Finally, the comfort control provides for a maximum acceptable rate of change in centripetal acceleration during curve entry. The *Green Book* indicates that this control is intended to provide for "comfort and safety" (*1*, p. 175).

All Rural Highways and High-Speed Urban Streets. The following equation illustrates the *Green Book* guidance for computing the minimum superelevation runoff length for RHS facilities:

TABLE 8 Design controls for superelevation transition design

Descriptor	Control Type	No.	Name	Facility Type[1]	Basis
Class & Type		1	Functional Classification (urban..., rural...)	all	Specified
		2	Movement Type (through, turning)	all	Specified
Design Control	Basic	3	Design Speed	all	Specified
		4	Facility Type (RHS, LS, & TR)[1]	--	Based on 1, 2 & 3
		5	Maximum Design Side Friction Factor	LS	Based on 1, 2 & 3
	Element-Specific	6	Maximum Relative Gradient	RHS,TR	Based on 3
		7	Minimum Travel Time on Runoff Section	RHS	Specified
		8	Max. Rate of Change in Lateral Acceleration	LS	Based on 3
		9	Minimum Length of Superelevation Runoff	all	Based on 3 to 8
		10	Minimum Length of Tangent Runout	RHS, ?	Based on 6 & 9
		11	Portion of Runoff Prior to Curve	RHS, ?	Range provided

[1] RHS: All rural highways and high-speed urban streets; LS: Low-speed urban streets; TR: Turning roadways.

$$L_r = Larger\ of: \begin{cases} \dfrac{w\,e_d}{\Delta} n_l b_w \\ 2\dfrac{V_d}{3.6} \end{cases} \quad (5)$$

where:

L_r = minimum length of superelevation runoff, m;
Δ = maximum relative gradient, percent;
b_w = adjustment factor for number of lanes rotated (b_w equals 1.0, 0.80, 0.75 and 0.67 for n_l equal to 1.0, 1.5, 2.0, and 3.0, respectively);
w = width of one traffic lane (typically 3.6 m), m;
e_d = design superelevation rate, percent;
V_d = design speed, km/h; and
n_l = number of lanes rotated, lanes.

The *Green Book* authors note that direct application of the maximum relative gradient yields runoff lengths that, while desirable, may not be feasible in many instances. As a result, they allow for the reduction of runoff length based on an empirical adjustment. This adjustment is achieved through the use of b_w in Equation 5; however, it should be noted that the *Green Book* authors explicitly discuss the adjustment in terms of citing recommended values for the product "$n_l\ b_w$."

The runoff lengths for one and two lanes rotated are reported in the *Green Book*'s design superelevation tables (i.e., Tables III-7 through III-11). The lengths for the two-lanes-rotated case are larger than those reported in previous editions of the *Green Book* due to an apparent change regarding the travel time control. A closer examination of these lengths led to the conclusion that the length provided by the travel time control was adjusted for the number of lanes rotated (i.e., the resulting lengths were multiplied by $n_l\ b_w$). This change resulted in a significant increase in the minimum runoff length for the two-lanes-rotated cases when the travel time control dictated this length. Subsequent published errata for the 1994 *Green Book* confirm that this modification to the travel time control was in error and that Equation 5 yields the correct runoff length.

The runoff length obtained from Equation 5 can be used to determine the "effective" maximum relative gradient. This quantity represents the grade of the pavement edge slope relative to that of the axis of rotation. The effective gradient reflects the influence of the variable b_w and can be computed as:

$$\Delta^* = \frac{w\,e_d}{L_r} n_l \quad (6)$$

where:

Δ^* = effective maximum relative gradient, percent.

When the travel time control dictates runoff length, the effective gradient is smaller than the maximum gradient recommended in the *Green Book* (i.e., Table III-13). When the number of lanes rotated exceeds 1.0, the effective gradient is larger than the recommended value.

The maximum relative gradients and corresponding superelevation runoff lengths for one and two lanes rotated are shown in Table 9. Equation 5 was used with a 3.6-m

TABLE 9 Minimum superelevation runoff length for RHS facilities[1,2]

No. of Lanes Rotated	Superelevation Rate (%)	Design Speed (km/h)									
		30	40	50	60	70	80	90	100	110	120
		Maximum Relative Gradient (%)[3]									
		0.75	0.70	0.65	0.60	0.55	0.50	0.48	0.45	0.42	0.40
One Lane	2	17	22	28	33	39	44	50	56	61	67
	4	19	22	28	33	39	44	50	56	61	67
	6	29	31	33	36	39	44	50	56	61	67
	8	38	41	44	48	52	58	60	64	69	72
	10	48	51	55	60	65	72	75	80	86	90
	12	58	62	66	72	79	86	90	96	103	108
Two Lanes	2	17	22	28	33	39	44	50	56	61	67
	4	29	31	33	36	39	44	50	56	61	67
	6	43	46	50	54	59	65	68	72	77	81
	8	58	62	66	72	79	86	90	96	103	108
	10	72	77	83	90	98	108	113	120	129	135
	12	86	93	100	108	118	130	135	144	154	162

[1] Based on 3.6-m lanes.
[2] Underlined runout lengths result from the travel time control; others result from the gradient control.
[3] Values obtained from Table III-13 (*1*).

lane width to compute the lengths shown. The underlined values represent those lengths dictated by the travel time control; all other values are based on the maximum relative gradient.

The runoff lengths shown in Table 9 are in close agreement with those in the *Green Book*'s design superelevation tables (i.e., Tables III-7 through III-11). The lengths shown for one lane rotated also generally agree with *Green Book* Table III-14; however, those in Table III-14 have been rounded up to the nearest 5 m. As noted previously, the runoff lengths reported in the *Green Book*'s design superelevation tables for two lanes of rotation incorrectly include an adjustment for number-of-lanes-rotated in the travel time control and are not comparable with Table 9 in all cases.

Low-Speed Urban Streets. For LS facilities, the minimum runoff length is based on providing a comfortable rate of change in lateral acceleration through the transition section. This control assumes that a spiral path will be adopted by drivers as they travel through the superelevation transition section. The findings documented in Appendix D indicate that this assumption is reasonable. The following equation can be used to compute the minimum runoff length, as recommended by the *Green Book*, for LS facilities:

$$L_r = \frac{V_d \, g \, f_{d,\,\max}}{3.6 \, C_l} \tag{7}$$

where:

L_r = minimum length of superelevation runoff, m;
$f_{d,\,\max}$ = maximum design side friction factor;
g = gravitational acceleration (= 9.807 m/s^2); and
C_l = maximum rate of change in lateral acceleration, m/s^3.

There is no guidance in the *Green Book* regarding the use of a travel time control to compute runoff length for LS facilities. On the other hand, there is some guidance regarding adjustment of the length obtained from Equation 7 for the number of lanes rotated. Specifically, the *Green Book* authors state that the length obtained from Equation 7 is applicable when the pavement is rotated about the centerline and that this length should be doubled when the pavement is rotated about the inside edge of traveled way. This statement implies that the runoff length obtained from Equation 7 should be multiplied by the number of lanes rotated n_l.

The minimum runoff lengths based on Equation 7 are shown in Table 10. This table also shows the values recommended in the *Green Book* for C_l and for the maximum design side friction factor $f_{d,\,\max}$. Both of these factors were used to compute the runoff lengths shown in column 4.

Table 10 also provides the effective maximum relative gradient, as computed with Equation 6. Gradients are shown for superelevation rates of 4.0 and 6.0 percent. The gradients for 4.0 percent are smaller than recommended in *Green Book* (see Table 9) whereas those for 6.0 percent are larger than the recommended values. From this comparison, it would appear that both the gradient and comfort-based controls yield similar runoff lengths for superelevation rates of 4.0 to 6.0 percent. However, the comfort-based control maintains the same length for all superelevation rates whereas the gradient control would produce shorter runoff lengths for smaller superelevation rates.

Turning Roadways. The *Green Book* provides guidance for TR facilities in Chapters III, IX, and X. Chapters III and IX provide guidance for low-speed TR facilities at intersections. Chapter X provides guidance for low- and high-speed TR facilities at interchanges.

The discussion in Chapter IX indicates that the gradient control used for RHS facilities also applies to TR facilities. In fact, Table IX-13 lists recommended maximum relative gradients for use on intersection curves that are the same as those recommended for RHS facilities. This table is also referenced in Chapter X as applicable to interchange ramps. Thus, the gradient control component of Equation 5 would also appear

TABLE 10 Minimum superelevation runoff lengths for LS facilities

Design Speed (km/h)	C_l[1] (m/s^3)	Maximum Side Friction[1], $f_{d,\max}$	Runoff Length (m)	Effective Gradient (%)[2]	
				4.0%	6.0%
30	1.20	0.312	21	0.69	1.03
40	1.15	0.252	24	0.60	0.75
50	1.10	0.214	27	0.53	0.67
60	1.05	0.186	29	0.50	0.62
70	1.00	0.163	31	0.46	0.58

[1] Values obtained from *Green Book* (*1*) Table III-15.
[2] Based on one, 3.6-m lane rotated to the superelevation rate shown in the column heading.

to be appropriate for TR facilities. There is no recommendation in Chapters IX or X regarding the use of the travel time control to determine runoff length for TR facilities.

Discussion in the *Green Book* that is associated with Table IX-13 indicates that the gradients listed are to be achieved over *two* lanes of rotated pavement. For Equation 5, this condition would be the equivalent of setting the adjustment factor b_w to 1.0 (as opposed to 0.75) when n_l equals 2.0. Application of this guidance will result in the minimum runoff length for a turning roadway being larger than that used on a street or highway curve.

Runoff Lengths Used by Highway Agencies. A comprehensive examination of state DOT design procedures was conducted for this research. This examination explored the DOTs' interpretations of and extensions to the *Green Book* guidance. It consisted of a review of 27 state DOT design manuals, a survey of engineers with 35 state DOTs, and a review of guideline documents published by 6 foreign countries. One objective of this examination was to identify the methods used to define runoff length.

The examination of state DOT manuals for RHS facility design indicates that most states are using some variation of the *Green Book* guidance for computing runoff length. Based on this examination, it was concluded that 28 percent of the DOTs follow the *Green Book* guidance, as described by Equation 5. Notably, 21 percent of the DOTs do not use the travel time component of Equation 5. It is believed that this omission is intended to avoid long transition lengths at small superelevation rates and thereby improve pavement drainage (this point is discussed further in "Issues Related to Superelevation Transition Design"). Finally, the majority of DOTs considered (72 percent) were found to use values for b_w that are very similar to those recommended in the *Green Book*. Slight differences in maximum relative gradient appear to be the result of differences in the approach used to define gradients for equivalent metric design speeds.

The examination of guidelines developed by international agencies indicated that a combination of controls is being used in other countries to define runoff length. The gradient control was recommended by all agencies included in the review. Rate of pavement rotation, drainage, and spiral rate controls were also recommended by one or more agencies. In contrast, the travel time control was not recommended by five of the six agencies reviewed.

The examination of state DOT manuals that describe LS facility design indicated that more DOTs are using the gradient control (i.e., Equation 5) than are using the comfort control (i.e., Equation 7) to define runoff length. Of those DOTs that are basing runoff length on gradient, the recommended maximum relative gradients tend to vary widely; although, they typically fall within the range of values shown in columns 5 and 6 of Table 10. Most important, all of the methods used by the DOTs (i.e., gradient or comfort-based) yield about the same runoff lengths for superelevation rates between 4.0 and 6.0 percent. It should also be noted that only two of the DOT manuals reviewed explicitly recommended consideration of the travel time control for LS facilities.

The number-of-lanes-rotated adjustment factor b_w was also considered in the examination of state DOT guidelines. In general, the adjustment for multilane cross sections is typically described in these guidelines as a factor representing the product $n_l\, b_w$; this is also true for the *Green Book*. Typical values for this product are shown in Table 11.

Several state DOTs provided adjustment factors for combinations of rotated lanes that were different from those listed in Table 11. These factors appeared to be based on interpolation or extrapolation of the trends in column 2 of Table 11. However, one DOT (i.e., Washington) recognized the linear trend in column 2 and used it to develop an equation for computing the adjustment factor. This equation is effectively represented as follows:

$$n_l\, b_w = 1 + 0.5(n_l - 1) \tag{8}$$

Minimum Length of Tangent Runout

RHS and TR Facilities. The *Green Book* discussion of tangent runout length is included in the section of Chapter III dealing with RHS facilities. This design control is not provided its own subsection; rather, it is dealt with in two subsections within the section titled "Superelevation Runoff." It is likely that this discussion of runout length also applies to LS and TR facilities; however, there is no specific guidance in this regard in the *Green Book*. Moreover, it is recognized that many turning roadways never

TABLE 11 Adjustment factor for number of rotated lanes

Number of Lanes Rotated, n_l	Product of "$n_l\, b_w$"	Adjustment Factor, b_w
1	1.0	1.00
1.5	1.2	0.80
2	1.5	0.75
3	2.0	0.67

have a normal cross section from which to transition and, hence, the subject of runout length on turning roadways is often not relevant.

In one location in the *Green Book*, the guidance indicates that the minimum runout length should *desirably* have the same relative gradient as used for the superelevation runoff length. The exact statement is worded as follows:

"The length of tangent runout is determined by the amount of adverse cross slope to be removed and the rate at which it is removed. This rate of removal should preferably be the same as the rate used to effect the superelevation runoff." (*1*, p. 180)

The advantage cited for having a constant relative gradient through the transition section is a smooth edge of pavement profile.

The *Green Book* authors also recognize that maintaining a constant gradient through the transition section can have disadvantages. These disadvantages occur when the travel time control dictates runoff length. First, the resulting effective gradient can be undesirably small such that drainage along the roadway is inadequate. Second, the length of roadway within the transition section having negligible cross slope (and thus, inadequate lateral drainage) can be undesirably large.

In recognition of the aforementioned disadvantages associated with a constant gradient, the *Green Book* authors have offered some additional guidance regarding an *acceptable* minimum runout length. Its exact wording is as follows:

> "On the basis of the relative slopes previously established, the tangent runout distance on two-lane roads varies from about 10 to 15 m for the cross slope rate of 1.5 percent and where there are 3.6 m lanes. . . . These are the lengths for curves with maximum superelevation. Where there is less than maximum superelevation, tangent runout lengths will be longer if the same relative slope as that for superelevation runoff is retained. It is desirable that these relative slopes be retained but where this is not possible the runout lengths should be at least equal to those required for a curve with maximum superelevation where the same relative slopes for tangent runoff and runout are retained." (*1*, p. 183–184).

This guidance is interpreted to mean that the acceptable minimum tangent runout length should be based on the maximum relative gradient, as listed in Table III-13 (or Table 9). The desirable minimum runout length should be based on maintaining a constant gradient through the transition section. If this interpretation of the above quotation is correct, then the following equation would be appropriate for computing the minimum tangent runout length:

$$L_t \begin{cases} \dfrac{e_{NC}}{e_d} & : \textit{Desirable Min.} \\ \dfrac{w\, e_{NC}}{\Delta} n_l b_w & : \textit{Acceptable Min.} \end{cases} \qquad (9)$$

where:

L_t = minimum length of tangent runout, m; and
e_{NC} = normal cross slope, percent.

The desirable and acceptable minimum tangent runout lengths predicted by Equation 9 are shown in Table 12. As this table indicates, the acceptable minimum runout lengths are unaffected by the design superelevation rate and its corresponding runoff length. In contrast, the desirable minimum lengths always equal or exceed the acceptable minimum values. As noted previously, the desirable lengths will exceed the acceptable lengths when the travel time control dictates the runoff length (i.e., this typically occurs when the superelevation rate is small or the speed is high).

Runout Lengths Used by Highway Agencies. As noted previously, a comprehensive examination of state DOT design procedures was conducted for this research. This examination explored the DOTs' interpretations of and extensions to the *Green Book* guidance. One objective of this examination was to identify the method used to define minimum tangent runout length.

On the basis of this examination, it was found that the guidelines for runout length adopted by 84 percent of the state DOTs surveyed could be generalized using the following equation:

$$L_t = \frac{e_{NC}}{e_d} L_r \qquad (10)$$

This equation is equivalent to the "desirable minimum" component of Equation 9. It should be noted that an additional 8 percent of the state DOTs modified Equation 10 only slightly by substituting a constant value (between 1.0 and 2.0 percent) for the variable e_{NC}.

Portion of Runoff Prior to Curve

RHS and TR Facilities. The *Green Book* discussion regarding the location of the runoff is included in Chapter III in a section dealing with RHS facilities. This discussion is provided its own subsection within the section titled "Superelevation Runoff." As noted previously, this guidance is explicitly directed to RHS facilities; however, it is likely that this discussion also applies to LS and TR facilities (although, there is no specific instruction in this regard in the *Green Book*).

The *Green Book* discussion regarding runoff location indicates that this location is relative to the point of curvature (PC) or to the point of tangency (PT) for a given horizontal curve. The location of the runoff is established as the portion

TABLE 12 Desirable and acceptable minimum tangent runout lengths for RHS and TR facilities

Control Condition	Superelevation Rate (%)	Design Speed (km/h)									
		30	40	50	60	70	80	90	100	110	120
Runout Length for One Lane Rotated[1,2]											
Desirable Minimum	2	17	22	28	33	39	44	50	56	61	67
	4	10	11	14	17	19	22	25	28	31	33
	6	10	10	11	12	13	15	17	19	20	22
	8	10	10	11	12	13	14	15	16	17	18
	10	10	10	11	12	13	14	15	16	17	18
	12	10	10	11	12	13	14	15	16	17	18
Acceptable Min.	all	10	10	11	12	13	14	15	16	17	18
Runout Length for Two Lanes Rotated[1,2]											
Desirable Minimum	2	17	22	28	33	39	44	50	56	61	67
	4	14	15	17	18	20	22	25	28	31	33
	6	14	15	17	18	20	22	23	24	26	27
	8	14	15	17	18	20	22	23	24	26	27
	10	14	15	17	18	20	22	23	24	26	27
	12	14	15	17	18	20	22	23	24	26	27
Acceptable Min.	all	14	15	17	18	20	22	23	24	26	27

[1] Based on 3.6-m lanes and a normal cross slope of 2 percent.
[2] Underlined runout lengths result from the travel time control; others result from the gradient control.

of its length placed prior to the PC (or following the PT). It is implicit in this location reference that the tangent runout section be located on the roadway tangent, adjacent to the runoff section.

The *Green Book* guidance for the "portion" control indicates a range of values are acceptable. Specifically, the range offered is 0.5 to 1.0; although, the preferred range is indicated to be 0.6 to 0.8 (*1*, p. 181). The provision of some of the superelevation prior to the curve is advantageous because some superelevation would be available immediately upon curve entry and thereby, be available to offset the associated centripetal acceleration. The disadvantage of this provision is that drivers on the tangent may have to steer in a direction opposite to that of the impending curve to counter the increasing superelevation. Placing all (or none) of the superelevation transition before the curve magnifies the effect of the aforementioned advantage and disadvantage.

Portions Used by Highway Agencies. A comprehensive examination of state DOT design procedures was conducted for this research. This examination explored the DOTs' interpretations of and extensions to the *Green Book* guidance. One objective of this examination was to identify the recommended portion of runoff to be located prior to the curve. Based on this examination, it was concluded that about 80 percent of state DOTs recommend using one value of the portion control for all roadway curves. About 90 percent of the DOTs used a portion in the range of 0.6 to 0.7. It should be noted that only one DOT allowed for the possible placement of all of the runoff prior to the curve.

Issues Related to Superelevation Transition Design

Pavement Drainage

As mentioned previously, there is a potential for inadequate pavement drainage in the superelevation transition section. Specifically, two drainage problems can arise:

1. Inadequate longitudinal drainage because of negligible edge of pavement grade, and
2. Inadequate lateral drainage because of negligible cross slope.

The first drainage problem occurs when the grade of the axis of rotation is equal to the effective relative gradient but opposite in sign. These adverse combinations are found in the outside lane when the axis of rotation has a slight downgrade during curve entry or in the inside lane when there is a slight upgrade during curve entry. The reverse trend is applicable to curve exit. When the edge of pavement has negligible grade, surface water depth increases, which increases the potential for hydroplaning. On curbed streets, this problem may be particularly acute as some longitudinal grade is necessary for water to reach the curb inlet. This drainage problem can be avoided by maintaining a minimum grade for both the centerline and the edge of pavement in the transition section.

The second drainage problem is found in that portion of the transition section where the cross slope is negligible. This

problematic segment begins at the start of the transition (where the cross section has a normal crown) and ends at the point where the roadway is superelevated at a rate equal to the normal cross slope. This segment includes the tangent runout section and an equal length of superelevation runoff. Within this segment, the pavement cross slope may not be steep enough to promote adequate lateral drainage. This problem cannot be eliminated; however, it can be minimized by either reducing the length of roadway affected (e.g., by increasing the relative gradient) or by maintaining a minimum centerline grade in the transition section.

Both of the aforementioned problems can create unsafe operating conditions during periods of intense rainfall. They create a short section of roadway where the lateral and longitudinal grades may not be adequate for drainage purposes. The problem is most likely to occur when the centerline grade is relatively flat (i.e., less than 1.0 percent). More important, the magnitude of the problem and its longitudinal extent are increased when the travel time control dictates runoff length. As noted previously, this control increases runoff length (relative to that obtained using the gradient control) which decreases the edge of pavement grade.

Guidelines published by governmental highway agencies in Germany, Sweden, and the U.K. also offer insight on potential solutions to transition-related drainage problems. To minimize drainage problems in the transition, the German highway design guideline (*5*) includes a recommendation that the grade of the pavement edge equal or exceed 0.5 percent; this value is reduced to an acceptable minimum of 0.2 percent for roadways without curbs. In addition, the German guideline includes a recommendation that the centerline grade equal or exceed 0.7 percent (1.0 percent desirably) in the transition section. Similarly, guidelines prepared by the Swedish (*6*) and U.K. (*7*) highway agencies recommend a minimum centerline grade of 0.5 percent in the transition section. It should also be noted that none of these agencies recommend the use of a travel time control to define transition length.

Transition-Control-Related Research

Location of Runoff Prior to the Curve. Several researchers (*14*, *15*) have used simulation studies to evaluate the effect of runoff location on the lateral acceleration experienced by the vehicle. Glennon et al. (*14*) investigated passenger car performance in transitions designed to have 20 and 70 percent of the runoff length located on the tangent section. Their simulation evaluated these two percentages using a range of speeds and superelevation rates. Based on their simulation results, they concluded that 70 percent was associated with better operating conditions (e.g., lower peak side friction demands) than 20 percent.

Blue et al. (*15*) focused their simulation study on trucks. Specifically, they investigated placing two-thirds and all (i.e., 67 and 100 percent) of the runoff on the tangent. Based on this investigation, they found that the design with two-thirds of the runoff length on the tangent resulted in significantly lower lateral accelerations to large trucks than that with all of the length on the tangent. Taken together, the findings of Glennon et al. (*14*) and Blue et al. (*15*) support the range of portions recommended in the *Green Book* (i.e., 0.6 through 0.8). It should be noted that "portion" and "percentage" are used interchangeably in this report; percentage being equal to portion after multiplication by 100. Hence, the portion 0.6 has the same meaning as 60 percent.

Adjustment for Number of Lanes Rotated. Another simulation study was conducted by Good (*16*). He investigated the relationship between transition length and vehicle steering stability. This stability was defined in terms of the magnitude of steer corrections required to negotiate the transition relative to the "ideal" steer response (i.e., one that is compatible with the roadway curvature).

For his investigation, Good (*16*) examined several variables used to define transition length. One of the variables investigated was rotated pavement width ($= w\ n_l\ b_w$). His investigation was based on simulation of vehicles traveling through transition sections with one and with three lanes rotated. The results of this investigation indicated that the magnitude and frequency of steer corrections increased with transition length. The reported results also indicate that the values of b_w listed in Table 11 limit the magnitude of steer angle corrections to acceptable levels (as defined by Good). This result provides some justification for these adjustment factors and suggests that the corresponding runoff lengths should be recognized as *design values* as opposed to minimums.

Pavement Edge Profile. Good (*16*) also investigated the length of vertical curve used at the breaks in grade at the start and end of the superelevation transition section. The 1990 edition of the *Green Book* indicated that the length of this vertical curve should be equal (in feet) to the numeric value of the design speed (in mph) (*17*, p. 184). This translates to 0.68 s travel time at the design speed. The research findings of Good (*16*) confirm the desirability of this guidance. It should be noted that the 1994 *Green Book* incorrectly recommends that the vertical curve length (in meters) be equal to the numeric value of the design speed (in km/h) (*1*, p. 185). This relationship translates into 3.6 s travel time which is much longer than the 0.68 s recommended in previous editions of the *Green Book*.

The minimum edge-of-pavement vertical curve length recommended in the *Green Book* indirectly bears on the minimum length of the superelevation transition section. As noted previously, the *Green Book* authors indicate that 2.0 s travel time in the runoff L_r is needed to avoid "abrupt" pavement edge profiles. However, the guidance regarding edge-of-pavement profile suggests that a transition length ($= L_r + L_t$) need only equal 0.68 s to provide a smooth transition.

Maximum Relative Gradient

As noted previously, the values of maximum relative gradient differ slightly between the 1990 and 1994 editions of the *Green Book*. This difference is most significant for the lowest and highest speeds. It is likely a result of the metric conversion for the 1994 edition rather than an intentional change in the magnitude of the control. The differences are shown in Figure 11.

As shown in Figure 11, the gradients in the 1994 *Green Book* tend to have a reduced sensitivity to speed (i.e., flatter slope) and a more significant "break" in slope at 80 km/h when compared to the gradients in the 1990 *Green Book*. When expressed as a percentage change, the differences are most significant for the higher design speeds. In fact, for speeds in excess of 80 km/h, the runoff lengths obtained using the gradients recommended in the 1994 *Green Book* tend to be about 5.0 percent shorter than those obtained from previous editions of this document.

Lateral Motion in the Superelevation Transition Section

A kinematic analysis of the lateral accelerations acting on a vehicle traveling through a tangent-to-curve transition section was conducted for this research. The results of this analysis indicated that all vehicles shift laterally in the transition section and that the magnitude of shift is influenced by the transition design. It was also noted that a non-zero lateral velocity at the end of the transition section could adversely affect side friction demand and steering stability. Additional details of this analysis are provided in Appendix D.

The relationship between transition design and a vehicle's lateral motion at the end of the transition was examined for this research. The objective of this examination was to define transition design controls that minimize lateral motion. Equations for estimating lateral velocity and shift are described in Appendix D. Equations 16 and 18 in this appendix were used to examine the relationship between runoff length, speed, steering time, and portion-of-runoff-prior-to-the-curve. The results of this examination are described in the remainder of this section.

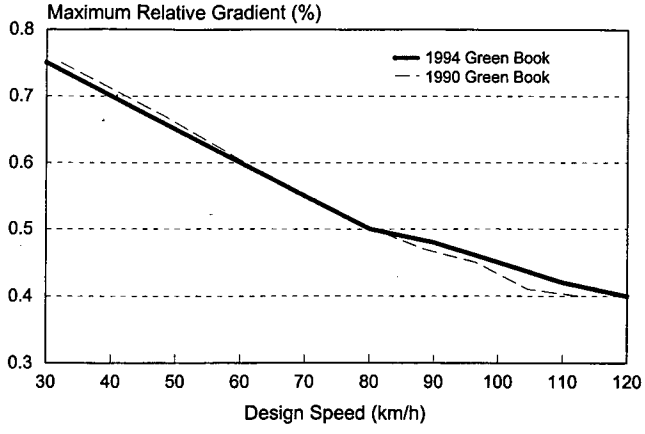

Figure 11. Comparison of maximum relative gradients recommended in the 1990 and 1994 Green Books.

Evaluation Criteria

As an overall goal, transition design elements should be sized such that a vehicle's lateral velocity and shift as it exits the transition section should be as small as possible. Recognizing that this goal may not always be achievable for both travel directions, three evaluation criteria were established to define maximum deviations from the overall goal:

1. Lateral velocity v_l should not exceed a rate equivalent to 0.3 m/s.
2. Lateral velocity should not be in an outward direction (relative to the curve).
3. Lateral shift y_l should not exceed 1.0 m.

With regard to Criterion 1, Equation 16 in Appendix D was derived to predict lateral velocity in units of "meters shift per meter of forward progress." A more intuitive representation of this velocity can be attained by multiplying v_l by the vehicle's speed v, which yields units of "meters shift per second." As indicated in Criterion 1, the velocity obtained from this product should not exceed 0.3 m of shift per second.

The findings documented in Appendix D on the direction of lateral velocity (or drift) provide the motivation for Criterion 2. It is argued that an outward drift during curve entry would require the driver to make a steering adjustment that would produce a path radius sharper than that of the roadway (i.e., a critical path radius). The negative aspect of this adjustment is that it produces a significant, momentary increase in side friction demand. It should be noted that the "outward" direction is defined to coincide with a positive lateral velocity for the left-hand (or outside) curve direction and a negative lateral velocity for the right-hand (or inside) curve direction.

Criterion 3 listed above minimizes the potential for encroachment into adjacent lanes. Equation 18 of Appendix D was used for this evaluation. The value of 1.0 m was established as an upper limit for the amount of shift based on the conservative assumption that the vehicle is located in the middle of the lane prior to entering the transition section.

Superelevation Rates Associated with Excessive Lateral Shift

A sensitivity analysis was conducted using Equation 18 (of Appendix D) to determine which design variables had the greatest influence on lateral shift. Variables considered included speed, superelevation rate, portion-of-runoff-prior-to-the-curve, number-of-lanes-rotated, and radius. In order to minimize the number of variables, the mathematical

relationship among superelevation rate, curve radius, and speed implied by the superelevation distribution method was used to eliminate radius. Specifically, it was determined that radius would be computed from the superelevation rate and 95th percentile speed. The distribution method used is that recommended in Chapter 3, which is consistent with *Green Book* Method 5.

Based on this analysis, it was found that speed and superelevation rate had a significant effect on lateral shift. In contrast, number-of-lanes-rotated and portion-of-runoff-prior-to-the-curve in the range of 0.5 to 1.0 had negligible effect. In general, lateral shift increased with increasing superelevation rate and with decreasing speed. In fact, it was found that a limiting superelevation rate existed for each speed. In general, rates in excess of the limiting rate were associated with lateral shifts of 1.0 m or more and an undesirable outward lateral velocity. These limiting superelevation rates are shown in Figure 12.

Both the 5th and 95th percentile speeds were considered in the analysis of lateral shift. These speeds were obtained from Table B-6 of Appendix B. Based on a consideration of both percentile speeds, the 95th percentile speed was used to define the limiting superelevation rates shown in Figure 12. The 95th percentile speed was selected over the 5th percentile speed because larger shifts were predicted by Equation 18 (of Appendix D) for higher speeds. Thus, the 95th percentile speed is recommended as the appropriate speed to use in defining limiting superelevation rates because slower speeds would be associated with less lateral shift.

Portion of Runoff Prior to Curve

Optimum Portion for One Travel Direction. Both components of Equation 16 (of Appendix D) were examined to determine the relationship between runoff length, speed, steering time, portion-of-runoff-prior-to-the-curve, and lateral velocity. Specifically, these components were algebraically manipulated to define a portion that would yield a lateral velocity of 0.0 m/s. The resulting equations are as follows:

$$P_{r,0}\begin{cases} 1-\dfrac{0.5t_s v}{L_r} & :P_{r,0} > \dfrac{0.5t_s v + L_t}{L_r} \\ \dfrac{L_r + L_t}{2L_r} & :P_{r,0} \le \dfrac{0.5t_s v + L_t}{L_r} \end{cases} \quad (11)$$

where:

$P_{r,0}$ = portion of superelevation runoff located prior to the curve that yields zero lateral velocity;
L_r = minimum length of superelevation runoff, m;
L_t = minimum length of tangent runout (negative for left-hand curves), m;
t_s = steering time (= 2.8 s), s; and
v = vehicle speed, m/s.

The two components of Equation 11 are necessary because the driver's steering and the superelevation development are modeled to occur independently along the transition. In this regard, the first equation is appropriate when the steer is initiated after the superelevation rotation begins. In contrast, the second equation applies when the steer is initiated prior to the point where superelevation rotation begins. It should be noted that the variable for tangent runout length is represented as a negative quantity when Equation 11 is applied to left-hand (or outside) curves.

Consideration of Both Travel Directions. Some generalization is possible regarding the two components of Equation 11. Specifically, the first component always applies to the left-hand (or outside) travel direction for typical values of P_r, L_t, and L_r. On the other hand, either component can be applicable to the right-hand (or inside) travel direction. The first component applies to right-hand curves with larger superelevation rates while the second component applies to right-hand curves with smaller superelevation rates.

Ideally, the portion of runoff located prior to the curve would be determined such that the lateral velocity is zero for both travel directions. Unfortunately, when each travel direction is considered separately, the value of $P_{r,0}$ appropriate for one direction does not always equal that for the other direction. From this finding, it is concluded that zero lateral velocity in both directions is not always attainable for a common value of $P_{r,0}$. As a result, it was determined that a compromise value of $P_{r,0}$ would be needed that minimized the combined lateral velocity for both curve directions.

Further analysis was conducted to determine the one value of $P_{r,0}$ that minimized the combined lateral velocity for both directions. The results of this analysis revealed there were two cases to consider: (1) when the first component of Equation 11 applies to both directions and (2) when the first component applies to the outside curve direction and the second compo-

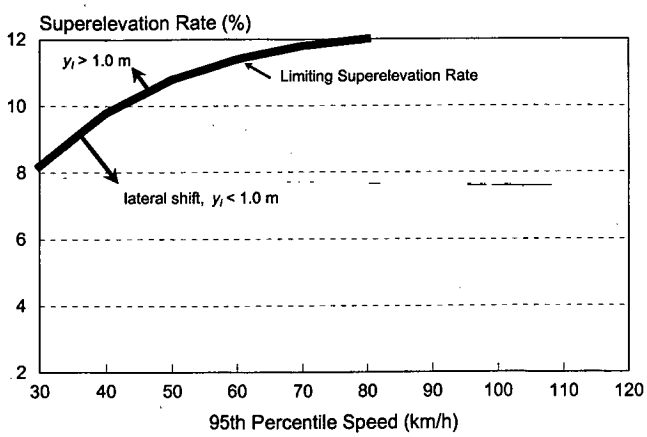

Figure 12. Superelevation rates associated with 1.0 m of lateral shift.

nent applies to the inside curve direction. Case 1 typically occurs for larger superelevation rates, Case 2 for lower rates. Application of Equation 11 for both cases revealed that Case 1 occurs when $P_{r,0}$ from the first component of Equation 11 is larger than $P_{r,0}$ obtained from the second component.

As the first component of Equation 11 applies to both curve directions for Case 1, it can be used to predict a value of $P_{r,0}$ that yields zero lateral velocity in both directions. Unfortunately, this result cannot be obtained for Case 2. Further analysis for Case 2 indicated that the minimum combined lateral velocity occurred when the lateral velocity for the inside direction is zero. This condition was always found to produce a small, negative velocity for the outside direction. The negative value of velocity was deemed acceptable because it implies an inward drift direction (i.e., it satisfies Criterion 2). Similarly, the magnitude of lateral velocity was found to be less than 0.3 m/s (i.e., it satisfies Criterion 1). Based on this analysis, it was determined that the second component of Equation 11 should be used to define $P_{r,0}$ for Case 2.

Defining Percentile Speed. A sensitivity analysis was conducted to determine if the 5th or 95th percentile speed represented the controlling condition for defining $P_{r,0}$. $P_{r,0}$ was computed for a wide range of 95th percentile speeds (i.e., $30 < V_{95} < 120$ km/h), superelevation rates, and rotated lanes. For each combination, $P_{r,0}$ was computed for the 95th percentile speed and then this value of $P_{r,0}$ was used to compute lateral velocity for both the 5th and 95th percentile speeds. This pattern was repeated for a $P_{r,0}$ computed for the 5th percentile speed. The trends shown in Figure 13 are fairly typical for the 95th percentile speeds considered; however, the absolute value of lateral velocity tended to decrease for 95th percentile speeds greater than 30 km/h.

Only the lateral velocity for the "worst-case" combination of speed and $P_{r,0}$ percentiles are shown in Figure 13. That is, if $P_{r,0}$ was defined using the 5th percentile, then it was evaluated for its effect on vehicles traveling at the 95th percentile speed because this group of vehicles does not have a $P_{r,0}$ "optimized" for their speed. The lateral velocity corresponded to the defining percentile speed (e.g., v_l for the 95th percentile speed when $P_{r,0}$ was based on the 95th percentile speed) is not shown in Figure 13 because it is, by definition, optimized to be zero in the inside direction and either zero or small-and-inward for the outside direction. Based on this analysis, it was found that basing the value of $P_{r,0}$ on the 5th percentile speed yielded the best operating conditions (i.e., in terms of Criteria 1 and 2) for the distribution of speeds.

Sensitivity Analysis. To illustrate the relationship between $P_{r,0}$ and superelevation rate, Equations 5 and 10 were combined with Equation 11 to produce the following equation:

$$P_r = Larger\ of: \begin{cases} 1 - \dfrac{t_s v_{c,5} \Delta}{2 e_d w n_l b_w} & : Case\,1 \\ 0.5\left(1 + \dfrac{e_{NC}}{e_d}\right) & : Case\,2 \end{cases} \qquad (12)$$

where:

P_r = portion of superelevation runoff located prior to the curve; and
$v_{c,5}$ = 5th percentile curve speed, m/s.

The relationship between the 95th and 5th percentile speeds is defined in Table B-6 of Appendix B. The subscript "0" in the variable $P_{r,0}$ is deleted in Equation 12 to recognize that zero velocity cannot be guaranteed for both travel directions in both cases (i.e., not in Case 2).

Trend lines corresponding to the two components of Equation 12 are shown in Figure 14. The first component is represented by the thin lines; the second component is represented by the thick line. As discussed in the section titled "Consideration of Both Travel Directions," the larger value

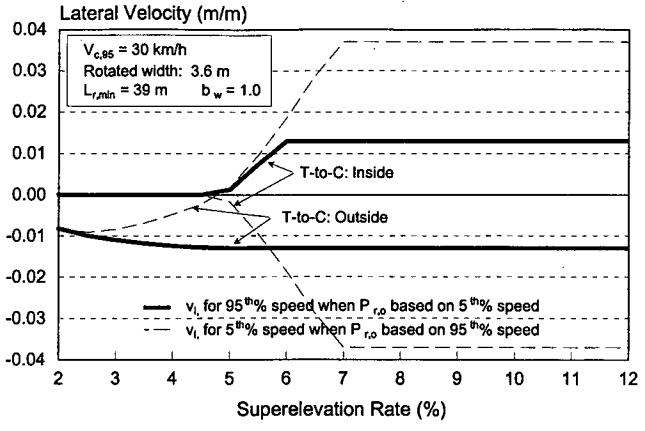

Figure 13. Effect of alternative definitions of $P_{r,0}$ on lateral velocity.

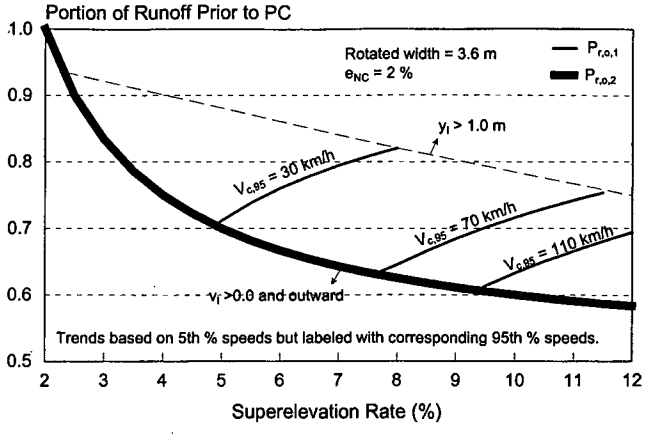

Figure 14. Effect of superelevation rate on P_r.

of P_r obtained from the two components of Equation 12 dictates the applicable case condition (i.e., Case 1 or 2). This larger value was also found to provide the best, or "optimum," operating conditions in terms of Criteria 1 and 2.

Figure 14 also includes some indication of the consequences of deviating from the optimal value of P_r. Values of P_r falling below the thick trend line should be avoided because they are likely to be associated with excessively large outward lateral velocities. Similarly, values of P_r falling above the dashed line should be avoided because the resulting lateral shift would likely exceed 1.0 m for faster drivers. This dashed line corresponds to the limiting superelevation rates described previously for Figure 12.

Figure 14 indicates that the optimum value for P_r is 0.67 when the 95th percentile speed is 70 km/h and the superelevation rate is 6 percent (this observation is consistent with the finding reported in Appendix D for Figure D-23). Alternatively, when the superelevation rate is 11.8 percent, the optimum value of P_r is 0.76. This example (and Figure 14 in general) indicates that the optimum value of P_r is moderately sensitive to superelevation rate. Unfortunately, recognition of this sensitivity in the portion-of-runoff-prior-to-the-curve control would overly complicate curve design by requiring the selection of a unique value of P_r for each curve. It is recognized that one value of P_r that provides acceptable operation for the full range of superelevation rates would be most desirable from a design perspective. The development of this compromise value of P_r is described in the next few paragraphs.

Desirable Values of the Portion Control. Based on the preceding paragraph, it was determined that a compromise value of P_r could be derived for each 95th percentile speed. This one value would yield acceptable operating conditions for the range of available superelevation rates. The compromise value was obtained by solving for the value of P_r at the intersection of the thin and dashed lines in Figure 14. This intersection point was computed using the limiting superelevation rates shown in Figure 12 and the first component of Equation 12. The values of P_r that result from this computation are listed in Table 13.

The values of P_r listed in Table 13 represent a single compromise value for a given 95th percentile speed. Theoretically, better values could be obtained for each speed and superelevation rate combination using Equation 12; however, such precision is not likely justifiable given the assumptions made to develop the underlying lateral motion model. The values listed in the table should minimize lateral velocity, prevent outward velocities (and associated critical radii), and prevent excessive lateral shifts. Moreover, they should provide these desirable characteristics for a wide distribution of speeds (i.e., 5th percentile and above) and superelevation rates (i.e., 2 to 12 percent) for both travel directions through the transition.

The values of P_r listed in Table 13 generally fall within the range recommended in the *Green Book* (i.e., 0.6 to 0.8). However, they tend to be on the high side of this range. Additional analysis indicates that slightly smaller values of P_r (i.e., those in the range of 0.6 to 0.7) will adequately serve drivers traveling at higher speeds but may increase the likelihood of an adverse outward lateral velocity for slower drivers. As mentioned previously, the values listed in Table 13 serve both fast and slow drivers. It should be noted that the maximum relative gradients shown in Table 13 are taken from Table III-13 in the 1994 *Green Book*, with the exception of those for speeds between 90 and 120 km/h. Gradients for speeds in this range were derived from the data in Table III-14 in the 1990 *Green Book* (*17*) because of an apparent inconsistency in the metrication in the 1994 *Green Book*.

TABLE 13 Portion of runoff located prior to the curve that minimizes lateral velocity and shift[1]

95th % Curve Speed (km/h)	5th % Curve Speed[2] (km/h)	Limiting Superelevation Rate (%)	Max. Relative Gradient[3] (%)	Portion of Runoff Before PC, P_r
30	17.8	8.2	0.75	0.82
40	24.9	9.8	0.70	0.81
50	32.3	10.8	0.65	0.79
60	39.9	11.4	0.60	0.77
70	47.8	11.8	0.55	0.76
80	55.8	12.0	0.50	0.75
90	64.1	12.0	0.47	0.73
100	72.5	12.0	0.44	0.71
110	81.0	12.0	0.41	0.70
120	89.6	12.0	0.38	0.69

[1] Based on one 3.6-m lane rotated.
[2] 5th percentile speeds obtained from Table B-6 of Appendix B.
[3] Maximum relative gradients for speeds between 90 and 120 km/h are based on the relationship between speed and gradient described in the 1990 *Green Book* (*17*).

CONTROLS FOR ALIGNMENT TRANSITION DESIGN

This section presents the findings from a critical review of the guidelines provided in the *Green Book* for designing the alignment transition section. An alignment transition section consists of a spiral curve or a series of compound curves that transition the roadway from the tangent to the horizontal curve. The guidelines for alignment transition design are described primarily in Chapters III and IX of the *Green Book*. The review of these guidelines includes a synthesis of *Green Book* guidance, a summary of state DOT practice, and a discussion of some problematic design issues related to transition design.

Review of Alignment Transition Design Controls

This section describes the design controls and values that apply to alignment transition design. This design component has several controls reflecting the many elements associated with its design. The controls applicable to alignment transition design vary with functional classification, movement type, design speed, and transition type. For transition type, the controls are specific to the two types of curves used in the alignment transition section (i.e., the spiral curve and the compound curve). The applicable design controls for the alignment transition are listed in Table 14.

The compound curve as a transition design element is generally described in the *Green Book* as applicable to TR facilities. The last three controls listed in Table 14 are described in sections dedicated to turning roadways in *Green Book* Chapters III and IX.

To facilitate discussion of the alignment transition design controls, the term "tangent-to-curve" transition design is used herein to refer to the situation where compound or spiral curvature is *not* used in the transition. Thus, in the tangent-to-curve design, the tangent section of the alignment intersects directly with the horizontal curve. There are no horizontal alignment-related controls associated with this design because there is no transition curve.

It should be recognized that the *Green Book* does *not* recommend or require the use of a compound or spiral curve in the alignment transition section of a horizontal curve on any facility type. However, it does encourage the use of spirals on TR facilities and it lists their advantages in the section dealing with RHS facilities. As a result, the decision to use a transition curve is left to the discretion of the design engineer, as directed by the design standards of the agency for which he or she works.

The *Green Book*'s treatment of transition design controls varies by the type of facility. The spiral curve is discussed in the context of both the RHS and low-speed TR facilities. The compound curve is addressed only in the context of both low- and high-speed TR facilities. Neither type of transition curve is described for LS facilities. The tangent-to-curve design is assumed (by lack of comment to the contrary) to be applicable to all three facility types.

A survey of state DOTs that was conducted for this research indicated that only 5 of 37 (14 percent) responding states use compound curves in transition areas. Of these five state DOTs, representatives of most indicated that the spiral curve was generally preferred for transition design because it more closely follows the natural path of the driver. Based on this preference, the remainder of this section focuses on design guidelines and controls for the spiral curve transition.

Spiral Curve Transition Guidance

Green Book Guidance. The *Green Book* does not explicitly define the conditions where a spiral curve transition would be most helpful or when to use a spiral curve instead of the tangent-to-curve design. However, the *Green Book*

TABLE 14 Design controls for alignment transition design

Descriptor	Control Type	No.	Name	Application[2]	Basis
Class & Type		1	Functional Classification (urban..., rural...)	both	Specified
		2	Movement Type (through, turning)	both	Specified
Design Control	Basic	3	Design Speed	both	Specified
		4	Facility Type (RHS, LS, & TR)[1]	both	Based on 1, 2 & 3
	Element-Specific	5	Max. Rate of Change in Lateral Acceleration	spiral	Based on 3
		6	Minimum Length of Spiral	spiral	Based on 3 to 5
		7	Maximum Ratio of Larger to Smaller Radius	comp.	Based on 1 & 3
		8	Maximum Deceleration Rate on Compound Curve	comp.	Specified
		9	Minimum Length of Circular Arc	comp.	Based on 1, 2 & 3

[1] RHS: All rural highways and high-speed urban streets; LS: Low-speed urban streets; TR: Turning roadways.
[2] "spiral": spiral curve transition; "comp." compound curve transition; "both": spiral and compound curve transitions.

does suggest that spirals may be appropriate for curves on RHS facilities that have a combination of "high speeds and sharp radii." The *Green Book* does discuss the use of spiral curves at the terminal portions of TR facilities and provides relatively detailed guidance on the design of these curves. No discussion is provided regarding the use of spiral curves on LS facilities; although it is noted that an equation from the "family" of spiral length equations is recommended for computing the minimum superelevation runoff length.

Spiral Guidance Used by Highway Agencies. A survey of state DOT design procedures was conducted to explore the DOT interpretations of and extensions to the *Green Book* guidance. This examination consisted of a review of 27 state DOT design manuals, a survey of engineers with 35 state DOTs, and a review of guideline documents published by 6 foreign countries. One objective of this examination was to identify the conditions where one or more agencies believe that a spiral curve transition is warranted.

Of the 27 state DOTs for which design manuals were obtained, 25 provided sufficient information on the topic of horizontal curve design to assess their policy on the use of spirals. A review of this information indicated that about 48 percent of the state DOTs (12 of 25) surveyed have a policy regarding the use of spirals. However, a closer examination of the guidance provided in the design manuals indicates that only about 28 percent of the DOTs (7 of 25) *require* spiral curves and then only for specific conditions. These conditions generally relate to the type of facility, its design speed, the curve superelevation rate, or its radius. Manuals for the remaining 20 percent of DOTs (5 of 25) that use spirals indicate that spirals are desirable but not required.

The state DOTs that provide guidance on when a spiral curve transition is appropriate typically do so by using one or two of the following controls: maximum radius, minimum superelevation rate, minimum design speed, minimum average daily traffic (ADT), and minimum spiral "throw" distance (i.e., circular curve offset). In addition to different combinations of these controls, the DOTs have identified a wide range of criteria for each control. Those controls that are related to speed and radius are shown in Figure 15.

Also shown in Figure 15 is the guidance provided in the 1984 *Green Book* (*8*). This guidance was initially provided in the 1954 AASHTO design policy for rural highways (*9*). The authors of the 1954 policy determined that the maximum radius for use of spirals should correspond to those curves having a design superelevation rate of 3 percent (based on distribution Method 5). The specific guidance provided in these tables in the 1954 through 1973 *Policies* was "Spirals [are] desirable but not as essential above [the] heavy line" (i.e., "above" meaning superelevation rates less than 3 percent). This guidance was changed in the 1984 *Green Book* to "Spirals [are] seldom used above the heavy line." As Figure 15 indicates, two state DOTs continue to use this guidance.

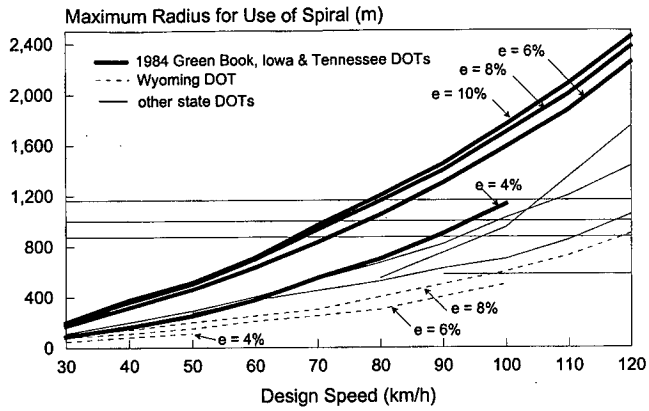

Figure 15. Comparison of maximum radii for use of spiral as defined by various agencies.

Based on the trends in Figure 15, it appears that there is little consensus among the state DOTs on the speed and radius combinations that would benefit from the use of spiral curve transitions. A review of international guidance in this regard also indicated a general lack of consensus on conditions justifying or amenable to the use of spiral curves in the transition section.

Minimum Spiral Length

All Rural Highways and High-Speed Urban Streets. The *Green Book* authors encourage the use of spiral curve transitions in recognition of their ability to provide a smooth transition between the tangent and circular curve portions of the horizontal alignment. The spiral curve transition is believed to introduce the lateral acceleration experienced by motorists in a gradual, constantly increasing manner up to that amount ultimately produced by the circular curve.

The length of spiral is based on one of two approaches. One approach is to have its length equated to that needed for the superelevation runoff. The other approach is to make the spiral sufficiently long to maintain a "comfortable" rate of change in lateral acceleration. Because the former approach yields a longer minimum length, the *Green Book* authors recommend that it be used to define the minimum spiral length. Hence, Equation 5 is used to compute the minimum spiral length as well as the minimum runoff length.

Low-Speed Urban Streets. The *Green Book* authors do not discuss alignment transition design for LS facilities. However, the equation provided for determining minimum runoff length (i.e., Equation 7) is used by some international agencies to compute spiral curve transition length. The use of this equation implies that minimum spiral length and minimum runoff length should be equal, which is consistent with the guidance provided for RHS facilities.

Turning Roadways. Based on a review of guidance in *Green Book* Chapters III and IX, it appears that the *Green Book* authors recommend the use of either spiral or compound curvature for turning roadways. With regard to the minimum spiral curve transition length, the following equation is recommended:

$$L_{s,\min} = 0.0214 \frac{V_d^3}{R C} \quad (13)$$

where:

$L_{s,\min}$ = minimum length of spiral, m;
V_d = design speed, km/h;
C = maximum rate of change in centripetal acceleration, m/s^3.

The *Green Book* authors provide (in Table III-17) recommended maximum values for C and minimum values for R, because they apply to low-speed turning roadways. They use these values (in Equation 13) to define a *minimum* spiral length for each design speed; these minimums are listed in Table 15. They recognize the ambiguity of having a "minimum" length defined by a "minimum" radius and note that these are minimum spiral lengths for use with the minimum radius and that "somewhat lesser lengths are suitable for above-minimum radii" (*1*, p. 198).

Figure 16 compares the minimum length of spiral curve transition recommended by the *Green Book* for RHS and low-speed TR facilities. In general, these lengths are similar in magnitude and increase with increasing design speed. The use of trend lines for RHS facilities versus data points for TR facilities is a reminder of the differences in design flexibility permitted for each facility type as related to design speed, radius, and superelevation rate.

Spiral Lengths Used by Highway Agencies. A survey of state DOT design procedures and a review of international agency guidelines was conducted for this research. One objective of this examination was to identify the guidance offered with regard to the minimum length of spiral curve transition.

A review of the design manuals provided by the state DOTs indicated that the *Green Book* guidance on spiral

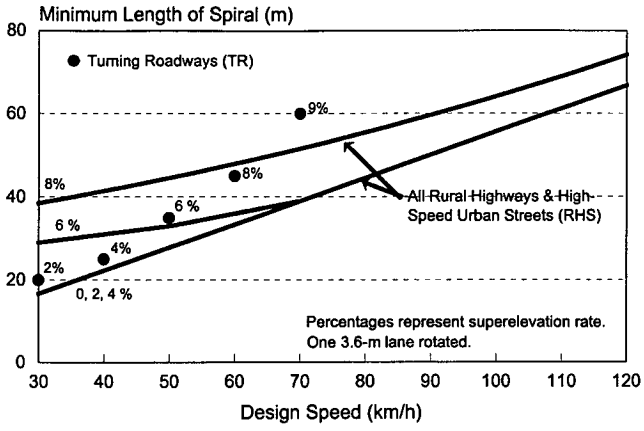

Figure 16. Comparison of minimum lengths of spirals for TR and RHS facility types.

length is consistently followed by each DOT. Specifically, all of the DOTs that use spiral curves determine the length of runoff first and then set the spiral length equal to the runoff length.

A review of international agency guidelines indicates that three types of controls are most commonly used to determine the minimum length of the spiral curve transition. These controls include consideration of roadway appearance, motorist comfort, spiral effectiveness, and lateral shift. The appearance consideration is reflected in the use of the maximum-relative-gradient and minimum-travel-time controls. The comfort consideration is reflected in the use of a maximum-rate-of-change-in-centripetal-acceleration control. The spiral effectiveness consideration is reflected in the use of a minimum deflection angle control. This control ensures that the spiral is long enough to provide a shift in the lane that is consistent with that produced by the vehicle's natural spiral path. The German (*5*) guideline defines minimum spiral length based on these considerations using the following equation:

$$L_{s,\min} = \frac{R}{9} \quad (14)$$

Finally, the lateral shift consideration is reflected in the use of a minimum-lateral-offset control. This control has the same intent as the spiral effectiveness control. The Australian (*2*)

TABLE 15 Minimum length of spiral for TR facilities

Design Speed (km/h)	C (m/s^3)[1]	Radius, R (m)[1]	Runoff Length (m)
30	1.2	25	19
40	1.1	50	25
50	1.0	80	33
60	0.9	125	41
70	0.8	160	57

[1] Values based on *Green Book* (*1*) Table III-17.

guideline defines minimum spiral length based on these considerations using the following equation:

$$L_{s,\min} = \sqrt{24 p_{\min} R} \quad (15)$$

where:

$p_{\min}$ = minimum lateral offset between the tangent and circular curve (= 0.25 m).

The Australian guideline recommends that a minimum offset $p_{\min}$ of 0.25 m be used to define the minimum radius. For moderate to small radii, the lengths obtained from Equation 15 are similar to those obtained from Equation 14 when $p_{\min}$ is about 0.2 m.

Several international guidelines (*4, 5, 6, 7*) suggest that the driver must also be able to look beyond the spiral to evaluate the curvature of the subsequent horizontal curve. Specifically, the U.K. (*7*) and French (*4*) guidelines suggest that drivers cannot perceive the true curvature of a bend when it is preceded by a "long" spiral. Their contention is that this situation promotes over-driving the curve, which increases the potential for "run-off-the-road" crashes. The French guidelines cite research conducted by Stewart et al. (*18*) who showed that curves with "long" spirals were associated with a high crash frequency.

Like the U.K. and French guidelines, the Swedish (*6*) and German (*5*) guidelines also note the need to avoid long spirals to avoid perceptual problems, especially on small radius curves. They recommend limiting spiral length to a value equal to the curve radius (i.e., $L_{s,\max} = R$).

A lateral shift control has also been used to define maximum spiral length. The U.K. guideline (*7*) recommends limiting the lateral offset to 1.0 m for sharper curves. The rationale for this control is that an excessive amount of lateral offset is inconsistent with the desired path of drivers upon curve entry. In addition, excessive offsets are generally associated with longer spiral lengths and shorter radii. As discussed previously, this combination can make it difficult for the driver to detect the curvature of the subsequent horizontal curve. The following equation is recommended in the U.K. guideline to define the *maximum* spiral length:

$$L_{s,\max} = \sqrt{24 p_{\max} R} \quad (16)$$

where:

$p_{\max}$ = maximum lateral offset between the tangent and circular curve (= 1.0 m).

The French guideline (*4*) recommends that the spiral curve length be kept short to help drivers assess the curvature of the horizontal curve. This guideline includes an equation for predicting the "desired" spiral length. Larger lengths are acceptable but not encouraged. Equation 16 yields lengths similar to that obtained from the equation in the French guideline for lateral offsets in the range of 0.5 to 1.0 m.

The aforementioned controls for spiral length are compared in Figure 17. In general, the trends in this figure suggest there is a relatively narrow range of spiral lengths suitable for any given radius. The gradient/travel time and comfort controls indicate a need to increase the spiral length with increasing curvature (= 1,000/*R*). On the other hand, the lateral shift controls indicate a need to decrease spiral length with increasing curvature. The gradient/travel time and comfort controls are based on Equations 5 and 13, respectively, for a design speed of 70 km/h. For Equation 13, a maximum value of *C* equal to 1.2 m/s^3 is used to define the acceptable minimum spiral length.

The minimum spiral length obtained from the gradient/travel time control (as defined by Equation 5) is shown in

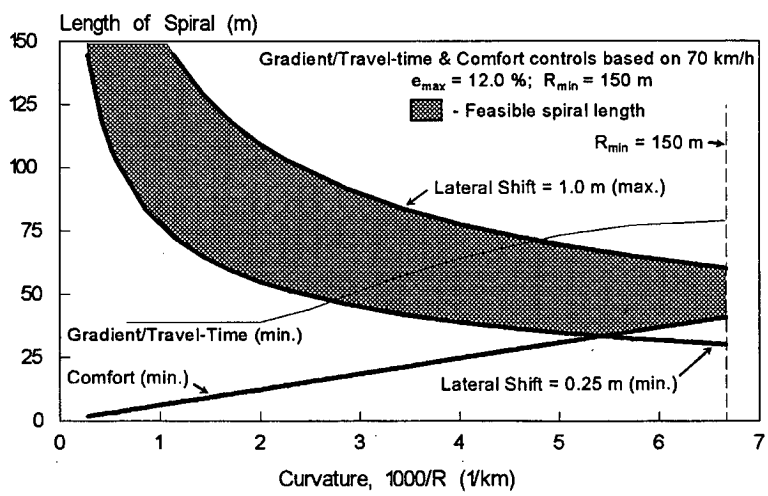

Figure 17. Comparison of alternative controls for defining spiral curve length.

Figure 17 with a thin trend line. This control is also shown to have no effect on the feasible spiral length region. This approach was taken because the gradient and travel time controls are based primarily on aesthetic considerations. Logically, a higher priority in spiral length determination should be given to motorist comfort and safety. For this reason, the feasible region boundaries shown in Figure 17 are based on the comfort and lateral shift controls.

Issues Related to Alignment Transition Design

The advantages of the spiral curve transition have been documented by several researchers (*14, 15, 19, 20, 21, 22, 23*). These researchers have based their findings on both field observation and simulation. Collectively, these studies found that spirals have the following attributes (relative to a tangent-to-curve transition):

1. A more gradual and comfortable change in lateral acceleration and truck roll angle (*15, 21*),
2. A reduced peak side friction demand (*14, 19*),
3. A path more consistent with the path drivers naturally take when entering a curve (*14*), and
4. A reduction in crash risk by about 5 percent under some conditions (*20, 22*).

Blue et al. (*15*) used simulation to study the effect of spiral curve transition design on the side friction demand and body roll of large trucks. Harwood et al. (*21*) (who collaborated with Blue and later summarized their study findings) concluded that spiral curves reduced the lateral acceleration acting on trucks but that the magnitude of this reduction is so small (i.e., about 0.01 *g*) that "the use of spirals is unlikely to provide a major reduction in rollover accidents."

Zegeer et al. (*20*) conducted a study of crash history at 10,900 horizontal curves located on two-lane highways in the state of Washington. Based on this study, Zegeer reported that spiral curves may reduce overall crash frequency by 2 to 9 percent, the exact amount dependent on the corresponding horizontal curve's radius and its central angle. An overall reduction of 5 percent was reported to be "most representative of the effect of spiral transitions."

The effect of spiral curve transitions on crash frequency was also examined by Council (*22*). Council re-examined the data assembled by Zegeer et al. (*20*). He used linear logistic modeling to quantify the effect of curve geometry and roadway cross section on the probability of one or more crashes in a 5-year period. As a result of his examination, Council concluded that spirals can reduce crash probability on horizontal curves in level terrain when the curve radius is less than 600 m. He also recommended that spirals seldom be used in mountainous terrain but, if used, that the roadway include wider lane and shoulder widths.

Lamm et al. (*23*) recently completed a synthesis of research on spiral curve transition safety. Based on their findings, they concluded that spiral curve transitions are likely to reduce crash risk when the horizontal curve radius is 200 m or less (*23*, p. 9.2). They also recommend the use of the tangent-to-curve transition for radii of 800 m or greater (1,000 m or more when the design speed is 105 km/h or greater) (*23*, p. 12.18).

The potential disadvantages of spiral curve transitions have been noted by several researchers. Most notably, Stewart (*24*) has questioned the usefulness of the spiral curve transition. He has argued that the spiral curve "hides" the true curvature of the roadway from the driver. He presents evidence that a consequence of this perceptual deception is that the driver overestimates the curve radius when it is preceded by a spiral curve. As a result, the resulting side friction demand is often larger than desired and may reach unsafe levels.

As mentioned previously, the French (*4*) guideline recognizes the merit of Stewart's argument and supporting data (*18, 24*). As a result, the French guideline recommends avoiding long spirals because they are most likely to deceive drivers.

Visual recognition of the curve beginning was noted in Appendix D as an essential component in the driver's vehicle control process. A tangent-to-curve design maximizes the driver's ability to detect the beginning of the curve and to initiate the curve steer maneuver process in a safe and efficient manner. In contrast, a spiral curve hides the introduction of curvature, which enhances the appearance of the roadway (*1*, p. 175) but may also make it more difficult for the driver to perceive the curve and navigate the transition sections.

Lateral Motion in the Alignment Transition Section

The relationship between spiral length and a vehicle's lateral motion at the end of the transition was examined using the lateral motion model described in Appendix D. The objective of this examination was to identify the effect of existing transition design controls on vehicle lane position and lateral velocity while traveling through the transition. The results of this examination are described in the following sections.

Evaluation Criteria

As an overall goal, transition design elements should be sized such that a vehicle's lateral velocity and shift, as it exits the transition section, should be as small as possible. Recognizing that this goal may not always be achievable for both travel directions, three evaluation criteria were established to define maximum deviations from the overall goal:

1. Lateral velocity v_l should not exceed a rate equivalent to 0.3 m/s.
2. Lateral velocity should not be in an outward direction.
3. Lateral shift y_l should not exceed 1.0 m.

An explanation of each of these criteria was provided previously in "Lateral Motion in the Superelevation Transition Section."

Lateral Acceleration

Equation 32 in Appendix D was used to examine the relationship between spiral length and peak lateral acceleration. A range of speeds was considered for this evaluation. Also considered was the location of the traffic lane with respect to the curve direction (i.e., the inside lane of a curve to the right and the outside lane of a curve to the left). The relationship between peak acceleration and spiral length for a 95th percentile curve speed of 70 km/h is shown in Figure 18.

As the trend lines in Figure 18 indicate, the peak lateral accelerations for both curve directions have a nearly common minimum value. This minimum value occurs at spiral lengths of 50 and 54 m for the inside and outside curve directions, respectively. The minimum acceleration is near zero for the outside direction and is about 0.1 m/s^2 for the inside direction. Further examination of the equation predicting lateral acceleration (i.e., Equation 32, Appendix D) indicates that the minimum acceleration for the outside movement occurs when spiral length is equal to the product of steering time t_s and speed v.

Lateral Velocity

Controls for Spiral Length. Equation 35 of Appendix D was used to evaluate the effect of spiral length on lateral velocity. Two cases were considered for this evaluation; however, for both cases, spiral length was set equal to and concurrent with the superelevation runoff length. For the first case, the minimum runoff/spiral length was based on the following equation:

$$L_s = Larger\ of: \begin{bmatrix} \dfrac{w\, e_d}{\Delta} n_l b_w \\ \\ t_s \dfrac{V_c}{3.6} \end{bmatrix} \quad (17)$$

where:

L_s = minimum length of spiral, m;
Δ = maximum relative gradient, percent;
b_w = adjustment factor for number of lanes rotated;
w = width of one traffic lane (typically 3.6 m), m;
e_d = design superelevation rate, percent;
t_s = steering time (= 2.8 s), s;
V_c = curve speed, km/h; and
n_l = number of lanes rotated, lanes.

For the second case, only the first component of Equation 17 was used to define runoff/spiral length.

Equation 17 contains two components—each representing a separate control. The first component represents the gradient control where runoff/spiral length is defined by the maximum relative gradient. The second component represents the "steering time" control where runoff/spiral length equals the distance traveled during the typical ramp steering maneuver (as discussed in Appendix D). The larger of these two controls is used to define runoff/spiral length.

The results of the analysis are shown in Figure 19. The thick lines shown represent the resulting lateral velocity when the spiral length is determined using the first case (i.e., both components); the dashed lines represent the second case.

As the trends in Figure 19 suggest, the exclusive use of the gradient control (i.e., Case 2) yields widely varying lateral velocities. The addition of the steering time control (i.e., Case 1) moderates the lateral velocities over the range of

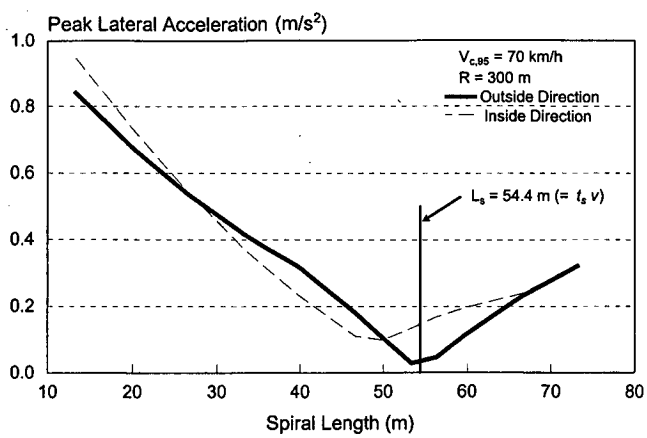

Figure 18. Effect of spiral length on peak lateral acceleration.

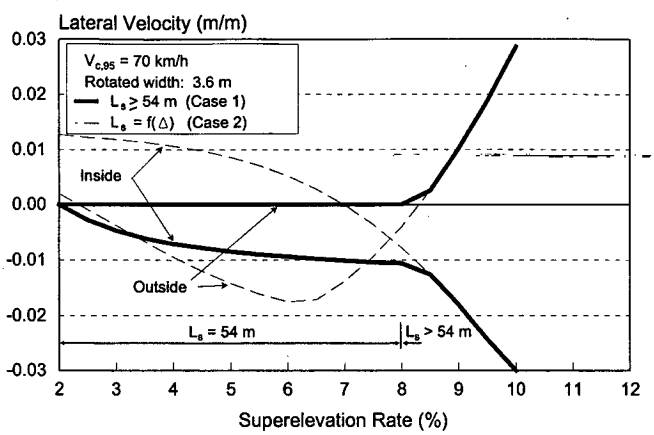

Figure 19. Effect of superelevation rate on lateral velocity.

superelevation rates to which it applies (i.e., rates below 8.5 percent). For both cases considered, the gradient control applies when the superelevation rate exceeds 8.5 percent. This limiting superelevation rate can be computed by setting both components of Equation 17 equal to one another and solving for superelevation rate.

The trends in Figure 19 indicate that imposition of the steering time control has a significant effect on lateral velocity. Specifically, this control results in the lateral velocity in the outside direction being equal to zero and the lateral velocity in the inside direction being equal to a small negative (or outward) value. This latter tendency results from the steer maneuver being implemented prior to the start of the superelevation in the inside direction.

Closer examination of the steering time control indicates that its use has both an advantage and a disadvantage. Its advantage is that it improves curve operation by reducing the combined lateral velocity for both directions. Its disadvantage is that the small negative lateral velocity produced for the inside curve direction is outward. A velocity in the outward direction is undesirable because it implies that the driver will have to adopt a "critical" travel path radius (i.e., $R_p < R$) to halt the resulting drift. Overall, it is believed that the advantage outweighs the disadvantage and that the use of the steering time control improves overall vehicle operations.

These findings, combined with those from the analysis of peak lateral acceleration, indicate that a runoff/spiral length approximately equal to the travel time during the steer maneuver should yield desirable operating conditions. Spiral lengths that are not equivalent to this steer distance, such as those dictated by the gradient control, may produce undesirably large peak lateral accelerations and lateral velocities. This finding is consistent with concerns raised by Stewart (*24*) regarding spiral lengths larger than the "natural" spiral that results from the driver's steering behavior during curve entry.

Defining Percentile Speed. A sensitivity analysis was conducted to determine if the 5th or 95th percentile speed represented the controlling condition for defining minimum spiral length based on the steering time control. Spiral length was computed for a wide range of 95th percentile speeds (i.e., $30 < V_{95} < 120$ km/h), superelevation rates, and rotated lanes. First, spiral length was computed for each combination based on the 95th percentile speed. This length was then used to compute the lateral velocity corresponding to a vehicle traveling at the 5th and at the 95th percentile speeds. Finally, this pattern was repeated for a spiral length based on the 5th percentile speed. The trends shown in Figure 20 are fairly typical for the 95th percentile speeds considered; although, the absolute value of lateral velocity tended to decrease for higher 95th percentile speeds.

Only the lateral velocity for the "worst-case" combination of speed and percentile-based length are shown in Figure 20. That is, if spiral length was defined using the 5th percentile, then it was evaluated only for its effect on vehicles traveling at the 95th percentile speed. This approach was followed

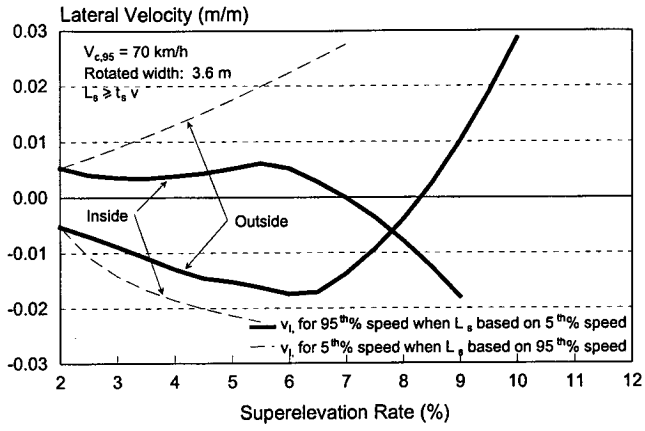

Figure 20. Effect of alternative definitions of minimum length of spiral on lateral velocity.

because lateral velocity for the "defining" percentile was negligibly small, as illustrated by the thick lines in Figure 19.

As shown by the trend lines in Figure 20, basing the spiral length on the 5th percentile speed has a decided advantage over basing it on the 95th percentile speed. In particular, it can be seen that the lateral velocities for vehicles traveling at the 95th percentile speed (on a spiral with length based on the 5th percentile speed) will be both small and inward (i.e., they are consistent with Evaluation Criteria 1 and 2) when the superelevation rate is less that 7.0 percent. This result is not provided when spiral length is defined by the 95th percentile speed. As a result, it is concluded that basing runoff/spiral length on the 5th percentile speed will yield the best operating conditions for the distribution of speeds in a typical traffic stream.

Peak Lateral Acceleration. The impact of basing spiral length on the 5th percentile speed was also investigated in terms of the resulting peak lateral acceleration. As expected, vehicles traveling at the 5th percentile speed had negligible peak lateral acceleration (this expectation is based on the discussion associated with Figure 18). This trend was found to be consistent for the range of 95th percentile speeds (i.e., $30 < V_{95} < 120$ km/h) considered.

The peak lateral acceleration for the 95th percentile driver was found to be small but not negligibly small. This acceleration results from the 95th percentile driver initiating the ramp steer maneuver prior to the start of the spiral. In other words, the desired balance among spiral curvature, superelevation rotation, and steer-induced lateral acceleration is not achieved for the 95th percentile driver when spiral length is based on the behavior of the 5th percentile driver.

The peak acceleration experienced by the 95th percentile driver (when traveling on a spiral with length defined by the 5th percentile speed) was examined further to determine if the magnitude of this acceleration could be generalized. Based on this analysis, it was concluded that the peak lateral

acceleration for the 95th percentile driver was about three-tenths (0.3) of the centripetal acceleration a_r. This can be compared to a peak lateral acceleration of 0.5 a_r found for the tangent-to-curve design. It should also be noted that these peaks are minimum values that would be realized when both transition types have runoff/spiral lengths defined using the equations described previously (i.e., Equation 5 for the tangent-to-curve and Equation 17 for the spiral curve transition).

The findings from this analysis were used to make relative comparisons between the peak lateral accelerations of the spiral and tangent-to-curve transition design. Specifically, it appears that a well-designed, tangent-to-curve transition produces a peak lateral acceleration about 67 percent (= 1 – 0.5/0.3) larger than that produced by a spiral curve transition. This trend is consistent with the findings of Glennon et al. (*14*) whose simulation data indicate that maximum side friction demands for the tangent-to-curve transition are about 50 to 60 percent larger than those of the spiral curve transition.

Lateral Shift

Equation 36 of Appendix D was used to evaluate the effect of spiral length on lateral shift. Trends similar to those shown in Figure 19 were obtained as a result of this analysis. In particular, lateral shift was nominal for small superelevation rates and excessively large when the limiting superelevation rate was exceeded. More important, it was found that lateral shifts less than 1.0 m are achieved when spiral length is based on the steering time control.

CHAPTER 3

INTERPRETATION, APPRAISAL, AND APPLICATIONS

This chapter describes the guidelines and control values recommended for use in designing horizontal curves for streets, highways, and turning roadways. These guidelines and values are developed from the separate consideration of theoretic principles, field data, and current practice. Details of the theoretic modeling and field data analysis are reported in Appendices A, B, C, and D. The findings from these efforts are reported in Chapter 2 as is a synthesis of the guidelines and control values being used in practice.

The recommended design guidelines and control values are presented in three sections. The first section describes the guidelines and values that control the selection of superelevation rate and radius for a horizontal curve. The second section describes the guidelines and values that control the length and location of the superelevation transition section. The last section describes guidelines and values that control the need for and length of the spiral curve transition.

CONTROLS FOR HORIZONTAL CURVE DESIGN

This section describes the recommended guidance and controls for horizontal curve design. Specifically, the following controls are discussed in this section:

- Curve Design Speed
- Maximum Design Side Friction Factor
- Minimum Radius
- Minimum Radius with Normal Cross Slope
- Superelevation Distribution

Curve Design Speed

Definition

Most curve design controls are sensitive to design speed, as noted previously with regard to Tables 1, 8, and 14. This sensitivity allows the elements of the curve to be sized such that a majority of drivers are able to navigate the curve in a safe and comfortable manner. For this reason, it is important that all controls that constrain element size be consistent in their association with the intended design speed.

Topographic constraints may occasionally require the design of sharp radius curves. The findings reported in Appendix A indicate that drivers tolerate sharp radius curves; however, they do so through a "compromise" approach. Specifically, they allow a small reduction in speed along the curve and tolerate a small increase in side friction demand (both relative to the speed and friction values intended by the designer).

In recognition of the drivers' tendency to reduce speed on sharp curves, the concept of "curve design speed" is coined for this research. Curve design speed is defined as the design speed associated with the curve. It is generally equal to the design speed of the roadway; however, it can be slightly below the roadway's design speed if an acceptable speed reduction is identified and used for the sharper curves. Thus, the curve design speed is equal to the roadway design speed less the magnitude of the acceptable speed reduction.

This definition of curve design speed provides the conceptual framework necessary for the uniform development of curve design controls. However, a more quantitative definition is essential to the consistent evaluation of existing controls and the accurate calibration of any new controls. The *Green Book* authors provide some guidance on the speed appropriate for curve design. Specifically, they indicate that the 95th percentile speed of the passenger car traffic stream is representative of a curve's design speed (*1*, pp. 193–194).

There is also a need to address vehicle density in the definition of curve design speed. In this regard, the curve design speed definition is refined to represent the speeds of "freely flowing" passenger cars. As a result, curve design speed reflects speeds during low-volume conditions where vehicle density does not influence driver speed choice.

In summary, curve design speed is defined as the expected 95th percentile speed of freely flowing passenger cars on the curve. For design applications, curve design speed is equivalent to the 95th percentile approach speed less an amount equal to the acceptable speed reduction associated with the curve. This speed reduction would be negligible for moderate to large radius curves but could have a small positive value for sharper curves.

Context

The recommended definition of curve design speed is primarily intended to clarify (rather than change) the *Green Book* design guidance for curve design. The notion of an

acceptable speed reduction in the context of curve design speed may appear to be a significant change from existing guidance. However, the models developed in Appendix A demonstrate that modest speed reductions currently result from the use of the *Green Book*'s maximum design side friction factors and curves of near-minimum radius. Thus, speed reductions result from the application of existing controls; the curve design speed concept provides a means of formally recognizing this result.

The benefit of explicitly recognizing "curve design speed" and "acceptable speed reduction" in the curve design process is that the designer is more aware of the implications of using sharp radius curves. As will be shown in "Minimum Radius," the minimum radius for each design speed recommended by the *Green Book* is essentially unchanged by these definitions, provided that the acceptable speed reduction ranges from 3 to 5 km/h.

Maximum Design Side Friction Factor

Percentile Value for Design

The side friction models described in Appendix A provide a logical basis for establishing maximum side friction factors for design. Their representation of an upper percentile of the driver population provides a conservative nature to the design process, consistent with that used to define other design controls in the *Green Book*. Of the two percentiles considered in the development of these models (i.e., 85th and 95th), the 95th percentile provides the more appropriate level of coverage for curve design.

The rationale for recommending the 95th percentile side friction demand as the basis for design is based primarily on consideration of the probability of "failure." Unlike the issue of stopping sight distance, where several "rare" events must combine to produce possible failure in the form of a collision, curve speed is the only "random" variable that dictates the successful negotiation of the curve (as it relates to side friction demand and Equation 2). In this context, failure is represented by an uncomfortable level of lateral acceleration and not by the loss of vehicle control.

Failure in stopping sight distance design requires that the reaction time, deceleration rate, and speed criteria will be at or below their "worst-case" values for a given driver. For example, if 85th percentile values of each control are used to define stopping sight distance, the probability of failure is about 1 in 300 (= $[1 - 0.85]^{-3}$). However, if this level of safety were also provided in curve design, the 99.7th percentile side friction demand (= 1 − 1/300) would need to be used. Practical considerations preclude the use of such an extreme value. On the other hand, the 85th percentile side friction demand is probably too low because 15 percent of drivers would have side friction demands in excess of the design value. Therefore, the 95th percentile side friction demand is believed to offer an appropriate compromise value for design applications.

Friction Factors for Curve Design

The side friction demands of both passenger cars and heavy trucks were evaluated for this research. The following equation was developed for predicting the side friction demand of the 95th percentile passenger car:

$$f_{D,95,pc} = 0.243 - 0.00187\,V_{a,95,pc} + (0.0135 - 0.0067\,I_{TR})\,dv_{95,pc} \quad (18)$$

where:

$f_{D,95,pc}$ = side friction demand factor for the 95th percentile passenger car;
$V_{a,95,pc}$ = 95th percentile passenger car approach speed, km/h;
$dv_{95,pc}$ = 95th percentile passenger car speed reduction (= $V_{a,95,pc} - V_{c,95,pc}$), km/h;
$V_{c,95,pc}$ = 95th percentile passenger car curve speed, km/h; and
I_{TR} = indicator variable (1 for turning roadways; 0 otherwise).

A similar relationship was developed for the 95th percentile truck. This relationship is as follows:

$$f_{D,95,tk} = 0.222 - 0.00140\,V_{a,95,tk} + (0.0101 - 0.0063 I_{TR})\,dv_{95,tk} \quad (19)$$

where:

$f_{D,95,tk}$ = side friction demand factor for the 95th percentile heavy truck;
$V_{a,95,tk}$ = 95th percentile heavy truck approach speed, km/h;
$dv_{95,tk}$ = 95th percentile heavy truck speed reduction (= $V_{a,95,tk} - V_{c,95,tk}$), km/h; and
$V_{c,95,tk}$ = 95th percentile heavy truck curve speed, km/h.

Additional discussion regarding the development of these models and their implications to curve design are provided in Appendix A.

A comparison of Equations 18 and 19 indicated similar side friction demands for both car and truck drivers. Specifically, it was found that truck drivers demand slightly less side friction on low-speed facilities than do passenger car drivers (and slightly more friction on high-speed facilities). However, from a practical standpoint, the differences in friction demand are not significant for the two vehicle types. Therefore, it is recommended that the side friction factors for passenger cars be used to define the maximum side friction demand factors for curve design. In this regard, Equation 18 is redefined as follows:

$$f_{d,\max} = 0.243 - 0.00187\,V_{a,95} + (0.0135 - 0.0067\,I_{TR})\,dv_{95} \quad (20)$$

where:

$f_{d,\max}$ = maximum design side friction factor;
$V_{a,95}$ = 95th percentile approach speed, km/h;
dv_{95} = 95th percentile speed reduction (= $V_{a,95} - V_{c,95}$), km/h; and
$V_{c,95}$ = 95th percentile curve speed (i.e., curve design speed), km/h.

Hereafter, the factors obtained from Equation 20 are referred to as the "maximum design side friction factors" to denote that they represent maximum values for design applications.

Equation 20 includes the effect of speed reduction on side friction demand. Use of this equation to define the maximum design side friction factors requires determining what degree of speed reduction is acceptable. The side friction demand factor coincident with no speed reduction $f_{d,0}$ logically represents a *desirable* value for the maximum design side friction factor. A curve designed to require a side friction demand equal to or less than $f_{d,0}$ would operate with no speed reduction along the curve. However, in recognition of the desirability of providing a balance between motorist safety and construction cost, it may be more practical to designate a non-zero speed reduction for curve design. This speed reduction would be used with the side friction model to define an *acceptable* maximum design side friction factor $f_{d,r}$.

Based on the discussion in the preceding paragraph, a compromise speed reduction was used to define one maximum design side friction factor for each design speed. The compromise speed reduction was based on consideration of the measured speed reductions of cars and trucks on numerous curves as well as the implications of the corresponding friction factors on minimum radii for design. Based on these considerations, the acceptable speed reduction used to define the maximum design side friction factors was established at 3.0 km/h for design speeds of 90 km/h or less. For design speeds greater than 90 km/h, the acceptable speed reduction is gradually increased; with a maximum reduction of 4.55 km/h at 120 km/h.

The recommended maximum design side friction factors are shown in Figure 21. These factors were computed from Equation 20 using the acceptable speed reductions noted in the preceding paragraph. It should be noted that the aforementioned speed reductions, when used with Equation 20, specifically apply to passenger cars. However, Equation 19 can be used to show that the recommended friction factors equate to truck speed reductions that are very similar to those of passenger cars.

The recommended maximum design side friction factors reflect conditions found on street and highway curves. Similar levels of side friction demand were also observed on turning roadways; however, the speed reductions were found to be about twice those on streets and highways. A larger speed reduction on turning roadways is logical because drivers on these roadways anticipate sharp curvature and a significant speed reduction as they transition between intersecting facilities.

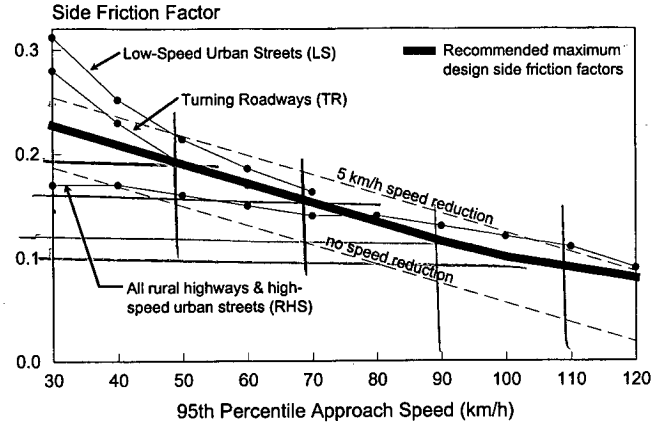

Figure 21. Maximum design side friction factors.

Minimum Radius

The minimum radius is a limiting value of curvature that is associated with a side friction demand equal to the design maximum when the curve has maximum superelevation and is traveled at the curve design speed. Use of sharper curvature would call for superelevation beyond the limit considered practical or side friction beyond the design maximum or both. Thus, the minimum radius is a significant control in horizontal alignment design.

Equation 2 defines the relationship among radius, side friction demand, and superelevation rate. This equation was used to develop the following equation for calculating the minimum radius:

$$R_{\min} = \frac{(V_{a,95} - dv_{95})^2}{127(0.01\,e_{\max} + f_{d,\max})} \quad (21)$$

where:

$R_{\min}$ = minimum radius at maximum superelevation rate, m; and
$e_{\max}$ = maximum superelevation rate, percent.

Recommended minimum radii for each combination of 95th percentile approach speed, maximum design side friction factor, and maximum superelevation rate are listed in Table 16. As noted previously, the speed reductions listed were selected in part to minimize differences between the radii recommended in Table 16 and those included in *Green Book* Table III-6.

TABLE 16 Recommended minimum radius using maximum superelevation and side friction

95th Percentile Approach Speed (km/h)	Speed Reduction (km/h)	Curve Design Speed (km/h)	Max. Design Side Friction Factor, $f_{d,\max}$	Minimum Radius (m)				
				Max. Superelevation Rate, e_{max} (%)				
				4	6	8	10	12
30	3.00	27	0.227	21	20	19	18	17
40	3.00	37	0.209	43	40	37	35	33
50	3.00	47	0.190	76	70	64	60	56
60	3.00	57	0.171	121	111	102	94	88
70	3.00	67	0.153	183	166	152	140	129
80	3.00	77	0.134	268	241	218	200	184
90	3.00	87	0.115	385	341	306	277	254
100	3.25	96.75	0.100	526	461	409	369	335
110	3.90	106.10	0.090	682	591	521	467	422
120	4.55	115.45	0.080	875	750	656	583	525

The speed reductions listed in Table 16 correspond to values observed on sharper curves, as described in Appendix A. Larger reductions will likely result if curve radii smaller than those listed are used. Experience indicates that the speed reductions listed in Table 16 represent a reasonable compromise between the designer's occasional need to use sharp radius curves and desire to maintain a consistent design speed along the roadway.

Minimum Radius with Normal Cross Slope

The minimum-radius-with-normal-cross-slope is defined as the smallest radius that can be used on a roadway with a normal cross section without causing an undesirable level of lateral acceleration. The normal cross slope is defined as the cross slope used in the typical cross section on tangent alignments. It equals or exceeds the minimum cross slope, as described in Chapter 2. By definition, radii smaller than the minimum-radius-with-normal-cross-slope would require superelevation at a rate at least equal to the normal cross slope rate.

The guidance provided by the *Green Book* authors with regard to the cross slope used to define the minimum-radius-with-normal-cross-slope control is limited to RHS facilities. For this facility type, the *Green Book* authors assume a normal cross slope of 1.5 percent. They do not specify a normal cross slope rate nor discuss a minimum-radius-with-normal-cross-slope for LS or TR facilities. It should be noted that a review of state DOT design manuals indicated that most DOTs define the normal cross slope as 2.0 percent for both RHS and LS facilities.

Equation 2 was modified to develop an equation for computing the minimum radius with normal cross slope. The following is the resulting equation:

$$R_{NC} = \frac{(V_{a,95} - dv_{95})^2}{127(0.01e_{NC} + f_{NC})} \quad (22)$$

where:

R_{NC} = minimum radius with normal cross slope, m;
e_{NC} = normal cross slope rate (typically −1.5 to −2.5 percent), percent; and
f_{NC} = maximum side friction with adverse cross slope.

As the terms in this equation indicate, the minimum-radius-with-normal-cross-slope is dependent on the normal cross slope rate and the maximum friction with adverse cross slope. It is recommended that this radius be based on passenger car speed because this speed is typically larger than that of trucks. As a result, a minimum radius based on passenger car speed will yield a truck side friction that is below the maximum side friction level (i.e., f_{NC}).

The dependence of Equation 22 on friction also suggests some association with facility type. The *Green Book* authors have defined appropriate levels of side friction for each facility type. For LS facilities, the *Green Book* authors recommend that side friction demand on the sharpest curves equal the design maximum. Hence, the minimum radius for LS facilities would logically be based on f_{NC} being equal to the maximum design side friction factor $f_{d,\max}$, as defined by Equation 20.

For RHS facilities, the *Green Book* authors do not explicitly define a specific value for f_{NC}. Rather, the parabolic distribution equation that underlies Distribution Method 5 must be "back-solved" to determine the radius that corresponds to a recommended design superelevation rate of 1.5 percent (i.e., the normal cross slope rate). This solution technique was used to develop *Green Book* Table III-12 (*1*, p. 172). The values in this table indicate that f_{NC} varies from 0.031 to 0.038 for speeds ranging from 30 to 120 km/h.

A review of design guideline documents from several international highway agencies indicated that there is no consensus on the magnitude of the maximum side friction control f_{NC}. The Swedish (*6*), Australian (*2*), and U.K. (*7*) guidelines recommend a constant value for this control. The German (*5*) guideline recommends that f_{NC} equal 10 percent of the maximum design side friction factor; thus, f_{NC} decreases with

increasing design speed. In contrast, only the United States (i.e., *Green Book*) and Canadian (*3*) guidelines use distribution methods that indirectly produce values for f_{NC} that *increase* with increasing design speed. In addition, Australia, Germany, and the U.K. recommend values of f_{NC} that collectively lie in the range of 0.05 to 0.10. As a result, their values for the minimum-radius-with-normal-cross-slope are much smaller than those recommended in the *Green Book*.

After considering the aforementioned range in international practice, it is recommended that the maximum side friction demand control f_{NC} be defined as a constant value. This approach would represent a deviation from the procedure used in the *Green Book* to define the minimum-radius-with-normal-cross-slope control for RHS facilities (i.e., it currently is a by-product of the parabolic distribution equation). However, it offers the benefit of simplicity of computation and elimination of its dependence on distribution method. In addition, the use of a constant value for f_{NC} is more consistent with international practice and is more defensible from a theoretic standpoint.

Based on the preceding discussion, the following values are recommended for use in determining the minimum radius with normal cross slope:

$$e_{NC} = -2.0\% \qquad f_{NC,RHS} = 0.04 \qquad f_{NC,LS} = f_{d,\max}$$

It should be noted that the value of f_{NC} for RHS facilities (i.e., 0.04) implies a minimum nominal speed reduction, as it relates to Equation 20, for 95th percentile approach speeds of 110 and 120 km/h. In particular, Equation 20 can be used to compute speed reductions of 0.20 and 1.58 km/h for speeds of 110 and 120 km/h, respectively. For LS facilities, an acceptable speed reduction of 3.0 km/h was considered reasonable and consistent with observed driver behavior. Moreover, this level of speed reduction yields minimum radii that are very similar to those recommended in the *Green Book* (*1*, Figure III-18).

The recommended values for minimum-radius-with-normal-cross-slope obtained from Equation 22 are listed in Table 17. The values listed in *Green Book* Table III-12 and shown in Figure III-18 are also repeated in this table for comparative purposes.

A comparison of the recommended minimum radii (as listed in Table 17) with those provided in the *Green Book* indicates that they are in general agreement. For RHS facilities, the recommended radii are within ±10 percent of the *Green Book* values (except for the 30 and 40 km/h approach speeds where the recommended radii are 20 percent smaller than the *Green Book* values). For LS facilities, the recommended radii are within ± 4 m of the *Green Book* values.

Superelevation Distribution

The distribution of superelevation rate and side friction demand is described in this section. Initially, boundary values for minimum and maximum superelevation rates are defined. Then, these boundary values are used to evaluate the superelevation rates recommended in the *Green Book*. Finally, modifications to the *Green Book* distribution methods are described that overcome some of their observed limitations.

Controlling Superelevation Rates

This section describes the development of equations that bound the region of acceptable superelevation rates. For this

TABLE 17 Recommended minimum radius with normal cross slope

95th % Approach Speed (km/h)	RHS Facilities			LS Facilities		
	95th % Speed Reduction[1] (km/h)	Minimum Radius (m)	*Green Book*[2] Min. Radius (m)	95th % Speed Reduction[3] (km/h)	Minimum Radius (m)	*Green Book*[4] Min. Radius (m)
30	0.00	354	450	3.0	28	24
40	0.00	630	800	3.0	57	54
50	0.00	984	1,110	3.0	102	101
60	0.00	1,417	1,520	3.0	169	171
70	0.00	1,929	2,000	3.0	266	270
80	0.00	2,520	2,480			
90	0.00	3,189	3,010			
100	0.00	3,937	3,680			
110	0.20	4,746	4,240			
120	1.58	5,521	4,960			

[1] Speed reduction implied by the specification of f_{NC} = 0.04, as it relates to Equation 20.
[2] Minimum radius listed in *Green Book* Table III-12 (*1*, p. 172).
[3] Speed reduction used in Equation 20 to determine f_{NC} (= $f_{d,\max}$).
[4] Minimum radius obtained from *Green Book* Figure III-18 (*1*, p. 190).

purpose, an equation is developed that predicts the minimum superelevation rate that can be used without causing excessive side friction demand. A second equation is developed that predicts the maximum superelevation rate that can be used without causing excessive counter steer. These extreme behaviors are associated with undesirable operating conditions that can reduce the level of safety for drivers. The minimum and maximum rates described in this section reflect the side friction demands of both passenger car and truck drivers.

Minimum Superelevation Rate Based on the 95th Percentile Driver. The minimum superelevation rate suitable for curve design should be that rate necessary to ensure that the side friction demand of the majority of drivers is not excessively large. The intent of this control is to minimize the portion of drivers that would have a side friction demand in excess of the maximum comfortable limit (as a result of a combination of high speed, small superelevation rate, or both). The problems associated with an excessively high side friction demand are a reduced margin of safety and a large speed reduction upon curve entry, both of which have adverse safety implications.

The minimum superelevation rate is intended to provide a safe design for all but the fastest drivers. Thus, this control is based on the side friction demand of the 95th percentile driver as defined by the distribution of speeds. The maximum side friction demand associated with this control would be that value corresponding to the threshold of motorist comfort, as defined by the maximum design side friction factor.

The relationship among superelevation rate, side friction demand, speed, and radius that is necessary to quantify this control is defined in Equation 2. Specifically, this equation can be used to compute the minimum superelevation rate when the speed is assumed equal to the curve design speed ($= V_{a,95} - dv_{95}$) and the side friction demand is equated to the maximum design side friction factor $f_{d,\max}$. Thus, the minimum superelevation rate is computed as follows:

$$e_{\min,95} = 100\left(\frac{(V_{a,95} - dv_{95})^2}{127R} - f_{d,\max}\right) \quad (23)$$

where:

$e_{\min,95}$ = minimum superelevation rate based on the 95th percentile driver, percent; and
R = radius of curve, m.

The minimum superelevation rates for passenger cars and heavy trucks, as predicted by Equation 23, are shown in Figure 22. The trend lines shown in this figure correspond to a 95th percentile passenger car approach speed of 70 km/h and an acceptable speed reduction of 0 km/h; hence, the curve design speed is also 70 km/h (= 70 − 0). The slope of each line increases for higher speeds. If a small speed reduction (say, 3 to 5 km/h) were considered acceptable for design, then the trend lines would shift downward slightly.

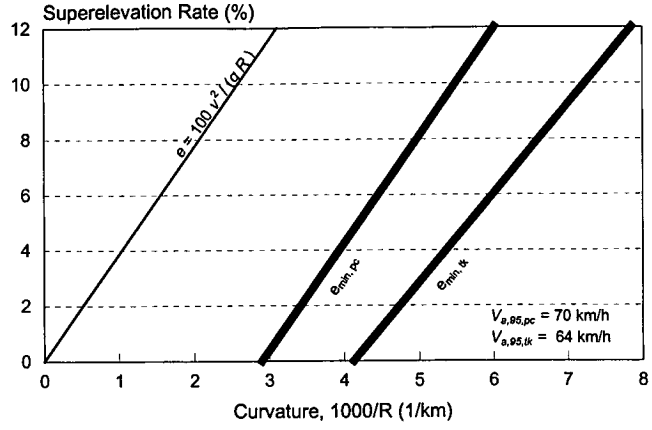

Figure 22. Minimum superelevation rates for passenger cars and heavy trucks.

Development of the trend lines shown in Figure 22 required the identification of "concurrent" 95th percentile speeds for the passenger car and heavy truck vehicle classes. In this regard, concurrent speeds are those that would be found to occur for the respective vehicle types on the same facility, in the same traffic stream, and under the same environmental conditions. A relationship between the speeds of these two vehicle classes was defined for this research using car and truck speeds observed on numerous roadways. Analysis of these data indicated that a 95th percentile passenger car speed of 70 km/h is consistent with a 95th percentile truck speed of 64.0 km/h. Additional details of this relationship are provided in Appendix B.

A comparison of the car and truck trend lines in Figure 22 indicates that passenger cars require a larger minimum rate. This trend is consistent for all 95th percentile passenger car speeds in the range of 30 to 120 km/h. Thus, the passenger car (i.e., the faster vehicle type) represents the design vehicle for this control.

Maximum Superelevation Rate Based on the 5th Percentile Driver. The maximum superelevation rate suitable for curve design should be that rate necessary to ensure that the side friction demand of the majority of drivers is not excessively small. The intent of this control is to minimize the portion of drivers that would have a side friction demand less than zero (because of a combination of slow speed, large superelevation rate, or both). The problem associated with a negative side friction demand is that it requires drivers to steer in the opposite direction of the curve (i.e., to counter steer), which is logically unsafe.

This maximum superelevation rate is intended to provide a safe design for all but the slowest drivers. Thus, this control is based on the side friction demand of the 5th percentile driver as defined by the distribution of speeds. The minimum side friction demand associated with this control would be that value corresponding to the side friction experienced on

a tangent roadway segment with a normal cross slope. Chapter IV of the *Green Book* indicates that "Cross slopes up to 2.0% are barely perceptible as far as effect on vehicle steering is concerned . . . "(*1*, p. 330). Thus, a minimum side friction demand was conservatively established as –0.015, corresponding to a cross slope of 1.5 percent.

The relationship among superelevation rate, side friction demand, speed, and radius that is necessary to quantify this control is defined by Equation 2. Specifically, this equation can be used to compute the maximum superelevation rate when the speed is assumed equal to the 5th percentile curve speed and the side friction demand is equated to –0.015. Thus, the maximum superelevation rate is computed as follows:

$$e_{\max,5} = 100\left(\frac{(V_{a,5} - dv_5)^2}{127R} + 0.015\right) \quad (24)$$

where:

$e_{\max,5}$ = maximum superelevation rate based on the 5th percentile driver, percent;
$V_{a,5}$ = 5th percentile approach speed, km/h;
dv_5 = 5th percentile speed reduction (= $V_{a,5} - V_{c,5}$), km/h; and
$V_{c,5}$ = 5th percentile curve speed, km/h.

The maximum superelevation rates for passenger cars and heavy trucks, as predicted by Equation 24, are shown in Figure 23. For comparative purposes, the minimum superelevation rate trend lines from Figure 22 are also shown. The trend lines shown in this figure correspond to a 95th percentile passenger car approach speed of 70 km/h and an acceptable speed reduction of 0 km/h; hence, the curve design speed is also 70 km/h (= 70 – 0). The slope of the lines corresponding to the maximum rate increase for higher speeds. If a small speed reduction (e.g., 3 to 5 km/h) were considered acceptable for design, then the line slope would decrease slightly.

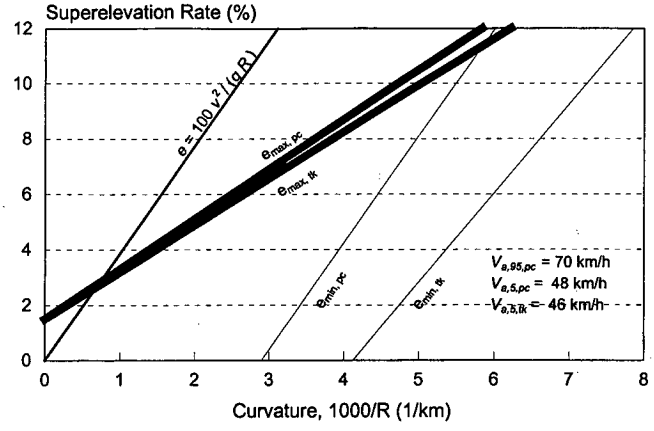

Figure 23. Maximum superelevation rates for passenger cars and heavy trucks.

Development of the trend lines shown in Figure 23 required the identification of concurrent 5th percentile speeds for the passenger car and heavy truck vehicle classes, when the 95th percentile passenger car speed is defined to be 70 km/h. A relationship between the speeds of these two vehicle classes was defined for this research using car and truck speeds observed on numerous roadways. Analysis of these data indicated that a 95th percentile passenger car speed of 70 km/h is consistent with a 5th percentile car speed of 47.8 km/h and a 5th percentile truck speed of 46.3 km/h. The relationship used to estimate these speeds is described in Appendix B.

A comparison of the car and truck trend lines in Figure 23 indicates that heavy trucks require a smaller minimum rate because of their lower speed. This trend is consistent for all 95th percentile passenger car speeds in the range of 30 to 120 km/h. Thus, the heavy truck represents the design vehicle for this control.

Further examination of Figure 23 indicates that the minimum and maximum superelevation rate controls intersect at a common superelevation rate and radius. In Figure 23, this intersection occurs at a superelevation rate of about 11 percent and a radius of 170 m (i.e., a curvature of 5.9 km^{-1}). This intersection point shifts toward the right as the acceptable speed reduction increases beyond 0.0 km/h. Over a range of speed reductions, this point represents the maximum superelevation rate for the 5th percentile driver (i.e., it extends Equation 24).

Equations 23 and 24 can be combined to determine the aforementioned maximum superelevation rate when the acceptable speed reduction dv exceeds zero. The equation resulting from this combination is as follows:

$$e^*_{\max} = 100\frac{r_v f_{d,\max} + 0.015}{1 - r_v} \quad (25)$$

with

$$r_v = \frac{(V_{a,5,tk} - dv_{5,tk})^2}{(V_{a,95,pc} - dv_{95,pc})^2} \quad (26)$$

where:

$e^*_{\max}$ = maximum superelevation rate based on the 5th percentile driver ($dv > 0$), percent; and
r_v = speed ratio.

The maximum rate obtained from Equation 25 can be combined with Equation 23 or 24 to obtain the corresponding minimum radius. The result of this combination with Equation 23 is as follows:

$$R^*_{\min} = \frac{(V_{a,95} - dv_{95})^2}{127(0.01e^*_{\max} + f_{d,\max})} \quad (27)$$

where:

R^*_{min} = minimum radius based on the 5th percentile driver ($dv > 0$), m.

Equations 20, 25, and 27 were used to compute the maximum superelevation rate based on the 5th percentile driver and the corresponding minimum radius for a range of 95th percentile approach speeds. The speed reductions assumed for this computation are those listed in Table 16. The resulting superelevation rates and minimum radii are listed in Table 18.

Superelevation and Radius Regions. Figure 24 illustrates five regions of superelevation and curvature for a 95th percentile approach speed of 70 km/h and acceptable speed reductions of 0 and 5 km/h. This approach speed and speed reduction correspond to curve design speeds between 65 and 70 km/h. The five regions are defined by the controls described in the previous two sections.

The equations used to develop the trend lines in Figure 24 required estimating several speeds; all of these estimates were based on a 95th percentile approach speed of 70 km/h. These estimates include the concurrent 5th percentile truck approach speed and the acceptable reduction in the 5th percentile speed. All of these estimates were based on equations described in Appendix B.

The trend lines in Figure 24 create five regions of possible combinations of superelevation rate and radius. Regions A and B include combinations suitable for curve design because they reflect the best operational characteristics. Region A represents "desirable" combinations as they would provide almost all motorists with an acceptable level of side friction demand (i.e., $-0.015 < f_D < f_{d,max}$) and no speed reduction. In other words, the superelevation rates and radii in this region satisfy the two controls defined in Equations 23 and 24.

Region B represents "acceptable" combinations because they would provide almost all motorists with an acceptable level of side friction demand and a speed reduction less than 5 km/h. However, the braking associated with a speed reduction effectively consumes some of the friction supply and thereby, reduces the friction margin of safety. This margin of safety may be further reduced on sharp downgrade curves because some additional braking is needed for speed maintenance. Hence, combinations in Region B may not be appropriate for curves on steeper downgrades (e.g., 5 percent or more), especially for facilities with significant truck traffic.

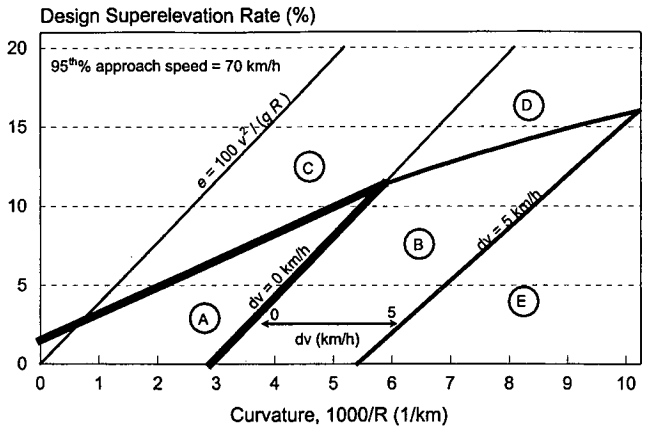

Figure 24. Regions of superelevation rate and radius combinations as defined by the minimum and maximum superelevation rate controls.

The remaining three regions should be avoided in design because they compromise one or both of the aforementioned controls. Region C represents combinations of rate and radius that would yield large negative friction demands for slower drivers (e.g., truck drivers). Region D represents combinations that would yield both large negative friction demands and speed reductions between 0 and 5 km/h. Region E represents combinations that produce speed reductions in excess of 5 km/h.

Regions of acceptable combinations of superelevation rate and radius can be developed for each 95th percentile speed. Examples of this type of development are provided in Figures 25 and 26. Also shown for comparative purposes are

TABLE 18 Maximum superelevation rate based on the 5th percentile driver

95th Percentile Approach Speed (km/h)	Speed Reduction (km/h)	Curve Design Speed (km/h)	Maximum e, e^*_{max} (%)	Minimum R, R^*_{min} (m)
30	3.00	27	12.2	16.4
40	3.00	37	13.5	31.4
50	3.00	47	14.1	52.5
60	3.00	57	14.3	81.4
70	3.00	67	14.3	119.5
80	3.00	77	13.9	171.2
90	3.00	87	13.2	241.6
100	3.25	96.75	12.6	326.4
110	3.90	106.10	12.3	416.2
120	4.55	115.45	11.9	527.7

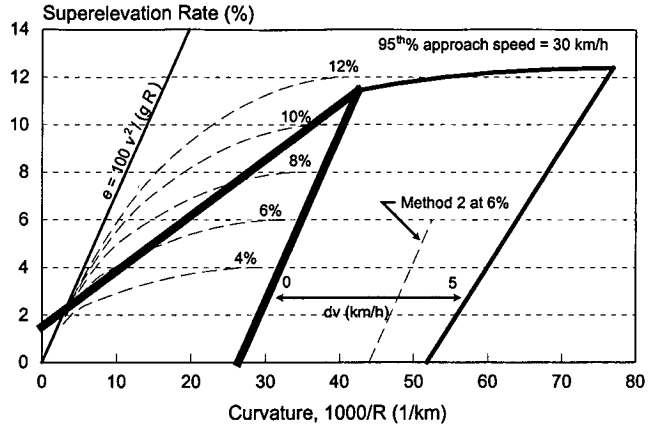

Figure 25. Regions of acceptable superelevation rate and radius combinations for a 95th percentile approach speed of 30 km/h.

the superelevation rates (and corresponding distribution methods) recommended in the *Green Book*. The percentages shown in each figure correspond to the maximum superelevation rate associated with each distribution curve. It is assumed that the *Green Book* design speed is equivalent to the 95th percentile approach speed for this comparison.

The trends shown in Figures 25 and 26 suggest that some of the superelevation rates recommended in *Green Book* Tables III-7 through III-11 may subject slower drivers to negative side friction demands. This problem is most notable for the lower design speeds, as suggested by Figure 25. However, the problem also occurs for the larger maximum superelevation rates at the higher design speeds, as suggested by Figure 26.

As shown in Figure 25, the trend lines associated with the recommended minimum superelevation rate control (i.e., Equation 23) and Distribution Method 2 are similar in slope. This similarity stems from their common basis in Equation 2

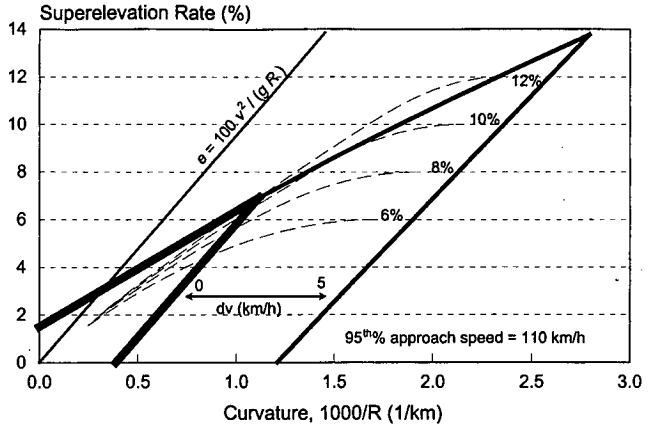

Figure 26. Regions of acceptable superelevation rate and radius combinations for a 95th percentile approach speed of 110 km/h.

and their use of the maximum design side friction factor. The slight difference between the slopes is due to the maximum side friction demand factors used to define each control. In general, the recommended minimum superelevation rate would be effectively equal to that obtained from Method 2 if a curve speed reduction of about 3 km/h were allowed.

Superelevation Distribution Method for RHS Facilities

The *Green Book* distribution of superelevation rate for RHS facilities (i.e., Method 5) is based on the desire to emphasize superelevation and minimize side friction demand. However, based on the discussion in the preceding sections, this distribution method has some deficiencies:

1. It violates the maximum-superelevation-rate-based-on-the-5th-percentile-driver control (i.e., Equations 24 and 25) under some conditions, as noted in the discussion of Figures 25 and 26.
2. Its use of separate distribution curves for each candidate maximum superelevation rate (e.g., 6 percent, 8 percent) and design speed leads to violation in design consistency, as noted in the discussion of Table 6.

The recommended distribution method is intended to satisfy the *Green Book* authors' desire to emphasize superelevation as well as resolve the aforementioned deficiencies. The recommended distribution method is based on the following equation:

$$e_d = e^*_{\max}\left(\frac{R^*_{\min}}{R}\right)^{n_e} \tag{28}$$

with

$$n_e = \frac{\ln(-0.01e_{NC}) - \ln(0.01e^*_{\max})}{\ln(R^*_{\min}) - \ln(R_{NC})} \tag{29}$$

where:

e_d = design superelevation rate, percent;
$e^*_{\max}$ = maximum superelevation rate based on the 5th percentile driver ($dv > 0$), percent;
$R^*_{\min}$ = minimum radius based on the 5th percentile driver ($dv > 0$), m;
n_e = shape factor;
$\ln(x)$ = natural log of x; and
R = radius of curve, m.

This equation satisfies two logical boundary conditions. First, it predicts a design superelevation rate equal to $e^*_{\max}$ when the curve radius equals $R^*_{\min}$. Second, the shape factor n_e obtained from Equation 29 forces Equation 28 to predict a design superelevation rate equal to the normal cross slope

rate when the curve radius equals R_{NC}. The resulting values of n_e range from 0.59 to 0.76 for design speeds ranging from 30 to 120 km/h. As these values are all less than 1.0, the distribution curve has a concave shape that emphasizes superelevation over side friction.

Kanellaidis (*25*) has shown that the distribution method in the German highway design guideline (*5*) is equivalent to Equation 28 when $n_e = 0.76$. Thus, the recommended distribution method is generally consistent with the distribution method used by German engineers.

The recommended distribution method does not explicitly include the maximum-superelevation-rate-based-on-the-5th-percentile-driver control, as predicted by Equation 24. However, an examination of Equation 28 (as calibrated by Equation 29) indicates that the distributed superelevation rates are very consistent with this control. Specifically, the rates from Equation 28 yield side friction demands for trucks that are always larger than – 0.024. While this value is lower than the recommended minimum sided friction demand of –0.015 for some radii, the difference is not of practical significance and the range of radii affected is small. Thus, the use of Equation 28 effectively overcomes Deficiency 1 and the use of one distribution "curve" for a given 95th percentile approach speed overcomes Deficiency 2. The recommended distribution is shown in Figure 27 for a 95th percentile approach speed of 70 km/h and an acceptable speed reduction of 3 km/h.

All state DOTs have defined a maximum superelevation rate (i.e., 4, 6, 8, 10, or 12 percent) based on practical considerations of climate, terrain, area type, and the frequency of slow-moving vehicles. This maximum superelevation rate can be "imposed" on the recommended distribution defined by Equation 28. In this regard, if Equation 28 yields a superelevation rate larger than the agency-defined maximum rate, then the latter rate would be used instead of that obtained from Equation 28. Recognition of an imposed maximum superelevation rate in conjunction with Equation 28 provides the necessary sensitivity to these practical considerations. It also allows for the use of multiple maximum rates.

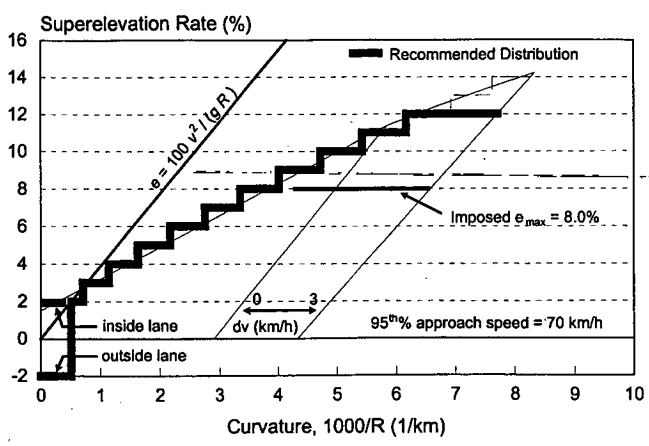

Figure 27. Recommended superelevation distribution for RHS facilities.

Figure 27 illustrates the "imposition" of an 8.0 percent maximum superelevation rate on the recommended distribution. In this situation, Equation 28 would be applicable to radii that yield a computed superelevation rate of 8.0 percent or less. Therefore, as indicated in Figure 27, this equation is applicable to radii of 249 m (i.e., 4.0 km^{-1}) or larger. Equation 28 yields larger superelevation rates for radii less than 249 m; however, such rates would not be used because they exceed the imposed maximum rate of 8.0 percent. Hence, the imposed rate of 8.0 percent is used for these smaller radii. The imposed maximum rate of 8.0 percent would apply to radii over the range of 152 to 249 m (i.e., 6.6 to 4.0 km^{-1}). Of course, radii between 152 m (6.6 km^{-1}) and 201 m (5.0 km^{-1}) would be associated with a speed reduction between 0 and 3 km/h.

One drawback from the use of an imposed maximum superelevation rate is that it eliminates the guarantee of design consistency for those superelevation rate and radius combinations falling on the "imposed" portion of the distribution. These particular rates and radii may also be obtained from the distributions for other maximum superelevation rates *provided* the agency allows consideration of multiple maximum rates. For example, Figure 27 indicates that a radius of 250 m (4.0 km^{-1}) could have a design superelevation rate of 4, 6, or 8 percent (if the agency recognizes these three rates as acceptable maximum rates). Fortunately, this overlap only occurs for smaller radii; unique values of rate and radius will always exist for the larger radii. In fact, unique values will always exist if the agency allows only one maximum superelevation rate.

The recommended distribution is shown in Figure 27 as being "stair-stepped" to illustrate the range of feasible radii for integer superelevation rates. In this regard, it is also recommended that the presentation of superelevation rate-radius guidance in the *Green Book* be based on integer superelevation rates (e.g., 3, 4, 5 percent) and a corresponding range of applicable radii. Values at each stair "corner" represent the application of Equation 28 to compute the radius R twice; once using $e_d - 0.5\%$ and then again using $e_d + 0.5\%$. This approach corresponds to a superelevation rate precision of ±0.5 percent.

There are two advantages to using integer superelevation rates. First, they yield unique combinations of rate and radius for a given design speed; thus, they promote design consistency. Second, integer superelevation rates are more consistent with the limits of cross slope construction tolerance.

There is one exception to the recommended use of integer superelevation rates. For higher speeds, it is recommended that the precision be reduced to ± 0.25 percent such that superelevation rates of 2.5, 3.5, 4.5, 5.5, and 6.5 percent may also be used. This modification is intended to ensure unique radius and superelevation combinations. In other words, if 2.5 percent were not used to define a range of radii for 90 km/h, the

resulting radius ranges for integer rates of 2 and 3 percent would overlap with those for 80 and 100 km/h speeds.

The use of integer superelevation rates is not expected to have an adverse impact on curve speed. This expectation is based on an examination of the relationship between speed change, superelevation rate precision, and radius. Specifically, Equation 2 was differentiated to determine the desired relationship. The resulting equation is as follows:

$$dv = \frac{gR}{200v} de \tag{30}$$

This equation indicates that a superelevation precision de of ± 0.5 percent equates to a variation in speed dv of less than ± 4 km/h over the range of typical radii and design speed combinations. Moreover, the speed variation is less than ± 1.5 km/h for sharper radii (which are of greater concern from the standpoint of safety and operations). In other words, a driver's speed would be essentially indifferent to the use of a 6.0 or 7.0 percent superelevation rate (or any other pair of rates that differ by no more than 1.0 percent) on a sharp curve. The use of a precision of ±0.025 percent for smaller superelevation rates reduces the aforementioned speed variation by 50 percent.

Tables 19 and 20 represent the recommended superelevation distribution tables for RHS facilities. Table 19 presents superelevation rate and radius combinations for high-speed streets and highways. Table 20 presents combinations for low-speed rural highways (low speed is defined herein as design speeds between 30 and 70 km/h). The radius ranges in each table are designed to yield the desired unique relationship among speed, radius, and rate. The only exception to this trend is with the combination of low superelevation rates and high speeds; however, the degree of range overlap in radius is minimal.

In general, the radii in the columns labeled "High" and "Low" define the maximum and desirable minimum radii for a given 95th percentile approach speed and superelevation rate. Radii in each range represent the horizontal part of a "step" in the stair-stepped form of the distribution. If the superelevation rate coincides with the imposed maximum superelevation rate, then the radius provided in the column labeled "Min. $dv = x$" (where $x = 3$, 4, or 5) can be considered the minimum acceptable radius. Thus, for superelevation at the maximum rate, the range of candidate radii is thereby expanded to include all radii from the "High" value to the "Min. $dv = x$" value. Radii equal to the "Min. $dv = x$" value have superelevation and side friction at their maximum

TABLE 19 Superelevation distribution table for high-speed streets and highways

Super-elevation Rate e_d (%)	95th Percentile Approach Speed (km/h)																			
	80				90				100				110				120			
	Range of Design Radii (m)																			
	High	Low	dv=0	Min. dv=3	High	Low	dv=0	Min. dv=3	High	Low	dv=0	Min. dv=3	High	Low	dv=0	Min. dv=4	High	Low	dv=0	Min. dv=5
NC	tan.	2,520	--	--	tan.	3,189	--	--	tan.	3,937	--	--	tan.	4,746	--	--	tan.	5,521	--	--
2	2,520	2,139	--	--	3,189	2,714	--	--	3,937	3,356	--	--	4,746	4,053	--	--	5,521	4,727	--	--
2.5	2,139	1,619	--	--	2,714	2,062	--	--	3,356	2,557	--	--	4,053	3,097	--	--	4,727	3,628	--	--
3	1,619	1,283	--	--	2,062	1,640	--	--	2,557	2,039	--	--	3,097	2,475	--	--	3,628	2,911	--	--
3.5	1,283	1,052	--	--	1,640	1,348	--	--	2,039	1,680	--	--	2,475	2,043	--	--	2,911	2,411	--	--
4	1,052	884	378	268	1,348	1,136	556	385	1,680	1,418	820	526	2,043	1,727	1,232	682	2,411	2,044	1,935	875
4.5	884	757	--	--	1,136	975	--	--	1,418	1,219	--	--	1,727	1,488	--	--	2,044	1,765	--	--
5	757	618	--	--	975	798	--	--	1,219	1,065	--	--	1,488	1,301	--	--	1,765	1,547	--	--
5.5	--	--	--	--	--	--	--	--	1,065	941	--	--	1,301	1,151	--	--	1,547	1,372	--	--
6	618	490	329	241	798	635	474	341	941	797	679	461	1,151	1,030	979	591	1,372	1,230	na	750
6.5	--	--	--	--	--	--	--	--	--	--	--	--	1,030	929	--	--	1,230	1,111	--	--
7	490	402	--	--	635	522	--	--	797	657	--	--	929	806	--	--	1,111	967	--	--
8	402	337	291	218	522	440	412	306	657	554	579	409	806	682	na	521	967	820	na	656
9	337	289	--	--	440	377	--	--	554	477	--	--	682	587	--	--	820	708	--	--
10	289	251	261	200	377	329	365	277	477	416	na	369	587	513	na	467	708	620	na	583
11	251	222	--	--	329	290	--	--	416	368	--	--	513	454	--	--	620	550	--	--
12	222	197	na	184	290	259	na	254	368	335	na	335	454	422	na	422	550	525	na	525

[1] NC: normal cross slope (2.0 percent assumed).

[2] "High": maximum radius for corresponding superelevation rate and design speed. "Low": desirable minimum radius. "dv=0": smallest radius for which there is no speed reduction. "Min. dv=x": minimum radius at maximum superelevation and side friction; corresponds to a speed reduction of x km/h. "na": radii between the High and Low values are associated with some speed reduction. "tan.": tangent section (i.e., infinite radius).

[3] All superelevation rate and radius combinations in this table represent preferable values for turning roadways.

TABLE 20 Superelevation distribution table for low-speed rural highways

Super-elevation Rate e_d (%)	95th Percentile Approach Speed (km/h)																			
	30				40				50				60				70			
	Range of Design Radii (m)																			
	High	Low	dv=0	Min. dv=3	High	Low	dv=0	Min. dv=3	High	Low	dv=0	Min. dv=3	High	Low	dv=0	Min. dv=3	High	Low	dv=0	Min. dv=3
NC	tan.	354	--	--	tan.	630	--	--	tan.	984	--	--	tan.	1,417	--	--	tan.	1,929	--	--
2	354	243	--	--	630	443	--	--	984	704	--	--	1,417	1,025	--	--	1,929	1,406	--	--
3	234	137	--	--	443	261	--	--	704	425	--	--	1,025	629	--	--	1,406	873	--	--
4	137	89	31	21	261	176	60	43	425	291	104	76	629	437	166	121	873	612	254	183
5	89	64	--	--	176	128	--	--	291	216	--	--	437	326	--	--	612	460	--	--
6	64	48	29	20	128	98	55	40	216	168	94	70	326	256	149	111	460	363	224	166
7	48	37	--	--	98	79	--	--	168	135	--	--	256	208	--	--	363	297	--	--
8	37	30	27	19	79	64	51	37	135	112	86	64	208	173	134	102	297	249	201	152
9	30	25	--	--	64	54	--	--	112	95	--	--	173	148	--	--	249	212	--	--
10	25	21	25	18	54	46	47	35	95	82	79	60	148	128	123	94	212	184	182	140
11	21	18	--	--	46	40	--	--	82	71	--	--	128	112	--	--	184	162	--	--
12	18	17	na	17	40	35	na	33	71	63	na	56	112	99	na	88	162	144	na	129

[1] NC: normal cross slope (2.0 percent assumed).
[2] "High": maximum radius for corresponding superelevation rate and design speed. "Low": desirable minimum radius. "dv=0": smallest radius for which there is no speed reduction. "Min. dv=x": minimum radius at maximum superelevation and side friction; corresponds to a speed reduction of x km/h. "na": radii between the High and Low values are associated with some speed reduction. "tan.": tangent section (i.e., infinite radius).
[3] All superelevation rate and radius combinations shown in this table represent preferable values for turning roadways.
[4] A rate of 4.0, 6.0, 8.0, or 10 percent is considered the desirable maximum superelevation rate for low-speed turning roadways.

design levels. These radii yield average speed reductions of 3, 4, or 5 km/h, as indicated by the variable x.

The column labeled "dv = 0" defines the smallest radius associated with no speed reduction. The range of radii between the values in the columns labeled "dv = 0" and "Min. dv = x" are associated with speed reductions from 0 to x km/h (where x = 3, 4, or 5). For the higher superelevation rates, the range of radii denoted by the "High" and "Low" columns lies within the range of radii associated with a speed reduction. In this situation, there is no radius available that is associated with a "zero" speed reduction; this condition is identified with the notation "na." In general, radii associated with a speed reduction should be avoided for downgrades of 5 percent or more on facilities with significant truck traffic. This guidance is based on the fact that braking associated with speed reduction and with speed maintenance on downgrade effectively consume some of the friction supply. In combination, these factors can significantly reduce the friction margin of safety (especially for trucks).

As noted in Chapter 2, "Effect of Lateral Shift on the Travel Path Radius," the effective radius of the travel path may be larger than that of the roadway curve. This condition is limited to relatively short curves and may not occur frequently in practice. However, if the curve length is less than 140 m, the effective path radius may be much larger than that of the roadway. If this situation exists, the effective radius can be computed as the sum of the roadway curve radius and the increase-in-radius dr (from Equation 3). This effective radius may be considered during the selection of an appropriate superelevation rate from Table 19 or 20.

To illustrate the use of Tables 19 and 20, consider a highway with a 95th percentile approach speed of 110 km/h and an imposed maximum superelevation rate of 6.0 percent. If a radius of 2,000 m is being used by the designer, Table 19 indicates that the design radius lies in the range of 1,727 to 2,043 m which corresponds to a superelevation rate of 4.0 percent. However, if a radius of 900 m is needed, then the design superelevation rate will be limited by the 6.0 percent imposed rate. Because this value is smaller than the "dv = 0" radius of 979 m, a speed reduction will be incurred by motorists. This reduction can be estimated as 0.8 km/h by interpolation (= 4 * (979 – 900)/(979 – 591)). Alternatively, Equation 7 in Appendix A can be used to compute a curve design speed of 109.4 km/h, which corresponds to a speed reduction of 0.6 km/h. The minimum acceptable radius that could be considered for this design is 591 m, which would correspond to a curve design speed of 106 km/h (= 110 – 4).

Superelevation Distribution Method for LS Facilities

The *Green Book* distribution of superelevation rate for LS facilities (i.e., Method 2) is based on the desire to minimize superelevation in urban areas. As a result, this method maximizes side friction demand. Moreover, it does not share the

two deficiencies associated with Method 5 (as discussed in the previous section). Unlike the guidance for RHS facilities, the *Green Book* does not recommend values for the minimum-radius-with-normal-cross-slope R_{NC} and normal-cross-slope-rate e_{NC} controls for LS facilities.

The distribution method recommended herein is intended to minimize superelevation as well as to explicitly recognize the R_{NC} control. The recommended distribution method is based on providing superelevation equal to the minimum-superelevation-rate-based-on-the-95th-percentile-driver, as predicted by Equation 23. An acceptable speed reduction of 3.0 km/h is also recommended because this magnitude of reduction yields superelevation rates that are very nearly equivalent to those obtained from the *Green Book*'s Distribution Method 2.

It is also recommended that the maximum superelevation rates currently used by the state DOTs (i.e., 4.0 and 6.0 percent) be imposed on the recommended distribution. If Equation 23 yields a superelevation rate larger than the imposed maximum superelevation rate, then the latter rate would be used instead of that obtained from Equation 23. The recommended distribution is shown in Figure 28 for a 95th percentile approach speed of 70 km/h and an acceptable speed reduction of 3.0 km/h.

The recommended distribution shown in Figure 28 is "stair-stepped" to illustrate the range of feasible radii for integer superelevation rates. As discussed previously, it is recommended that integer superelevation rates be used for design purposes. It should be noted that the "stair-steps" are

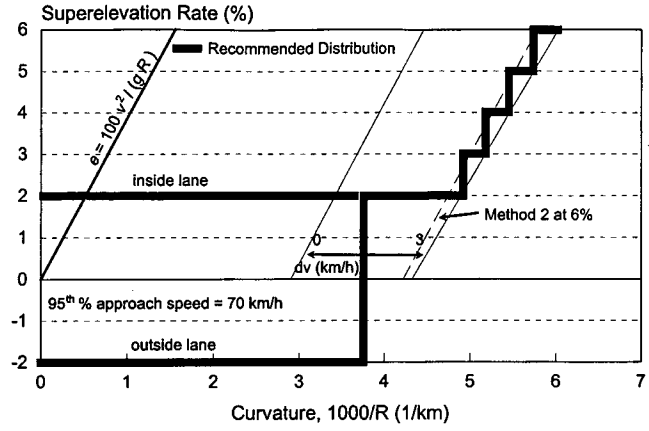

Figure 28. Recommended superelevation distribution for LS facilities.

positioned such that no one rate and radius combination yields a side friction demand that exceeds the maximum design side friction factor.

The recommended superelevation distribution table for LS facilities is provided in Table 21. The radius ranges in each table are designed to yield the desired unique relationship among speed, radius, and rate.

The use of Table 21 follows that for Tables 19 and 20. In general, the radii in the columns labeled "High" and "Low" define the range of desirable radii for a given 95th percentile approach speed and superelevation rate. The column labeled

TABLE 21 Superelevation distribution table for low-speed urban streets

Super-elevation Rate e_d (%)	95th Percentile Approach Speed (km/h)																			
	30				40				50				60				70			
	Range of Design Radii (m)																			
	High	Low	dv=0	Min. dv=3	High	Low	dv=0	Min. dv=3	High	Low	dv=0	Min. dv=3	High	Low	dv=0	Min. dv=3	High	Low	dv=0	Min. dv=3
NC	tan.	28	--	--	tan.	57	--	--	tan.	102	--	--	tan.	169	--	--	tan.	266	--	--
2	28	23	--	--	57	47	--	--	102	83	--	--	169	134	--	--	266	205	--	--
3	23	22	--	--	47	45	--	--	83	79	--	--	134	127	--	--	205	193	--	--
4	22	21	na	21	45	43	na	43	79	76	na	76	127	121	na	121	193	183	na	183
5	21	21	--	--	43	42	--	--	76	72	--	--	121	116	--	--	183	174	--	--
6	21	20	na	20	42	40	na	40	72	70	na	70	116	111	na	111	174	166	na	166
7	20	19	--	--	40	39	--	--	70	67	--	--	111	106	--	--	166	159	--	--
8	19	19	na	19	39	37	na	37	67	64	na	64	106	102	na	102	159	152	na	152
9	19	18	--	--	37	36	--	--	64	62	--	--	102	98	--	--	152	146	--	--
10	18	18	na	18	36	35	na	35	62	60	na	60	98	94	na	94	146	140	na	140

1 NC: normal cross slope (2.0 percent assumed)

2 "High": maximum radius for corresponding superelevation rate and design speed. "Low": desirable minimum radius. "dv=0": smallest radius for which there is no speed reduction. "Min. dv=3": minimum radius at maximum superelevation and side friction; corresponds to a speed reduction of 3 km/h. "na": radii between the High and Low values are associated with some speed reduction. "tan.": tangent section (i.e., infinite radius).

3 All superelevation rate and radius combinations shown in this table represent *acceptable* values for turning roadways. They should be considered when adverse impacts to adjacent property drainage or the frequency of slow-moving vehicles are important reasons to be conservative in the use of superelevation. It is also acceptable to consider the rates and radii in this table for the terminal sections of low-speed turning roadways, especially those with a significant number of trucks.

4 A rate of 4.0 or 6.0 percent is considered the desirable maximum superelevation rate for low-speed urban streets.

"$dv = 0$" is not used in Table 21 because all radii shown are associated with a speed reduction of about 3 km/h. In fact, the radii in the columns labeled "Low" and "Min. $dv = 3$" are equal because both are based on a 3 km/h speed reduction.

The effective radius of the travel path may be larger than that of the roadway curve. In particular, if the curve length is less than 140 m, the effective path radius may be much larger than that of the roadway. If this situation exists, the effective radius can be computed as the sum of the roadway curve radius and the increase-in-radius dr (from Equation 3). This effective radius may be considered during the selection of an appropriate superelevation rate from Table 21.

To illustrate the use of Table 21, consider an urban street with a 95th percentile approach speed of 60 km/h and an imposed maximum superelevation rate of 6.0 percent. If a radius of 120 m is used by the designer, Table 21 indicates that the design radius lies in the range of 116 to 121 m, which corresponds to a superelevation rate of 5.0 percent. An average speed reduction of 3.0 km/h will be incurred by motorists. A better estimate of the speed reduction can be obtained using Equation 7 in Appendix A. This equation indicates that the speed reduction will be about 2.6 km/h, which would correspond to a curve design speed of 57.4 km/h (= 60 – 2.6).

Superelevation Distribution Method for TR Facilities

The *Green Book* distribution of superelevation rate for TR facilities is not as clearly defined as that for RHS or LS facilities. As described previously for Table 5, the *Green Book* authors offer a relatively wide range of superelevation rates for low-speed TR facilities. Examination of these ranges for radii from 75 to 1,000 m indicates that the recommended rates tend to vary between rates that would be obtained from Distribution Methods 1 and 2. However, guidance in the *Green Book* (*1*, p. 729) indicates that preference should be given to rates near those obtained from Method 1. Hence, preference is given to the more generous application of superelevation.

Guidance in the *Green Book* for high-speed TR facilities emphasizes interchange ramp design. In contrast, high-speed intersection curve design is not discussed in the *Green Book*. For high-speed interchange ramps, the *Green Book* authors indicate that superelevation rate Tables III-7 through III-11 are appropriate for ramp design. Thus, the recommended superelevation rates for these facilities are based on Distribution Method 5.

The distribution method recommended herein for TR facilities complies with the *Green Book* authors' general guidance, as summarized in Chapter 2. However, the recommended distribution also provides more consistency among the three facility types in terms of their distribution methods and underlying controls. Finally, the recommended distribution method includes all types of low- and high-speed TR facilities. It should also be noted that maximum superelevation rates for TR facilities are limited to 4, 6, 8, or 10 percent (as described for Table 4).

It is recommended that the distribution method recommended for RHS facilities (i.e., Tables 19 and 20) be considered for use with TR facilities. For low-speed TR facilities, it should be considered acceptable to use the distribution method recommended for LS facilities (i.e., Table 21) when adverse impacts to adjacent property drainage or the frequency of slow-moving vehicles are important reasons to be conservative in the use of superelevation. It is also acceptable to consider the rates and radii in Table 21 for the terminal sections of low-speed turning roadways, especially those with a significant number of trucks.

As indicated in Equation 20, drivers on turning roadways have a reduced sensitivity to speed reduction. The result of this reduced sensitivity is that the speed reductions cited for RHS and LS facilities are effectively doubled when the corresponding distributions are applied to TR facilities. Thus, the 3-km/h speed reduction cited in the preceding sections would be effectively equivalent to a 6-km/h speed reduction for a TR facility. To illustrate, consider a superelevation rate and radius combination selected from the RHS (or LS) distribution that is associated with a 2.5-km/h speed reduction. If this rate and radius were applied to a turning roadway, it would result in a speed reduction of about 5 km/h.

Evaluation of Existing Horizontal Curves

The controls developed in the preceding sections (e.g., $e_{min,95}$, $e_{max,5}$, R_{min}) can be used to evaluate the geometry of an existing horizontal curve. It is recognized that a wide range of superelevation rates can adequately serve traffic for a given combination of speed and radius. Curves having rates other than those recommended in Tables 19, 20, and 21 do not necessarily have poor or unsafe operating conditions; however, they may not be consistent with the driver's expectation.

The evaluation can be based on the concepts described for Figure 24. Specifically, Equations 23 through 27 can be used to define the minimum and maximum superelevation rates for a given speed and radius (Figures 24, 25, and 26 illustrate the use of these equations for design speeds of 70, 30, and 110 km/h, respectively). Existing curves that have a superelevation rate falling between the minimum and maximum rates (i.e., that fall in Regions A or B) should provide acceptable operating conditions for a large majority of drivers and, as a result, not require reconstruction. Those curves that do not satisfy the minimum and maximum rates (i.e., those in Regions C, D, and E) may have an undesirable operational character. The existence of this condition should be verified and, if confirmed, steps should be taken to modify the curve's superelevation rate or radius to eliminate the undesirable characteristics.

CONTROLS FOR SUPERELEVATION TRANSITION DESIGN

This section describes the recommended guidance and controls for the design of the superelevation transition section that is associated with a horizontal curve. Specifically, the following controls are discussed in this section:

- Minimum Length of Superelevation Runoff
- Minimum Length of Tangent Runout
- Portion of Runoff Prior to the Curve
- Limiting Superelevation Rates
- Minimum Transition Grades

The findings reported in Chapter 2 indicate that state DOTs and international agencies are using many different controls to establish critical superelevation transition design dimensions. An examination of the effect of these control values on a vehicle's lateral motion while in the transition section indicates that many alternative combinations of these controls exist that yield similar operational performance. Hence, other factors were considered with regard to defining the most suitable combination of control values for transition design. Factors considered include drainage, comfort, safety, and appearance. The recommended superelevation transition controls described in this section reflect the results of this examination.

The most fundamental recommendation is that the superelevation transition controls described in this chapter be applied to all three facility types. In other words, it is recommended that no distinction be made between the different facility types in transition design. It has been noted that many state DOTs are currently applying this concept in their design practice. The primary advantage of the recommended approach is design consistency. It also has the advantage of simplicity in terms of the universal application of common design methods for all facility types.

Minimum Length of Superelevation Runoff

This section describes the recommended method for determining the minimum runoff length for the "tangent-to-curve" design. As noted in Chapter 2, this term is used herein to refer to the situation where compound or spiral curvature is not used in the transition. Thus, in the tangent-to-curve design, the tangent section of the alignment intersects directly with the horizontal curve. Recommended controls for runoff length, when used with a spiral curve transition, are provided in "Length of Spiral."

In general, the recommended method for determining superelevation runoff length is based exclusively on the gradient control. This control is intended to provide both a comfortable and aesthetically pleasing transition design. It is also recommended that the gradient-based runoff length be adjusted for number-of-lanes-rotated, as is currently recommended by the *Green Book* authors. Research by Good (*16*) indicates that this adjustment is helpful for minimizing steering effort. Finally, it is recommended that the travel time control not be considered when selecting runoff length. The rationale for these recommendations is provided in the subsequent paragraphs.

Gradient Control

The *Green Book* authors indicate that, for appearance and comfort, the length of superelevation runoff should be based on a maximum acceptable difference between the longitudinal grades of a two-lane roadway's centerline and edge of pavement (*1*, p. 177). More generally, it is the difference between the longitudinal grades of the axis of rotation (e.g., centerline, profile grade line) and the edge of pavement opposite this axis. Current practice is to limit this difference, referred to as the maximum relative gradient, to a value of 0.75 percent for two-lane roadways. However, to reflect a sensitivity to speed (in terms of travel time through the transition) this limiting maximum relative gradient is decreased for the higher design speeds.

The maximum relative gradients provided in *Green Book* Table III-13 are also used herein to determine the minimum runoff length. As noted for Figure 11, the gradients in the 1994 *Green Book* tend to have a flatter slope and a significant "break" in this slope at 80 km/h, relative to prior editions. It is recommended that the gradients for the higher speeds be adjusted slightly to improve their consistency with the gradients provided in previous editions of the *Green Book*. The recommended maximum relative gradients are listed in Table 22.

Travel Time Control

The *Green Book* advises that the runoff length equal or exceed 2.0 s travel time at the design speed. Research into the basis for this travel time control and its resulting effect on road drainage and driver behavior indicate that it should not be used to define runoff length for the tangent-to-curve transition design. The exclusion of this control is based on the following findings:

1. The *Green Book* authors do not discuss the need for a travel time control for LS or TR facilities.
2. Several state DOTs do not use the travel time control for defining runoff length.
3. According to the *Green Book* authors, the "appearance" aspect of runoff length is provided through the use of the gradient control (*1*, p. 177).
4. Most international highway agencies do not recommend consideration of a travel time control.
5. The travel time control tends to aggravate drainage problems in the transition section by dictating long runoff lengths.

TABLE 22 Maximum relative gradients

95th Percentile Approach Speed (km/h)	Maximum Relative Gradient (%)	Equivalent Maximum Relative Slope
30	0.75	1:133
40	0.70	1:143
50	0.65	1:150
60	0.60	1:167
70	0.55	1:182
80	0.50	1:200
90	0.47	1:213
100	0.44	1:227
110	0.41	1:244
120	0.38	1:263

6. The analysis of lateral motion conducted for this research indicates that the travel time control is only helpful in some situations (and then only in a very small way) for minimizing lateral velocity and shift at the end of the transition section.
7. The *Green Book* guidance on vertical curve length for the edge-of-pavement profile indicates that smooth profiles can be attained when the runoff length is less than 1.0 s travel time.

An analysis of accelerations acting on the motorist in the transition section was conducted to assess the effect of runoff length on driver comfort. This analysis considered both the change in lateral acceleration and the magnitude of rotational acceleration experienced by motorists as a result of the transition. The results of this analysis indicate that the change in lateral acceleration because of superelevation is less than 0.3 m/s^3, which is about one-third of the value considered acceptable for spiral curve transition design. The results also indicate that rotational acceleration is negligibly small (i.e., less than 0.01 m/s^2).

The analysis of accelerations also focused on the effect of travel time control on lateral acceleration. This analysis indicated that the lateral and rotational acceleration increased slightly when the travel time control was not considered. However, as noted in the preceding paragraph, the accelerations are both very small for typical designs. These findings led to the conclusion that a minimum runoff length based on the gradient control is still likely to be comfortable, even if this length is shorter than 2.0 s travel time. Finally, it should be noted that simulation studies by Glennon et al. (*14*) indicate that peak side friction demands are *lower* when the runoff length is shorter than that recommended by the *Green Book* (lengths as short as 1.2 and 1.5 s travel time were studied).

Recommended Minimum Runoff Length

It is recommended that the gradient control be used to establish runoff lengths for all facility types. An advantage of this approach is that runoff length for all facilities will have a similar sensitivity to superelevation rate and number of lanes rotated. These sensitivities are not reflected in the existing equations for computing runoff length for LS facilities. It may be due to this limitation that several state DOTs currently use the gradient control to define runoff length for LS facilities.

The following equation and associated table represent the recommended method of computing the minimum superelevation runoff length:

$$L_r = \frac{we_d}{\Delta} n_l b_w \tag{31}$$

where:

L_r = minimum length of superelevation runoff, m;
Δ = maximum relative gradient, percent;
b_w = adjustment factor for number of lanes rotated (as listed in Table 23);
w = width of one traffic lane (typically, 3.6 m), m; and
e_d = design superelevation rate, percent.

The adjustment factors listed in column 3 of Table 23 for 1, 2, and 3 lanes rotated are the same as those recommended in the *Green Book*. The factors for 2.5 and 3.5 lanes rotated have been included to expand the guidance for alternative cross sections. These factors were computed using an equation reported in the Washington DOT design manual (i.e.,

TABLE 23 Recommended adjustment factor for number of lanes rotated

Number of Lanes Rotated, n_l	Product of "$n_l b_w$"	Adjustment Factor, b_w
1	1.0	1.00
1.5	1.25	0.83
2	1.5	0.75
2.5	1.75	0.70
3	2.0	0.67
3.5	2.25	0.64

Note: For other values of n_l, use the equation $b_w = (1 + 0.5\ (n_l - 1)) \div n_l$.

Eq. 8). This equation was also used to compute the factor for 1.5 lanes rotated (i.e., 0.83). As a result, the computed value differs slightly from that recommended in the *Green Book* (i.e., 0.80).

The minimum superelevation runoff lengths obtained from Equation 31 are listed in Table 24. The lengths shown represent cases where one and two lanes are rotated about the pavement edge. The former case can be found on two-lane roadways where the pavement is rotated about the centerline or on one-lane interchange ramps where rotation is about an edge line. The latter case can be found on four-lane undivided roadways where the pavement is rotated about the centerline or on four-lane divided roadways where rotation is about an edge line.

In most cases, the runoff lengths shown in Table 24 are equivalent to those obtained using the guidance provided in the 1994 *Green Book*. The recommended maximum relative gradients (listed in Table 22) result in a 2.0 to 5.0 percent increase in runoff length, depending on speed. Lengths for the case of "1.5 lanes rotated" have increased about 4.0 percent because of the change in the adjustment factor b_w (i.e, from 0.80 to 0.83). Elimination of the travel time control has resulted in shorter lengths for smaller superelevation rates or for higher speeds. However, even the shortest lengths (corresponding to a superelevation rate of 2.0 percent) have travel times of 0.6 s or more. This length is about twice that needed for a smooth edge-of-pavement profile using a parabolic vertical curve at the beginning and end of the transition.

The minimum runoff length obtained from Equation 31 should be considered a "desirable" minimum value. Values for the portion-of-runoff-located-prior-to-the-curve control, discussed in "Portion of Runoff Prior to the Curve," are derived to be consistent with the runoff lengths obtained from Equation 31. If larger lengths are used, Equation 12 can be used to compute a more appropriate value of the "portion" control. In general, larger values of the portion control are helpful for larger runoff lengths.

Minimum Length of Tangent Runout

Based on the review of *Green Book* guidance and state DOT practice, it is recommended that the relative gradient used within the superelevation runoff be maintained through the tangent runout section. This approach has the advantage of maintaining a smooth pavement edge throughout the transition section. When the travel time control is not used to define runoff length, this recommendation is entirely consistent with *Green Book* guidance. The following equation represents the recommended method of computing the minimum tangent runout length:

$$L_t = \frac{e_{NC}}{e_d} L_r \tag{32}$$

where:

L_t = minimum length of tangent runout, m; and
e_{NC} = normal cross slope rate, percent.

The tangent runout lengths obtained from Equation 32 are listed in Table 24.

TABLE 24 Recommended minimum superelevation runoff and runout lengths[1]

Design Element	Superelevation Rate (%)	95th Percentile Curve Speed (km/h)									
		30	40	50	60	70	80	90	100	110	120
One Lane Rotated											
Runoff	2	10	10	11	12	13	14	15	16	18	19
	4	19	21	22	24	26	29	31	33	35	38
	6	29	31	33	36	39	43	46	49	53	57
	8	38	41	44	48	52	58	61	65	70	76
	10	48	51	55	60	65	72	77	82	88	95
	12	58	62	66	72	79	86	92	98	105	114
Runout[2]	any	10	10	11	12	13	14	15	16	18	19
Two Lanes Rotated											
Runoff	2	14	15	17	18	20	22	23	25	26	28
	4	29	31	33	36	39	43	46	49	53	57
	6	43	46	50	54	59	65	69	74	79	85
	8	58	62	66	72	79	86	92	98	105	114
	10	72	77	83	90	98	108	115	123	132	142
	12	86	93	100	108	118	130	138	147	158	171
Runout[2]	any	14	15	17	18	20	22	23	25	26	28

[1] Based on 3.6-m lanes and the maximum relative gradients listed in Table 22.
[2] Based on a 2.0 percent normal cross slope rate.

TABLE 25 Recommended portion of runoff located prior to the curve[1,2]

95th Percentile Approach Speed (km/h)	No. of Lanes Rotated			
	1.0	1.5	2.0–2.5	3.0–3.5
30–70	0.80	0.85	0.90	0.90
80–120	0.70	0.75	0.80	0.85

[1] Values shown should adequately serve drivers traveling at the 5th percentile and higher speeds.
[2] Values shown are based on the maximum relative gradients listed in Table 22.

Portion of Runoff Prior to the Curve

As discussed in Chapter 2, the portion of superelevation runoff located prior to the beginning of the curve P_r has a significant influence on a vehicle's lateral velocity and lane position at the end of the transition. Values of P_r that minimize lateral velocity and shift for both travel directions were developed and presented in Table 13.

The methods used to develop Table 13 were also used to develop the recommended values of P_r shown in Table 25. The values listed in this table are suitable for a range of design speeds and number-of-lanes-rotated. It should be noted that these values are consistent with the range of values recommended in the *Green Book* as well as the findings of previous research projects (*14,15*).

Limiting Superelevation Rates

An analysis of the vehicle's lateral motion when traveling through the transition section was conducted using the models described in Appendix D. This analysis indicated that upper limits of superelevation rate existed for the lower range of 95th percentile speeds. Superelevation rates in excess of this limiting value would likely be associated with a lateral shift of 1.0 m or more when driven at speeds in excess of the 95th percentile speed. The recommended limiting superelevation rates are listed in Table 26.

It is recommended that superelevation rates larger than the limiting rates listed in Table 26 be avoided when possible. If rates larger than these limits are used, some consideration should be given to increasing the width of the traveled way along the curve to minimize encroachment into the adjacent lane or shoulder.

Minimum Transition Grades

Two pavement surface drainage problems were described in Chapter 2, "Issues Related to Pavement Drainage," as being of significant concern in the transition section. One problem concerns the lack of adequate longitudinal grade along both the roadway centerline and the edge of pavement. The other problem concerns inadequate lateral drainage because of negligible cross slope during pavement rotation.

Two techniques were recommended by several international agencies to minimize transition drainage problems. One technique is to use a minimum centerline grade in the transition section. The second technique ensures a minimum edge of pavement grade in the transition section. Based on this review of international practice, the following grade controls are recommended (based primarily on guidance in Reference 5):

1. A minimum centerline grade of 0.5 percent should be maintained through the transition section.
2. A minimum edge of pavement grade of 0.2 percent (0.5 percent for curbed streets) should be maintained through the transition section.

The second grade control is equivalent to the following series of equations relating centerline grade and effective maximum relative gradient:

$$\begin{aligned} G &\le -\Delta^* - 0.2 \\ G &\ge -\Delta^* + 0.2 \\ G &\le \Delta^* - 0.2 \\ G &\ge \Delta^* + 0.2 \end{aligned} \quad (33)$$

where:

G = roadway grade, percent; and
Δ^* = effective maximum relative gradient (computed with Equation 6), percent.

The value of "0.2" represents the minimum edge of pavement grade for uncurbed highways (in percent). If Equation 33 is applied to curbed streets, it is recommended that the value "0.2" be replaced with "0.5".

TABLE 26 Recommended upper limit superelevation rates for low-speed facilities

	95th Percentile Approach Speed (km/h)				
Limiting Superelevation Rate (%)[1,2]	30	40	50	60	70
	8.2	9.8	10.8	11.4	11.8

[1] Values shown should adequately serve drivers traveling at the 95th percentile and lower speeds.
[2] Values are only applicable to tangent-to-curve transition designs.

To illustrate the combined use of the two grade controls, consider an uncurbed highway curve having an effective maximum relative gradient of 0.65 percent in the transition section. The first control would exclude centerline grades between – 0.50 and + 0.50 percent. The second grade control would exclude grades in the range of – 0.85 to – 0.45 percent (via the first two components of Equation 33) and those in the range of 0.45 to 0.85 percent (via the last two components of Equation 33). Given the overlap between the ranges for Controls 1 and 2, the centerline grade within the transition would have to equal or exceed ± 0.85 percent to satisfy both controls and provide adequate road surface drainage.

CONTROLS FOR ALIGNMENT TRANSITION DESIGN

This section describes the recommended guidance and controls for the design of the alignment transition section that is associated with a horizontal curve. Specifically, the following controls are discussed in this section:

- Maximum Radius for Use of a Spiral Curve Transition
- Minimum Length of Spiral Curve Transition
- Maximum Length of Spiral Curve Transition
- Desirable Length of Spiral Curve Transition

The review of practice described in Chapter 2 indicated that there is a lack of consensus on spiral curve transition use and design. Many different controls are currently being used to identify conditions suitable for spiral use. Similarly, many controls are being used to identify limiting values for the length of this spiral. The literature review indicated that spirals may have a safety benefit but only when used with the sharpest horizontal curves. A kinematic analysis of the vehicle's lateral motion in the transition indicated that excessively short and excessively long spirals have a negative influence on vehicle operations. These findings and others were used to develop the recommended spiral curve transition guidance described in this section.

The most fundamental recommendation is that the spiral curve transition controls described in this section be applied to all three facility types. In other words, it is recommended that no distinction be made between the different facility types in the *Green Book* with regard to guidance on spiral curve transition design. The primary advantage of the recommended approach is design consistency. It also has the advantage of simplicity in terms of the universal application of a common design method for all facility types.

Guidance on the Use of Spiral Curve Transitions

General Guidance

The findings reported in Chapter 2 suggest that the spiral curve transition may offer some safety and operational benefit. Specifically, there is some evidence that spirals have a small safety benefit when used with sharp horizontal curves (*20,22,23*). There is also some evidence that spirals of moderate length can reduce the peak lateral acceleration experienced in the transition (see Figure 18). However, there is also evidence that spirals of excessive length can reduce safety (*18,24*). This evidence is not conclusive; however, it suggests that any effect a spiral is likely to have on safety and operations is relatively small and relegated to a narrow range of conditions.

In recognition of the aforementioned findings, it is recommended that the *Green Book* continue to recognize the use of spiral curve transitions. However, as a minimum, additional guidance should be provided that identifies the conditions where a spiral is likely to offer a tangible benefit, relative to the tangent-to-curve transition design. Guidance on spiral curve transition length is also needed for the purpose of ensuring a safe and comfortable design.

Maximum Radius for Use of a Spiral Curve Transition

Guidance regarding conditions suitable for a spiral curve transition are developed in this section; however, it is offered only as guidance to those agencies that desire to use spirals. This guidance is not intended to be used as a spiral "warrant."

The review of state DOT and international agency design guidelines indicated a general lack of consistency in identifying conditions suitable for use of a spiral curve transition. The trends shown in Figure 15 suggest that a maximum radius for use of a spiral curve transition could be conservatively defined by identifying the sharpest radii that satisfy most, if not all, of the criteria referenced in Figure 15. By this approach, all of the referenced agencies should agree that the resulting range of sharp radii are likely to benefit from the use of a spiral curve transition. The trends in Figure 15 suggest that the maximum radius associated with this "aggregate" (or "consensus") range be based on a parabolic relationship between speed and radius, as would be obtained by defining a "minimum centripetal acceleration." Such a relationship is represented by the following equation:

$$R_{s,\max} = \frac{(V_{a,95})^2}{13\,a_r} \tag{34}$$

where:

$R_{s,\max}$ = maximum radius for use of a spiral, m;
$V_{a,95}$ = 95th percentile approach speed, km/h; and
a_r = minimum centripetal acceleration (= 1.3 m/s^2).

The acceleration used to define the maximum radius should logically produce values that are consistent with the aggregate range. Moreover, the acceleration rate used should be associated with those sharper radii known to realize some

safety benefit from the use of spiral curve transitions. In this regard, Council (*22*) found that radii less than 600 m were associated with a safety benefit from the use of spirals. This range is consistent with the findings reported by Lamm et al. (*23*). A radius of 600 m and a design speed of 100 km/h, when combined with Equation 34, yields a minimum centripetal acceleration of 1.3 m/s^2.

Based on the aforementioned findings, a minimum centripetal acceleration of 1.3 m/s^2 is recommended for use in defining the maximum-radius-for-use-of-a-spiral control. The resulting relationship between speed and radius is shown in Figure 29.

The thick trend line in Figure 29 represents the maximum radius for use of a spiral curve transition, as predicted by Equation 34. Radii smaller than this maximum may benefit from the use of a spiral for reduced crash potential and reduced peak lateral acceleration (relative to the tangent-to-curve transition design). The shaded area represents the range of radii that can be considered for a given speed. The lower limit of this range corresponds to the minimum radius, as listed in Table 16. The trend line associated with this lower limit is based on an e_{max} of 8.0 percent; any other value of e_{max} (e.g., 4, 6, 10, or 12 percent) can be used to define this lower limit. Finally, the thin trend lines represent the range of guidance provided in previous editions of the *Green Book* and by various state DOTs. These trend lines were previously described for Figure 15 and are provided here for comparative purposes.

Length of Spiral

This section describes three controls that can be used to determine the length of the spiral curve transition. These controls include a minimum, maximum, and desirable length of spiral. Collectively, they can be used to provide a transition that is aesthetically pleasing, comfortable, and relatively safe.

Minimum Length of Spiral Curve Transition

Several international agencies define a minimum length of spiral based on consideration of motorist comfort and lateral shift. The comfort control is intended to produce a spiral length that allows for a comfortable increase in centripetal acceleration associated with the curve. The lateral shift control is intended to ensure that the spiral is long enough to provide a shift in the lane that is consistent with that produced by the vehicle's natural spiral path. It is recommended that these two controls be used together to determine the minimum length of spiral. This minimum spiral length can be computed as follows:

$$L_{s,\,min} = Larger\ of: \left[\sqrt{24 p_{min} R};\ 0.0214\frac{(V_{a,95})^3}{RC}\right] \quad (35)$$

where:

$L_{s,\,min}$ = minimum length of spiral, m;
p_{min} = minimum lateral offset between the tangent and circular curve (= 0.20 m).
R = radius of curve, m;
$V_{a,95}$ = 95th percentile approach speed, km/h; and
C = maximum rate of change in centripetal acceleration (= 1.2 m/s^3).

The first component of Equation 35 represents the lateral shift control; the second represents the comfort control.

Two controlling variable values have been specified for application of Equation 35. A value of 0.20 m is recommended for p_{min}. This value is consistent with the minimum lateral shift that occurs as a result of the natural steer behavior of most drivers. A value of 1.2 m/s^3 is recommended for C. This value represents the largest (or maximum) value that should be used, which is consistent with the intent of any upper limit control. The use of lower values will yield longer, more "comfortable"

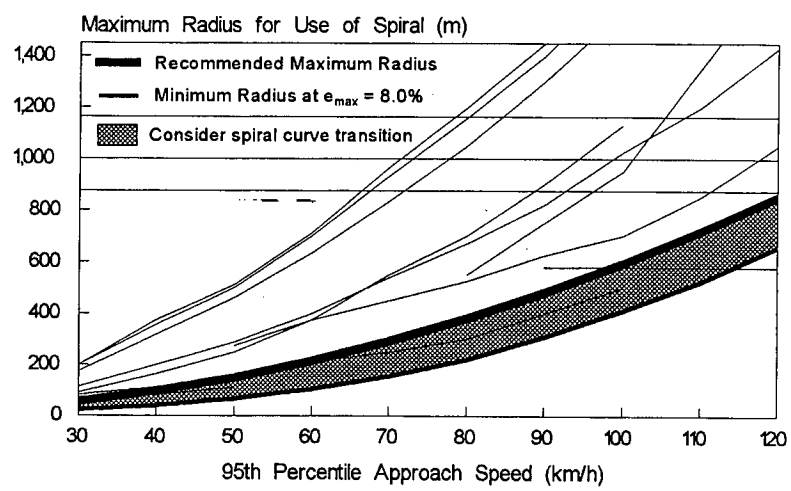

Figure 29. Maximum radius for use of a spiral curve transition.

lengths; however, these lengths would not represent the *minimum* length associated with the comfort limit.

Maximum Length of Spiral Curve Transition

Most international agencies recognize the need to limit spiral length. This need stems from safety problems occurring on longer spirals (relative to the length of the curve). These problems occur when the spiral is so long that the driver is misled about the sharpness of the impending curve. A conservative maximum length of spiral that avoids these problems can be computed as follows:

$$L_{s,\max} = \sqrt{24_{\max} R} \tag{36}$$

where:

$L_{s,\max}$ = maximum length of spiral, m; and
$p_{\max}$ = maximum lateral offset between the tangent and circular curve (= 1.0 m).

A value of 1.0 m is recommended for $p_{\max}$. This value is consistent with the maximum lateral shift that occurs as a result of the natural steer behavior of most drivers. It also provides a reasonable balance between the length of spiral and the radius of the curve.

Desirable Length of Spiral Curve Transition

The kinematic analysis of a vehicle's lateral motion in the transition section provided considerable insight about the effect of spiral length on vehicle operation. Specifically, the most desirable operating conditions were noted when the spiral length was approximately equal to the length of the "natural" spiral adopted by the driver during curve entry. Deviations between these two lengths may result in operational problems for a large lateral velocity or shift at the end of the transition section. Specifically, a large lateral velocity in an outward direction (relative to the curve) requires the driver to make a corrective steer maneuver that produces a path radius sharper than that of the roadway curve. Such a critical radius produces an undesirable increase in peak side friction demand. Moreover, a lateral velocity of sufficient magnitude to shift the vehicle into an adjacent lane (without corrective steering) is also undesirable for safety reasons.

The kinematic analysis considered the length of spiral curve transition needed by both slower and faster drivers. The results of this analysis indicated that the best overall operations were obtained when the length of spiral equaled 2.8 s travel time at the 5th percentile speed. This travel time is representative of the natural spiral path produced by the driver's steering motion; hence, it is referred to as the steering time control. Further consideration of these steering time and speed relationships indicated that the length obtained from the 5th percentile speed and 2.8 s steering time was equivalent to that obtained from the 95th percentile speed and 2.0 s steering time. Because the latter speed is consistent with design speed, the recommended desirable spiral length is based on 2.0 s travel time.

Based on the preceding discussion, the following equation represents the recommended method of computing the desirable length of spiral curve for transition design:

$$L_s = 2.0 \frac{V_{a,95}}{3.6} \tag{37}$$

where:

L_s = desirable length of spiral, m.

This control is intended to provide an operationally efficient and functionally safe transition design. Deviations from the desirable length will likely increase lateral acceleration, velocity, and shift. The spiral length obtained from this control should also define, and be physically concurrent with, the superelevation runoff length. The spiral lengths obtained from Equation 37 are listed in Table 27.

It should be noted that the desirable length obtained from Equation 37 does not supercede the minimum spiral lengths obtained from Equation 35. In some instances (e.g., lower design speeds and sharper radii), the minimum length obtained from Equation 35 will be slightly larger than the "desirable" value obtained from Equation 37. In these instances, the minimum length should be used for spiral design.

Spiral Length Comparison

The spiral lengths obtained from the steering time control were compared with the lengths obtained from the minimum and maximum spiral length controls described previously. The result of this comparison is shown in Figure 30. In gen-

TABLE 27 Recommended desirable length of spiral curve transition

	95th Percentile Approach Speed (km/h)									
Desirable Length of Spiral (m)	**30**	**40**	**50**	**60**	**70**	**80**	**90**	**100**	**110**	**120**
	17	22	28	33	39	44	50	56	61	67

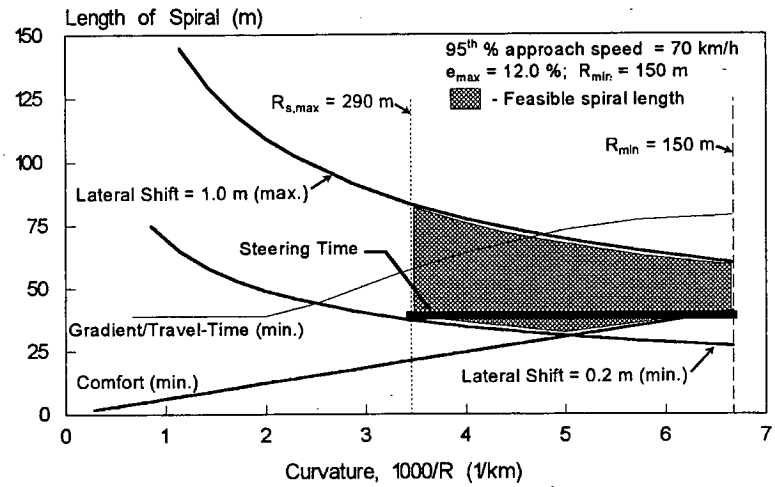

Figure 30. Comparison of minimum, maximum, and desirable spiral lengths.

eral, the trends in this figure suggest that the steering time control yields lengths that are within the range of maximum and minimum lengths—albeit at the shorter end of this range. In fact, the steering time control yields lengths that are effectively equal to those from the travel time control (it being based on 2.0 s at the design speed). The "feasible" region is limited on the left side by the maximum radius obtained from Equation 34.

CHAPTER 4

CONCLUSIONS AND SUGGESTED RESEARCH

CONCLUSIONS

Several conclusions have been reached as a result of this research. These conclusions relate to horizontal curve design, superelevation transition design, and alignment transition design. They are described in the following three sections.

This research also led to the formulation of several recommended revisions to the guidance provided in the 1994 edition of the *Green Book* (*1*). These recommendations were described in Chapter 3. They are also more formally presented in Appendix E, as recommended revisions to the *Green Book*. The material in Appendix E is offered to the AASHTO Task Force on Geometric Design for consideration and possible inclusion in the next update of the *Green Book*.

Conclusions for Horizontal Curve Design

The major conclusions of the research for horizontal curve design guidelines are as follows:

1. Drivers slow on sharp horizontal curves. The magnitude of their speed reduction reflects a compromise between a desire for a comfortable level of lateral acceleration and a desire to minimize travel time. From a curve design standpoint, designers should avoid curves that are so sharp that they promote a speed reduction. However, a nominal speed reduction of 3 to 5 km/h appears to be an acceptable compromise between driver comfort and the occasional need for sharp curvature.
2. Drivers have similar side friction demands when traveling on street and highway curves. Thus, the use of separate side friction factors for the design of curves on low- and high-speed urban streets does not appear justified. Differences among the *Green Book* design friction factors for each facility type are likely due to differences in (1) the average speed reduction at the facilities studied and (2) the method of measurement (e.g., test subject interview with inquiry about comfort/discomfort versus computation of the 95th percentile speed and friction demand of observed traffic streams).
3. In contrast to the observations noted in Item 2 above, drivers were observed to accept larger side friction demands when traveling on turning roadway curves, relative to street or highway curves with the same radius. The larger demand reflects a significantly larger speed differential that typically exists between the turning roadway and the through roadways it intersects.
4. Measurements of the side friction demands of both passenger car drivers and heavy truck drivers indicate that such demands are very nearly the same for the same speed and curve geometry. Truck drivers appear to have slightly lower friction demands than car drivers on low-speed facilities. The reverse of this trend is true for high-speed facilities.
5. Significant roadway grade depletes the friction supply available for cornering. This depletion results from the use of a portion of the friction supply to provide the necessary tractive or braking forces required to maintain speed on up or downgrades, respectively. The reduction in side friction supply reduces the margin of safety afforded vehicles traveling on horizontal curves on grade. The reduction in margin of safety is particularly significant for heavy trucks because of their greater weight and higher peak side friction demands.
6. A review of the design guidelines developed by several international transportation agencies indicates that a wide variety of superelevation distribution methods are being used. A comparison of the superelevation rates obtained from these distribution methods indicates that a wide range of rates can be used for the same design speed and radius. This finding, combined with additional analysis of the effect of superelevation on side friction demand, leads to the conclusion that there is considerable flexibility in the selection of an appropriate superelevation rate for a given roadway curve.
7. Superelevation Distribution Method 5, in combination with the use of multiple maximum superelevation rates, does not promote design consistency. Method 5 can yield different superelevation rates for the same speed and radius depending on the designer's choice of maximum superelevation rate. Field measurements at several curves in five states have revealed that this flexibility in design has resulted in superelevation rates ranging from a low of 2 percent to a high of 11 percent for the same 250-m radius design.
8. To achieve consistency in curve design, a superelevation distribution method is needed that provides a unique relationship among design speed, radius, and

superelevation rate. This type of distribution method was developed for this research and is described in Chapter 3.

Conclusions for Superelevation Transition Design

The major conclusions of the research for superelevation transition design guidelines are as follows:

1. A kinematic analysis of a vehicle's lateral motion within the transition section indicates that proper design of this section can minimize or eliminate lateral shift. This shift is manifest as a "drift" within the traffic lane; however, it is actually the result of unbalanced lateral accelerations acting on the vehicle as it travels through the transition. An outward shift is particularly troublesome because it requires a corrective steering action by the driver, which precipitates a "critical" path radius that is sharper than that of the curve. A critical radius is associated with a peak side friction demand that exceeds that intended by the designer.
2. The kinematic analysis of lateral motion indicated that larger superelevation rates, when used with a tangent-to-curve transition design, are sometimes associated with excessive lateral shift. Specifically, rates in excess of 8, 10, 11, 11, and 12 percent for 95th percentile approach speeds of 30, 40, 50, 60, and 70 km/h, respectively, are likely associated with shifts in excess of 1.0 m. The magnitude of shift for speeds of 80 km/h and greater are not likely to be excessive provided that the superelevation rate is 12 percent or less.
3. The kinematic analysis of lateral motion indicated that the portion of the superelevation runoff located prior to the curve can also influence the magnitude of lateral shift. The portion that minimizes this shift varies from 0.70 to 0.90 (i.e., 70 to 90 percent) and depends on speed and the number of lanes in the transition section.
4. A review of several state DOT design manuals and the guidelines developed by several international transportation agencies indicates that many of these DOTs and agencies are not maintaining a minimum superelevation runoff length equal to 2.0 s travel time at the design speed. Rather, these agencies are using controls that dictate runoff length based only on a maximum relative gradient or a maximum rate of pavement rotation. This finding and the results from a kinematic analysis of vehicle motion in the transition section indicate that adherence to the "travel time" control is not essential in tangent-to-curve transition design because it does not appear to improve motorist comfort or safety.
5. The *Green Book* does not explicitly address the topic of road surface drainage in the transition section. The warping of the roadway in this section can result in inadequate longitudinal or lateral slope for drainage purposes. Poorly drained road surfaces can result in a significant reduction in the friction supply during wet weather conditions. Inadequate drainage in the transition section is particularly hazardous because additional friction demands are placed on the tire-pavement interface during curve entry. Techniques that can be used to avoid drainage problems are described in Chapter 3.

Conclusions for Alignment Transition Design

The major conclusions of the research for alignment transition design guidelines are as follows:

1. A review of the literature on the safety and operational benefits of spiral curve transitions indicates that these benefits are small, relative to the use of tangent-to-curve transitions. These marginal benefits are likely to be one reason why so many state DOTs (estimated to exceed 70 percent) do not require the use of spirals.
2. A review of several state DOT design manuals and the guidelines developed by several international transportation agencies indicate that there is little consensus on the conditions suitable for use of a spiral curve transition. Studies have shown that unneeded or excessively long spirals can increase crash potential. Studies have also shown that, under certain conditions, spirals can decrease crash potential. Guidelines regarding conditions suitable for use of a spiral curve transition are described in Chapter 3.
3. There is evidence that spiral curve transition length can have a significant effect on operations and safety. Several international agencies have adopted controls that define both a maximum and a minimum spiral length. Excessively long spirals have been found to mislead drivers about the sharpness of the impending curve. Excessively short spirals were found to offer no significant operational benefit. A kinematic analysis of a vehicle's lateral motion while traveling along the spiral indicates that lateral shift in the lane can be minimized when the spiral length is equal to the motorist's steering time (i.e., about 2.0 s travel time). The spiral length selected for design must reflect all of the aforementioned considerations for its operational and safety benefits to be realized. Guidelines regarding minimum, maximum, and desirable spiral curve lengths are described in Chapter 3.

SUGGESTED RESEARCH

Several topics for future research were identified during the conduct of this research. These topics represent extensions to the research conducted for this report because they go beyond its scope. The suggested topics are briefly described

in this section. It is believed that this research will provide additional insight into the safe and efficient design of roadway curves for both new and existing alignments.

1. Additional research is needed regarding the extension of the guidelines developed for this research to "3R" (i.e., resurfacing, restoration, and rehabilitation) or minor reconstruction projects. Specifically, this research should examine the cost-effectiveness of any deviation from the recommended control values. The measure of effectiveness used should reflect impacts to both safety and operations.
2. The findings of this research indicate that transition design is dependent on many design controls and that alternative combinations of control values can yield similar levels of safety and comfort. In this regard, additional research is needed that (1) evaluates the effect of a sub-optimal control value on safety and operations and (2) identifies alternative combinations of control values that provide similarly acceptable operating conditions. Such information could be useful when evaluating existing curve designs.
3. Additional research is needed regarding driver steer behavior during curve entry, because this behavior is affected by the transition design and curve geometry. The focus of this research should be on (1) defining the relationship between geometry and steer behavior and (2) quantifying the effect of this behavior on vehicle stability and control. The kinematic model developed for this research (described in Appendix D) could form the basis for further research. However, it is recommended that additional field data be collected to refine its formulation and validate its predictive ability.
4. Currently available vehicle simulation models (e.g., highway-vehicle-object simulation model [HVOSM] and PHASE 4) do not appear to have sufficiently detailed driver-control algorithms to permit an accurate assessment of the effect of transition design or curve geometry on vehicle stability and control. In this regard, additional research is needed to develop a realistic driver-control algorithm for use in these models. In addition, the development of a graphical user interface for these models will be essential to their widespread use. Simulation models have the potential to be very helpful in evaluating complicated combinations of vehicle type and curve geometry. For example, they could be used to simulate a driver-controlled truck traveling on a significant grade under power as it travels through a sharp horizontal curve. Unfortunately, HVOSM and PHASE IV are not able to accurately simulate these conditions at this time.
5. Additional research is needed on pavement surface drainage in the transition section. This research should consider the section length, rotated width, longitudinal slope of the centerline and edge lines, cross slope rate, change in cross slope rate, tire-pavement friction properties, and rainfall intensity. Such research is especially needed for undivided multilane roadways and roadways with closely-spaced horizontal curves. This research should identify the longest drainage path in the transition section as well as the depth of water and its velocity along the path. This research should provide transition design guidance that, if followed, will minimize water depth and drainage path lengths.
6. Additional research is needed on the design of the transition sections of adjacent horizontal curves when separated by a relatively short section of tangent. It is likely that drivers' expectations in these sections are different from those on longer tangents. In this regard, higher levels of lateral acceleration may be tolerated; however, the kinematics of lateral motion in the transition section may dictate excessive lateral shift under some conditions. Guidance is needed on the minimum length of tangent necessary to develop superelevation runoff for both the reverse and broken-back curve arrangements. Pavement drainage problems can be particularly problematic in these sections. The guidelines developed for this research should consider the full range of design controls for both the superelevation and alignment transitions.

REFERENCES

1. *A Policy on Geometric Design of Highways and Streets.* American Association of State Highway and Transportation Officials, Washington, D.C. (1994).
2. *Rural Road Design: Guide to the Geometric Design of Rural Highways.* Austroads, Sydney, Australia (1989).
3. *Manual of Geometric Design Standards for Canadian Roads.* Transportation Association of Canada, Ontario, Canada (1986).
4. *Highway Design Guide—Technical Guide.* French Administration for the Technical Studies of Roads and Motorways, Bagneux, France (August 1994).
5. *Richtlinien für die Anlage von Straßen, RAS, Teil: Linienführung, RAS-L.* Forschungsgesellschaft für Strassen–und Verkehrswesen (in German), Kirschbaum Verlag, Bonn, Germany (1995).
6. *Trafikleder på landsbygd. (Standard Specifications for Geometric Design of Rural Roads).* National Swedish Road Administration, Borlänge, Sweden (1986).
7. *Road Layout and Geometry: Highway Link Design.* Departmental Standard TD 9/81. Department of Transport: Highways and Traffic, United Kingdom (1986).
8. *A Policy on Geometric Design of Highways and Streets.* American Association of State Highway and Transportation Officials, Washington, D.C. (1984).
9. *A Policy on Geometric Design of Rural Highways.* American Association of State Highway Officials, Washington, D.C. (1954).
10. ITE Technical Council Committee 5-5, *Guidelines for Urban Major Street Design.* Institute of Transportation Engineers, Washington, D.C. (1984).
11. Hayward, J.C., Highway Alignment and Superelevation: Some Design-Speed Misconceptions. *Transportation Research Record 757,* Transportation Research Board, National Research Council, Washington, D.C. (1980) pp. 22–25.
12. Krammes, R.A., R.Q. Brackett, M.A. Shafer, J.L. Ottsen, I.B. Anderson, K.L. Fink, K.M. Collins, O.J. Pendleton, and C.J. Messer, *Horizontal Alignment Design Consistency for Rural Two-Lane Highways.* Report FHWA-RD-94-034, Federal Highway Administration, U.S. Department of Transportation, Washington, D.C. (1995).
13. Emmerson, J., "Speeds of Cars on Sharp Horizontal Curves." *Traffic Engineering & Control* (July 1969) pp. 135–137.
14. Glennon, J.C., T.R. Neuman, and J.E. Leisch, *Safety and Operational Considerations for Design of Rural Highway Curves.* Report FHWA-RD-86-035, Federal Highway Administration, U.S. Department of Transportation, Washington, D.C. (1985).
15. Blue, D.W. and B.T. Kulakowski, "Effects of Horizontal-Curve Transition Design on Truck Roll Stability." *Journal of Transportation Engineering,* Vol. 117, No. 1, American Society of Civil Engineers, New York, New York (1991) pp. 91–103.
16. Good, M.C., "Evaluation of Transition Curve Design Parameters Using an Analytical Vehicle Model." *Australian Road Research,* Vol. 7, No. 2. Australian Road Research Board (June 1977) pp. 14–22.
17. *A Policy on Geometric Design of Highways and Streets.* American Association of State Highway and Transportation Officials, Washington, D.C. (1990).
18. Stewart, D. and C.J. Chudworth, "A Remedy for Accidents at Bends." *Traffic Engineering & Control,* Vol. 31, No. 2. (February 1990) pp. 88–93.
19. Segal, D.J. *Highway-Vehicle-Object Simulation Model—1976 User's Manual.* Report FHWA-RD-76-162, Federal Highway Administration, U.S. Department of Transportation, Washington, D.C. (1976).
20. Zegeer, C.V., J.R. Stewart, F.M. Council, D.W. Reinfurt, and E. Hamilton, Safety Effects of Geometric Improvements on Horizontal Curves. *Transportation Research Record 1356,* Transportation Research Board, National Research Council, Washington, D.C. (1992) pp. 11–19.
21. Harwood, D.W. and J.M. Mason, Horizontal Curve Design for Passenger Cars and Trucks. *Transportation Research Record 1445,* Transportation Research Board, National Research Council, Washington, D.C. (1994) pp. 22–33.
22. Council, F.M., Safety Benefits of Spiral Transitions on Horizontal Curves on Two-Lane Rural Roads. *Transportation Research Record 1635,* Transportation Research Board, National Research Council, Washington, D.C. (1998) pp. 10–17.
23. Lamm, R., B. Psarianos, and T. Mailaender, *Highway Design and Traffic Safety Engineering Handbook.* McGraw-Hill, New York, New York (1999).
24. Stewart, D., "The Case of the Left-Hand Bend." *The Highway Engineer,* Vol. 24(6). Institution of Highway Engineers (1977) pp. 12–17.
25. Kanellaidis, G., "Aspects of Highway Superelevation Design." *Journal of Transportation Engineering,* Vol. 117, No. 6. American Society of Civil Engineers, New York, New York (1992) pp. 624–632.

APPENDIX A

SIDE FRICTION DEMAND AND CURVE SPEED

This appendix describes the development and calibration of two models that collectively explain the relationship among curve speed, side friction demand, and curve geometry. One model is based on an empirical relationship between side friction demand and speed; the other model is based on a theoretical relationship among curve speed, geometry, and side friction demand. The inclusion of side friction demand in both models is evidence that friction demand is one of the most influential controls used in horizontal curve design. Hence, a clear understanding of the factors that affect this demand and its relationship to curve geometry is essential to effective horizontal curve design.

SIDE FRICTION AS A DESIGN CONTROL

The literature is replete with the published results of examinations of curve speed and side friction demand. Examinations of curve speed generally recognize speed as the dependent variable and the geometric attributes of the curve as independent variables. Calibrated models from such examinations are often used to predict the expected speed on a curve of known radius, superelevation rate, grade, and so forth. This type of application is consistent with the information needed to assess an alignment's design consistency.

Examinations of side friction demand generally recognize friction demand as the dependent variable and curve speed as the independent variable. Calibrated models from such examinations tend to be focused on defining an upper limit on comfortable side friction demand for purposes of horizontal curve design. It should be noted that the side friction demand referred to in this appendix is computed from a kinematic model of circular motion; it is not a directly measured quantity.

To date, what has not been examined is the combined effect of side friction demand and curve geometry on speed. It is hypothesized that friction demand and geometry are independent variables that influence a driver's curve speed choice. It is theorized that this influence is evidenced by a speed reduction upon entry to the curve (especially sharper curves). The extent of the reduction is believed to represent a compromise between the driver's desire to maintain speed and the desire to minimize the degree of discomfort associated with lateral accelerations stemming from side friction demand.

Current curve design practice (as described in *A Policy on Geometric Design of Highways and Streets* [*1*]) is based on two principles: (1) there is an upper limit on the amount of side friction demand deemed comfortable by motorists and (2) curve radii used in design should yield side friction demands at or below the "comfort limit" when they are driven at or below the design speed. In spite of these principles, findings from recent curve speed studies (*2*,*3*) suggest that (1) faster drivers on moderate to sharp curves routinely accept side friction demands in excess of the design side friction factor, (2) these drivers tend to reduce speed as they enter the curve, and (3) larger speed reductions are associated with larger side friction demand levels.

One objective of this research was to develop models of curve speed and side friction demand that could be used to define appropriate friction factors for horizontal curve design. These two models would be used to define the speed and friction demand experienced by an upper percentile of motorists when such speeds are limited by curve geometry. The model of curve speed would be used to assess the uniformity of speeds along a roadway segment. The model of side friction demand could be used to define the limiting (or maximum) side friction demand factors used for curve design.

Side Friction Demand

When a vehicle moves in a circular path, it undergoes a centripetal acceleration that acts toward the center of curvature. This acceleration is sustained by the friction between the tire and pavement and, if the road is superelevated, by a component of gravity. The relationship among side friction, superelevation rate, speed, and radius is commonly expressed as follows:

$$f_D = \frac{v^2}{gR} - \frac{e}{100} \tag{1}$$

where:

f_D = side friction demand factor;
e = superelevation rate, percent;
v = vehicle speed, m/s;
g = gravitational acceleration (= 9.807 m/s^2); and
R = radius of curve, m.

Side friction demand is often considered as dimensionless; however, it is sometimes useful to recognize that it represents an equivalent number of gravity forces (or g-forces) and thus, has units of "g's."

Maximum Design Side Friction Factors

One of the most fundamental controls related to horizontal curve design is the maximum design side friction factor. This factor is commonly used to define the minimum radius available for curve design. Maximum design side friction factors recommended by several international highway agencies are shown in Figure A-1.

There are several trends depicted in Figure A-1 that are worth noting at this point. One trend is the decrease in side friction factor with increasing speed. This trend is recognized by five of the six agencies represented. Many researchers believe the trend reflects a driver's desire to maintain an acceptable margin of safety relative to tire-pavement friction supply (which has a similar trend with speed). The most speed-sensitive factors are those used by the Australians for rural highway design (*4*). In contrast, factors used in the U.K. (*5*) are insensitive to speed. A second trend is the general agreement among the U.S. (*1*), Canadian (*6*), German (*7*), and Swedish (*8*) factors for speeds greater than 60 km/h.

The factors attributed to the "U.S." in Figure A-1 are obtained from *A Policy on Geometric Design of Highways and Streets* (*1*) (i.e., the *Green Book*). This guideline offers unique maximum design side friction factors for three different facility types:

- All Rural Highway and High-Speed Urban Streets (RHS);
- Low-Speed Urban Streets (LS); and
- Turning Roadways (TR).

The factors shown in Figure A-1 correspond to RHS and LS facilities; those for TR facilities lie between those for RHS and LS facilities and range in speed from 15 to 60 km/h.

The factors recommended in the *Green Book* for RHS facilities are based on five studies conducted in the 1930s and 1940s. These studies attempted to define the effective side friction corresponding to a curve speed that, if exceeded, would impart a reaction from passenger car occupants. This reaction varied from "awareness of being on a curve" to "distinct discomfort." The side friction obtained from these studies ranges from about 0.17 to 0.10—lower values being associated with higher speeds.

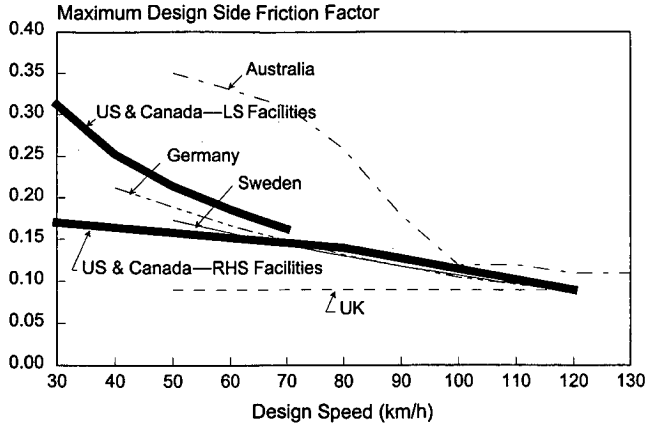

Figure A-1. Maximum design side friction factors recommended by several highway agencies.

The source of the recommended factors for LS facilities is not explicitly identified in the *Green Book*. These factors were first introduced in the *Green Book*'s 1984 edition. The discussion in this edition of the recommended factors suggests that they are based on the same studies that were used to define factors for RHS facilities.

The friction factors recommended by the *Green Book* for TR facilities were derived from four studies conducted between 1948 and 1952. Collectively, these four studies documented the relationship between driver speed and turn radius at 34 locations. The authors of the *Green Book* synthesized the results of these studies by extracting the 95th percentile speed, superelevation rate, and radius for each curve location. In this context, the *Green Book* authors' acknowledge that the 95th percentile speed is representative of the curve's design speed.

Curve Speed Prediction

Many curve speed models have been developed in the past 30 years. All of these models include the effect of curvature on speed. Several others also include the effect of approach speed. Recently, McLean (*9*) compared eight of the more widely used models and found them to predict fairly similar speeds. All of the models reviewed by McLean (*9*) predict the 85th percentile speed that, in the international design community, is generally recognized as the "operating" speed.

McLean (*9*) also compared the reported effects of superelevation rate, curve sight distance, lane width, shoulder width, and grade on curve speed. On the basis of this comparison, he concluded that only lane width appeared to have a practically significant effect on speed—specifically, that wider lanes were associated with higher curve speeds. However, he qualified this finding by suggesting that the observed effect of lane width may have truly been due to its correlation with the roadway's functional classification.

An examination of the models reviewed by McLean (*9*) indicates that there are two classes of curve speed model. The first class (Class 1) includes those models based only on radius. These models predict higher curve speeds with larger radii. The second class (Class 2) includes those models based on both radius and approach speed. These models generally predict higher curve speeds with higher approach speeds or larger radii.

The approach speed term in the Class 2 models is used as a surrogate for the "speed environment" of the roadway. In this regard, speed environment represents the driver's desired speed, as influenced by terrain, trip length, access control, and area type. A roadway's speed environment can

be estimated using observed driver speeds on long tangents under low-volume conditions. It is worth noting that the R^2 of the Class 2 models (as reported by McLean [*9*]) was consistently higher than that of the Class 1 models (i.e., 0.87 to 0.93 vs. 0.65 to 0.80) suggesting that the inclusion of approach speed can improve a model's predictive ability.

The relationship among speed, radius, and approach speed for three Class 2 models (*10,11,12*) is shown in Figure A-2. The agreement among the three models is quite good considering that each has a different mathematical form and was calibrated using data from a different country. The inclusion of approach speed in these models results in separate curves for each approach speed considered. As a result, a curve with a 120-m radius can have a curve speed of 55, 68, or 80 km/h, when the approach speed is 60, 80, or 100 km/h, respectively.

Two points can be made regarding the variation in speeds noted in the preceding paragraph. First, drivers reduce speed for the curve. It is likely that they do so to maintain an acceptable level of side friction demand (as experienced through lateral acceleration). Second, drivers do not slow to one, common curve speed for a given radius. From these two points, it appears that drivers seek to find a compromise or balance between the conflicting goals of maintaining the desired speed and adopting an acceptable level of lateral acceleration.

Equation 1 and the curve speed model reported by McLean (*12*) were used together to examine the relationship between speed reduction and side friction demand. A curve with a 120-m radius and a 6.0 percent superelevation rate was considered for the examination. The results are shown in Figure A-3.

The trend shown in Figure A-3 indicates that drivers accept higher side friction with higher speed reductions. The slope of this line represents a driver behavior characteristic in terms of the accepted change in side friction relative to the accepted speed reduction. The trend line having a non-zero slope is evidence that drivers increase the amount of side

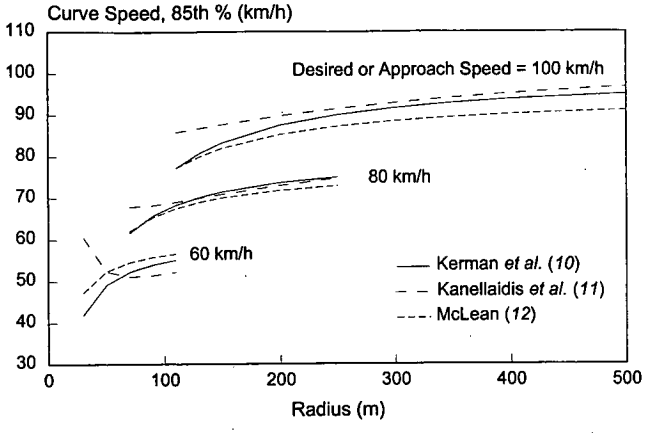

Figure A-2. Curve speed model comparisons for a range of radii and approach speeds.

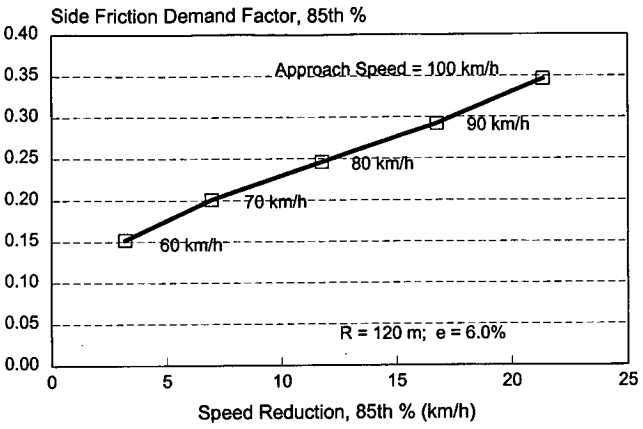

Figure A-3. Relationship between speed reduction and side friction demand.

friction they will accept to minimize the speed reduction associated with a given approach speed. Extrapolation of the trend line shown suggests that drivers on this curve would not reduce speed if the approach speed were 50 km/h; this speed corresponds to a side friction demand of 0.10. If it can be assumed that no speed reduction is "desired" by the driver, then the side friction demand that coincides with a zero speed reduction (i.e., 0.10 in Figure A-3) can be referred to as a "desired" side friction demand.

To illustrate the implications of the trends in Figure A-3, consider a driver approaching a curve with a 120-m radius and 6.0 percent superelevation rate. If the driver believes the roadway environment supports travel at 100 km/h, the driver will slow only to 79 km/h (and accept a side friction factor of 0.35) to negotiate the curve. However, when this same driver believes the environment supports travel at 60 km/h, he or she will slow to 57 km/h (and accept a friction factor of 0.15). Note that in this latter scenario, the driver does not speed up to 79 km/h or maintain the 60-km/h speed. Rather, the driver chooses to reduce speed slightly to provide an equitable balance between the desired side friction demand of 0.10 and the desired speed of 60 km/h.

MODEL DEVELOPMENT

Side Friction Model

A two-term side friction model was formulated to reflect the trends shown in Figures A-1 and A-3. One model term recognizes the decrease in side friction demand with increasing approach speed, as suggested by Figure A-1. A second term recognizes the increase in friction demand with increasing speed reduction, as suggested by Figure A-3. The form of the model is as follows:

$$f_D = b_0 - b_1 V_a + b_2 (V_a - V_c) I_v \qquad (2)$$

where:

f_D = side friction demand factor;
V_a = approach speed, km/h;
V_c = curve speed, km/h;
b_0, b_1, b_2 = calibration coefficients; and
I_v = indicator variable (= 1.0 if $V_a > V_c$; 0.0 otherwise).

The model formulation is sufficiently general as to permit its application to the prediction of expected side friction demand for individual drivers. The model formulation can also be used to predict the side friction corresponding to a specific percentile speed at a selected curve site. For design applications, the model should be calibrated using a specific upper percentile speed. A percentile value in the range of 85 to 95 is generally considered appropriate.

One objective of this research was to define side friction values for design applications. Hence, it was deemed necessary that the data used to calibrate the side friction model reflect situations where curve geometry was a dominant factor influencing speed choice. This need was first pointed out by Haile (*13*). He suggested that one indicator of this influence is when the vehicle is observed to have a lower speed on the curve than on the approach tangent. In this situation, it is highly likely that those drivers who decrease their speed do so in reaction to curve geometry. It follows then, that side friction demands predicted by Equation 2 will be most suitable for design application when they reflect the true effect of curve geometry on driver behavior.

Curve Speed Model

Equations 1 and 2 can be combined to obtain an equation for predicting curve speed for a given radius, superelevation rate, and approach speed. The variable relationships in these two equations require the use of the quadratic formula to obtain a closed-form solution for curve speed. The results of this combination are the following two equations:

$$V_c = 63.5R\left(-b_2 + \sqrt{b_2^2 + \frac{4c}{127R}}\right) \leq V_a \quad (3)$$

with

$$c = \frac{e}{100} + b_0 + (b_2 - b_1)V_a \quad (4)$$

where:

b_1, b_2, b_3 = calibration coefficients (obtained from Equation 2).

The inequality in Equation 3 results from the indicator variable in Equation 2 and serves to ensure that the curve speed predicted by the equation does not illogically exceed the approach speed. Any predicted curve speed that is lower than the approach speed represents a situation where curve geometry influences speed choice. In contrast, when the speed predicted by Equation 3 equals the approach speed, curve geometry is not likely to have any influence on driver speed choice.

STUDY DESIGN AND DATA COLLECTION

This section describes the development of the database used to calibrate the side friction demand and curve speed models. This development includes the identification of relevant database characteristics and a description of the data collection methods. At the end of this section, a brief summary of the database characteristics is provided to demonstrate the database's depth and breadth of coverage.

Database Characteristics

Study Site Characteristics

The study sites included in the database were selected to represent a wide range of street and highway curves. To ensure that this representation was attained, curve study sites were selected to offer a range of values in several key areas:

1.	Facility Type:	All rural highways and high-speed urban streets (RHS); Low-speed urban streets (LS); and Turning roadways (TR).
2.	Curve Radius:	50 to 900 m
3.	Speed Limit:	40 to 120 km/h
4.	Environment:	Urban, Rural
5.	Superelevation Rate:	–2 to +12%
6.	Curve direction:	Left, Right
7.	Grade:	–8 to +8%
8.	Geographic Diversity:	Northern and southern climates
9.	Vehicle Type:	Passenger cars and heavy trucks (vehicles with more than four tires)

It should be noted that a "study site" was defined as one direction of travel along one horizontal curve.

The study sites were also evaluated to ensure that they were representative of good design practice and of sufficient length to have some impact on driver behavior. Each study site was checked to verify that its geometric elements were in compliance with the *Green Book* controls. Finally, all sites satisfied the following conditions:

1. Lane widths between 3.0 and 3.6 m;
2. Sight distance everywhere along the curve in excess of stopping sight distance;

3. Curve lengths in excess of 3 s travel time at the design speed; and
4. Travel time on tangent prior to curve in excess of 4 s.

The type of alignment transition (i.e., with or without spiral) was not used to screen sites. The rationale for this approach was that the type of transition used would have negligible effect on curve speed.

Traffic Characteristics

The study sites were also selected to provide a wide range in traffic behavior. A study site had to have moderate traffic volumes (1,000 veh/day/ln or more), some truck activity (10 percent or more), and a nominal percentage of drivers who reduced their speed during curve entry. These attributes were needed to calibrate the curve speed and side friction models for a design application. Such application requires the speeds of free-flowing, car and truck drivers whose speed choice was likely influenced by curve geometry.

Only sites with moderate traffic volumes were included in the database because low- and high-volume sites tended to yield small sample sizes. Sample sizes at high-volume sites were generally low because they tended to have few free-flowing vehicles. Free-flowing vehicles were considered desirable because their speeds are presumably affected primarily by geometry and terrain. A vehicle was defined as free-flowing if (1) the headway between it and the vehicle in front (i.e., leading headway) was more than 4 s and (2) the headway between it and the vehicle in back (i.e., following headway) was more than 3 s. The minimum following headway was relaxed to 2 s if the subject vehicle was a large truck. This modification was instituted because it was believed that closely following vehicles had less of an effect on a truck driver's speed than on a passenger car driver's speed.

Data Collection Approach

The need for geographic representation and a wide range of geometric conditions together with a modest field study budget required an innovative data collection approach. After some investigation, it was determined that the most cost-effective means of assembling the database would be to aggregate the data collected for several previous research projects and to supplement this data with data collected for this research project.

Four previous studies were identified as having the desired site and traffic characteristics. Two of these studies (*14,15*) focused on rural two-lane highways, a third (*16*) addressed suburban arterials, and a fourth (*17*) examined free right-turn lanes (a type of turning roadway) at rural highway intersections. In all cases, the study sites and the data collected at each site were evaluated for consistency with the site and traffic characteristics established for this research project. Only those sites that satisfied these criteria were included in the combined database.

Several different data collection efforts were undertaken at each study site. These efforts included a survey of the geometric elements at each site as well as the measurement of vehicle speeds in advance of and along the subject horizontal curve. A description of the data collection procedures is provided in the following paragraphs. These procedures describe the studies conducted for this research project; however, they are very consistent with the methods used in the four previous studies.

Vehicle Measurements

Four characteristics were measured for each vehicle observed during a study: speed, leading headway, following headway, and vehicle classification. Speeds were measured using one of two methods. One method was based on the use of computer-monitored pavement sensors. The other method was based on the use of manually-operated laser speed guns. Both methods were designed to collect speeds in advance of the curve and at its midpoint. When the sensor method was used, a video camcorder was used to record traffic events along the curve. This videotape record was used to screen out unusual conditions and to verify the accuracy of the processed sensor data.

The preferred method of speed measurement was based on the pavement sensors. This preference stems from the sensor system's ability to electronically record precise measurements of headway, speed, and wheelbase for each vehicle without the immediate presence of the field study team. Laser speed guns were used whenever traffic conditions were such that deployment of the sensors presented a significant risk to the study team. Whenever speed guns were used, each study team member was positioned at a vantage point such that he or she was hidden from the subject driver's view.

Both leading and following headways were measured for each vehicle. Both were used to screen out drivers whose speed might have been influenced by traffic density.

For a given study site, the method of determining vehicle classification was dependent on the method used to measure speed. For the sensor method of measurement, the videotape record was used in conjunction with the computed wheelbase to determine vehicle type. For the laser gun method, the vehicle classification was noted at the time of the speed measurement.

Vehicle speed and headway measurements were taken at two locations. One location was on the approach tangent, the other was at the curve midpoint. These locations are illustrated in Figure A-4 for a two-lane highway or street. For all multilane locations, the measurements were taken in the outside (or curb) lane.

The approach tangent speed was used for two purposes: (1) to calibrate the curve speed prediction model and (2) to discriminate between drivers who did and did not increase

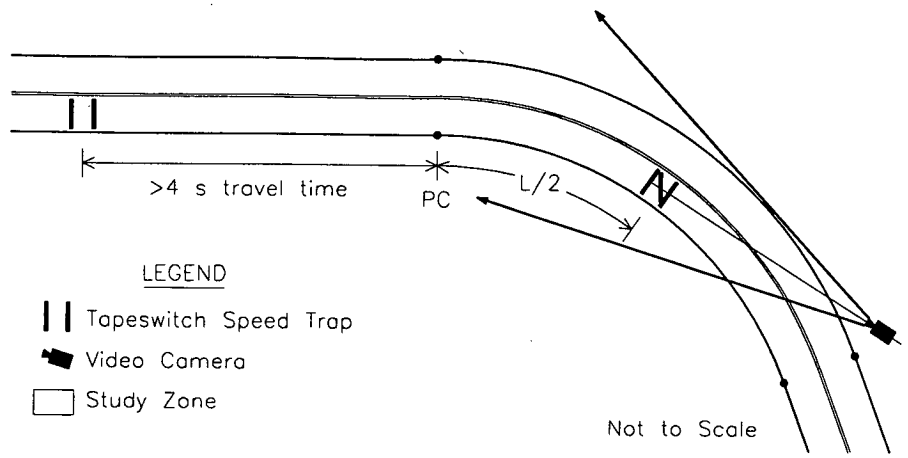

Figure A-4. Field study design for a typical horizontal curve.

their speed between the approach and curve measurement points. Drivers who slowed or maintained their speed were presumed to reflect a speed that was suitable for the curve. It was rationalized that those drivers who increased their speed did not yield useful information about the impact of the curve geometry on their speed choice. Thus, only those drivers who slowed or maintained their speed were used to define the relationship between side friction demand and speed.

Site Survey

The physical layout of the roadway was surveyed for each study site. The following geometric elements were measured during this survey:

1. Curve radius,
2. Deflection angle (or curve length),
3. Width of traffic lanes and entire roadway,
4. Superelevation at curve midpoint, and
5. Grade along the curve.

In addition to these measurements, several other important attributes were noted for each study site. One set of attributes relates to the type of traffic control signs posted in the site vicinity. Also, the speed limit as well as any advisory speed in advance of the subject curve was recorded during the site survey. A second set of attributes relates to the weather and road surface conditions present during the field study. These conditions were noted at the onset of each study. It should be noted that no studies were conducted when the roads were wet or on highways with a highly uneven pavement surface.

The curve radius was measured using the "chord and offset" method. The precision of the computed radius by this method is limited by the size of the middle ordinate. A small error made while measuring a short middle ordinate can lead to a relatively large error in the estimate of radius. In recognition of the limited precision of the chord-and-offset method, the measured radius was only used to confirm the radius obtained from the as-built plans for the subject curve.

A surveyor's level and rod were used to facilitate the computation of superelevation rate and grade. For superelevation rate, this rate was computed from elevations taken at the edge of the subject traffic lane combined with cross section width measurements. Superelevation rates were measured at the curve midpoint. The longitudinal grade of the roadway was estimated by taking elevations at the curve midpoint and at the beginning of the curve (i.e., PC). This grade was confirmed using the as-built plans for the subject curve.

Video and photo logs were created to provide a visual record of site conditions. The video log was created using a camcorder. This camcorder recorded roadway conditions during a "drive-through" of the study site. The recording started about 10 s in advance of the curve and continued until a point about 5 s downstream was reached. The photo log consisted of four photos taken at each site; all photos were taken facing the travel direction of interest. One photo was taken at each of the following locations: (1) just upstream of the point where tangent speeds were measured, (2) halfway between the tangent point and the curve PC, (3) at the curve PC, and (4) at the curve midpoint.

Data Collection Methods

Two methods of data collection were used for this project. The first method employed computer-monitored pavement sensors. The second method used manually-operated laser speed guns. The first method was used whenever possible; however, it was sometimes difficult to install sensors on high-volume roadways. This difficulty stemmed from the need for two or three 1-min gaps in traffic to adhere each pair of sensors to the pavement. When these gaps were not available and when discrete vantage points could be obtained, laser guns were used instead of the pavement sensors.

All data were collected during weekday, daytime periods between the hours of 7:00 a.m. and 7:00 p.m. The study

period generally included the hours of peak traffic demand at the study site. Data were not collected during inclement weather or during unusual traffic conditions (e.g., traffic accident).

Summary of Database Characteristics

The combined database represents 55 curve study sites in eight states (i.e., Arizona, Minnesota, Nebraska, New York, Oregon, Pennsylvania, Texas, and Washington). The data obtained from previous studies accounted for 39 sites in 7 states; 16 sites in 2 states (i.e., Arizona and Texas) were studied for this research. The distribution of the 55 study sites is shown in Table A-1.

In general, there is broad geographic representation in the database. This representation also extends to the various facility types listed in Table A-1. One facility type, "low-speed rural highway," was relatively difficult to find. The two sites that were found were in rolling terrain on alignments with several closely-spaced, sharp curves. The low-speed nature of the highway was based on an estimate of the likely design speed using the *Green Book* superelevation tables combined with the measured curve radius and superelevation rate.

Table A-2 lists the range of study site characteristics in the combined database. As indicated in this table, a wide range of values are provided for each facility type. Collectively, the study sites satisfy the desired site characteristics defined previously.

DATA REDUCTION AND ANALYSIS

This section describes the reduction and analysis of the combined database. Initially, the methods of data reduction are summarized. Then, several model variables are examined for potentially harmful correlations. Finally, the data are examined more rigorously using analysis of variance techniques. This later examination is intended to identify factors that have a significant effect on side friction demand.

Data Reduction

The combined database was developed using a four-step data reduction process. As a first step, the data collected with the computer-monitored pavement sensors was manually reviewed for accuracy. This review included a subjective comparison of the computed vehicle characteristics with visual estimates of the same quantities as obtained from videotape recordings.

The second step in the reduction process involved a complete and thorough review of the materials gathered from the four previous studies. These materials included photo and video logs, site survey forms, and, when speed guns were used, the original data collection forms. These materials were

TABLE A-1 Geographic distribution of study sites in the combined database

State	Through Street or Highway				Turning Roadway	Total
	Urban		Rural			
	Low-speed	High-speed	Low-speed	High-speed		
Arizona	3	1			1	5
Minnesota				1		1
Nebraska					2	2
New York				5		5
Oregon			2	4		6
Pennsylvania				3		3
Texas	9	7		10	3	29
Washington				4		4
Total:	12	8	2	27	6	55

TABLE A-2 Range of study site characteristics

Facility Type		Posted Speed (km/h)	Radius (m)	Def. Angle (°)	Super-elevation (%)	Grade (%)
Urban	Low-speed	40–64	29–315	20–96	-2.9–2.9	-2.8–1.8
	High-speed	72	108–990	13–74	-2.3–3.8	-8.4–1.6
Rural	Low-speed	89	109–125	33–45	5.5–6.5	-0.5–6.0
	High-speed	89–113	97–1747	5–91	1.9–12	-7.0–8.0
Turning Roadways		64–105	48–206	90–290	4.0–9.8	-5.9–4.5

scrutinized for quality of data collection and consistency with the site and traffic characteristics needed for this research project. More than 100 study sites from the four previous studies were evaluated in this manner to obtain the 39 sites ultimately included in the database.

The third step in the data reduction process was to convert all of the existing site and traffic data into a common database format. Frequently, this step required only that an existing computer data file be converted into the file format devised for this project. Several software programs were developed for this conversion process. In contrast, speed gun data for several sites had to be entered manually into the database. The database constituted 8,219 observations from 55 curve sites.

The fourth step in the data reduction process involved the examination of the data for inconsistencies. The distribution of speeds observed at each site was examined for outliers. Twenty-eight speed observations were excluded as a result of this process. A SAS (*18*) statistical procedure (i.e., UNIVARIATE) was used for outlier identification. The cause of each speed "outlier" was investigated by consultation with the original data files, videotape, or data collection forms. In most cases, the reason for the outlier was obvious (e.g., vehicle turning onto the roadway near the curve, transposing two numbers when recording them) while in other cases no logical reason could be identified. After removal of the outliers, 8,191 valid speed observations remained in the database.

Preliminary Examination

The data were initially examined to determine the relationship between curve speed, approach speed, and curve speed reduction. As noted previously, drivers observed to increase speed from the approach to mid-curve measurement points were not considered to offer a valid representation of driver curve speed choice, as influenced by curve geometry. It is believed that such behavior resulted from drivers going slower than their desired speed on the approach tangent and accelerating toward this speed as they entered the curve. This hypothesis was investigated further through the examination of approach speed versus speed reduction at several sites. A typical relationship between these two characteristics is shown in Figure A-5, as found at one study site.

The data in Figure A-5 indicate that the drivers who increased speed were always the slower drivers. This finding is consistent with the aforementioned belief that accelerating drivers were not representative of all drivers (just slower ones) and that their speed was not likely challenged by curve geometry. As a result, it was concluded that these drivers conveyed little useful information about the effect of curve geometry on desired speed and that these few slow drivers should be screened from the database.

Further examination of the database indicated that 13 percent of the observed drivers (i.e., 1,098) had higher speeds on the curve than on the approach tangent. Moreover, an examination of the average speed change for each study site indicated that 95 percent (i.e., 52) of the 55 sites exhibited a decrease in average speed from the approach tangent to the curve. From this examination, it was concluded that the number of observations excluded from the analysis was minimal and that the curves studied were sufficiently sharp as to have some influence on the driver's speed choice.

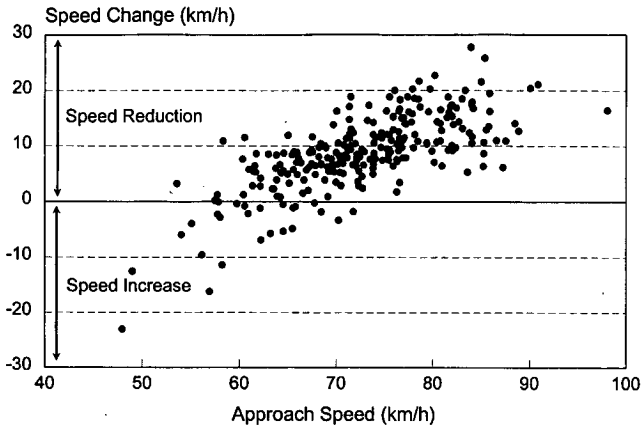

Figure A-5. Relationship between approach speed and speed reduction at one site.

Possible correlations between key model variables were also investigated. From a statistical standpoint, correlation among independent variables can bias the regression coefficients. This investigation focused on two relationships. The first relationship examined was that between the speed change $V_a - V_c$ and approach speed V_a variables. Both of these variables are included in the side friction model and both include the effect of approach speed. The results of this examination are shown in Figure A-6.

The data shown in Figure A-6 indicate that there is no correlation (i.e., $R^2 = 0.02$) between the two variables. The lack of correlation stems from the fact that curve speed is a random variable that varies with approach speed. As a result, the

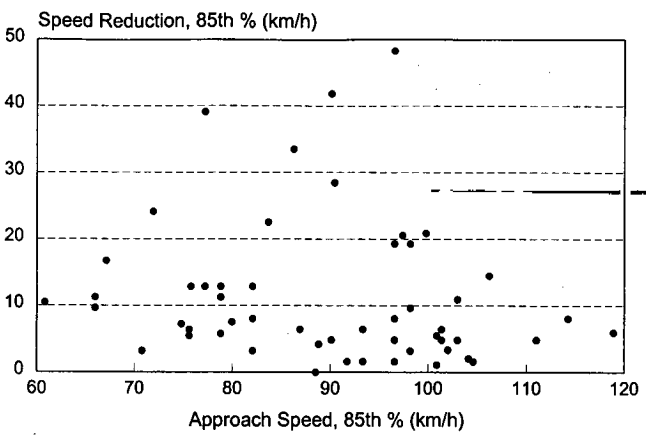

Figure A-6. Relationship between approach speed and speed reduction.

difference of two highly correlated, random variables is also a random variable having little association with either of the original two variables. The lack of correlation between approach speed and speed reduction is also evidence that screening observations associated with a speed increase from the database did not introduce a bias into the database.

The second relationship examined was the possible correlation between superelevation rate e and radius R. This investigation was motivated by the inclusion of both factors in the curve speed model. It is logical that such a correlation might exist because the *Green Book* guidelines recommend the selection of superelevation rate based on the magnitude of the radius. However, the results of this investigation indicated that there was no correlation (i.e., $R^2 = 0.004$) between superelevation rate and radius. This finding is consistent with observations made by Krammes et al. (*14*).

The relationships between approach speed, speed class, area type (i.e., urban vs. rural), vehicle type and side friction demand are shown in Figure A-7. The data in this figure represent the 85th percentile approach speed observed at each site and the 85th percentile side friction demand. For this examination, the 85th percentile side friction was computed using Equation 1 and the 85th percentile curve speed. Similar trends were found for the 95th percentile speeds and side friction factors.

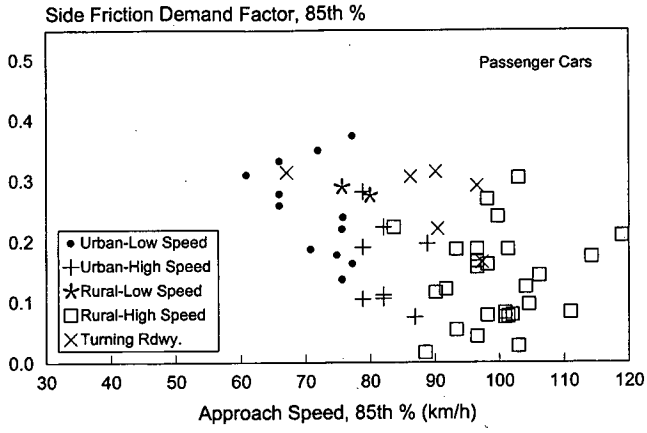

a. Passenger car side friction demand.

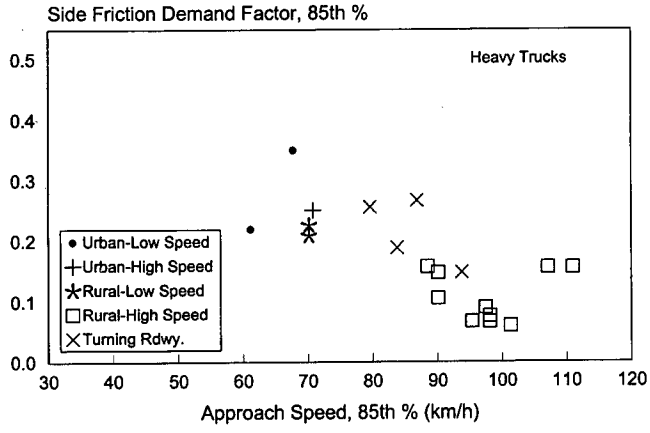

b. Heavy truck side friction demand.

Figure A-7. Effect of approach speed on side friction demand for cars and trucks.

The number of observations at each curve site varied widely. To minimize the variability resulting from small sample sizes, only those sites with 10 or more observations are shown in Figure A-7 (this minimum requirement eliminated 12 sites from Figure A-7b).

Examination of the data in Figure A-7 indicates that several trends exist. One trend is that side friction demand generally decreases with increasing speed. A second trend is that there is very little difference in side friction demand among urban and rural facilities. A third trend is that heavy trucks (i.e., vehicles with more than four tires) have friction demands similar in magnitude to those of passenger cars. Figures A-7a and A-7b also confirm that the database includes sites that collectively have a wide range of friction demands and approach speeds for both passenger cars and trucks.

Data Analysis

Statistical Considerations

A two-stage statistical analysis procedure was used to identify the factors affecting side friction demand. The first stage of the analysis was based on the use of analysis of variance to evaluate the effect of several factors that could have some influence on curve speed and side friction demand. The second stage of the analysis involved the use of nonlinear regression to calibrate the curve speed model (i.e., Equation 3). The regression coefficients obtained from this calibration were then used in the side friction model (i.e., Equation 2).

The SAS nonlinear regression procedure (NLIN) was used for model calibration. Linear regression was not used to calibrate the curve speed model because its form does not have linear components. While the side friction model has a linear form and is suitable for linear regression, it is not the preferred model for coefficient calibration for three reasons. First, the dependent variable (i.e., friction) is a "computed" value rather than a truly "measured" quantity. Second, computed friction is not normally distributed as assumed for least-squares regression modeling; rather, its standard deviation is linearly related to mean curve speed. Third, computed friction is based on curve speed which, when used with Equation 2, effectively puts the effect of curve speed on both sides of the equal sign in the friction model. These reasons limit the appeal of using Equation 2 as the regression model because they can result in biased coefficient estimates.

The curve speed model as a regression model does not share the aforementioned limitations. The nonlinear regression approach combined with Equation 3 (as the appropriate

model form) offers an unbiased means of quantifying the true relationship between curve speed and approach speed. The regression coefficients obtained from this regression analysis can then be substituted into Equation 2 to obtain the true relationship between speed and side friction demand.

Analysis of Factor Effects

The SAS analysis of variance procedure (i.e., GLM) was used to identify factors affecting side friction demand. Because side friction demand is a fundamental control in curve design and also believed to have a fundamental influence on driver curve speed choice, it was reasoned that the analysis of variance should focus on factors affecting friction demand.

The side friction model was used for the analysis of variance. It was recognized that this model form has the aforementioned limitations regarding coefficient calibration; however, it is believed that these limitations are not so significant that they would adversely affect an examination of influential factors. In general, the GLM procedure is well suited to detecting significant factor effects in the presence of unbalanced, incomplete data. It is also efficient at detecting significant differences in the presence of mild non-normality of the residual errors.

For all analyses, a confidence level of 95 percent ($\alpha = 0.05$) was used as a cutoff value for significance tests. This confidence level limits to 5 percent the probability of erroneously concluding that the effect is significant when in fact it is not.

The analysis of variance was used to evaluate the effect of several site-related characteristics. These factors include the following:

1. Facility type:
   - Low-speed urban streets (LS)
   - All rural highways and high-speed urban streets (RHS)
   - Turning roadways (TR)
2. Curve direction:
   - Curve to the left
   - Curve to the right
3. Grade
4. Deflection angle
5. Posted speed limit
6. Vehicle Type:
   - Passenger car
   - Heavy Truck (more than 4 tires)

The dependent variable (i.e., side friction demand) for this analysis was computed using Equation 1.

The analysis of "vehicle type" was conducted first. This analysis compared the individual curve speed measurements for both heavy trucks and passenger cars. The results of this analysis indicated that truck side friction demand is significantly different from passenger car demand. Specifically, it was found that truck friction is about 0.028 g's (units of side friction) less than that of a passenger car.

The analysis of the other factors in the preceding list (i.e., factors 1, 2, 3, 4, and 5) was conducted using the average speed and side friction demand for each study site. Because the number of observations at each site was not the same, the squared residuals were weighted using the reciprocal of the squared standard error of side friction. This quantity was computed for each site with the following equation:

$$W_f = \frac{n}{\sigma_v^2}\left(\frac{gR}{2v_c}\right)^2 \quad (5)$$

where:

W_f = weight function for analysis of variance of side friction demand;
σ_v^2 = curve speed variance, m^2/s^2;
n = number of observations for the subject site;
v_c = curve speed, m/s;
g = gravitational acceleration (= 9.807 m/s^2); and
R = radius of curve, m.

Based on the analysis of variance, it was determined that curve direction, grade, speed limit, and deflection angle do not have significant effects on side friction demand. The lack of any significant effect of grade is consistent with a finding reported by McLean (*9*). There was some evidence that side friction was higher on curves with larger deflection angles. However, this effect was not significant and was strongly correlated with facility type. When only LS and RHS facilities were examined, the effect of deflection angle was not significant. From this analysis, it was concluded that the effect of deflection angle was more likely due to differences in driver behavior on turning roadways (TR) (they tended to have the largest deflection angles).

As noted in the preceding paragraph, "facility type" was found to be associated with significantly different side friction demands. Specifically, TR facilities were found to have significantly more side friction demand than LS or RHS sites. Further examination revealed that the effect of facility type was most influential when it was combined with the speed reduction term (i.e., $V_a - V_c$) in Equation 2. In other words, the regression coefficient for this term was significantly different for turning roadways than for the other facility types. This finding suggested that drivers on TR facilities are more willing to reduce their speed; possibly because they anticipate a "yield" condition where the turning roadway joins the crossing street or highway.

The analysis of variance indicated that both terms in Equation 2 (i.e., approach speed and speed reduction) were significantly correlated with side friction demand. The relationship between side friction and approach speed was noted previously in Figure A-7. The effect of speed reduction is shown in Figure A-8. The trends shown in this figure indicate that higher side friction is tolerated by motorists when they have to significantly reduce their approach speed to

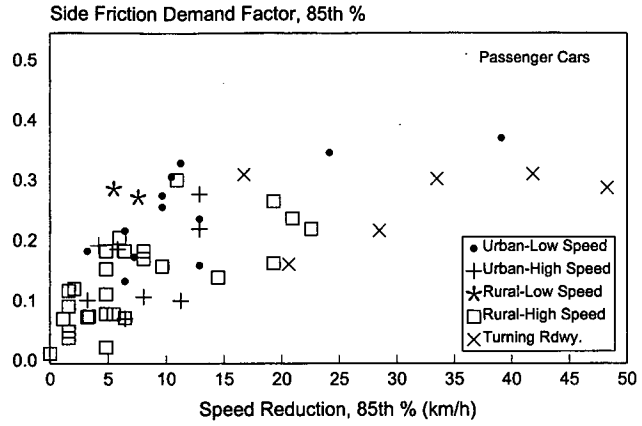

a. Passenger car side friction demand.

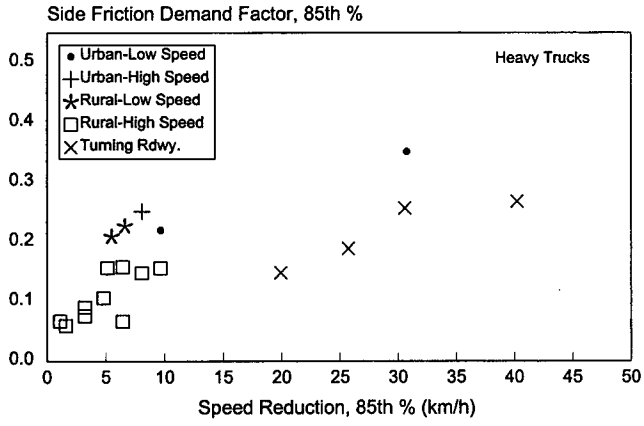

b. Heavy truck side friction demand.

Figure A-8. Effect of speed reduction on side friction demand for cars and trucks.

negotiate the curve. This trend is consistent with that noted for Figure A-3.

MODEL CALIBRATION

Model Calibration

Based on the findings from the analysis of factor effects, it was determined that the side friction model needed revision to reflect differences between drivers on TR facilities relative to drivers on other facility types. The form of the revised model is as follows:

$$f_D = b_0 - b_1 V_a + (b_2 + b_3 I_{TR})(V_a - V_c) \quad (6)$$

where:

V_c = curve speed, km/h;
V_a = approach speed, km/h;
b_3 = incremental effect of speed reduction on side friction demand at TR facilities; and
I_{TR} = indicator variable (= 1.0 for turning roadways; 0.0 otherwise).

Combining Equations 3 and 6 yields the curve speed model used for the regression analysis. The form of this model is as follows:

$$V_c = 63.5R\left(-(b_2 + b_3 I_{TR}) + \sqrt{(b_2 + b_3 I_{TR})^2 + \frac{4c}{127R}}\right) \quad (7)$$
$$\leq V_a$$

with

$$c = \frac{e}{100} + b_0 + (b_2 + b_3 I_{TR} - b_1)V_a \quad (8)$$

where:

b_0, b_1, b_2, b_3 = calibration coefficients; and
e = superelevation rate, percent.

The number of observations at each site was not the same. Thus, the squared residuals were weighted during the regression using the reciprocal of the squared standard error of speed. This quantity was computed for each site using the following equation:

$$W_v = \frac{n}{\sigma_v^2} \quad (9)$$

where:

W_v = weight function for nonlinear regression of curve speed;
σ_v^2 = curve speed variance, and
n = number of observations for the subject site.

The regression analysis was based on both the 85th and 95th percentile speeds measured at each site; one model was developed for each percentile. The 95th percentile speed model provides a defensible relationship between design speed and side friction demand. Precedent for this has been established in the 1994 *Green Book* Figure III-19.

The 85th percentile speed model was calibrated to facilitate comparison of these research findings with those reported in the literature. The 85th percentile speed is generally recognized as an appropriate means of assessing a curve's operational character in terms of design consistency. In fact, many international design agencies define the 85th percentile speed as the operating speed.

The 85th percentile curve speed model may also be useful to those design engineers who have some indication of the speed limit to be used on the facility under design. This application follows the generally accepted practice of equating the speed limit with the 85th percentile speed. Thus, the use of

both the 85th and 95th percentile models in a design situation provides a means for establishing a desirable relationship between design speed and speed limit.

The results of the regression analysis are summarized in Tables A-3 and A-4 for the 95th and 85th percentile speeds. The statistics shown in each of these tables indicate that the calibrated model is a very reliable predictor of curve speed. The quality of fit to the 95th percentile curve speeds is shown in Figure A-9. The fit for the 85th percentile speed form of the model had a pattern very similar to that shown in this figure.

It should be noted that the data points shown in Figure A-9 represent only those sites with more than 10 observations. All sites were used for model calibration; however, sites with only a few observations were not shown in the figure in order to better convey the trends in the data. This restriction only affected the number of sites represented in Figure A-9b.

The regression coefficients from the calibrated curve speed model were combined with Equation 6 to form the side friction model. The forms of this model for each combination of vehicle type and percentile speed are as follows:

$$f_{D,95,pc} = 0.243 - 0.00187V_{a,95,pc} + (0.0135 - 0.0067\,I_{TR})(V_{a,95,pc} - V_{c,95,pc}) \quad (10)$$

$$f_{D,95,tk} = 0.222 - 0.00140V_{a,95,tk} + (0.0101 - 0.0063\,I_{TR})(V_{a,95,tk} - V_{c,95,tk}) \quad (11)$$

TABLE A-3 Calibrated speed-comfort equilibrium model statistics—95th percentile

Model Statistics		Passenger Car			Heavy Truck		
R^2:		0.95			0.97		
Root Mean Square Error (km/h):		4.1			3.6		
Observations:		55 (sites)			31 (sites)		
Range of Model Variables							
Var.	Variable Name	Units	Min.	Max.	Units	Min.	Max.
f_D	Side friction demand factor	g's	0.02	0.41	g's	0.07	0.38
V_a	Approach speed	km/h	66	128	km/h	63	114
V_c	Curve speed	km/h	40	118	km/h	39	106
Calibrated Coefficient Values							
Coeff.	Coefficient Definition	Value	Std. D.	t-stat.	Value	Std. D.	t-stat.
b_0	Intercept	0.243	0.0882	2.8	0.222	0.0585	3.8
b_1	Effect of approach speed	0.00187	0.0009	2.0	0.00140	0.0006	2.3
b_2	Effect of speed reduction	0.0135	0.0018	7.4	0.0101	0.0015	6.6
b_3	Effect of Turning Roadways	-0.0067	0.0017	-4.0	-0.0063	0.0014	-4.4

TABLE A-4 Calibrated speed-comfort equilibrium model statistics—85th percentile

Model Statistics		Passenger Car			Heavy Truck		
R^2:		0.96			0.99		
Root Mean Square Error (km/h):		3.5			2.2		
Observations:		55 (sites)			31 (sites)		
Range of Model Variables							
Var.	Variable Name	Units	Min.	Max.	Units	Min.	Max.
f_D	Side friction demand factor	g's	0.02	0.37	g's	0.06	0.35
V_a	Approach speed	km/h	61	119	km/h	61	109
V_c	Curve speed	km/h	38	113	km/h	37	102
Calibrated Coefficient Values							
Coeff.	Coefficient Definition	Value	Std. D.	t-stat.	Value	Std. D.	t-stat.
b_0	Intercept	0.256	0.0750	3.4	0.258	0.0456	5.7
b_1	Effect of approach speed	0.00223	0.0008	2.7	0.00196	0.0005	4.1
b_2	Effect of speed reduction	0.0133	0.0018	7.4	0.0093	0.0013	7.3
b_3	Effect of Turning Roadways	-0.0074	0.0016	-4.5	-0.0057	0.0011	-5.0

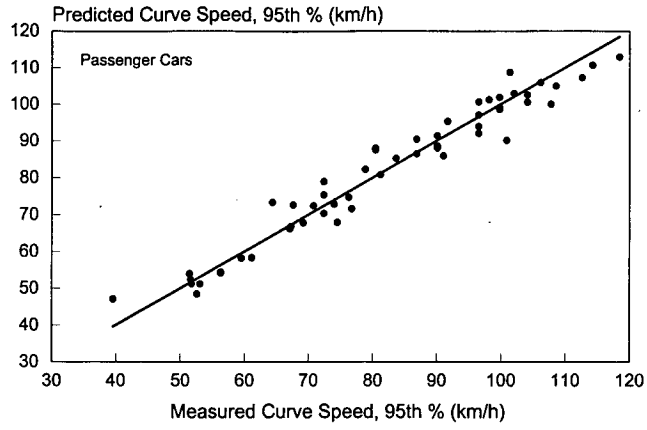

a. Passenger car speeds.

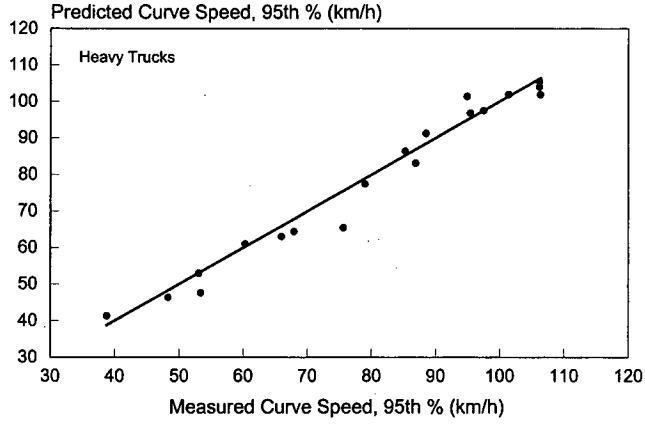

b. Heavy truck speeds.

Figure A-9. Comparison of measured and predicted curve speeds for cars and trucks.

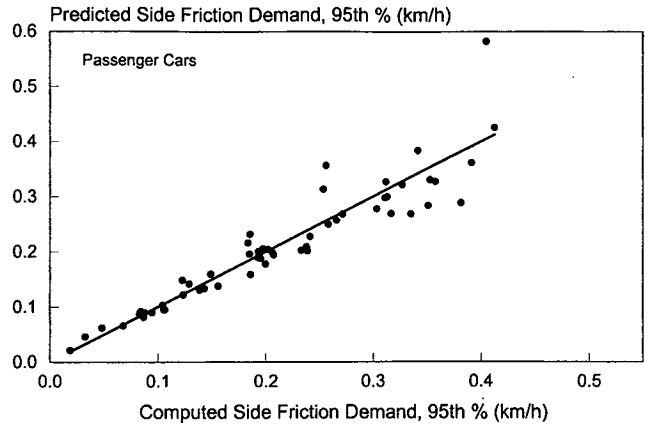

a. Passenger car side friction demand.

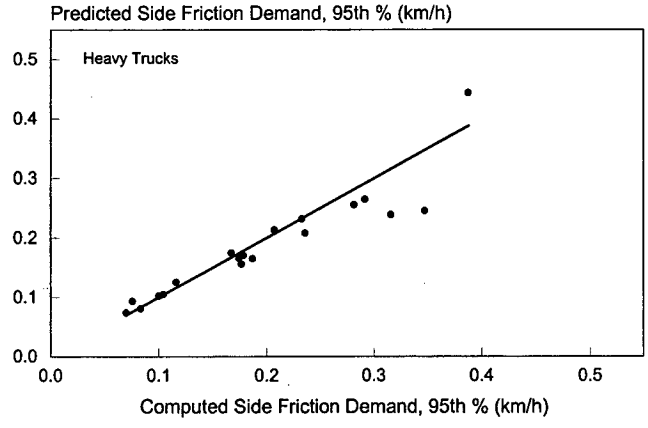

b. Heavy truck side friction demand.

Figure A-10. Comparison of computed and predicted side friction demand for cars and trucks.

$$f_{D,85,pc} = 0.256 - 0.00223V_{a,85,pc} + (0.0133 - 0.0074\, I_{TR})(V_{a,85,pc} - V_{c,85,pc}) \quad (12)$$

$$f_{D,85,tk} = 0.258 - 0.00196V_{a,85,tk} + (0.0093 - 0.0057\, I_{TR})(V_{a,85,tk} - V_{c,85,tk}) \quad (13)$$

The calibrated side friction model was also examined for its quality of fit to the data. Specifically, Equation 1 was used to compute the side friction demand for each site based on its observed 95th percentile speed and measured superelevation rate and radius. These computed values are compared with the side friction demand predicted by Equations 10 and 11 for each curve site. The results of this comparison are shown in Figure A-10.

The trends shown in Figure A-10 indicate a fit nearly as good as that obtained from the curve speed model. For the passenger car friction model shown in Figure A-10a, the R^2 value is 0.86 and the root mean square error (i.e., the standard deviation of the predicted quantity) is 0.039 g's. For the truck model, the R^2 value is 0.87 and the root mean square error is 0.034 g's.

Model Verification

The calibrated curve speed model was compared with the three models described previously for Figure A-2. The results of this analysis are shown in Figure A-11. In general, the trend lines associated with the proposed model are in very good agreement with existing models. This agreement, combined with the quality of model fit to the data collected for this study, provides strong support for the hypothesized relationship between side friction demand and curve speed, as modeled by Equation 6.

Sensitivity Analysis

The calibrated side friction model was used to examine the relationship between side friction demand and approach speed. This relationship is shown graphically in Figure A-12. Also shown in Figure A-12 are the maximum design side friction factors recommended in the *Green Book*. The proposed

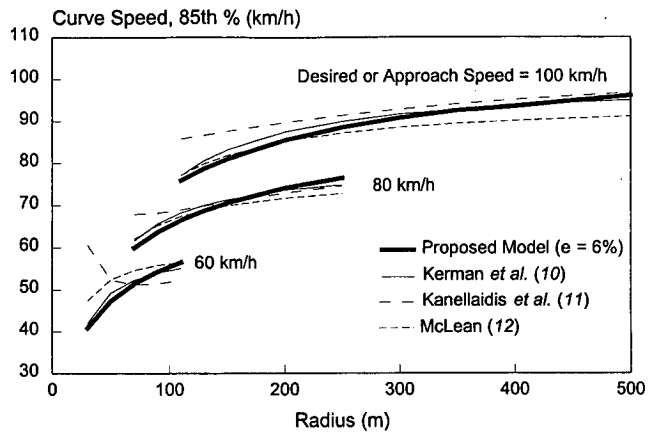

Figure A-11. Comparison of the calibrated curve speed prediction model with other models.

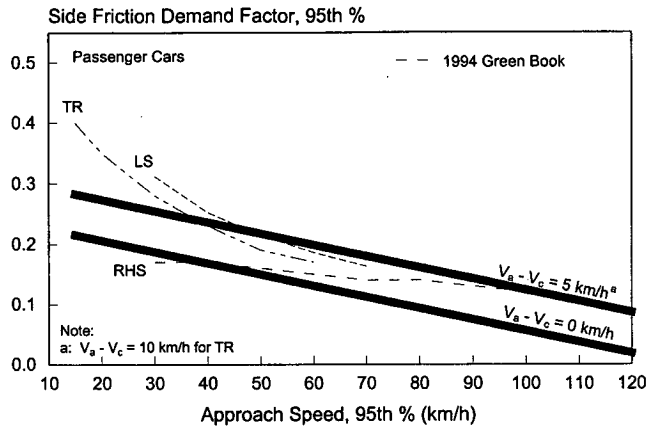

a. Passenger car side friction demand.

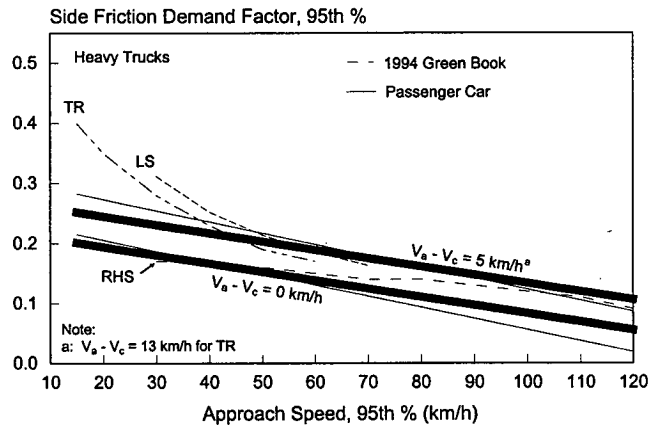

b. Heavy truck side friction demand.

Figure A-12. Predicted maximum side friction demand factors for a range of approach speeds for cars and trucks.

model predicts a decrease in side friction demand with an increase in approach speed. In addition, the proposed model indicates that side friction demand increases with increasing speed reduction (i.e., $V_a - V_c$).

A comparison of the friction factors obtained from the proposed model with those recommended in the *Green Book* indicates that a nominal speed reduction of 5 to 10 km/h is expected of drivers traveling on curves designed with near-minimum radii. In contrast, curves with moderate to large radii that yield side friction demands below the "$V_a - V_c = 0$" trend line are not likely to induce a speed reduction.

The trend line shown in Figure A-12 that coincides with a 5-km/h speed reduction is applicable to RHS and LS facilities. As mentioned previously, the analysis indicated that drivers on TR facilities tend to accept about twice the speed reduction for the same side friction demand and approach speed. Hence, the "$V_a - V_c = 5$" trend line in Figure A-12a coincides with a 10-km/h speed reduction for passenger cars on TR facilities; that shown in Figure A-12b coincides with a 13-km/h reduction for trucks.

An examination of Figure A-12b indicates that heavy trucks have slightly lower side friction demands than passenger cars on low-speed facilities. The reverse of this trend is true for high-speed facilities. Alternatively, it can be suggested that the "flatter" slope of the friction trend line for heavy trucks suggests that truck drivers have a reduced sensitivity to speed in their choice of side friction demand.

DESIGN IMPLICATIONS

Maximum Design Side Friction Factors

The calibrated side friction models described in the preceding section provide a logical basis for establishing maximum side friction factors for design. Their representation of an upper percentile of the driver population provides a conservative nature to the design process, consistent with that used to define other design controls in the *Green Book*. Of the two percentiles considered (i.e., 85th and 95th), the 95th percentile provides the more appropriate level of coverage for curve design.

The rationale for selecting the 95th percentile side friction demand as the basis for design is based primarily on considering the probability of "failure." Unlike the issue of stopping sight distance, where several "rare" events must combine to produce possible failure in the form of a collision, curve speed choice is the only random variable that dictates the successful negotiation of the curve (as it relates to side friction demand and Equation 1).

Failure in stopping sight distance design requires that the reaction time, deceleration rate, and speed criteria will be at or below their "worst-case" values for a given driver. For example, if 85th percentile values of each control are used to define stopping sight distance, the probability of failure is about 1 in 300 (= $(1 - 0.85)^{-3}$). If this level of safety were also provided in curve design, the 99.7th percentile side friction demand (= 1 – 1/300) would need to be used. Practical

considerations preclude the use of such an extreme value; however, the 85th percentile side friction demand is likely too low because 15 percent of drivers would have side friction demands in excess of the design value. Such an excess implies motorist discomfort and a possible vehicle control failure.

Based on the discussion in the preceding paragraphs, it is recommended that the maximum design side friction factors used for curve design be based on the 95th percentile side friction demand. Following this recommendation, it is also recommended that the curve design speed be based on the 95th percentile curve speed. It should be noted that this rationale and recommendation are consistent with the statements made in the *Green Book* (*1*, pp. 193–194), as they relate to curve design for turning roadways.

The calibrated side friction model coefficients indicate that side friction demand varies by vehicle type. Specifically, truck drivers prefer slightly less side friction on low-speed facilities than do passenger car drivers. Hence, the maximum design side friction factors for low-speed facilities serving a significant percentage of trucks could be based on the side friction trends for heavy trucks. However, from a practical standpoint, the differences in friction factors are not significantly different for the two vehicle types. Hence, it is recommended that the maximum design side friction factors used for curve design be based on those observed for passenger cars because they are effectively equivalent to those observed for trucks.

The calibrated side friction model structure recognizes an effect of speed reduction on side friction demand. This naturally raises the question of what degree of speed reduction is acceptable for curve design. The side friction demand factor coincident with no speed reduction $f_{d,0}$ logically represents a *desirable* value for the maximum design side friction factor. A curve designed to require a side friction demand equal to or less than $f_{d,0}$ would operate with no speed reduction along the curve. However, in recognition of the desirability of providing a balance between motorist safety and construction cost, it may be more practical to designate a non-zero speed reduction for curve design. This speed reduction would be used with the side friction model to define an *acceptable* maximum design side friction factor $f_{d,r}$.

The allowable speed reduction for curve design could be based on consideration of facility type, design speed, or both. On the other hand, in an effort to minimize the number of values associated with the side friction design control, it could also be determined that one maximum speed reduction should be used for all conditions. Based on the trends shown in Figure A-12a, it appears that a reasonable maximum allowable speed reduction would be about 5 km/h.

As a compromise approach, the allowable speed reduction used to define the maximum design side friction factors varies from 3.0 to 4.55 km/h (for passenger cars). This range was selected after consideration of the speed reduction of trucks as well as the implications of these factors on corresponding minimum radius (at the maximum superelevation rate). The resulting maximum design side friction factors deemed suitable for both vehicle types are shown in Table A-5. The factors shown in this table are computed from Equation 10. The speed reductions shown are for passenger cars; Equation 11 can be used to show that these friction factors produce truck speed reductions of less than 5.0 km/h.

Curve Speed Relationships

The curve speed model developed for this research is based on the hypothesis that the speed adopted by a driver when traveling along a curve is based on approach speed, curve radius, and curve superelevation rate. In general, a driver's curve speed will equal the approach speed except when it is limited to lower values through the use of sharp curvature or minimal levels of superelevation. The maximum design side friction factors recommended in the *Green Book* correlate with speed reductions of 10 km/h or more on the sharpest curves.

The calibration coefficients listed in Table A-3 were used to develop relationships between speed, radius and superelevation rate. These relationships are shown in Figures A-13

TABLE A-5 Proposed maximum design side friction factors

95th Percentile Approach Speed (km/h)	Speed Reduction (km/h)	Maximum Design Side Friction Factor, $f_{d,max}$
30	3.00	0.227
40	3.00	0.209
50	3.00	0.190
60	3.00	0.171
70	3.00	0.153
80	3.00	0.134
90	3.00	0.115
100	3.25	0.100
110	3.90	0.090
120	4.55	0.080

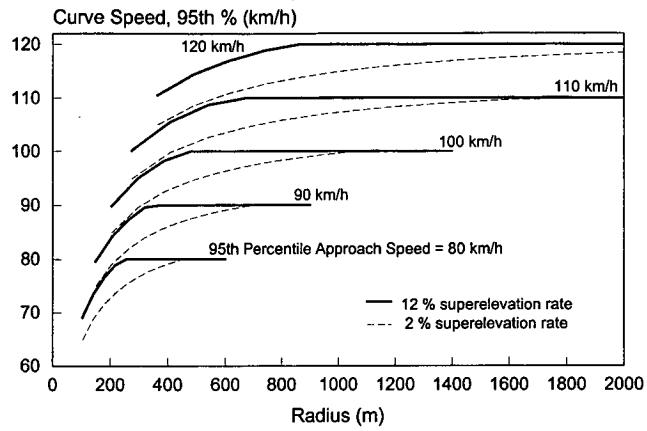

a. High-speed streets and highways.

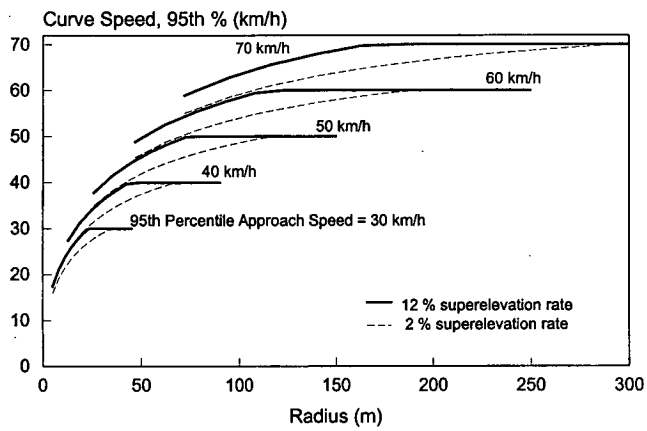

b. Low-speed streets.

Figure A-13. Expected curve speeds for streets and highways.

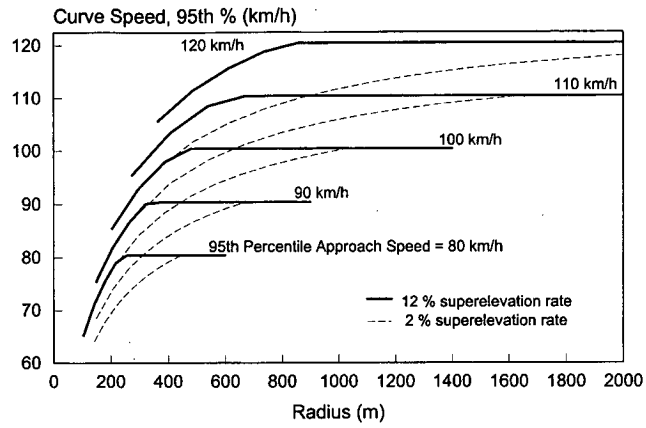

a. High-speed turning roadways.

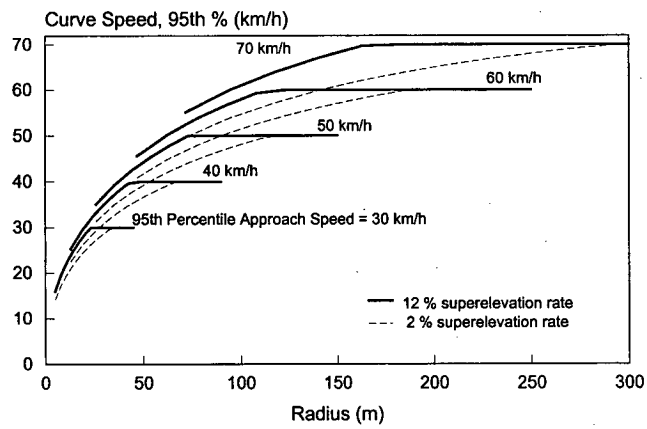

b. Low-speed turning roadways.

Figure A-14. Expected curve speeds for turning roadways.

and A-14. Those relationships shown in Figure A-13 apply to RHS and LS facilities; those in Figure A-14 apply to TR facilities. The trends shown are based on the coefficients for passenger cars. The trends for trucks were very similar; however, truck speeds tend to be slightly slower than those of passenger cars. The difference in speeds is dependant on curve radius with differences as large as 6 percent found on the sharper curves.

The trends shown in Figures A-13 and A-14 indicate that speed reductions only occur on the sharper curves. A comparison of these figures indicates that speed reductions on turning roadways are larger than those on street or highway curves. This trend suggests that drivers on turning roadways with sharp radii tend to accept larger speed reductions as they transition between intersecting facilities. In general, the average speed reduction on a turning roadway curve is between 50 and 80 percent larger than that on a RHS or LS facility for the same radius and superelevation rate.

To illustrate the use of Figure A-13, consider a curve with a radius of 500 m and a superelevation rate of 2.0 percent. Figure A-13 indicates that such a curve on a roadway with a 95th percentile speed of 80 km/h would impose no speed reduction. However, if the 95th percentile approach speed was 100 km/h, the 95th percentile curve speed would be about 95 km/h. The field data indicate that this 5-km/h speed reduction would be adopted by all drivers (not just the 95th percentile driver). Finally, if the 95th percentile approach speed was 120 km/h, the typical speed reduction would be on the order of 11 km/h.

SUMMARY

The curve speed and side friction models represent an improvement over existing models for three reasons. First, they offer a human-behavior-based explanation for driver curve speed choice. The influence of curve geometry on speed is explained using the concept of a motorist-selected balance between delay and comfort. Drivers minimize delay by limiting the magnitude of speed reduction necessary to negotiate the curve; drivers maximize comfort by limiting

the magnitude of lateral acceleration that stems from side friction demand.

A second improvement offered by the proposed models is that they provide a rational, direct linkage between curve speed and side friction demand. Calibration coefficients obtained from the curve speed model are used directly in the side friction model. The side friction model does not require explicit calibration.

A third improvement offered by the proposed models is that they include a sensitivity to superelevation rate. The statistical analysis conducted for this research indicates that superelevation rate has a significant effect on curve speed. Its effect on speed is illustrated in Figures A-13 and A-14. This factor is not considered in many curve speed relationships including those reported by McLean (*9,12*), Kerman et al. (*10*), Kanellaidis et al. (*11*), and the *Green Book* (*1, p. 197*).

REFERENCES

1. *A Policy on Geometric Design of Highways and Streets.* American Association of State Highway and Transportation Officials, Washington, D.C. (1994).
2. Chowdhury, M.A., D.L. Warren, and H. Bissell, "Analysis of Advisory Speed Setting Criteria." *Public Roads*, Vol. 55, No. 3, Federal Highway Administration, U.S. Department of Transportation, Washington, D.C. (1991) pp. 65–71.
3. Fitzpatrick, K., C. Shamburger, R. Krammes, and D. Fambro, Operating Speed on Suburban Arterial Curves. *Transportation Research Record 1579*, Transportation Research Board, National Research Council, Washington, D.C. (1977) pp. 89–96.
4. *Rural Road Design: Guide to the Geometric Design of Rural Highways.* Austroads, Sydney, Australia (1989).
5. *Road Layout and Geometry: Highway Link Design.* Departmental Standard TD 9/81. Department of Transport: Highways and Traffic, United Kingdom (1986).
6. *Manual of Geometric Design Standards for Canadian Roads.* Transportation Association of Canada, Ontario, Canada (1986).
7. *Richtlinien für die Anlage von Straßen, RAS, Teil: Linienführung, RAS-L.* Forschungsgesellschaft für Strassen–und Verkehrswesen (in German), Kirschbaum Verlag, Bonn, Germany (1995).
8. *Trafikleder på landsbygd. (Standard Specifications for Geometric Design of Rural Roads).* National Swedish Road Administration (1986).
9. McLean, J.R, "An International Comparison of Curve Speed Prediction Relations." *Road and Transport Research,* Vol. 4, No. 3 (1995) pp. 6–15.
10. Kerman, J.A., M. McDonald, and G.A. Mintsis, "Do Vehicles Slow Down on Bends? A Study into Road Curvature, Driver Behavior, and Design." *PTRC, 10th Summer Annual Meeting, Proceedings Seminar K.* (1982) pp. 57–67.
11. Kanellaidis, G., J. Golias, and S. Efstathiadis, "Drivers' Speed Behavior on Rural Road Curves." *Traffic Engineering & Control*, Vol. 31, No. 7 (July 1990) pp. 414–415.
12. McLean, J., "Driver Speed Behavior and Rural Road Alignment Design." *Traffic Engineering & Control*, Vol. 22, No. 4 (April 1981) pp. 208–211.
13. Haile, E.R., "Discussion of Friction Factors and Superelevation." Discussion paper published with: Barnett, J., "Safe Side Friction Factors and Superelevation Design." *Proceedings of the Highway Research Board*, Vol. 16, Highway Research Board, Washington, D.C. (1936) pp. 69–80.
14. Krammes, R.A., R.Q. Brackett, M.A. Shafer, J.L. Ottsen, I.B. Anderson, K.L. Fink, K.M. Collins, O.J. Pendleton, and C.J. Messer, *Horizontal Alignment Design Consistency for Rural Two-Lane Highways.* Report FHWA-RD-94-034, Federal Highway Administration, U.S. Department of Transportation, Washington, D.C. (1995).
15. Fitzpatrick, K. and J.M. Collins, *User's Guide to Data Base for Two-Lane Highway Design Consistency.* Report FHWA/7283-1, Federal Highway Administration, U.S. Department of Transportation, Washington, D.C. (1997).
16. Fitzpatrick, K., J.D. Blaschke, C.B. Shamburger, R.A. Krammes, and D.B. Fambro, *Compatibility of Design Speed, Operating Speed, and Posted Speed.* Report FHWA/TX-95/1465-2F, Texas Department of Transportation, Austin, Texas (Oct. 1995).
17. McCoy, P.T., R.R. Bishu, J.A. Bonneson, J.W. Fitts, M.D. Fowler, S.L. Gabor, M.E. Lutjeharms, B.A. Moen, and D.L. Sicking, *Guidelines for Free Right-Turn Lanes at Unsignalized Intersections on Rural Two-Lane Highways.* Report No. TRP-02-32-95, Nebraska Department of Roads, Lincoln, Nebraska (1995).
18. *SAS/STAT User's Guide, Version 6,* 4th ed. SAS Institute, Inc., Cary, North Carolina (1990).

APPENDIX B

HORIZONTAL CURVE SPEED CHARACTERISTICS

This appendix describes the characteristics of free-flowing traffic streams on horizontal curves. These characteristics are represented as speed statistics and include the average, 5th, and 95th percentile speeds of both cars and heavy trucks. Vehicle speed was also measured on the tangent approach to the curve to provide statistical control.

The characteristics described in this appendix were used to calibrate the recommended horizontal curve design controls described in Chapter 3. In general, simple relationships were developed that can be used to predict (1) the 5th and 95th percentile approach speeds of both cars and trucks, (2) the relationship between car and truck speeds on the same curve, and (3) the reduction in the 5th and 95th percentile approach speed of both cars and trucks as a result of curve geometry. These relationships permit the evaluation of side friction demand for both slow and fast drivers as a function of curve radius and superelevation. As such, they were useful in the evaluation and revision of the superelevation distribution methods described in *A Policy on Geometric Design of Highways and Streets* (*1*) (i.e., the *Green Book*).

DATABASE DEVELOPMENT

The database used to quantify and define the aforementioned speed characteristics is described in Appendix A. This database includes the geometry of 55 horizontal curves located in eight states. These curves represent all combinations of rural/urban and low-/high-speed conditions. Six of the curves are located on turning roadways (including four interchange ramps). Data recorded for each curve include radius, superelevation rate, grade, deflection angle (or curve length), curve direction (i.e., left or right), posted speed limit, and advisory speed limit (when applicable).

DATA REDUCTION AND ANALYSIS

The database development task for this research included several quality-control steps. Specifically, the field data were reviewed for accuracy and consistency. The geometric data were verified through the use of survey measurements, photo logs, and the comparison of survey measurements with as-built plans, when available. The speed data that were manually recorded on data collection sheets were reduced in duplicate by different technicians; the speed data that were collected with sensors were verified using videotape records. The details of the data reduction and analysis process are described in Appendix A.

The reduced database included 8,191 valid vehicle observations. Each observation included a measurement of the vehicle's approach speed, curve speed, and classification (i.e., car or heavy truck). About 90 percent of the observations in the database represent passenger cars; the balance represents heavy trucks (i.e., those with more than two axles).

MODEL CALIBRATION

Three types of model were calibrated for this research:

1. Percentile-Speed Model,
2. Car-Truck Speed Model, and
3. Speed Reduction Model.

The first model type predicts a percentile speed using average speed as the independent variable. Separate variations of this model were developed to predict the 5th and 95th percentile speeds. The second model type predicts average truck speed using the average passenger car speed as the independent variable. Finally, the third model type predicts a percentile speed reduction using average speed reduction as the independent variable. Separate variations of this model were also developed to predict the 5th and 95th percentile speed reductions.

The calibration of each model is described in the remainder of this section. This calibration includes a regression analysis, a presentation of the calibrated model form, and an assessment of its quality of fit.

Percentile Speed Models

This section describes the development of regression relationships between the average and selected percentile approach speeds for both cars and trucks. Specifically, two relationships are defined, one between the average and 95th percentile speed and a second between the average and 5th percentile speed.

95th Percentile Approach Speed

The relationship between the 95th percentile and average speeds is shown in Figure B-1. Each data point shown represents the speeds measured at one study site (i.e., one travel

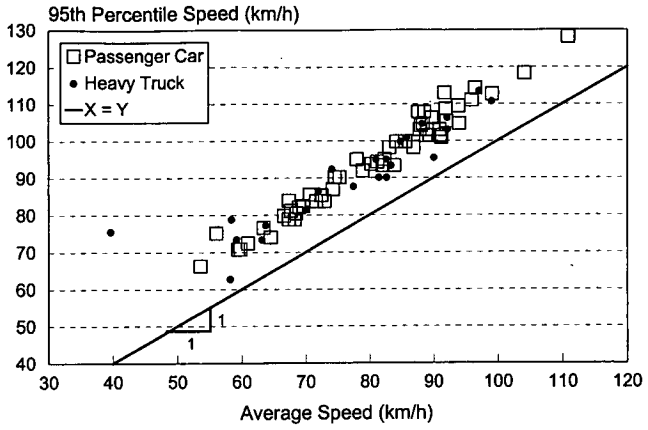

Figure B-1. Relationship between the 95th percentile and average approach speeds.

direction of one horizontal curve). The trends shown indicate that the 95th percentile speed is about 10 to 20 km/h greater than the average speed. The data corresponding to heavy trucks suggest that truck speeds are slightly slower than passenger car speeds. However, the truck data are also slightly more variable than the car data because of lower numbers of observations underlying each "truck" data point.

The data shown in Figure B-1 were used to calibrate a relationship between the average and 95th percentile speeds. Based on the distribution of data in this figure, it was determined that least-squares regression would be appropriate. However, because the number of observations differed among the various curve sites, the regression residuals were weighted using the reciprocal of the squared standard error of speed. This quantity was computed for each site using the following equation:

$$W_v = \frac{n}{\sigma_v^2} \quad (1)$$

where:

W_v = weight function for regression of curve speed,
σ_v^2 = variance of curve speed, and
n = number of observations for the subject site.

Several alternative model forms were considered to account for any differences in passenger car versus truck speeds. The model form that was found to offer the best compromise between simplicity and sensitivity to vehicle type was as follows:

$$V_{a,95} = (b_0 + b_1 I_{tk}) V_a'^{b_2} \quad (2)$$

where:

$V_{a,95}$ = 95th percentile approach speed, km/h;
V_a' = average approach speed, km/h;
I_{tk} = indicator variable (1.0 for heavy trucks; 0.0 for passenger cars); and
b_i = calibration coefficients (i = 0, 1, 2).

The results of the regression analysis are summarized in Table B-1. The statistics shown in this table indicate that the calibrated model is a very reliable predictor of the 95th percentile speed.

The regression coefficients from Table B-1 were combined with Equation 2 to form the 95th percentile approach speed model. The form of this model is as follows:

$$V_{a,95} = (1.681 - 0.057 I_{tk}) V_a'^{0.917} \quad (3)$$

In application, this equation can be used to predict the 95th percentile speed for either passenger cars or trucks. When applied to passenger cars, the average speed used in Equation 3 would correspond to the average passenger car speed. Similarly, the average truck speed would be used to predict the 95th percentile truck speed.

TABLE B-1 Calibrated 95th percentile approach speed model

Model Statistics							
R^2:	0.96						
Root Mean Square Error (km/h):	3.2						
Observations:	86 (55 sites with cars and 31 sites with trucks)						
Range of Model Variables		**Passenger Car**			**Heavy Truck**		
Var.	Variable Name	Units	Min.	Max.	Units	Min.	Max.
$V_{a,95}$	95th percentile approach speed	km/h	66	128	km/h	42	113
V_a'	Average approach speed	km/h	54	111	km/h	42	99
Calibrated Coefficient Values							
Coeff.	Coefficient Definition	Value		Std. Deviation		t-statistic	
b_0	Intercept	1.681		0.169		9.9	
b_1	Effect of heavy trucks	-0.057		0.016		-3.6	
b_2	Effect of average speed	0.917		0.021		43.7	

The relationship between the average and 95th percentile speeds, as predicted by Equation 3, is shown in Figure B-2. Also shown in this figure is the relationship between design speed and average running speed (under low-volume conditions) as shown in *Green Book* (*1*) Figure II-22 and Table III-12.

The trends shown in Figure B-2 indicate that the 95th percentile speed is approximately equal to the design speed for average speeds between 70 and 90 km/h. On the other hand, these trends imply that design speed is above the 99.9th percentile for average speeds greater than 100 km/h and below the 60th percentile for average speeds of 40 km/h. These percentiles appear to be overly conservative for high speeds and overly liberal for low speeds. It should be noted that the *Green Book* authors do not document the rationale for the relationship shown in their Figure II-22. However, in their discussion of turning roadway design, the *Green Book* authors indicate that the 95th percentile speed can be assumed to be representative of design speed (*1*, p. 194).

5th Percentile Approach Speed

The relationship between the 5th percentile and average speeds is shown in Figure B-3. Each data point shown represents the speeds measured at one study site. The trends shown indicate that the 5th percentile speed is about 10 to 20 km/h lower than the average speed.

The data shown in Figure B-3 were used to calibrate a relationship between the average and 5th percentile speeds. As with the 95th percentile speed analysis, several alternative model forms were considered to account for differences in passenger car and truck speeds. The model form that was found to offer the best compromise between simplicity and sensitivity to vehicle type was as follows:

$$V_{a,5} = (b_0 + b_1 I_{tk}) V_a'^{b_2} \quad (4)$$

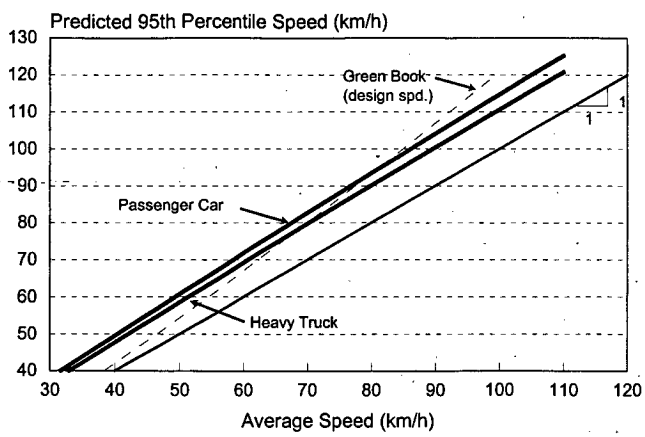

Figure B-2. Predicted relationship between the 95th percentile and average approach speeds.

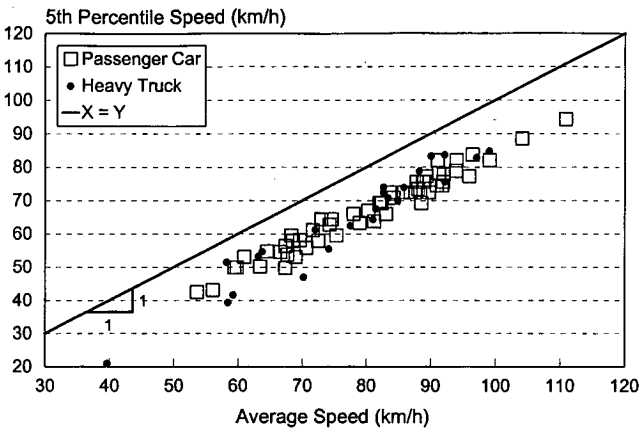

Figure B-3. Relationship between the 5th percentile and average approach speeds.

where:

$V_{a,5}$ = 5th percentile approach speed, km/h.

The results of the regression analysis are summarized in Table B-2. The statistics shown in this table indicate that the calibrated model is a very reliable predictor of the 5th percentile speed.

The regression coefficients from Table B-2 were combined with Equation 4 to form the 5th percentile approach speed model. The form of this model is as follows:

$$V_{a,5} = (0.616 - 0.021 I_{tk}) V_a'^{1.07} \quad (5)$$

In application, this equation can be used to predict the 5th percentile speed for either passenger cars or trucks. When applied to passenger cars, the average speed used in Equation 5 would correspond to the average passenger car speed. Similarly, the average truck speed would be used to predict the 5th percentile truck speed.

The relationship between the average and 5th percentile speeds, as predicted by Equation 5, is shown in Figure B-4. The trends shown suggest that the 5th percentile speed for heavy trucks is slightly higher than that of the passenger cars, for the same average speed. However, this does not mean that the 5th percentile truck has a faster speed than the 5th percentile speed of a passenger car on a given curve. In fact, the reverse is generally true because the average truck speed is typically slower than the average passenger car speed. This relationship between the average speed of cars and trucks on the same curve is described in more detail in the next section.

Car-Truck Speed Model

The relationship between the average speeds of cars and trucks on the same highway segment is shown in Figure B-5. The trends shown in this figure indicate that the average truck

TABLE B-2 Calibrated 5th percentile approach speed model

Model Statistics							
R^2:	0.93						
Root Mean Square Error (km/h):	3.5						
Observations:	86 (55 sites with cars and 31 sites with trucks)						
Range of Model Variables		**Passenger Car**			**Heavy Truck**		
Var.	Variable Name	Units	Min.	Max.	Units	Min.	Max.
$V_{a,5}$	5th percentile approach speed	km/h	42	94	km/h	20	91
V_a'	Average approach speed	km/h	54	111	km/h	42	99
Calibrated Coefficient Values							
Coeff.	Coefficient Definition	Value		Std. Deviation		t-statistic	
b_0	Intercept	0.616		0.076		8.1	
b_1	Effect of heavy trucks	0.021		0.009		2.3	
b_2	Effect of average speed	1.070		0.032		33.4	

speed is slightly below the average car speed. One study site was not consistent with this trend. It is represented in Figure B-5 as the data point with an average truck speed of 40 km/h. This particular site was on a significant downgrade and had signing for the truck drivers advising them to remain in a lower gear and maintain a low speed. This site was excluded from further analysis of these data.

An analysis of the distribution of data shown in Figure B-5 indicated that least-squares regression would be appropriate. However, because of the variation in the number of car and truck observations at each site, it was determined that the regression residuals should be weighted. The following equation was used to compute the weight for each site:

$$W_v = \frac{1}{\frac{\sigma^2_{v,pc}}{n_{pc}} + \frac{\sigma^2_{v,tk}}{n_{tk}}} \quad (6)$$

As with the previous analysis, several alternative linear model forms were considered. The model form that was found to offer the best compromise between simplicity and sensitivity to vehicle type was as follows:

$$V'_{tk} = b_0 V'_{pc} \quad (7)$$

where:

V'_{tk} = average heavy truck approach speed, km/h; and
V'_{pc} = average passenger car approach speed, km/h.

The results of the regression analysis are summarized in Table B-3. The statistics shown in this table indicate that the calibrated model is a very reliable predictor of the average truck speed.

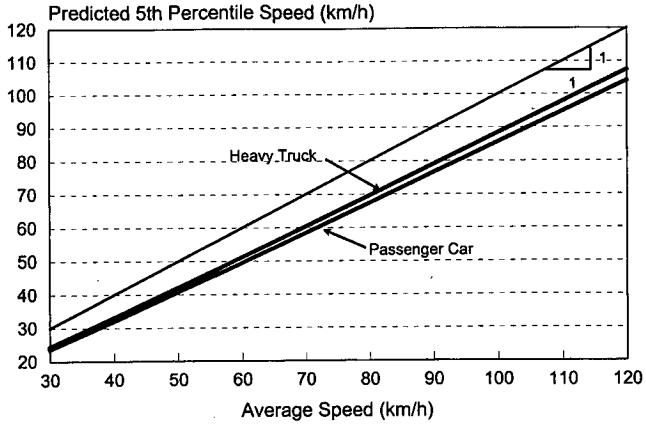

Figure B-4. Predicted relationship between the 5th percentile and average approach speeds.

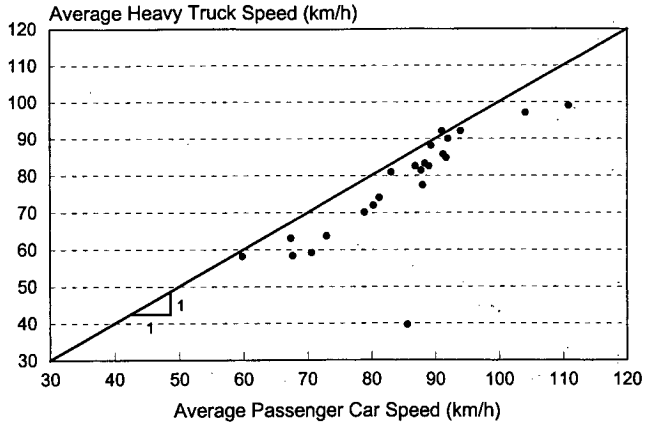

Figure B-5. Relationship between average passenger car and heavy truck speeds

TABLE B-3 Calibrated average truck approach speed model

Model Statistics							
R^2:	0.92						
Root Mean Square Error (km/h):	2.2						
Observations:	31 (sites with both cars and trucks)						
Range of Model Variables		**Passenger Car**			**Heavy Truck**		
Var.	Variable Name	Units	Min.	Max.	Units	Min.	Max.
V'	Average approach speed	km/h	54	111	km/h	42	99
Calibrated Coefficient Values							
Coeff.	Coefficient Definition	Value		Std. Deviation		t-statistic	
b_0	Effect of average passenger car speed	0.941		0.008		117.6	

The regression coefficient from Table B-3 was combined with Equation 7 to form the average truck approach speed model. The form of this model is as follows:

$$V'_{tk} = 0.941 V'_{pc} \quad (8)$$

The relationship between the average truck and car speeds, as predicted by Equation 8, is shown in Figure B-6. Also shown in this figure are data reported in Table 2-26 of the *ITE Traffic Engineering Handbook* (*2*). This table lists the mean speeds of both cars and trucks as measured on facilities with a specified speed limit. The speed limits included in Table 2-26 range from 40 to 90 km/h. The data indicate that the average truck speed is about 93 percent (± 4 percent) of the average car speed. These data provide some validation of the calibrated regression model.

Speed Reduction Models

The relationship between the approach and curve speed distributions was also examined. This relationship was examined in the context of the reduction in 95th and 5th percentile speeds relative to the reduction in average speed. Models for predicting these relationships are described in the following paragraphs.

95th Percentile Speed Reduction

The relationship between the reduction in 95th percentile and average speeds is shown in Figure B-7. In general, there is a one-to-one relationship between the 95th and average speed reductions. However, there is a tendency for some deviation from this trend when the speed reduction is large.

The data shown in Figure B-7 were used to calibrate a relationship between the average and 95th percentile speed reductions. Specifically, a linear model was calibrated using weighted least-squares regression. The weight function was similar to Equation 6; however, the approach and curve speed variances ($\sigma^2_{v,a}/n_a$ and $\sigma^2_{v,c}/n_c$) were used to compute the weight instead of the car and truck speed variances ($\sigma^2_{v,pc}/n_{pc}$ and $\sigma^2_{v,tk}/n_{tk}$).

Several alternative model forms were considered to evaluate the effect of vehicle type. However, the results of this pre-

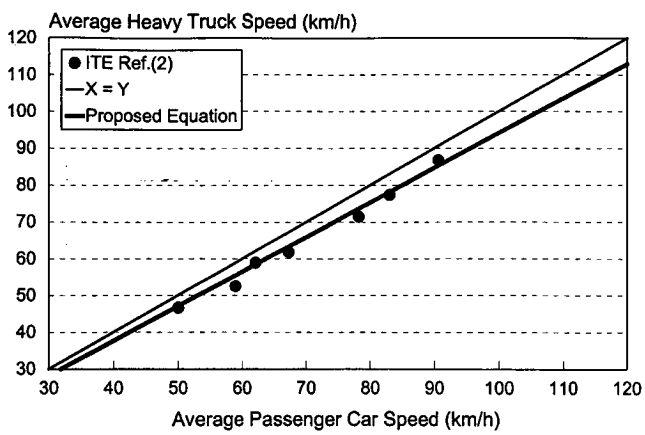

Figure B-6. Predicted relationship between the average car and truck approach speeds.

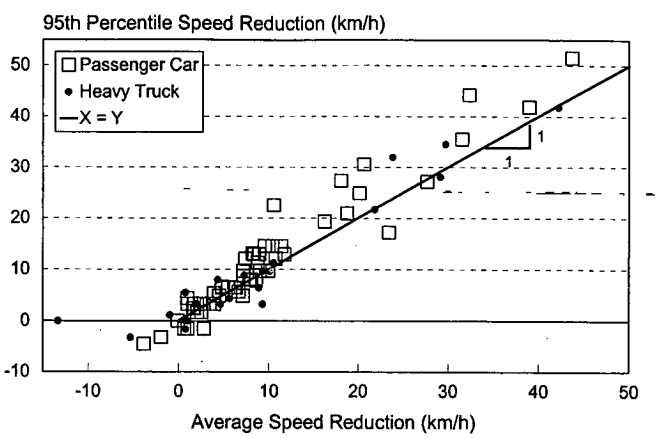

Figure B-7. Relationship between 95th percentile and average speed reduction.

TABLE B-4 Calibrated 95th percentile speed reduction model

Model Statistics							
R^2:	0.97						
Root Mean Square Error (km/h):	4.3						
Observations:	86 (55 sites with cars and 31 sites with trucks)						
Range of Model Variables		**Passenger Car**			**Heavy Truck**		
Var.	Variable Name	Units	Min.	Max.	Units	Min.	Max.
dv_{95}	95th percentile speed reduction	km/h	-5	51	km/h	-3	45
dv'	Average speed reduction	km/h	-4	44	km/h	-13	42
Calibrated Coefficient Values							
Coeff.	Coefficient Definition	Value		Std. Deviation		t-statistic	
b_0	Effect of average speed reduction	1.13		0.02		56.5	

liminary analysis indicated that there was no significant difference between the speed reductions of cars and trucks. Thus, the form of the model used for calibration was as follows:

$$dv_{95} = b_0\, dv' \tag{9}$$

where:

dv_{95} = 95th percentile speed reduction (= $V_{a,95} - V_{c,95}$), km/h;
dv' = average speed reduction (= $V_a' - V_c'$), km/h;
$V_{a,95}$ = 95th percentile approach speed, km/h;
$V_{c,95}$ = 95th percentile curve speed, km/h;
V_a' = average approach speed, km/h; and
V_c' = average curve speed, km/h.

The results of the regression analysis are summarized in Table B-4. The statistics shown in this table indicate that the calibrated model is a very reliable predictor of the 95th percentile speed reduction.

The regression coefficient from Table B-4 was combined with Equation 9 to form the 95th percentile speed reduction model. The form of this model is as follows:

$$dv_{95} = 1.13\, dv' \tag{10}$$

In application, this equation can be used to predict the 95th percentile speed reduction for either passenger cars or trucks. When applied to passenger cars, the average speed reduction used in Equation 10 would correspond to the average passenger car speed. Similarly, the average truck speed reduction would be used to predict the 95th percentile truck speed reduction.

5th Percentile Speed Reduction

The relationship between the reduction in 5th percentile and average speeds is shown in Figure B-8. In general, there is a one-to-one relationship between the 5th and average speed reductions. However, there is a tendency for some deviation from this trend for larger reductions.

The data shown in Figure B-8 were used to calibrate a relationship between the average and 5th percentile speed reductions. Several alternative model forms were considered to evaluate the effect of vehicle type. However, the results of this preliminary analysis indicated that there was no significant difference between the speed reductions of cars and trucks. Thus, the form of the model used for calibration was as follows:

$$dv_5 = b_0\, dv' \tag{11}$$

where:

dv_5 = 5th percentile speed reduction (= $V_{a,5} - V_{c,5}$), km/h; and
dv' = average speed reduction (= $V_a' - V_c'$), km/h.

The results of the regression analysis are summarized in Table B-5. The statistics shown in this table indicate that the

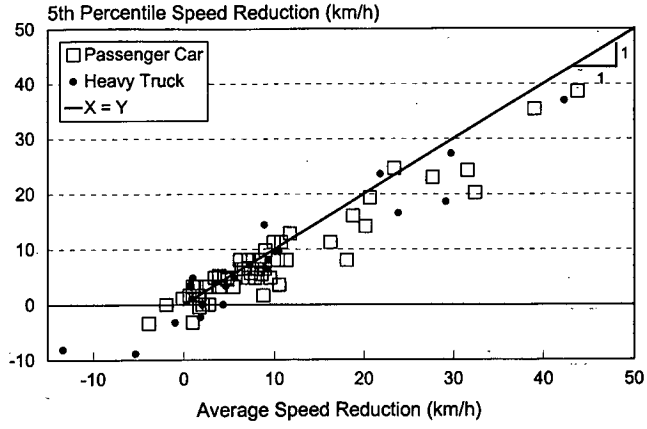

Figure B-8. Relationship between 5th percentile and average speed reduction.

TABLE B-5 Calibrated 5th percentile speed reduction model

Model Statistics							
R^2:	0.96						
Root Mean Square Error (km/h):	4.3						
Observations:	86 (55 sites with cars and 31 sites with trucks)						
Range of Model Variables		**Passenger Car**			**Heavy Truck**		
Var.	Variable Name	Units	Min.	Max.	Units	Min.	Max.
dv_5	5th percentile speed reduction	km/h	-3	39	km/h	-9	37
dv'	Average speed reduction	km/h	-4	44	km/h	-13	42
Calibrated Coefficient Values							
Coeff.	Coefficient Definition	Value		Std. Deviation		t-statistic	
b_0	Effect of average speed reduction	0.862		0.020		43.1	

calibrated model is a very reliable predictor of the 5th percentile speed reduction.

The regression coefficient from Table B-5 was combined with Equation 11 to form the 5th percentile speed reduction model. The form of this model is as follows:

$$dv_5 = 0.862\,dv' \tag{12}$$

In application, this equation can be used to predict the 5th percentile speed reduction for either passenger cars or trucks. When applied to passenger cars, the average speed reduction used in Equation 12 would correspond to the average passenger car speed. Similarly, the average truck speed reduction would be used to predict the 5th percentile truck speed reduction.

The relationship between the average and the percentile speed reductions, as predicted by Equations 10 and 12, is shown in Figure B-9. The trends shown in this figure suggest the magnitude of the percentile speed reduction deviates from the average reduction in direct proportion to the amount of reduction. In addition, the slope for the 95th percentile speed reduction is greater than 1.0 and that for the 5th percentile speed reduction is less than 1.0. These slopes suggest that the variance in the distribution of curve speeds decreases with increasing speed reduction.

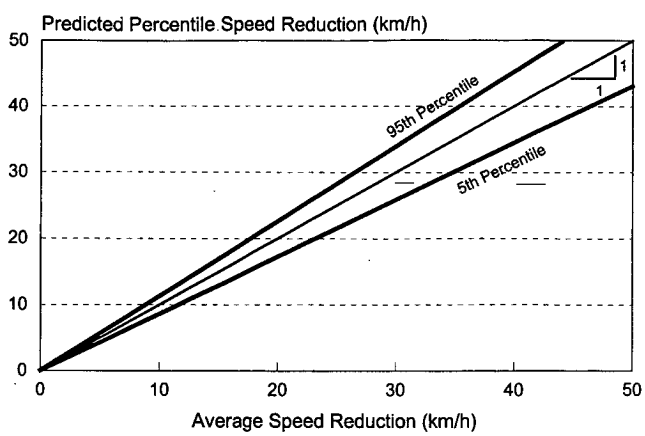

Figure B-9. Relationship among average, 95th, and 5th percentile speed reductions.

SPEED RELATIONSHIPS

Equations 3, 5, and 8 were used to define the relationship between passenger car and truck approach speeds. This relationship is shown in Table B-6 for the average, 95th, and 5th percentile speeds for each vehicle type. The 95th percentile speed for the passenger car was defined in 10 km/h increments; all other speeds shown were computed using Equations 3, 5, and 8.

The data in Table B-6 suggest that a curve with a 95th percentile passenger car speed of 70 km/h would likely have an average passenger car speed of 58.4 km/h and a 5th percentile speed of 47.8 km/h. Furthermore, the 95th percentile, average, and 5th percentile truck speeds on this same curve are likely to be 64.0, 54.9, and 46.3 km/h, respectively.

Equations 10 and 12 can be used to convert the approach speeds shown in Table B-6 into curve speeds once an appropriate speed reduction is identified. As described in Appendix A, the amount of speed reduction is dependent on curve geometry and approach speed. Specifically, the curve speed model in Appendix A can be used to determine the resulting speed reduction for a selected radius, superelevation rate, and approach speed.

To illustrate the use of Equations 10 and 12, assume that a curve geometry is selected that results in a 3-km/h reduction in the 95th percentile speed. This speed reduction translates into a 2.7-km/h (= 3.0/1.13) average speed reduction and a 2.3-km/h (= 2.7 * 0.862) 5th percentile speed reduction. Thus,

TABLE B-6 Relationship between passenger car and heavy truck approach speeds

Passenger Car Approach Speed			Heavy Truck Approach Speed		
95th Percentile (km/h)	Average (km/h)	5th Percentile (km/h)	95th Percentile (km/h)	Average (km/h)	5th Percentile (km/h)
30.0	23.2	17.8	27.4	21.8	17.2
40.0	31.7	24.9	36.5	29.8	24.1
50.0	40.4	32.3	45.7	38.1	31.3
60.0	49.3	39.9	54.8	46.4	38.7
70.0	58.4	47.8	64.0	54.9	46.3
80.0	67.5	55.8	73.1	63.5	54.1
90.0	76.8	64.1	82.2	72.2	62.1
100.0	86.1	72.5	91.4	81.0	70.2
110.0	95.5	81.0	100.5	89.9	78.5
120.0	105.0	89.6	109.6	98.9	86.8

when the 95th percentile passenger car approach speed is 70 km/h and the curve is sufficiently sharp as to warrant a 3-km/h 95th percentile speed reduction, the 5th percentile passenger car curve speed can be estimated as 45.5 km/h (= 47.8 – 2.3) and the 5th percentile truck curve speed can be estimated as 44.0 km/h (= 46.3 – 2.3).

REFERENCES

1. *A Policy on Geometric Design of Highways and Streets*. American Association of State Highway and Transportation Officials, Washington, D.C. (1994).
2. *Traffic Engineering Handbook*, 4th ed. J.L. Pline, editor, Institute of Transportation Engineers. Prentice Hall, New Jersey (1992).

APPENDIX C

VEHICLE DYNAMICS ON ROADWAY CURVES

This appendix examines the factors affecting side friction demand and supply. These factors include speed, curve radius, superelevation rate, vehicle type, and roadway grade. In the context of vehicle type, the effects of a vehicle's suspension, weight distribution, and physical dimension are considered. Special attention is given to an examination of the effect of grade on friction supply and demand. This examination provides a theoretic insight into the concept of side friction demand and supply, as it relates to the roadway design process. These insights formed the basis for the side friction demand model described in Appendix A.

The factors affecting side friction demand and friction supply are described in the next section. Then, a kinematic model is developed to predict side friction demand as well as the impact of selected geometric factors on this demand. Next, two friction supply models are developed. One of these models describes the slide failure mode and another describes the roll failure mode. Finally, the demand and supply models are compared using a margin of safety analysis.

SIDE FRICTION DEMAND AND SUPPLY

Side Friction Demand

The following equation is given in the *Green Book* (*1*) as defining the relationship among side friction demand, superelevation, speed, and radius:

$$f_{y,D} = \frac{v^2}{gR} - \frac{e}{100} \quad (1)$$

where:

e = superelevation rate, percent;
$f_{y,D}$ = side friction demand factor;
v = vehicle speed, m/s;
g = gravitational acceleration (= 9.807 m/s^2); and
R = radius of curve, m.

This equation is based on the representation of the vehicle as a "point-mass." With this approach, all force vectors are assumed to intersect at the vehicle's center of gravity; the distribution of forces to the individual tires is neglected. As a result, differences in vehicle type (e.g., small car, large truck) are not explicitly recognized by the model.

Equation 1 represents a force balance in the lateral direction. As a result, a factor for grade is not included because its primary effect is in the longitudinal direction.

Equation 1 is derived to predict the side friction demand at the tire-pavement interface for a given driver-selected speed v when traveling on a curve of radius R and superelevation rate e. However, the friction demand predicted by Equation 1 is more of a conceptual convenience than it is a true measure of tire-pavement friction. The predicted friction demand offers an intuitive means of understanding speed choice as a function of curve geometry. Specifically, the predicted friction is approximately equal to the lateral acceleration (in g's) experienced by the driver (in fact, motorists experience a slightly larger level of acceleration because of vehicle body roll). Logically, drivers would reduce speed if the lateral acceleration that is expected (or experienced) during curve entry exceeds a level that is deemed comfortable or, if they are in a hurry, tolerable.

Influence of Grade

The *Green Book* authors discuss the effect of grade on several roadway design controls. This discussion suggests that grade has a significant effect on climbing lane design and highway level of service. In these situations, the effect of grade stems from the performance capabilities of heavy trucks. The *Green Book* authors also describe the effect of grade on stopping sight distance; however, there are no firm recommendations offered regarding the use of adjusted values of stopping sight distance on grades. With regard to controls for horizontal curve design, those discussed in the *Green Book* do not have a sensitivity to alignment grade.

The *Green Book* authors do recognize a possible effect of grade on horizontal curve design. Specifically, the *Green Book* authors suggest that speeds may increase in the downgrade direction resulting in an increase in lateral acceleration. They suggest that separate consideration of the upgrade and downgrade directions (with regard to design speed and superelevation rate) is an option, although it is generally not necessary. It should be noted that, in a recent review of published studies of curve speed, McLean (*2*) found that grade did not have a significant effect on curve speed.

Dunlap et al. (*3*) re-examined the point-mass model with a focus on the effect of grade. They found that grade did have a secondary effect in that the vehicle weight component (and hence the normal force) was reduced slightly as a result of grade. The equation they derived is as follows:

$$f_{y,D} = \frac{v^2}{gR}\cos(0.01e) - \sin(0.01e)\cos(G) \quad (2)$$

where:

G = roadway grade, m/m.

Dunlap et al. (*3*) compared Equations 1 and 2 and concluded that grade had a negligible effect on side friction demand. They found that the difference in predicted friction demands equated to about 0.7 percent of the side friction demand predicted by Equation 2. More important, they found that grade had negligible effect on this difference. Based on this examination, Dunlap et al. Concluded that "... the AASHTO curve design formula [Equ. 1] is virtually equivalent to the exact formula [Equ. 2] and is essentially independent of grade" (*3*, p. 443).

Dunlap et al. (*3*) also used simulation to examine the effect of grade on turning vehicle performance. Specifically, they used the HVOSM (*4*) simulation program to simulate a passenger car traveling along a horizontal curve. They used this program to determine the maximum safe speed V_{LOC} that could be sustained on a given curve without "loss of control." The results of this examination are consistent with those noted previously. Specifically, that grade had negligible effect on a vehicle's turning ability.

Other Factors Affecting Side Friction Demand

Two additional factors have been identified that influence side friction demand. The first factor relates to the friction demands of heavy vehicles. Specifically, a study by MacAdam et al. (*5*) indicated that the side friction demand for large trucks exceeds that predicted by Equation 1 by about 10 percent because of variations in tire-to-tire friction.

A second factor relates to the radius of the vehicle path. Glennon and Weaver (*6*) found that drivers tend to track transient paths sharper in curvature than that of the roadway. They found that the radius of the highway curve was 1.1 to 1.5 times larger than the radius of the tracked path at a "critical" point along the curve. These findings are also consistent with those of MacAdam et al. (*5*) who reported that side friction demand is 15 percent higher than that predicted by Equation 1 because of "steering fluctuations" along the curve.

The tendency for the path radius to oscillate about the curve radius was observed again by Glennon et al. (*7*) in a second study. This study observed the critical radius to occur just after the beginning of the curve.

Based on the aforementioned factors, the following equation can be used to more accurately predict the maximum side friction demand on curves:

$$f_{y,D} = b_v\left(b_s\frac{v^2}{gR} - \frac{e}{100}\right) \quad (3)$$

where:

$f_{y,D}$ = side friction demand factor,
b_v = vehicle-type adjustment factor (1.0 for passenger cars, 1.10 for large trucks), and
b_s = steering fluctuation factor (= $R_{actual}/R_{critical} \approx 1.15$).

Side Friction Supply

Two types of failure are possible when traversing a highway curve: slide or roll. A failure occurs when the lateral acceleration (i.e., $v^2/R - g\,e/100$) is sufficient to (1) overcome the offsetting force of friction or (2) provide an overturning moment that rotates the vehicle about its outside tires. In general, the center of gravity of most passenger cars is sufficiently low that slide failure occurs before roll failure. However, the reverse is true for many trucks because of the greater height of their mass center, particularly when fully loaded.

The next two sections describe the side friction supply for both cars and trucks. The first section describes the friction supply associated with slide failure. The second section describes the friction supply associated with roll failure.

Side Friction Supply Based on Slide Failure

The friction supply applicable to travel along a curved path is more precisely referred to as the peak side friction supply provided by the tire-pavement interface under a minimal slip (i.e., "static") condition. When side friction demand exceeds the static friction supply, the vehicle will slide off the roadway. The *Green Book* does not report static friction supply factors; however, it does provide the friction factors for a locked-wheel, forward skid. The factors for a locked-wheel skid represent a maximum slip (or "dynamic") condition as the tire is moving relative to the pavement surface.

The dynamic friction factors provided in the *Green Book* are shown in column 2 of Table C-1. These factors are applicable to a locked-wheel skid on a worst-case combination of poor, wet pavement and worn tires. More representative dynamic friction factors can be found in Figure III-1 of the *Green Book*. Such values are more useful in the comparison of typical friction supply and demand values. The values selected from Figure III-1 as representative of the median dynamic friction factor are shown in column 3 of Table C-1. They compare favorably with the median friction factors measured by Wehner (*8*) (as reported by Lamm [*9*]) on German highways.

Olson et al. (*10*) have developed an equation that can be used to estimate the maximum side friction supply for slide failure (i.e., the static friction factor) using the friction factors for the forward skid:

$$\begin{aligned} f_{y,\max,sl} &= 0.20 + 1.12 f_{x,\max,sk} \quad &: \textit{passenger car} \\ f_{y,\max,sl} &= 1.01 f_{x,\max,sk} \quad &: \textit{passenger car} \end{aligned} \quad (4)$$

TABLE C-1 Side friction supply for slide failure

Design Speed (km/h)	Max. Design Forward Friction Factor, $f_{x,d,max}$ [1]	Max. Forward Friction Supply for Skid Failure, $f_{x,max,sk}$ [2]	Maximum Side Friction Supply for Slide Failure, $f_{y,max,sl}$	
			Passenger Car	Heavy Truck
30	0.40	0.53	0.79	0.54
40	0.38	0.48	0.74	0.49
50	0.35	0.44	0.69	0.45
60	0.33	0.40	0.65	0.41
70	0.31	0.36	0.60	0.37
80	0.30	0.34	0.58	0.35
90	0.30	0.33	0.57	0.33
100	0.29	0.31	0.55	0.31
110	0.28	0.30	0.54	0.30
120	0.28	0.29	0.52	0.29

[1] Design friction values reported in Table III-1 of the *Green Book* (*1*).
[2] Median friction values based on trends in Figures III-1A and III-1B of the *Green Book* (*1*).

where:

$f_{y,\max,sl}$ = maximum side friction supply for slide failure (median value for wet pavement); and
$f_{x,\max,sk}$ = maximum forward friction supply for skid failure (median value for wet pavement).

These equations were used to compute median values of the maximum side friction factor for slide failure. These factors are shown in Table C-1 in columns 4 and 5 as they apply to passenger cars and heavy trucks, respectively.

Kontaratos et al. (*11*) examined the effect of grade on the minimum curve radius control. This examination required quantification of the maximum side friction factor for design. They postulated that this factor represents the maximum side friction supply provided by the tire-pavement interface less that friction used to overcome the forces retarding forward motion (e.g., air resistance and grade). The tractive force applied to the drive wheels uses some of the friction supply to counter the retarding forces. This approach is based on an elliptic representation of friction supply in the longitudinal x and lateral y directions and the recognition that the use of friction in one direction reduces the available friction supply in the other direction.

The friction ellipse concept leads to the following equation for predicting the available maximum side friction supply for slide failure:

$$f^*_{y,\max,sl} = f_{y,\max,sl}\sqrt{1-\left(\frac{f_{x,D}}{f_{x,\max,sl}}\right)} \qquad (5)$$

where:

$f^*_{y,\max,sl}$ = available maximum side friction supply for slide failure;
$f_{y,\max,sl}$ = maximum side friction supply for slide failure;
$f_{x,\max,sl}$ = maximum forward friction supply for slide failure (approximately equal to $f_{y,\max,sl}$); and
$f_{x,D}$ = tractive or braking friction demand factor.

The analysis by Kontaratos et al. (*11*) revealed that an upgrade can have a significant effect on side friction supply because the vehicle's tractive forces expend some of the friction otherwise available in the lateral direction. Based on their analysis, Kontaratos et al. suggested that there was a need to increase the minimum curve radius for upgrade conditions beyond that recommended by the *Green Book*.

Side Friction Supply Based on Roll Failure

In addition to slide failure, a vehicle can roll over as it traverses a curve if its center of gravity is sufficiently high as to produce an overturning moment. A static force and moment analysis of a vehicle traveling on a curved path yields the following relationship between the height of the center of gravity, track width, superelevation, and the centripetal acceleration term at impending roll failure:

$$b_r\frac{t}{2h} = b_s\frac{v^2}{gR} - \frac{e}{100} \qquad (6)$$

where:

t = track width of the vehicle, m;
h = height of the vehicle's center of gravity, m; and
b_r = calibration factor (typically, $0.4 < b_r < 0.8$).

The calibration factor b_r included in this equation is based on the work reported by Ervin et al. (*12*). They found that the quantity $t/(2h)$ in Equation 6 overestimated a vehicle's roll stability (especially for trucks) because it did not account for

the vehicle's suspension system and the tendency for the sprung mass (i.e., vehicle engine and body) to "roll" or lean out while turning.

Equation six can be combined with Equation 3 to yield the equivalent side friction supply at impending roll failure $f_{y,\max,r}$. This friction level can be considered a maximum or limiting value because "failure" (by rollover) occurs when it is exceeded by actual demand (as predicted by Equation 1). As a result, $f_{y,\max,r}$ is considered a maximum side friction supply for the purposes of this research. This representation of friction-demand-at-roll-failure as a side friction supply facilitates the comparison of it with actual side friction demand and with the side friction supply for slide failure. The equivalent maximum side friction supply for roll failure can be computed as follows:

$$f_{y,\max,r} = b_v(RT - 0.01e) = b_v b_r \frac{t}{2h} \quad (7)$$

with

$$RT = b_r \frac{t}{2h} + \frac{e}{100} \quad (8)$$

where:

$f_{y,\max,r}$ = equivalent maximum side friction supply for roll failure,
RT = rollover threshold factor, and
b_v = vehicle-type adjustment factor (1.0 for passenger cars, 1.10 for large trucks).

Equation 7 predicts a maximum side friction factor $f'_{y,\max,r}$ of about 1.2 for passenger cars and about 0.4 for trucks of "average" load condition. Ervin et al. (*12*) suggest that the rollover threshold RT can be in the range of 0.24 to 0.34 for a truck with a full load of low-density material when traveling on an unsuperelevated roadway. In this situation, $f_{y,\max,r}$ can vary from 0.26 to 0.36 based on a roadway cross slope of 2.0 percent.

Comparison of Side Friction Supply and Demand

At this point, it is useful to compare the side friction supply and demand values obtained from the relationships described in the previous two sections. For this comparison, Equation 3 was used to compute the side friction demand for both cars and trucks. The radius used in this equation was set to the minimum radius values recommended in the *Green Book*. For speeds less than or equal to 70 km/h, the minimum radii recommended for low-speed urban streets were used. For speeds 80 km/h and greater, the minimum radii recommended for rural highways and high-speed urban streets were used. In all cases, a superelevation rate of 6.0 percent was used.

Equation 5 was used to estimate the available maximum side friction supply for slide failure. The maximum side friction supply factors were obtained from Table C-1. A nominal tractive/braking friction factor of 0.05 was used in Equation 5 to replicate typical friction demands used to propel or slow the turning vehicle.

Finally, Equation 7 was used to estimate the equivalent maximum side friction supply for roll failure. These friction factors were previously estimated as 1.2 and 0.43 for average cars and trucks, respectively. Because the value of 1.2 is significantly larger than the car's side friction supply for slide failure, almost all cars will fail by sliding out rather than by rolling over.

The predicted supply and demand friction factors are shown in Figure C-1. Also shown are the maximum design side friction factors recommended in the *Green Book* for three roadway facility types.

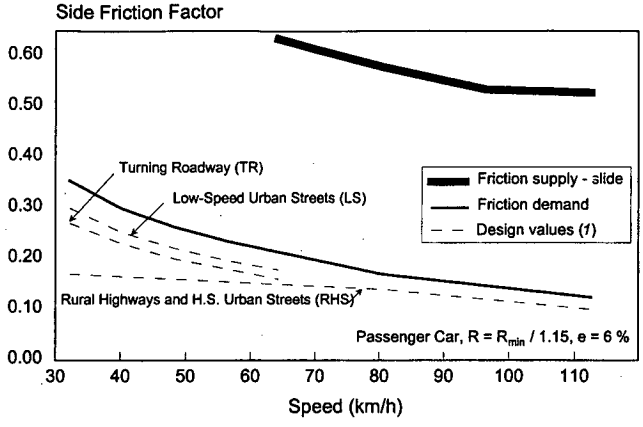

a. Passenger car.

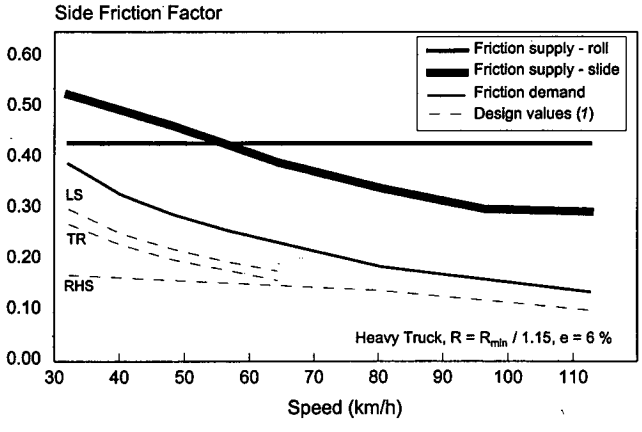

b. Heavy truck.

Figure C-1. Preliminary comparison of side friction supply and demand

The trends shown in Figure C-1 indicate that passenger cars have a larger margin of safety than trucks because cars have a lower peak friction demand and a higher friction supply. Moreover, the trends indicate that trucks can experience either slide or roll failure, depending on their speed and center of gravity height. In general, a fully loaded truck traveling on a low-speed curve of near-minimum radius is more likely to overturn than slide out. On the other hand, trucks are more likely to slide out under moderate- to high-speed conditions.

SIDE FRICTION DEMAND MODEL

This section describes the development of a side friction demand model. This model is based on a static analysis of the forces acting on a turning vehicle. A primary focus of this examination is the effect of grade on side friction demand, however; other factors such as speed, radius, and superelevation rate are also considered. The side friction demand model is based on a "bicycle" representation of a two-axle vehicle. The bicycle representation is shown in Figure C-2.

The bicycle representation provides an added level of modeling complexity, relative to the point-mass representation. Specifically, the normal and longitudinal forces are distributed among the two axles, as opposed to being combined at the center of gravity. This extension to the point-mass representation provides additional sensitivity to the effect of gravity because it recognizes the uneven distribution of forces to the two axles.

Model Development

Two or more coordinate systems can be defined to represent the system of forces acting on the vehicle. One coordinate system is fixed to the earth. The forces acting in this system can be described by a triplet of unit vectors (X, Y, Z). In this system, the X axis points in the direction of the roadway centerline and the Y axis points to the right; both axes lie in a horizontal plane relative to the direction of gravity. The Z axis points downward in the direction of gravitational acceleration.

The other coordinate systems are fixed to the vehicle; the number of systems is somewhat dependent on the representation of the vehicle system. For the bicycle representation, two coordinate systems can be used. One system is fixed to the vehicle's center of gravity and the other is fixed to its

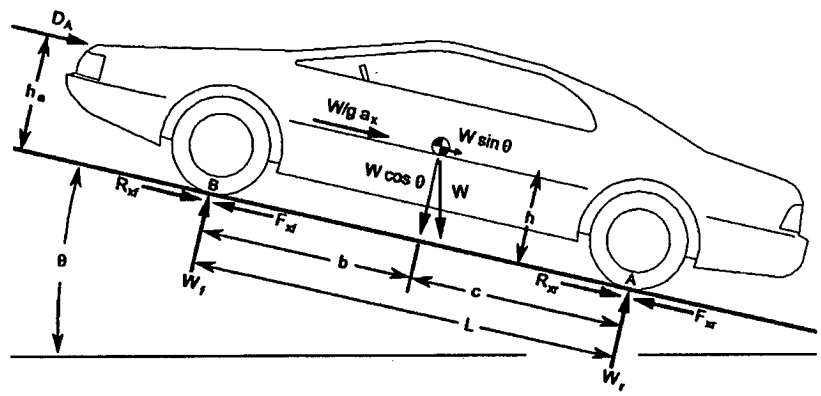

a. Forces acting on the vehicle as viewed from the side.

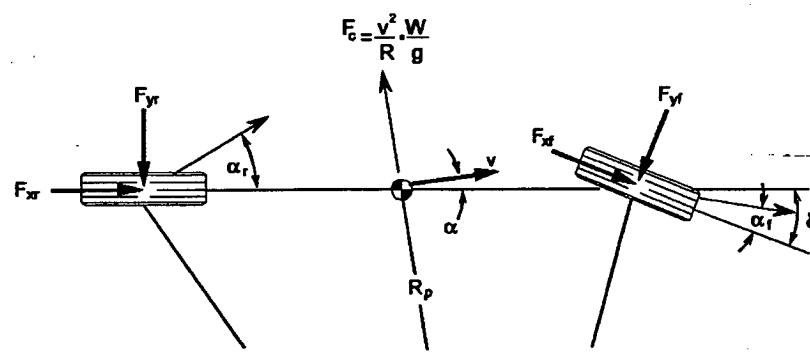

b. Forces acting on the vehicle as viewed from above.

Figure C-2. Bicycle model representation of two-axle vehicle (adapted from Ref. 13).

front tire. The system fixed to the center of gravity would have the x axis pointing in the forward direction of the vehicle, the y axis pointing to the right side of the vehicle, and the z axis pointing perpendicular to the x-y plane in a downward direction. This system is shown in Figure C-3. The system fixed to the front tire would have the same z axis; however, the x axis would be pointing in the direction the front tire is pointing and the y axis would be pointing to the right side of the front tire.

Each vehicle coordinate system has its own yaw angle α (i.e., angle of rotation about the z axis. For the system fixed to the center of gravity, this angle represents the angle between the vehicle's x axis and the velocity vector (i.e., X axis). This angle is defined as: $\alpha_1 = \alpha_r - c/R$, where α_r is the slip angle of the rear tire. For the system fixed to the front tire, the yaw angle represents the angle between the x axis and the velocity vector of the front tire, this angle is defined as: $\alpha_2 = \delta + \alpha_r - c/R$, where δ is the steer angle.

Development of a side friction demand model using two vehicle coordinate systems results in a relatively intractable model that requires an iterative solution approach. A simplified system is obtained by assuming that the two yaw angles (α_1 and α_2) are approximately equal and can be represented by one variable α (i.e., $\alpha = \alpha_1 = \alpha_2 = \alpha_r - c/R$). This angle α is sometimes referred to as the vehicle sideslip angle β.

The compromise vehicle coordinate system is essentially a system that is referenced to the vehicle center of gravity. As will be shown in the remainder of this section, the use of this system yields a closed-form solution for side friction demand. An examination of the error that results from the aforementioned assumption indicated that side friction demand is underestimated by no more than 5.0 percent for grades ranging from −10 to +10 percent, the error of magnitude increasing with the absolute value of grade.

The relationship between the earth coordinate system and the compromise vehicle coordinate system is defined by the yaw angle α, the grade G, and the superelevation rate e as each represent angles of rotation about the Z, Y, and X axes, respectively. The transformation matrix between the earth and vehicle coordinate systems is as follows:

$$\begin{bmatrix} X \\ Y \\ Z \end{bmatrix} = \begin{bmatrix} 1 & Ge - \alpha & G + \alpha e \\ \alpha & \alpha Ge + 1 & \alpha G - e \\ -G & e & 1 \end{bmatrix} \begin{bmatrix} x \\ y \\ z \end{bmatrix} \quad (9)$$

This transformation matrix takes advantage of the fact that the angles of rotation about each of the three axes are small. Specifically, it is assumed that $tan(\Theta) = G$, $sin(\Theta) = G$ and $cos(\Theta) = 1$, where Θ is the angle of incline of the roadway. A similar, small-angle assumption is made for α and e (in this instance e is defined as a rate in m/m in Equation 9 and not as a percentage). An examination of the implications of the small-angle assumption was conducted wherein the trigonometric functions were used to develop the aforementioned matrix. A comparison of the predicted side friction demands obtained from the two forms of the matrix indicated that the matrix shown in Equation 9 introduced less than 1.0 percent error relative to the use of the functions.

The forces acting on a cornering vehicle are shown in Figure C-2. These forces and their vector directions are summarized as follows:

Weight:	$W\overline{Z}$	
Rolling Resistance:	$-(R_{xf} + R_{xr})\overline{x}$	
Air Resistance:	$-_A \overline{x}$	
Traction/Braking:	$(F_{xf} + F_{xr})\overline{x}$	(+ traction, − brake)
Side Friction:	$(F_{yf} + F_{yr})\overline{y}$	
Normal:	$-(W_f + W_r)\overline{z}$	

In addition, the accelerations acting on the vehicle can be represented as forces to facilitate the static force analysis. These "equivalent" forces and their vector directions are as follows:

Centripetal Acceleration Force:	$-_c \overline{Y}$	
Thrust/Braking Acceleration Force:	$F_T \overline{x}$	(+ thrust, − brake)

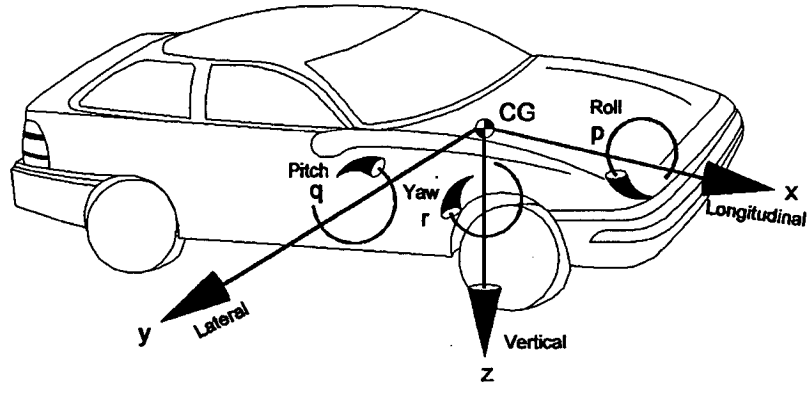

Figure C-3. Vehicle coordinate system (adapted from Ref. 13).

with

$$F_c = \frac{v^2}{R}\frac{W}{g} \tag{10}$$

$$F_T = a_x \frac{W}{g} \tag{11}$$

where:

v = vehicle speed (on the curve), m/s;
a_x = forward acceleration rate, m/s^2; and
W = vehicle weight, N.

In addition to the assumptions discussed in this section, the following assumptions were made for this analysis:

1. The driver will apply sufficient engine power to maintain a desired curve speed. Upgrades that require more power than is available are not considered.
2. The driver slows upon entry to the curve. Field observations reported in Appendix A indicate that drivers reduce speed to negotiate sharper curves. Observations by Lamm et al. (*14*) indicate that a deceleration rate of 0.85 m/s^2 is representative of most vehicles. Hence, the "acceleration" rate a_x is equal to −0.85 m/s^2.
3. The vehicle has rear wheel drive (i.e., $F_{xf} = 0$ when a tractive force is exerted). A preliminary analysis indicated that rear-wheel drive vehicles have a larger side friction demand than those with front-wheel drive.
4. All two or three factor products in the transformation matrix (Equation 9) are assumed to be effectively equal to zero and thus, can be eliminated from the matrix.
5. The height of the center of gravity h and the height of the center of the frontal area h_a are effectively equal.

Based on these assumptions, the following equations are derived by summing the forces in the x, y, and z directions:

$$\sum F_x: \quad -WG - F_c\alpha - D_A - R_{xr} - R_{xf} + (F_{xr} + F_{xf}) = a_x \frac{W}{g} \tag{12}$$

$$\sum F_y: \quad W(0.01e) - F_c + F_{yr} + F_{yf} = 0 \tag{13}$$

$$\sum F_z: \quad W + F_c(0.01e) - W_f - W_r = 0 \tag{14}$$

Equation 12 can be rewritten to yield the traction/braking force necessary to yield the acceleration rate a_x:

$$F_x = a_x \frac{W}{g} + D_A + R_x + WG + F_c\alpha \quad \le F_{x,\max} \tag{15}$$

with

$$F_{x,\max} = \frac{1000\eta}{vP}\frac{W}{g} \tag{16}$$

$$D_A = 0.6082 C_D A_f v^2 \tag{17}$$

$$R_x = R_{xf} + R_{xr} = W(b_0 + b_1 v^{b_2}) \tag{18}$$

$$\alpha = \alpha_r - \frac{c}{R} \tag{19}$$

$$\alpha_r = \frac{F_c - W(0.01e)}{CC \times W} \tag{20}$$

where:

F_x = tractive or braking force, N;
η = drive train efficiency (= 0.90);
P = mass/power ratio, kg/kw;
$F_{x,\max}$ = maximum tractive force available from engine, N;
D_A = aerodynamic drag force, N;
C_D = aerodynamic drag coefficient of vehicle;
A_f = frontal area of the vehicle, m^2;
R_x = rolling resistance of the front R_{xf} and rear R_{xr} wheels, N;
b_0, b_1, b_2 = calibration coefficients;
α = yaw angle, radians;
α_r = slip angle of the rear tire, radians; and
CC = cornering coefficient of tires, radians^{-1}.

$$W_r = [W + F_c(0.01e)]\frac{b}{L} + (D_A + WG + F_c\alpha)\frac{h}{L} \tag{21}$$

Moments taken about the front and rear tire-pavement interfaces (i.e., points B and A, respectively, in Figure C-2a) yield the following equations:

$$W_f = [W + F_c(0.01e)]\frac{c}{L} - (D_A + WG + F_c\alpha)\frac{h}{L} \tag{22}$$

$$F_{yf} = [F_c - W(0.01e)]\frac{c}{L} \tag{23}$$

$$F_{yr} = [F_c - W(0.01e)]\frac{b}{L} \tag{24}$$

Finally, the side friction demand for the front and rear tires can be computed as follows:

$$f_{yr,D} = \frac{F_{yr}}{W_r}; \qquad f_{yf,D} = \frac{F_{yf}}{W_f} \tag{25}$$

The larger of the friction demands is considered to represent the "critical" side friction demand. If this demand were to exceed the side friction supply, a failure in the form of slide or rollover would occur. Therefore, the critical side friction demand is defined as follows:

$$f_{y,D} = \textit{Larger of}: [f_{yf,D}, \quad f_{yr,D}] \tag{26}$$

Sensitivity Analysis

Equation 26 was used to compute the side friction demand for a range of vehicle types and geometric conditions. The focus of the examination was the effect of grade on side friction demand; however, the effect of speed, radius, superelevation, and vehicle type were also considered. To highlight differences between the side friction predicted by Equation 26 and that predicted by Equation 1, their ratio was computed as follows:

$$r_D = \frac{f_{y,D,26}}{f_{y,D,1}} 100 \quad (27)$$

where:

r_D = friction demand ratio, percent.

Three vehicle types are included in the investigation. Two of the vehicle types represent passenger cars: a compact and a full-size sedan. The other vehicle represents a single-unit truck. The characteristics of these vehicles are listed in Table C-2.

In general, the characteristics in Table C-2 were selected to represent "typical" vehicles. However, two exceptions were incorporated to provide a conservative representation of the vehicle population. Specifically, the tire properties (i.e., cornering coefficient and maximum side friction factor) for all vehicle types were selected to represent relatively poor tires, as might be found on about the 10th percentile of all tires. Second, the single-unit truck was configured to represent a vehicle that is fully loaded with a low-density cargo (i.e., it has a high center of gravity).

The side friction demand model was exercised for a range of speeds, radii, superelevation, vehicle types, and grades. In general, a full range of values for each variable was considered. These ranges are as follows:

Speed (km/h):	50, 110
Radius (m):	for 50 km/h: 45, 60, 120 for 110 km/h: 230, 335, 825
Superelevation (%):	0, 12
Vehicle types:	Compact car, Full-size car, Single-unit truck
Grade (%):	−10, −8, −6, −4, −2, 0, 2, 4, 6, 8, 10

A non-zero deceleration rate a_x complicates the application of the side friction demand model because this model includes a variable for speed, which is by definition not constant. However, recognizing that the speed change is typically small, a constant speed is used to simplify the analysis. Thus, the speed used in the model is conservatively considered to represent that occurring on the curve near the end of the deceleration. Subsequent to the deceleration, this speed is maintained for the remaining travel along the curve.

Two conditions were considered for the assessment of maximum side friction demand. The first condition represents the side friction demand of a braking vehicle (i.e., $a_x = -0.85$ m/s^2); the second represents the demand with no braking (i.e., $a_x = 0$). The first condition produces a larger friction demand on downgrades whereas the latter condition produces the larger friction demand on upgrades. Of the two, that condition producing the larger friction demand is recognized as the one that defines the maximum side friction demand for this analysis.

The results of the analysis are shown in Figures C-4 and C-5. These figures illustrate the combined effect of speed, radius, superelevation, and grade *beyond any effect accounted for in Equation 1*. In other words, values of the friction

TABLE C-2 Vehicle characteristics for side friction demand analysis

Characteristic	Vehicle Type			Source
	Compact Car	Full-Size Car	Single-Unit Truck	
Vehicle weight, W (N)	8,900	17,800	80,100	Ref. 15, p. 30
Wheelbase, L (m)	2.39	3.02	6.10	--
Rear axle to C.G. dist., c (m)	1.31	1.61	3.05	--
Height of C.G., h (m)	0.56	0.56	1.40	Ref. 13, p. 312
Frontal area, A_f (m^2)	2.07	2.29	5.29	--
Drag coefficient, C_D	0.40	0.40	0.70	Ref. 15, p. 35
Rolling resistance, b_0	0.011	0.010	0.0066	Ref. 13, pp. 117-118
b_1	1.70×10^{-6}	1.21×10^{-6}	103×10^{-6}	
b_2	2.5	2.5	1.0	
Mass/Power ratio, P (kg/kw)	18.2	13.4	42.6	Ref. 13, p. 24; Ref. 1, p. 232
Cornering coeff., CC (rad.$^{-1}$)	6.88	6.88	6.88	Ref. 13, p. 352

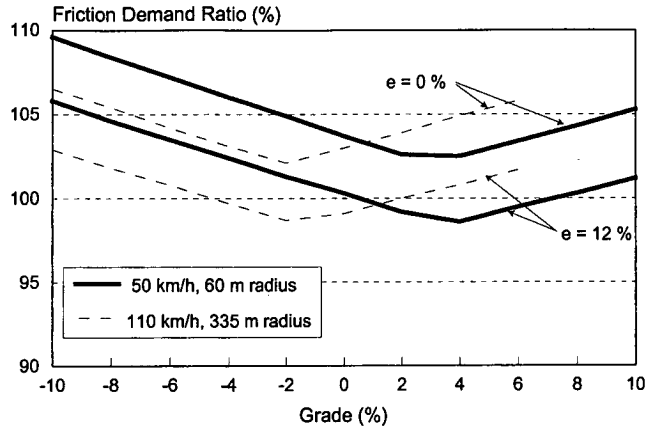

Figure C-4. Effect of grade, speed, and superelevation on side friction demand.

demand ratio r_D that are different from 100 percent indicate that the effect of a factor is not fully represented by Equation 1. Values less than 100 percent indicate that the effect is overestimated; values greater than 100 percent indicate that the effect is underestimated. In the case of speed, radius, and superelevation, any deviation from 100 percent represents an incremental effect because these terms are included in Equation 1. In contrast, the full effect of grade shown in Figures C-4 and C-5 as a grade term is not included in Equation 1.

Figure C-4 illustrates the effect of grade, speed, and superelevation. The trends shown indicate that side friction demand increases with positive or negative grade. However, the trends also indicate that the effect of grade is relatively small. In fact, it is generally within 5.0 percent of the value predicted by Equation 1 for most typical grades and superelevation rates. This trend is consistent with that found by Dunlap et al. (*3*) (i.e., Equation 2). However, the magnitude of the effect is larger than that suggested by Equation 2.

The trends shown in Figure C-4 also suggest that Equation 1 generally underestimates side friction demand, especially for curves that are not superelevated. In contrast, Equation 1 generally overestimates side friction demand for curves that have significant superelevation and smaller grades.

Speed tends to shift the "low point" of the curve left or right. In general, higher speeds shift the curve to the left. Closer examination indicates that this low point is approximately equal to the grade that requires a forward thrust that is equal and opposite to the combined forces of gravity, rolling resistance, and aerodynamic drag.

Figure C-5 illustrates the effect of grade and radius on side friction demand. The trends shown indicate that Equation 1 overestimates side friction demand for small radii and moderate grades. In contrast, it underestimates side friction demand for large radii. It should be noted that the 825-m radius curve was believed sufficiently flat to preclude the need to decelerate, unlike the two sharper curves. It is for this reason that the trend line for the 825-m radius overlaps that of the other trend lines.

The HVOSM simulation model (*4*) was used to examine the side friction demands of a full-size sedan for two different combinations of speed and radius over a wide range of grades. The results of this examination are shown in Figure C-6. Also provided in this figure is the side friction demand predicted by Equation 1.

The trends shown in Figure C-6 indicate that grade has a small effect on side friction demand; however, the magnitude of the effect is not necessarily consistent over the range of grades nor is it consistent between the two speed/radius combinations. There is some evidence that side friction is higher for upgrades than for level roadways. The trends shown also suggest that side friction demand increases on downgrades for low speeds but decreases on high-speed highways. The former trend is consistent with that predicted by the side friction demand model. In general, the variability within the plotted data points suggests that the small effect of grade may be obscured by the limited precision of the simulation model output.

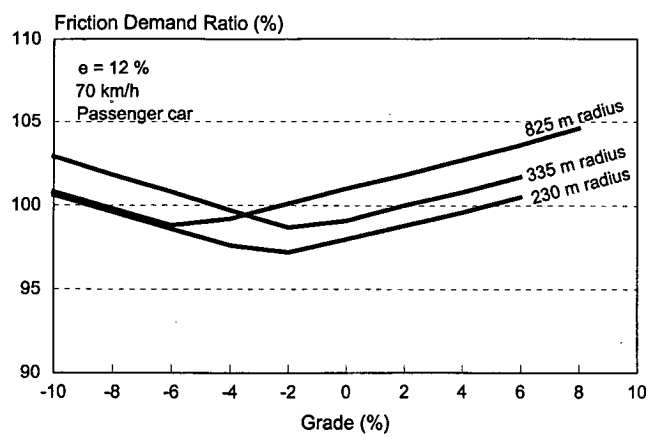

Figure C-5. Effect of grade and radius on side friction demand.

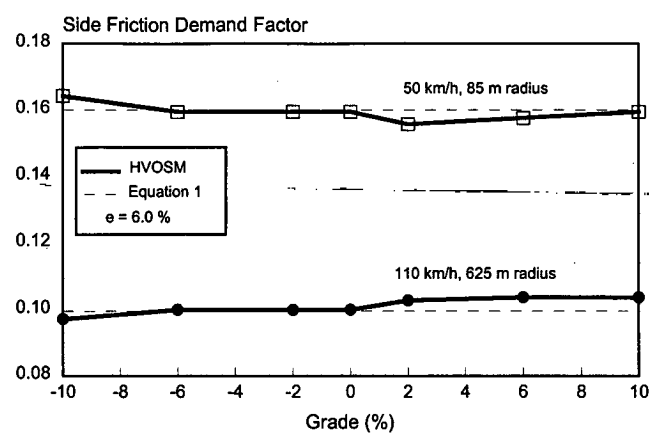

Figure C-6. Effect of grade on side friction demand as predicted by HVOSM.

SIDE FRICTION SUPPLY MODELS

Two types of failure are possible when traversing a highway curve: slide or roll. A failure occurs when the lateral acceleration is sufficient to (1) overcome the offsetting force of friction or (2) provide an overturning moment that rotates the vehicle about its outside tires. This section describes two models, one for each failure condition. This description will show that the friction supply available for turning is affected by the physical attributes of the vehicle. Hence, some of the equations developed for the side friction demand model are also used in the side friction supply models.

Slide Failure Model

Model Development

This section describes the development of a side friction supply model for slide failure. It is generally recognized that friction supply is based primarily on tire and pavement surface properties (although vehicle speed and weight also have some effect). However, in the analysis of *side* friction supply, it is useful to assume that the supply available for cornering is that remaining after the friction demand for accelerating or braking has been removed. The mechanism for "removing" this friction demand is based on the "friction-ellipse" concept. The mutually orthogonal vectors of forward and side friction are combined using the mathematical representation of the ellipse. From this modeling approach, the available maximum side friction factor for a slide failure can be computed as follows:

$$f^*_{y,\,\max,\,sl} = f_{y,\,\max,\,sl}\sqrt{1-\left(\frac{f_{x,\,D}}{f_{x,\,\max,\,sl}}\right)^2} \tag{28}$$

with

$$f_{x,\,D}\begin{cases}\dfrac{F_x}{W_r} & : F_x \geq 0\\[2ex] \dfrac{F_x}{W} & : F_x < 0\end{cases} \tag{29}$$

where:

$f^*_{y,\,\max,\,sl}$ = available maximum side friction supply for slide failure;
$f_{y,\,\max,\,sl}$ = maximum side friction supply for slide failure;
$f_{x,\,\max,\,sl}$ = maximum forward friction supply for slide failure (approximately equal to $f_{y,\,\max,\,sl}$);
$f_{x,\,D}$ = tractive or braking friction demand factor;
F_x = tractive or braking friction force, N (see Equation 15); and
W_r = normal force on the rear tires, N (see Equation 21).

As with the side friction demand model, two conditions were considered for the assessment of available side friction supply. The first condition represents the side friction demand for a braking vehicle (i.e., $a_x = -0.85$ m/s^2); the second represents the demand with no braking (i.e., $a_x = 0$). Of the two, that producing the larger friction demand and thereby, smaller friction supply, is the one that defines the available side friction supply for slide failure.

Sensitivity Analysis

The slide failure model was used to compute the available side friction supply for a range of speeds, radii, superelevation rates, vehicle types, and grades. Of these factors, speed, vehicle type, and grade were found to have the most significant effect. To facilitate a uniform comparison of the relative effect of these factors, the following variable was computed:

$$r_{sl} = 100\sqrt{1-\left(\frac{f_{x,\,D}}{f_{x,\,\max,\,sl}}\right)^2} \tag{30}$$

where:

r_{sl} = friction supply ratio for slide failure, percent.

The value obtained from this equation represents the ratio of the available side friction supply $f^*_{y,\,\max,\,sl}$ to the absolute maximum side friction supply $f_{y,\,\max,\,sl}$.

The results of the sensitivity analysis are shown in Figure C-7. As the trends in this figure indicate, the available side friction supply decreases significantly with an increasing rate of upgrade. It also decreases significantly with an increasing rate of downgrade for the single-unit truck. The trend lines are not extended beyond the + 4 percent for the truck because its engine has insufficient power to maintain speed on steeper grades. The trends shown are for the high-speed (110 km/h)

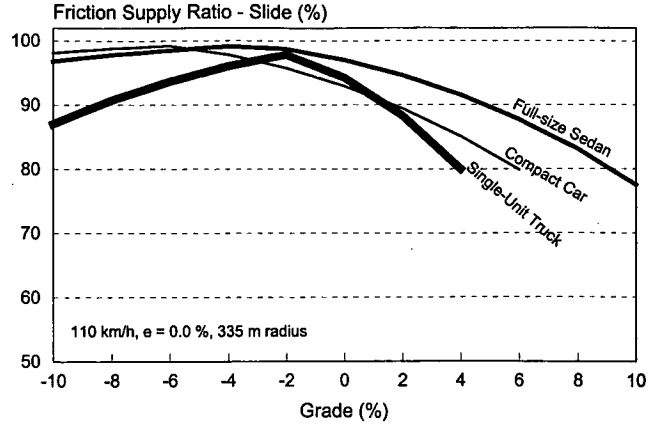

Figure C-7. Effect of vehicle type and grade on side friction supply for slide failure.

condition. The friction supply ratio is less sensitive to grade for lower speeds.

Roll Failure Model

Model Development

This section describes the development of a side friction supply model for roll failure. The side friction supply defined by this model is not a true friction "supply." Rather, it is side friction *demand* that would have to be developed to create a side force sufficient to cause the vehicle to roll over. Referring to it as a friction supply facilitates the comparison of actual friction demand to friction levels that would promote either a slide or a roll failure.

The roll failure model developed in this section is based on a static analysis of the forces acting on a cornering vehicle. Development of this model requires expansion of the bicycle representation described previously. This expansion introduces the width of the vehicle as a key parameter defining roll failure. It also incorporates the effect of body roll. This roll results from the lateral load transfer that occurs when a vehicle travels along a curve. The load "transfers" by shifting a portion of the vehicle's weight from the inside to the outside tires as a result of the vehicle body rotating in the cradle of the suspension system.

The forces acting on a cornering vehicle are shown in Figure C-8. The vehicle body is represented as a "sprung" mass whose center of gravity is located a distance h above the roadway. During cornering, the body's mass center rotates about the vehicle's roll center, which is located a distance h_r above the roadway.

Summing the moments about the roll center yields the following equation for predicting the vehicle roll angle φ as a function of centripetal acceleration, vehicle weight, and roll stiffness properties of the vehicle suspension:

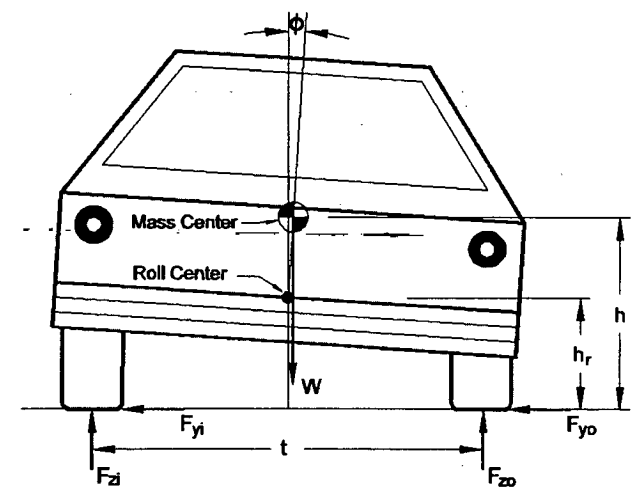

Figure C-8. Forces acting on a vehicle turning to the left (adapted from Ref. 13).

$$\varphi = \frac{F_c - (0.01e)W}{\frac{K_{\varphi r} + K_{\varphi f}}{p_s(h - h_r)} - (0.01e)F_c - W} \tag{31}$$

where:

φ = roll angle, radians;
$K_{\varphi r}$ = roll stiffness for the rear axle, N-m/radian;
$K_{\varphi f}$ = roll stiffness for the front axle, N-m/radian; and
p_s = sprung/total mass ratio.

In a similar manner, summing the moments about the outside (right) tires yields the following equations for the normal forces on the inside front and inside rear tire:

$$F_{zi,r} = \frac{1}{t}\left[W_r\left(\frac{t}{2} - \varphi(h - h_r)\right) - hF_{yr}\right] \tag{32}$$

$$F_{zi,f} = \frac{1}{t}\left[W_f\left(\frac{t}{2} - \varphi(h - h_r)\right) - hF_{yf}\right] \tag{33}$$

The condition necessary to precipitate a roll over is that the normal force on the inside front or rear tire equals zero. Inspection of the variable relationships in Equations 31, 32, and 33 indicates that it is impossible to algebraically manipulate them to achieve a closed-form solution for the speed or radius that would satisfy the roll failure condition. As a result, an iterative solution technique is required.

The solution technique begins with an initial assumption of radius (for a given speed, superelevation, vehicle type, and grade). The resulting normal forces on the inside tires are then computed. If neither of the normal forces equals zero then a new, smaller estimate of the radius is chosen. The process repeats until a radius is found that yields a normal force of zero for the front or rear inside tire. After there is convergence in this manner, the equivalent maximum side friction supply at roll over can be computed as follows:

$$f_{y,\max,r} = Smaller\ of: \left[f_{yr} = \frac{F_{yr}}{W_r};\quad f_{yf} = \frac{F_{yf}}{W_f}\right] \tag{34}$$

where:

$f_{y,\max,r}$ = equivalent maximum side friction supply for roll failure.

The smaller of the computed front and rear axle friction values in Equation 34 (as opposed to the larger) is used to facilitate a conservative comparison with the side friction demand computed by the side friction demand model in "Side Friction Demand Model." This model uses the larger of the friction demands on the front or rear axle to define the side friction demand. Together, the larger friction demand and smaller supply yield a conservative estimate of the margin of safety for the specified conditions.

As with the side friction demand model, two conditions were considered for the assessment of equivalent side friction supply. The first condition represents the effect of a braking vehicle (i.e., $a_x = -0.85$ m/s^2); the second represents the effect of no braking (i.e., $a_x = 0$). Of the two, that condition producing the smaller friction supply is the one that defines the equivalent side friction supply for roll failure.

Sensitivity Analysis

Equation 34 was used to compute the maximum side friction factor for a range of vehicle types and geometric conditions. The focus of the examination was the effect of grade on side friction supply; however, the effect of speed, radius, superelevation, and vehicle type were also considered. To highlight differences between the side friction supply predicted by Equation 34 and that predicted by Equation 7 (using $b_v = 1.0$ and $b_r = 1.0$), their ratio was computed as follows:

$$r_r = \frac{f_{y,\max,r,34}}{f_{y,\max,r,7}} 100 \quad (35)$$

where:

r_r = friction supply ratio for roll failure, percent; and
$f_{y,\max,r,7}$ = equivalent maximum side friction supply for roll failure from Equation 7 (evaluated with $b_v = 1.0$ and $b_r = 1.0$).

By using this approach, the friction supply ratio r_r is algebraically equal to the product of two calibration factors: b_v and b_r (i.e., $r_r = 100\ b_v\ b_r$). As mentioned previously, these factors are included in the computation of friction demand to reflect a sensitivity to differences in the tire and suspension characteristics of trucks and passenger cars.

Three vehicle types are included in the investigation of roll failure. Two of the vehicle types represent passenger cars: a compact and a full-size sedan. The other vehicle represents a single-unit truck. The characteristics of these vehicles are listed in Table C-3. The characteristics in this table were selected to represent "typical" vehicles.

The side friction supply model for roll failure was exercised for a range of speeds, superelevation rates, vehicle types, and grades. In general, a full range of values for each variable was considered:

Speed (km/h):	50, 110
Superelevation (%):	0, 12
Vehicle types:	Compact car, Full-size car, Single-unit truck
Grade (%):	−10, −8, −6, −4, −2, 0, 2, 4, 6, 8, 10

The results of the analysis are shown in Figure C-9. This figure illustrates the combined effect of superelevation, vehicle type, and grade *beyond any effect accounted for in Equation 7*. In other words, values of the friction supply ratio r_r that are different from 100 percent indicate that the effect of a factor is not fully represented by Equation 7. As the trends in Figure C-9 suggest, the ratio is always less than 100 percent indicating that the value computed by Equation 7 overestimates the true side friction supply for roll failure.

The trends shown in Figure C-9 indicate that Equation 7 lacks a reasonable sensitivity to the vehicle's body roll effect. This effect significantly reduces the side friction supply for roll failure because of the lateral shift of the vehicle's weight during cornering. Equation 7 is most notably in error for trucks. It should also be noted that the friction supply ratio r_r found for the single-unit truck (about 0.55 after conversion to portion) is nearly equal to the value of 0.60 recommended by Ervin et al. (*12*) for b_r.

Figure C-9 indicates that superelevation and grade have a small effect on side friction supply for roll failure. There is a trend toward reduced supply with larger superelevation rates. Grade has a minimal effect on supply. The analysis also found that speed and radius have a negligible effect on side friction supply for roll failure. It should be noted that the truck has insufficient power to maintain a speed of 100 km/h or more on grades in greater than 4 percent. No significant difference in supply was found between the full-size sedan and the compact passenger cars.

TABLE C-3 Vehicle characteristics for side friction supply analysis

Characteristic	Vehicle Type			Source
	Compact Car	Full-Size Car	Single-Unit Truck	
Track width, t (m)	1.40	1.57	1.78	Ref. 13, p. 312
Roll center height, h_r (mm)	91	150	560	Ref. 16, p. 413 Ref. 17, p. 45
Sprung/total mass ratio, p_s	0.90	0.90	0.89	--
Front Roll Stiff., $K_{\varphi f}$ (N-m/rad)	17,600	36,600	38,800	Ref. 16, p. 413 Ref. 17, p. 47
Rear Roll Stiff., $K_{\varphi r}$ (N-m/rad)	16,300	16,300	64,700	

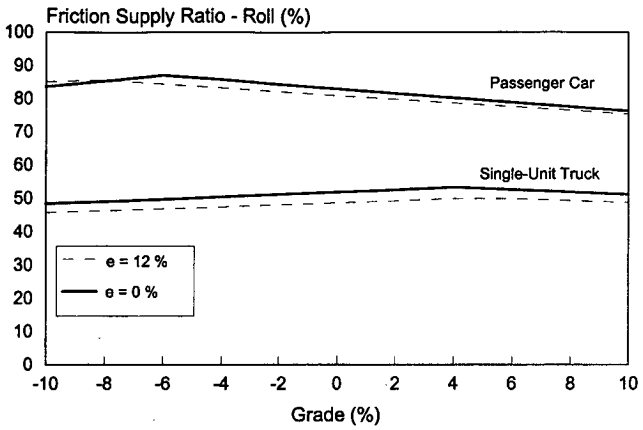

Figure C-9. Effect of vehicle type and grade on side friction supply for roll failure.

MARGIN OF SAFETY ANALYSIS

The margin of safety against slide or roll failure is traditionally defined as the difference between the side friction demand and supply. This latter quantity represents an upper limit on the amount of side friction demand that is available for cornering. If side friction demand reaches or exceeds the maximum available, then a skid or roll failure is eminent. The particular type of failure that occurs is represented by the failure condition with the smaller maximum side friction supply. In accordance with these definitions, the margin of safety can be computed as follows:

$$MS = f_{y,\max} - f_{y,D} \tag{36}$$

with

$$f_{y,\max} = \textit{Smaller of: } (F^{*}_{y,\max,sl},\ f_{y,\max,r}) \tag{37}$$

where:

MS = margin of safety against failure, and
$f_{y,\max}$ = maximum side friction supply.

The models developed in the preceding sections were used to examine the combined effect of speed, vehicle type, and grade on side friction demand and supply. For this examination, the side friction demand factor, available maximum side friction supply for slide failure, and the equivalent maximum side friction factor for roll failure were computed and compared graphically. The objective of this examination was to obtain a general sense of the margin of safety, as influenced by the aforementioned factors.

It was determined that conditions at the "critical" point on the curve would be considered in this examination of demand and supply. The radius chosen for a given speed would have the minimum value, based on the maximum design side friction factors recommended in Appendix A (Table A-5). This radius would be divided by 1.15 to account for the impact of steering fluctuations on path radius. The result of this division yields the critical radius that was used in the side friction demand model for the margin-of-safety analysis. Thus, the critical radius is computed as follows:

$$R_c = \frac{v^2}{g(0.01e + f_{d,\max})} \times \frac{1}{1.15} \tag{38}$$

where:

$f_{d,\max}$ = maximum design side friction factor; and
R_c = path radius at the critical point, m.

A superelevation rate of 6.0 percent and grades ranging from −10 to +10 percent were considered for this analysis.

The findings reported in Appendix A indicated that *drivers tend to reduce their speed prior to and through the initial portion of sharp horizontal curves.* On downgrades, this speed reduction likely requires the application of the vehicle's brakes; on upgrades, the speed reduction is likely achieved by a reduction in the applied engine power (i.e., through a reduction in pressure on the accelerator pedal). This observed behavior was considered in the margin-of-safety analysis by the separate analysis of two conditions, one with a braking force applied and one with a tractive force applied (in an amount necessary to maintain speed).

Figures C-10 and C-11 illustrate the effect of speed, grade, and braking on the margin of safety for passenger cars and trucks, respectively. In each figure, two scenarios are represented: one scenario represents a downgrade condition where the driver will likely brake to achieve a nominal speed reduction; the second scenario represents an upgrade condition where it is assumed that the driver will use the available engine power to maintain speed (i.e., no speed reduction). Both of these scenarios represent realistic, albeit worst-case, combinations of traction/braking and grade. It is recognized that the upgrade scenario is particularly conservative because it is possible that many drivers (especially truck drivers) will allow some speed reduction and thereby, increase the available side friction supply above that shown in Figures C-10b and C-11b.

The side friction supply shown in Figure C-10 is based on the slide failure condition. The equivalent factors for the roll condition were much larger than those for the slide condition; hence, slide failure is always the dominant failure mode for passenger cars on curves. The friction demands shown reflect values larger that those recommended for design in Chapter 3 because of the use of a critical path radius.

The trends in Figures C-10 and C-11 illustrate the effect of grade on side friction demand, side friction supply, and their difference (margin of safety). In general, friction demand and supply (for slide failure) both decrease with increasing speed. This trend tends to yield a margin of safety that is relatively constant over the range of speeds. Also, the trends indicate that both upgrades and downgrades yield an increase in side

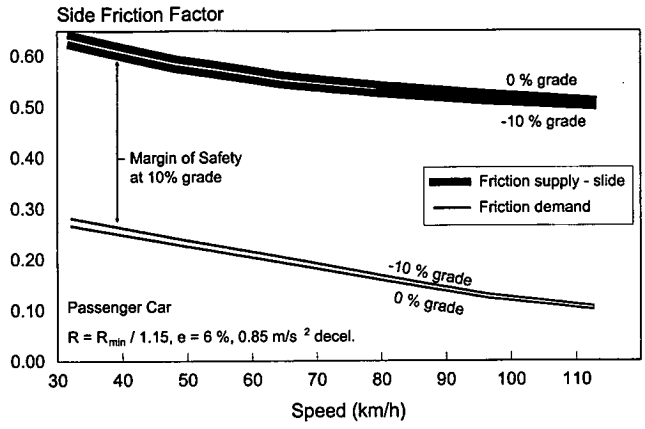

a. Speed reduction of 3 km/h.

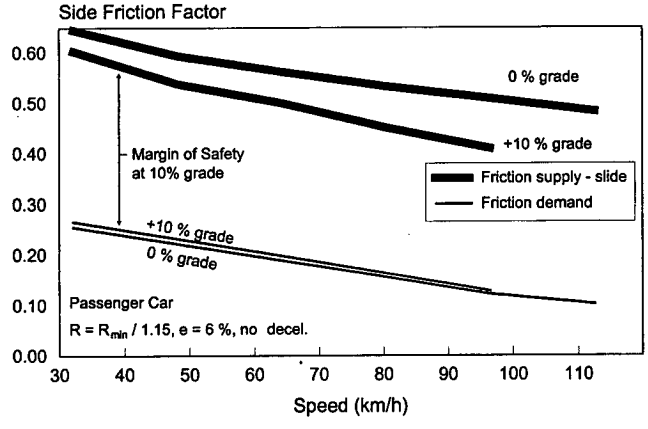

b. No speed reduction.

Figure C-10. Comparison of side friction supply and demand for passenger cars.

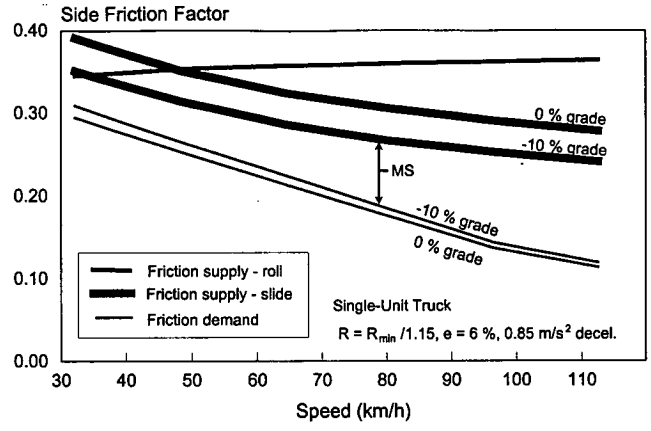

a. Speed reduction of 3 km/h.

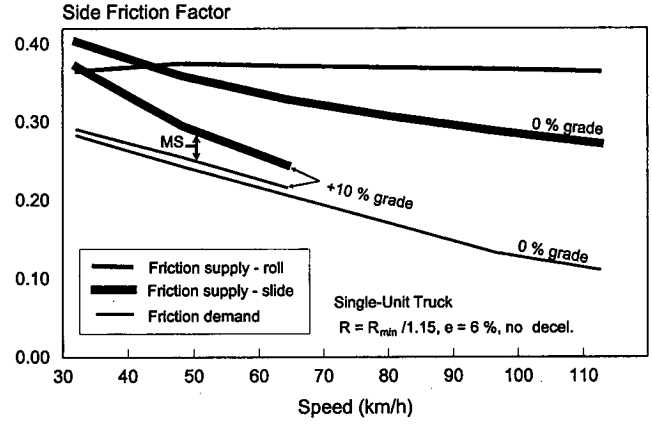

b. No speed reduction.

Figure C-11. Comparison of side friction supply and demand for single-unit trucks.

friction demand and a decrease in side friction supply. *The result is a significant decrease in the margin of safety resulting from roadway grade.*

Figure C-11 illustrates the relationship between friction supply and demand for the single-unit truck. The side friction demand trend lines shown in Figure C-11 were adjusted to account for variations in tire-to-tire friction (as discussed previously for variable b_v in "Other Factors Affecting Side Friction Demand"). The adjustment was in the form of a 10 percent increase in friction demand.

The truck side friction supplies for both roll and slide failure are shown in Figure C-11. With the exception of the slowest speeds, the supply trend lines indicate that slide failure will occur before roll failure. The friction supply for the 10 percent upgrade condition in Figure C-11b does not extend beyond 65 km/h because the engine has insufficient power to maintain higher speeds on this grade.

A comparison of the trends shown in Figures C-10 and C-11 indicates that *trucks are provided significantly less margin of safety than passenger cars on sharp highway curves*. This trend is due to the larger friction demands associated with trucks. Tire-to-tire variations tend to increase the friction demand by 10 percent. Trucks are also associated with larger tractive and braking friction demands because of their greater weight. As noted with regard to Equation 28, these forward friction demands reduce the friction supply available for cornering.

Also shown in each figure are trend lines reflecting the level (no grade) condition. Comparison of these lines in Figures C-10a and C-10b (or C-11a and C-11b) indicates that deceleration because of braking reduces the side friction supply and is associated with an increase in the side friction demand. *Together, these changes result in a significant reduction in margin of safety because of braking* (about 17 percent and 35 percent for cars and trucks, respectively).

In summary, drivers tend to slow on sharp horizontal curves. When these curves are located on significant grades (up or down), both cars and trucks have a lower margin of safety than they would on a level roadway. Sharp curves on downgrades are of greater concern because (1) most drivers

will be compelled to brake to maintain a safe speed and (2) most drivers are also likely to brake an added amount to reduce speed during curve entry. These two events combine to significantly reduce the margin of safety for most vehicles. Finally, the reduction in margin of safety because of grade, braking, or both tends to be more critical for trucks than cars because a significant portion of the friction supply is effectively used to slow (or propel) the heavier truck.

SUMMARY

Three models were developed to examination the relationship between side friction supply and demand. A primary focus of this examination is the effect of grade on side friction supply and demand; however, other factors such as speed, radius, and superelevation rate were also considered. The side friction demand model is based on a "bicycle" representation of a two-axle vehicle. This modeling approach represents an improvement over the point-mass model because it provides additional sensitivity to the distribution of forces to the axles.

Three vehicle types are included in the investigation. Two of the vehicle types were passenger cars: a compact and a full-size sedan. The other vehicle was a single-unit truck. In general, the side friction models were exercised for a range of speeds, radii, superelevation, vehicle types, and grades. The examination of side friction demand indicated that demand increases with positive or negative grade. However, the effect of grade is relatively small. In fact, the expected friction demand is generally within 5.0 percent of the value obtained from the point-mass model (i.e., Equation 1). The marginal effect of grade on friction demand is consistent with the findings of several other researchers.

The point-mass model generally underestimates side friction demand on most curves, especially those that have steep grades, little superelevation, or large radii. In contrast, it generally overestimates side friction demand for curves with flat grades, significant superelevation, and small radii. Conditions where Equation 1 underestimates side friction demand is of the most concern because this situation represents a compromise in the margin of safety.

The available side friction supply for slide failure decreases significantly with an increasing rate of upgrade. This reduction in available side friction stems from the use of some friction for tractive forces. For the single-unit truck, the side friction supply also decreases significantly with an increasing rate of downgrade. This reduction in friction supply stems from the use of some friction for braking. As a result, it appears that trucks experience a significant reduction in their margin of safety on grades, especially downgrades where braking is very likely to occur.

Vehicle body roll during cornering significantly reduces the equivalent side friction supply for roll failure. This roll effect is most notable for trucks because of their high center of gravity. Superelevation has a very small effect on side friction supply for roll failure. The analysis also found that speed and grade have negligible effects on side friction supply for roll failure. No significant difference in the roll friction supply was found between the full-size and compact passenger cars.

When considering both side friction supply and demand on sharp horizontal curves, it was found that significant grades (up or down) yield lower margins of safety than would otherwise be attained on level roadways. Sharp curves on downgrades are likely to be most problematic because driver braking reduces the margin of safety even further. Finally, the reduction in margin of safety because of grade, braking, or both tends to be larger for trucks than for cars.

REFERENCES

1. *A Policy on Geometric Design of Highways and Streets.* American Association of State Highway and Transportation Officials, Washington, D.C. (1994).
2. McLean, J.R., "An International Comparison of Curve Speed Prediction Relations." *Road and Transport Research,* Vol. 4, No. 3 (1995) pp. 6–15.
3. Dunlap, D.F., P.S. Fancher, R.E. Scott, C.C. MacAdam, and L. Segel, *NCHRP Report 184: Influence of Combined Highway Grade and Horizontal Alignment on Skidding.* Transportation Research Board, National Research Council, Washington, D.C. (1978).
4. Segal, D.J., *Highway-Vehicle-Object Simulation Model—1976 User's Manual.* Report No. DOT-FH-11-8265, Federal Highway Administration, U.S. Department of Transportation, Washington, D.C. (1976).
5. MacAdam, C.C., P.S. Fancher, and L. Segal, *Side Friction for Superelevation on Horizontal Curves—Volume II, Technical Report.* Report FHWA-RD-86-025, Federal Highway Administration, U.S. Department of Transportation, Washington, D.C. (1985).
6. J.C. Glennon and G.D. Weaver, Highway Curve Design for Safe Vehicle Operations. *Highway Research Record 390,* Highway Research Board, National Research Council, Washington, D.C. (1972) pp. 15–26.
7. J.C. Glennon, T.R. Neuman, and J.E. Leisch, *Safety and Operational Considerations for Design of Rural Highway Curves.* Report FHWA-RD-86-035, Federal Highway Administration, U.S. Department of Transportation, Washington, D.C. (1985).
8. Wehner, "Results of Skid-Resistance Measurements and Traffic Safety." *Road and Autobahn,* Vol. 8, (1965).
9. Lamm, R., Driving Dynamic Considerations: A Comparison of German and American Friction Coefficients for Highway Design. *Transportation Research Record 960,* Transportation Research Board, National Research Council, Washington, D.C. (1984) pp. 13–19.
10. Olson, P.L., D.E. Cleveland, P.S. Fancher, L.P. Kostyniuk, and L.W. Scheider, *NCHRP Report 270: Parameters Affecting Stopping Sight Distance.* Transportation Research Board, National Research Council, Washington, D.C. (1984).
11. Kontaratos, M., B. Psarianos, and A. Yotis, Minimum Horizontal Curve Radius as Function of Grade Incurred by Vehicle

Motion in Driving Mode. *Transportation Research Record 1445*, Transportation Research Board, National Research Council, Washington, D.C. (1994) pp. 86–93.

12. Ervin, R.D., C.C. MacAdam, and M. Barnes, Influence of the Geometric Design of Highway Ramps on the Stability and Control of Heavy-Duty Trucks. *Transportation Research Record 1052*, Transportation Research Board, National Research Council, Washington, D.C. (1985) pp. 77–89.
13. Gillespie, T.D., *Fundamentals of Vehicle Dynamics*. Society of Automotive Engineers, Inc., Warrendale, Pennsylvania (1992).
14. Lamm, R., E.M. Choueiri, and J.C. Hayward, Tangent as an Independent Design Element. *Transportation Research Record 1195*, Transportation Research Board, National Research Council, Washington, D.C. (1988) pp. 123–131.
15. *Traffic Engineering Handbook*. 4th ed. J.L. Pline, Editor. Institute of Transportation Engineers, Washington, D.C. (1992).
16. Limpert, R., *Motor Vehicle Accident Reconstruction and Cause Analysis*. 3rd ed. The Michie Company, Charlottesville, Virginia, (1989).
17. Harwood, D.W., J.M. Mason, W.D. Glauz, B.T. Kulakowski, and K. Fitzpatrick, *Truck Characteristics for use in Highway Design and Operation, Volume I: Research Report*. Report No. FHWA-RD-89-226, Federal Highway Administration, U.S. Department of Transportation, Washington, D.C. (1990).

APPENDIX D

VEHICLE KINEMATICS IN CURVE TRANSITIONS

This appendix describes the effect of horizontal curve transition design on a vehicle's lateral speed and position in the traffic lane. Models are described in this appendix that relate the forces acting laterally on a vehicle as it travels through the superelevation and alignment transition sections. It is shown that these forces accelerate the vehicle in the lateral direction producing some shift (or drift) away from the center of the traffic lane. The models described in this appendix were used to develop the recommended transition design guidelines described in Chapter 3.

Two lateral motion models are described in this appendix. Both models consist of an equation for predicting the lateral velocity and an equation for predicting the lateral shift of a vehicle after it exits the transition section. One model has been developed for the tangent-to-curve transition design and a second has been developed for the spiral curve transition design. Both models were calibrated using published data describing observed vehicle shift on several curves. The calibrated form of the equations were then used to evaluate the sensitivity of lateral velocity and shift to various transition design values (e.g., design speed, radius, superelevation rate, length).

Initially, this appendix describes a review of the literature as it relates to driver behavior during curve entry and the resulting path of the vehicle. Driver behavior, in the context of steering input for vehicle control, is examined first. Then, models of this behavior are introduced and reviewed for their application to the curve negotiation process. Next, the model is calibrated using published data. Finally, an analysis of the relationship between driver steering behavior and the resulting lateral shift is described.

LITERATURE REVIEW

This section provides a review of the research literature on the topic of vehicle control and lane position. This topic is addressed first by reviewing research related to vehicle control as it relates to the driving process while entering a horizontal curve. Then, research into vehicle path and lane position during curve entry is reviewed.

Vehicle Control Through the Transition Section

Vehicle Control—The Driving Process

Numerous researchers (*1, 2, 3*) have described the driving process in the form of a real-time, closed-loop vehicle control model. Donges (*1*) and Godthelp (*2*) each describe a variation of this type of model as it relates to curve negotiation. This type of model uses anticipatory and compensatory response mechanisms to simulate driver behavior. The anticipatory mechanism serves the vehicle guidance function because it uses visual input about road conditions ahead to prepare and initiate appropriate vehicle control inputs (e.g., steer angle). This mechanism avoids errors in lane position, speed choice, or vehicle direction. The selection of an appropriate control input in response to this information is based largely on the driver's recollection of similar geometric conditions and successful responses (i.e., the driver's expectancy).

The compensatory mechanism serves the vehicle control function because it uses information about current vehicle lane position, speed, heading angle, and lateral acceleration to continuously revise the vehicle control inputs. This mechanism minimizes the magnitude of errors (or undesirable deviations) in vehicle control once they occur. Information for this mechanism is based on visual and kinesthetic sensory inputs. The control response to this information is based on the driver's understanding of their vehicle's performance in terms of the effect of changes in steering and speed control on vehicle position, heading angle, and stability.

Both Donges (*1*) and Godthelp (*2*) applied their vehicle control models to the study of driver behavior during curve entry. They calibrated their models by observing subject drivers negotiate a test course with curves of various radii and direction. All curves incorporated the tangent-to-curve transition design. Both researchers concluded that drivers start the steering action a short time before the curve begins (i.e., the PC) and end a short time after the PC. This time interval was defined as the "anticipatory time" t_a as it relates to the anticipatory response mechanism.

The finding by both Donges (*1*) and Godthelp (*2*) regarding drivers initiating their steering based on road curvature is important for alignment transition design. Their finding indicates that the break in alignment at the PC is a key piece of information available to the driver's anticipatory response mechanism. However, this apparent benefit of a tangent-to-curve transition is not generally acknowledged in the field of highway design. In fact, the AASHTO *Green Book* (*4*) indicates that one of the principal advantages of a spiral curve transition is that it "... avoids the noticeable breaks at the beginning and ending of circular curves [that use the tangent-to-curve design] ..." (*4*, p. 175). In the context of the aforementioned vehicle control model, the use of a spiral curve transition may require drivers to rely more on the "reactive"

compensatory response mechanism than on the "proactive" anticipatory mechanism.

Driver Steering Behavior During Curve Entry

Figure D-1 describes the relationship between steering wheel angle and curvature during the curve negotiation process. The curve shown in this figure uses the tangent-to-curve design. The trends shown indicate that the driver initiates the steer t_a seconds prior to the PC. Thereafter, the slope of steering-wheel angle increases at a constant rate until the angle needed to negotiate the curve δ_{sc} is reached. This type of steering maneuver is sometimes referred to as "ramp" steering and the duration of the ramp slope is referred to as the "steering time" t_s. The steering oscillations that follow the ramp slope result from the compensatory response mechanism as the driver attempts to stabilize the vehicle's lateral motion and adopt a circular, path-following driving mode.

Donges (*1*) measured the anticipatory time during a series of experiments using a driving simulator. He found that anticipatory time t_a averaged 1.1 s and that it was insensitive to vehicle speed. Donges also provided a plot of measured steering-wheel angle versus time (similar to that shown in Figure D-1). Examination of this plot indicates that the ramp steering input continues beyond the PC for a time approximately equal to t_a. This finding suggests that the steering time is approximately equal to twice the anticipatory time (i.e., $t_s \approx 2\ t_a$).

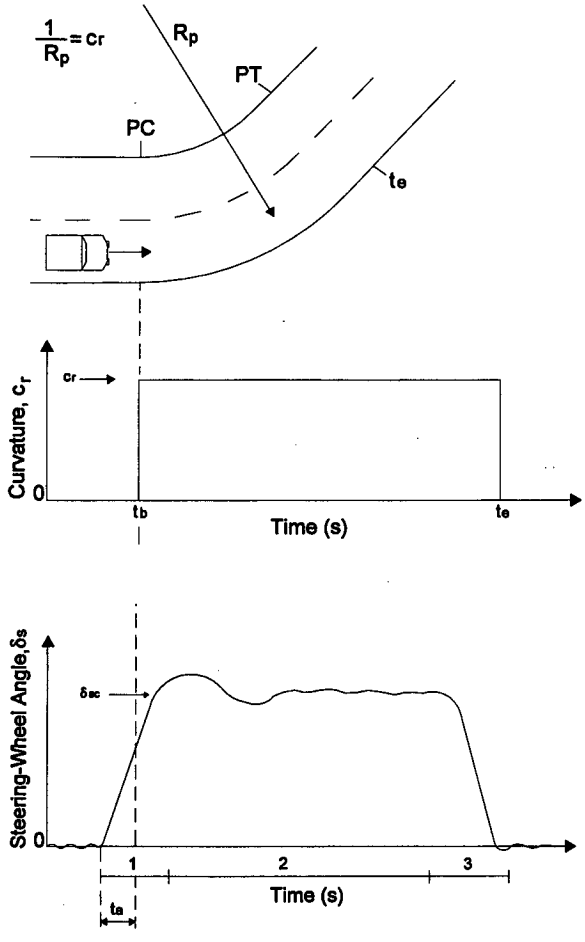

Figure D-1. Steering-wheel angle during curve entry (adapted from Ref. 2).

Stewart (*5*) examined the relationship between steering-wheel angle and curve PC at one 164-m curve on a rural highway. Specifically, he measured the time used to turn the steering wheel during curve entry (i.e., from $\delta_s = 0.0°$ to $\delta_s = \delta_{sc}$). He found this steering time t_s ranged from 2.0 to 3.1 s. He also noted that the steering time was approximately centered on the PC. A plot of the steering-wheel angle versus time provided by Stewart indicates a consistency with the ramp steering input described previously.

The mechanics of a vehicle's steering system produces the following relationship between steering-wheel angle and path curvature:

$$c_r = 1000 \frac{\delta_s}{r_s L(1 + 0.00199 v^2)} \qquad (1)$$

where:

c_r = roadway curvature (= 1000/R), km^{-1};
R = radius of curve, m;
δ_s = steering-wheel angle, rad;
r_s = steering-wheel to front-wheel angle ratio (typically about 20:1 for passenger cars);
L = wheelbase, m; and
v = vehicle speed, m/s.

The constant in the denominator of Equation 1 (i.e., 0.00199) represents the relationship between tire slip angle and speed for a typical passenger car. Slip angle increases with speed reflecting the higher friction demand associated with high-speed curves.

Equation 1 indicates that there is a linear relationship between steering-wheel angle and curvature. A unit change in steering-wheel angle produces a unit change in curvature. A constant rate of change in angle over time (or travel distance) produces a corresponding constant rate of change in curvature. Because the spiral shape represents a constant rate of change in curvature, the ramp steering behavior produces a spiral travel path. This point is noted by the Green Book authors (*4*, p. 174) and is also discussed by Stewart (*5*) and by Glennon et al. (*6*).

Stewart (*5*) examined the issue of differences between the steering-induced, "natural" spiral and the spiral curve used for highway design. Specifically, he considered the issue of differences in their length. After conducting a limited number of experiments of driver behavior on a highway curve and on a test track, he expressed some concern about spiral curve lengths that are different from the steering-induced spiral length. As noted previously, Stewart found that the steering-induced spiral length ranged from 2.0 to 3.1 s travel time.

Glennon et al. (*6*) measured the path curvature of vehicles entering six, two-lane rural highway curves. All curves had the tangent-to-curve transition design. Path curvature was estimated from videotape recordings of each vehicle using a grid of markers placed on the roadway. The typical travel path curvature observed by Glennon et al. is shown in Figure D-2.

Based on their analysis of vehicle path and curvature data, Glennon et al. (6) reported several findings that are consistent with those described in previous paragraphs. First, they found that vehicle path curvature increased in a linear manner from 0.0 km^{-1} to c_r in the vicinity of the PC. This linear change in curvature is consistent with a spiral travel path and is a product of the ramp steering behavior. Second, they found that the steering-induced spiral path was approximately centered on the PC. Third, they found that the spiral path was approximately 75 to 90 m in length during curve entry. Fourth, they estimated that very similar behavior occurred during curve exit (i.e., at the PT) except that the spiral path was slightly shorter (i.e., about 45 to 75 m). These spiral lengths correspond to about 3 to 4 s steering time during curve entry and 2 to 3 s during curve exit (based on the reported average speeds).

Glennon et al. (6) noted that a significant number of drivers deviated from the typical travel path curvature shown in Figure D-2. These drivers were observed to adopt a path radius sharper than that of the roadway (i.e., a "critical" radius) at some point along the curve. This steering behavior is depicted in Figure D-2 by the thin line oscillating about the roadway curvature. In the context of the vehicle control model described previously, the critical radius is likely a result of steering adjustments during the compensatory stage of the curve negotiation process.

Vehicle Path Through the Transition Section

Two accelerations act laterally on the vehicle during curve entry or exit. The first acceleration is due to driver steering behavior. This behavior introduces a friction-related centripetal acceleration that increases linearly with path curvature. The second acceleration is that due to gravity as affected through roadway superelevation. Prior to curve entry, these two accelerations are equal and opposite as the driver adopts a slight (almost imperceptible) steering angle to compensate for the normal cross slope. After curve entry, they combine to provide the centripetal acceleration needed to follow the highway curve. In between these two points, an unbalanced acceleration is realized that produces some lateral velocity and corresponding drift.

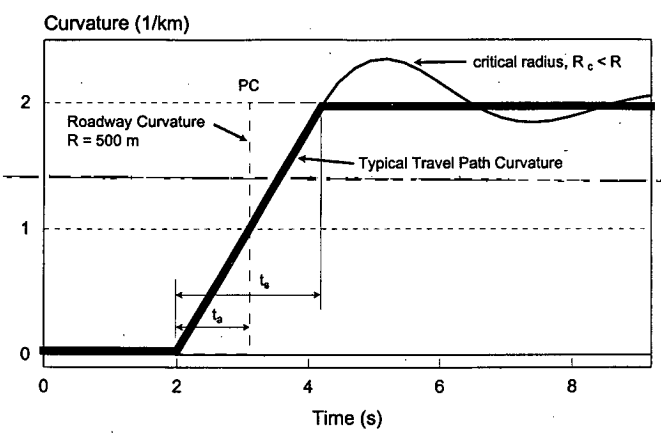

Figure D-2. Relationship between roadway curvature and travel path curvature in a tangent-to-curve transition design.

Two research teams (*7*, *8*) have measured the magnitude of vehicle drift during curve entry. Segal et al. (*7*) measured vehicle lane position by photographing study vehicles from a chase vehicle. Reference markers were placed along the roadside at 6.1- to 12.2-m intervals. Measurements were taken at two interchange off-ramp curves with a tangent-to-curve design and one interchange on-ramp curve with a spiral design.

Wong et al. (*8*) measured vehicle lane position by videotaping the subject vehicle from a series of cameras strategically located prior to and within the curve. Reference markers were placed at 10- to 12.5-m intervals along the lane lines at each site. Lane position measurements were taken at two, two-lane highway curves with spiral curve transitions.

Typical lateral shift distances reported from these two studies are reproduced in Figure D-3. The trends shown in both figures indicate that vehicles shifted inward during curve entry. The previous discussion suggests that this shift is a consequence of the two lateral accelerations acting on the vehicle during curve entry. It has also been suggested by Stewart et al. (*9*) and Emmerson (*10*) that this shift is the result of a driver's desire to flatten their path radius (i.e., cut the corner). However, models described in this appendix suggest that the shift results from lateral acceleration—a result that drivers take advantage of but do not explicitly seek during the initial stages of curve entry or exit.

The amount of lateral shift shown in Figure D-3 varies from 0.6 to about 1.5 m. This range is consistent with the shifts measured by Segal et al. (*7*) and Wong et al. (*8*) at the other curves they studied. Moreover, it is consistent with the lateral shifts of –0.1 to 0.9 m reported by Glennon et al. (*6*) for six highway curves. The observations provided by Segal et al. indicate that heavy trucks may shift slightly more than passenger cars. The observations provided by both Segal et al. and Wong et al. suggest that the shift amount is not significantly affected by transition design (spiral vs. tangent-to-curve).

Figure D-3b provides some clue regarding the relationship between steering initiation and curve beginning for the spiral transition design. Specifically, the trend lines in this figure indicate that a ramp steering input takes place along the spiral curve and that the corresponding steering time is about 3.0 s. There is some evidence that the steer may begin prior to the beginning of the spiral (TS) and end after the end of

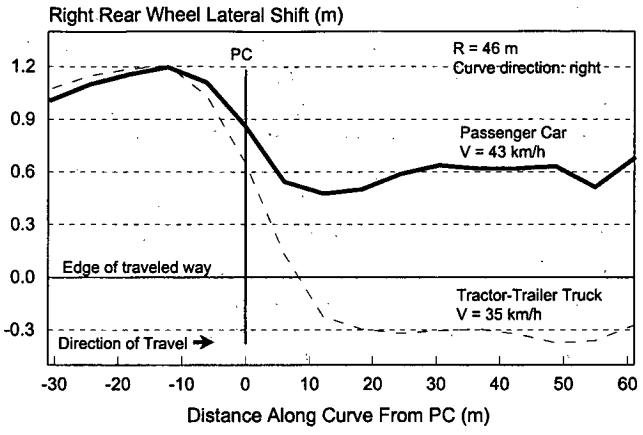

a. Observed lateral shift at a curve with a tangent-to-curve transition design (adapted from Ref. 7).

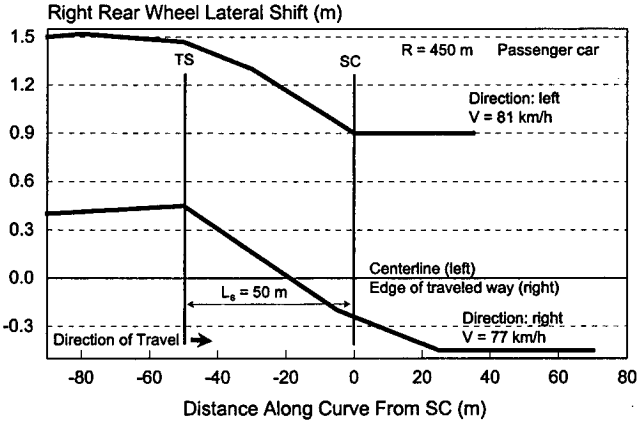

b. Observed lateral shift at a curve with a spiral transition design (adapted from Ref. 8).

Figure D-3. Lateral shift in lane position during curve entry.

spiral (SC). An examination of a similar plot provided by Segal et al. (*7*) also suggests that the steering input occurs during the spiral; however, the steering appears to begin very near the TS and end near the SC.

As mentioned previously, the spiral curve transition does not have a visually distinct point where the tangent ends and the curve begins. As a result, a spiral curve transition design may make the driver more reliant on kinesthetic information (e.g., superelevation change) to confirm the roadway's changing curvature. If so, the use of a spiral curve transition may require drivers to rely more on the compensatory response mechanism than on the anticipatory mechanism which could lead to the greater likelihood of steering oscillation (and adoption of a critical radius) following the ramp steering input. However, it is also possible that such oscillations may be damped significantly if the spiral curve transition length is about equal to the spiral path induced by the ramp steering behavior.

LATERAL MOTION MODELS

This section describes two kinematic models for predicting a vehicle's lateral motion after traveling through a transition section. One model is developed for the tangent-to-curve transition design; the other is developed for the spiral curve transition design. Both models consist of two equations. One equation is used to predict the vehicle's lateral velocity at the end of the transition section and the other is used to predict its lateral shift.

The lateral motion models are intended to provide a first-order approximation to the vehicle's lateral velocity and shift. They are based on an idealized ramp steering model and its associated duration (i.e., steering time). The model predictions are intended to be sufficiently accurate to estimate the relative merits of alternative transition design element values.

These models are not intended to be precise predictors of lateral velocity or shift because it is recognized that steering behavior is more complicated than can be described by the ramp steering model. Rather, the ramp steering behavior is believed to represent a "desirable" steering response. Thus, the models can be used to identify geometric conditions that enable drivers to reproduce a desirable steering response and thereby, minimize the need for corrective steering oscillations (and adoption of a critical path radius).

The HVOSM (*11*) simulation model was also considered to evaluate the effect of alternative transition design element values. However, exercise of this model indicated that simulation of transition sections was problematic and, as a result, not likely to produce information beyond that already available in the literature (*6*, *7*). (These problems are described "HVOSM Simulation Data.") More generally, simulation results are inherently difficult to interpret in terms of cause-and-effect and difficult to extrapolate to other conditions. On the other hand, the lateral motion models have a theoretic basis that is intuitive, bounded, and transferrable.

The remainder of this section is devoted to describing the lateral motion models. Initially, the tangent-to-curve transition model and associated equations are developed using a kinematic analysis of accelerations acting on the vehicle. Then, the spiral curve transition model equations are developed following a similar process.

Tangent-to-Curve Transition Model Development

The tangent-to-curve transition model is based on the lateral accelerations acting on the vehicle as it traverses the transition section. In general, there are two sources of lateral acceleration acting on the vehicle: (1) acceleration as a result of gravity and (2) acceleration as a result of tire-pavement friction. The first acceleration results from roadway superelevation and the second results from steering input. These accelerations tend to be equal and opposite prior to the transition and combine to equal the centripetal acceleration of the

curve after the transition. The variation of these accelerations through the transition section tends to result in lateral motion. These accelerations are shown in Figures D-4 and D-5 for curves to the left and right, respectively.

Sign Conventions and Assumptions

A comparison of Figures D-4 and D-5 indicates that many elements of the lateral accelerations are similar between the left- and right-hand curves. In particular, the steering-related and curve-related accelerations are identical between the left- and right-hand curves except for the fact that their magnitudes are opposite in sign. This characteristic is exploited in the subsequent model development by adopting a sign convention that allows the model to be applied to either left- or right-hand curves with only a change in the sign of selected variable values.

The sign convention adopted in this development is generally consistent with that used in the vehicle dynamics community. The positive x axis points in the forward direction of the vehicle, the positive y axis points to the right side of the vehicle, and the positive z axis points perpendicular to the x-y plane in a downward direction. Using this reference system, a side slope downward from left to right is positive. In addition, the

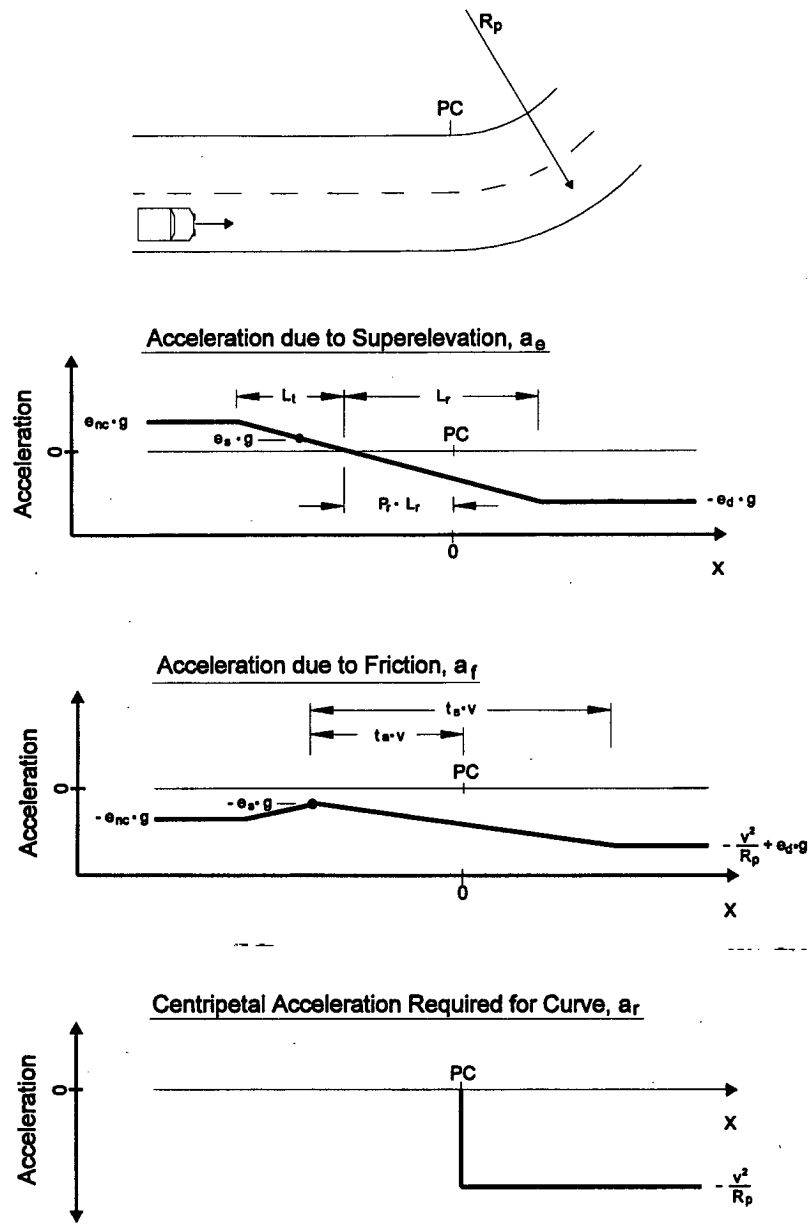

Figure D-4. Lateral accelerations during entry to a left-hand curve with a tangent-to-curve transition design.

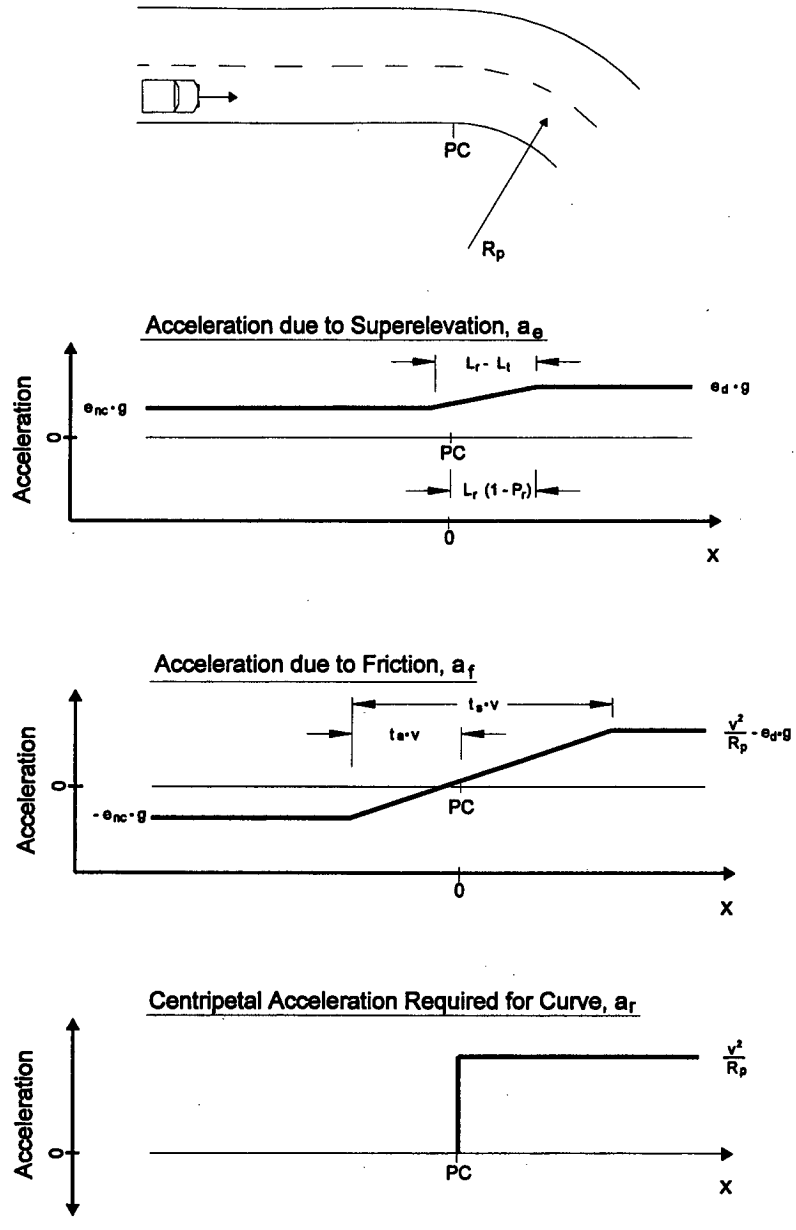

Figure D-5. Lateral accelerations during entry to a right-hand curve with a tangent-to-curve transition design.

vehicle is assumed to move from left to right in any graphic rendition such that its motion is in a positive direction along the x axis.

Based on the aforementioned sign convention, the sign conventions listed in Table D-1 have been adopted to permit the tangent-to-curve model to be used for both left- and right-hand curves. The model developed herein is for the inside or right-hand curve. The signs of the variable values listed in Table D-1 should be reversed when used in the corresponding equations for analysis of a left-hand curve. For example, a positive radius value would be used for the analysis of a right-hand curve; a negative radius value would be used for a left-hand curve.

In addition to the sign conventions, the following assumptions were made in developing the tangent-to-curve model:

1. The driver exerts whatever steering effort is needed to counter the normal cross slope and maintain a constant lane position up until t_a ($= t_s/2$) seconds prior to the PC. At this point in time, the driver is assumed to initiate the ramp steering behavior for t_s seconds.
2. Curve length exceeds the distance traveled during steering time ($L_c > t_s\, v$). This assumption should be fairly strong for rural applications because the *Green Book* recommends that curve length on highways exceed 10 s travel time.

TABLE D-1 Sign conventions

Variable	Outside (Left-Hand) Curve	Inside (Right-Hand) Curve
Normal Cross Slope Rate, e_{NC}	positive	positive
Design Superelevation Rate, e_d	negative	positive
Radius of Curve, R	negative	positive
Maximum Relative Gradient, Δ	negative	positive
Minimum Length of Tangent Runout, L_t	negative	positive

3. The superelevation runoff length is equal to the minimum length recommended in the *Green Book* (*4*), as computed using the following equation:

$$L_r = \textit{larger of:} \begin{cases} \dfrac{we_d}{\Delta} n_l b_w \\ 2 \dfrac{V_d}{3.6} \end{cases} \quad (2)$$

where:

L_r = minimum length of superelevation runoff, m;
Δ = maximum relative gradient (*Green Book* Table III-13), percent;
b_w = adjustment factor for number of lanes rotated (desirable minimum $b_w = 1.0$, acceptable minimum b_w equals 1.0, 0.80, 0.75 and 0.67 for n_l equal to 1.0, 1.5, 2.0, and 3.0);
w = width of one traffic lane (typically 3.6 m), m;
e_d = design superelevation rate, percent;
V_d = design speed, km/h; and
n_l = number of lanes rotated, lanes.

4. The tangent runout length equals that recommended in the *Green Book*, as computed using the following:

$$L_t = \frac{e_{NC}}{e_d} L_r \quad (3)$$

where:

L_t = minimum length of tangent runout, m; and
e_{NC} = normal cross slope rate (typically 2.0 percent), percent.

The runoff length obtained from Equation 2 can be used to determine the effective maximum relative gradient. This effective gradient can be computed as follows:

$$\Delta^* = \frac{we_d}{L_r} n_l \quad (4)$$

where:

Δ^* = effective maximum relative gradient, percent.

Lateral Acceleration As a Result of Superelevation

The acceleration as a result of superelevation can be computed as follows:

$$a_e(x) = g\, e(x)\, 0.01 \quad (5)$$

with

$$e(x) = \begin{cases} e_{NC} & : x \le x_1 \\ (e_d - e_{NC}) \dfrac{x - x_1}{x_3 - x_1} + e_{NC} & : x_1 < x < x_3 \\ e_d & : x \ge x_3 \end{cases} \quad (6)$$

$$x_1 = x_{PC} - (P_r L_r - L_t) \quad (7)$$

$$x_3 = x_{PC} + (1 - P_r) L_r \quad (8)$$

where:

$a_e(x)$ = acceleration sustained by superelevation at a distance x along the transition, m/s^2;
g = gravitational acceleration (= 9.807 m/s^2);
$e(x)$ = superelevation rate at a distance x along the transition section, percent;
P_r = portion of superelevation runoff located prior to the curve;
x_1 = location where superelevation begins its change from e_{NC} to e_d relative to the PC; and
x_3 = location where superelevation ends its change from e_{NC} to e_d relative to the PC.

Lateral Acceleration As a Result of Friction

The acceleration as a result of tire-pavement friction that results from the ramp steering behavior can be computed as follows:

$$a_f(x) = \begin{cases} -e(x) g\, 0.01 & : x \le x_a \\ \left(\dfrac{v^2}{R_p} - \dfrac{e_d}{100} g + \dfrac{e_s}{100} g \right) \dfrac{x - x_a}{x_b - x_a} - \dfrac{e_s}{100} g & : x_a < x < x_b \\ \dfrac{v^2}{R_p} - \dfrac{e_d}{100} g & : x \ge x_b \end{cases} \quad (9)$$

with

$$e_s = \begin{cases} (e_d - e_{NC})\dfrac{x_a - x_1}{x_3 - x_1} + e_{NC} & : x_a > x_1 \\ e_{NC} & : x_a \le x_1 \end{cases} \quad (10)$$

$$R_p = R - w(n_l - 0.5) \quad (11)$$

$$x_b = x_{PC} + \frac{t_s}{2} v \quad (12)$$

$$x_a = x_{PC} + \frac{t_s}{2} v \quad (13)$$

where:

$a_f(x)$ = acceleration sustained by friction at a distance x along the transition, m/s^2;
v = vehicle speed, m/s;
R_p = radius of travel path, m;
e_s = superelevation rate at the start of ramp steering, percent;
t_s = steering time, s;
x_a = location where ramp steering begins relative to the PC; and
x_b = location where ramp steering ends relative to the PC.

The accelerations resulting from superelevation and steering must combine to provide the centripetal acceleration required to track the traffic lane, as shown in the bottom portion of Figures D-4 and D-5. Any deviation from this requirement results in a lateral shift, as shown in Figure D-3. In fact, it is extremely unlikely that a driver could provide the instantaneous centripetal acceleration equal to that required at the PC because it would take a minimum nominal time to turn the wheel. Hence, a lateral shift is an evitable consequence of the two applied accelerations and their relationship to the required lane-tracking acceleration required by the curve.

Based on the observations made in the previous paragraph, it was determined that the difference between the applied lateral accelerations and the curve tracking acceleration equaled the acceleration available for lateral motion. This resultant lateral acceleration can be computed as follows:

$$a_l(x) = a_e(x) + a_f(x) - a_r \quad (14)$$

where:

$a_l(x)$ = resultant lateral acceleration at a distance x along the transition, m/s^2; and
a_r = centripetal acceleration (= v^2/R_p if $x > x_{PC}$; otherwise = 0.0), m/s^2.

Equations 5 through 14 were applied to a typical two-lane highway curve having a radius of 249 m and a superelevation rate of 8 percent. The average speed was assumed to be 61 km/h and the steering time was assumed to be 2.8 s. The resulting lateral accelerations are shown in Figure D-6.

The trend line shown in Figure D-6 (i.e., the thick line) indicates that the resultant lateral acceleration is initially equal to zero because the acceleration as a result of friction is equal and opposite to that required to maintain lane position on a normal cross slope. The driver initiates the ramp steering at 1.4 s (24 m) before the PC. At 21 m before the PC, the superelevation transition section is encountered and additional acceleration from gravity is introduced. The resultant acceleration increases to its maximum value just prior to the PC as the steering wheel angle and superelevation rates are gradually increased. As a result of these two accelerations, the vehicle drifts to the right.

After the PC, the centripetal acceleration required by the curve is large and not fully matched by the combined steering and superelevation-related accelerations. The resultant acceleration is also large and in a direction opposite to that experienced prior to the PC. As a result, the vehicle drift to the right begins to slow. As the vehicle moves further along the transition, the applied accelerations continue to increase until they match that required to track the curve radius. At this point (+24 m), the drift is significantly slowed (and possibly stopped).

The question of whether the drift is completely stopped can be answered by examining of the shaded areas of Figure D-6. Specifically, these areas can be integrated over travel distance to obtain lateral velocity. The area in the positive half of the y axis has a positive change in velocity; the area in the negative half has a negative change in velocity. When these two areas are equal, they balance in acceleration by the end of the transition section. This balance coincides with zero lateral velocity at the end of the transition. However, an inward lateral velocity still exists everywhere between the beginning and end of the transition. As a result, some lateral shift is guaranteed.

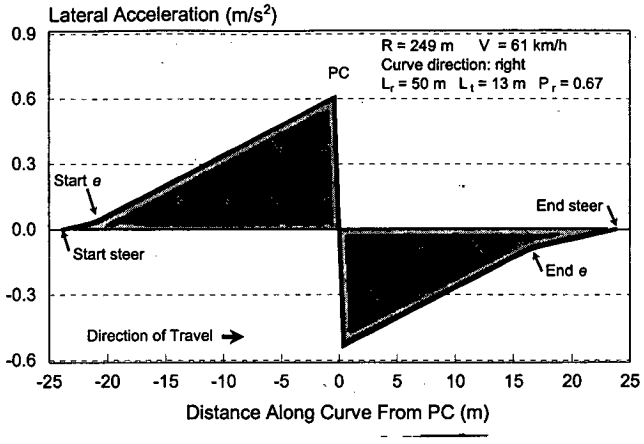

Figure D-6. Lateral acceleration during curve entry.

Lateral Velocity

Lateral velocity at any point can be computed by the integration of acceleration over time or distance. It was determined that integration over distance would be most helpful in satisfying the objectives of this project because many of the transition elements are represented by length along the roadway rather than travel time. Thus, the integral had the following basic form:

$$v_l(x) = \frac{1}{v^2}\int a_l(x)\,dx \tag{15}$$

where:

$v_l(x)$ = lateral velocity at a distance x along the transition, m/m.

The lateral velocity obtained from this equation represents meters of lateral shift for each meter of forward progress. Hence, it has units of meters per meter (i.e., m/m).

Figure D-7 illustrates the lateral velocity resulting from the example curve described for Figure D-6. The thick trend line shown indicates that lateral velocity is positive denoting a drift to the right (inward). This drift reaches its maximum value at the PC and then slows to a smal positive quantity. This non-zero lateral velocity at the end of the transition would require a small steering correction by the driver or inward drifting will continue.

The thin trend line shown in Figure D-7 illustrates the effect of placing more of the superelevation runoff on the curve (i.e., $P_r = 0.50$). The result is that there is less lateral acceleration prior to the PC and more after. In fact, the combined steering and superelevation accelerations are so large after the PC that they induce a negative (or outward) drift. This non-zero drift will require a small steering correction. More important, the outward direction of drift suggests that the correction required will be one of increased steering angle, which will create a critical path radius that is smaller than that of the highway curve.

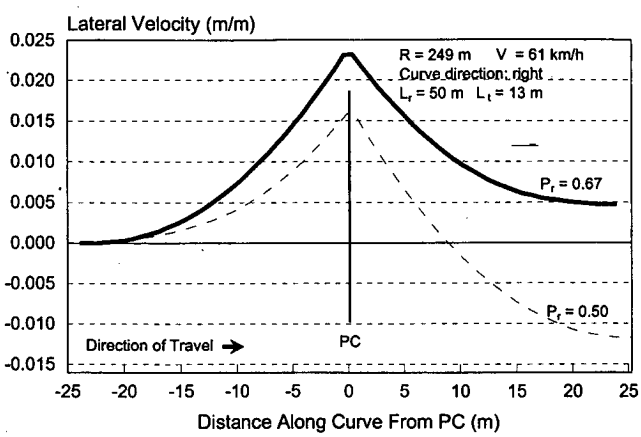

Figure D-7. Lateral velocity during curve entry.

Based on this analysis, it is desirable that lateral velocity equal zero at the end of the transition section. However, if the design has to produce a small lateral velocity, it would be preferable that this velocity be inward. In this manner, the probability that a driver incurs a critical path radius (i.e., $R_p < R$) can be minimized.

While knowledge of the lateral velocity at various points along the transition is useful, knowledge of this velocity at the end of the transition section is the key to understanding the effect of alternative transition designs. In recognition of this fact, Equation 15 was integrated to yield the following equation for predicting lateral velocity at the end of the tangent-to-curve transition:

$$v_l = \begin{cases} \dfrac{g\Delta^* 0.01}{2v^2 w n_l}\left[(0.5t_s v)^2 - L_r^2(1-P_r)^2\right] & : P_r > \dfrac{0.5t_s v + L_t}{L_r} \\ \dfrac{g\Delta^* 0.01}{2v^2 w n_l}\left[(P_r L_r - L_t)^2 - L_r^2(1-P_r)^2\right] & : P_r \le \dfrac{0.5t_s v + L_t}{L_r} \end{cases} \tag{16}$$

where:

v_l = lateral velocity at the end of the transition, m/m.

The two forms of the equation are needed because of the independence of the two applied accelerations. The first equation is appropriate when the ramp steering is initiated after the superelevation rotation begins. The second equation applies when the ramp steering is initiated prior to the point where superelevation rotation begins. It should be noted that the resultant lateral velocity predicted by Equation 16 is applicable to either curve entry or exit due to the integration process.

Lateral Shift

Lateral shift at any point can be computed by the integration of velocity over time or distance. It was determined that integration over distance would be most helpful in satisfying the objectives of this project. Thus, the integral had the following basic form:

$$y_l(x) = \int v_l(x)\,dx \tag{17}$$

where:

$y_l(x)$ = lateral shift at a distance x along the transition, m.

Figure D-8 illustrates the lateral shift resulting from the example curve described for Figure D-6. The thick trend line shown indicates that the lateral shift is positive, denoting a drift to the right (inward). The shift reaches its maximum value of about 0.42 m at the end of the steering time (as identified by point A).

The thin trend line shown in Figure D-8 illustrates the effect of placing more of the superelevation runoff on the curve. The combined steering and superelevation accelerations are so

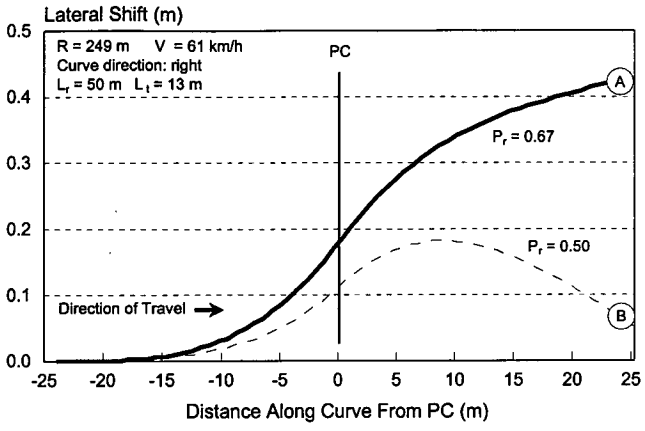

Figure D-8. Lateral shift during curve entry.

large after the PC that they induce a negative (or outward) drift that returns the vehicle to nearly the same lateral position it had prior to curve entry (as identified by point B). However, the outward lateral velocity that also exists at B (see Figure D-7) will require an increase in the steering angle to negate. This increase will create a critical path radius that is smaller than that of the highway curve.

In contrast to point B, the lateral velocity associated with point A is inward. A critical radius is not adopted; rather, the steering angle is decreased and the path radius flattened. As a result, the transition design represented by the thick trend line should be preferred to that represented by the thin line (provided the 0.42-m lateral shift can be safely accommodated in the roadway).

While knowledge of the lateral shift at various points along the transition is useful, knowledge of this shift at the end of the transition section is key to understanding the effect of alternative transition designs. Equation 17 was integrated to yield the following equation for predicting lateral shift at the end of the tangent-to-curve transition:

$$y_l = y_s + y_g - y_R \tag{18}$$

with

$$y_s = \left[\frac{1}{R_p} - \frac{g\Delta^* 0.01}{v^2 w n_l}(x_p)\right]\left[\frac{x_s^2}{2} + \frac{t_s v x_s}{2} + \frac{(t_s v)^2}{6}\right] \tag{19}$$

$$y_g = \frac{g\Delta^* 0.01}{v^2 w n_l}(x_p)\left(\frac{x_g^2}{2} + \frac{x_p x_g}{2} + \frac{x_p^2}{6}\right) \tag{20}$$

$$y_R = \frac{x_b^2}{2R_p} \tag{21}$$

$$x_p = \begin{cases} 0.5t_s v + L_r(1 - P_r) & : P_r > \dfrac{0.5t_s v + L_t}{L_r} \\ L_r - L_t & : P_r \le \dfrac{0.5t_s v + L_t}{L_r} \end{cases} \tag{22}$$

$$x_b = \textit{larger of: } [0.5t_s v, \quad L_r(1 - P_r)] \tag{23}$$

$$x_s = x_b - 0.5t_s v \tag{24}$$

$$x_g = x_b - L_r(1 - P_r) \tag{25}$$

where:

y_l = lateral shift at the end of the transition, m/m.

The two variations within Equation 22 are needed because of the independence of the two applied accelerations. The first equation is appropriate when the ramp steering is initiated after the superelevation rotation begins. The second equation applies when the ramp steering is initiated prior to the point where superelevation rotation begins. It should be noted that the resultant lateral shift predicted by Equation 18 is applicable to either curve entry or exit due to the integration process.

Spiral Curve Transition Model Development

The spiral curve transition model is based on the lateral accelerations acting on the vehicle as it traverses the transition section. As with the tangent-to-curve model, there are two sources of lateral acceleration acting on the vehicle in this section: (1) acceleration as a result of gravity and (2) acceleration as a result of tire-pavement friction. The variation of these accelerations through the transition section tends to result in lateral motion. These accelerations are shown in Figures D-9 and D-10 for curves to the left and right, respectively.

Sign Conventions and Assumptions

As with the tangent-to-curve model, the use of a sign convention allows the spiral model equations to be applied to either inside or outside curves with only a change in the sign of selected variables. This sign convention is the same as that listed in Table D-1.

The spiral model is developed for the inside (or right-hand) curve. The signs of the variables listed in Table D-1 should be reversed when used in the corresponding equations for analysis of an outside (or left-hand) curve.

In addition to the sign conventions, the following assumptions were made in developing the spiral curve transition model:

1. The driver exerts whatever steering effort is needed to counter the normal cross slope and maintain a constant lane position up until t_s seconds prior to the SC. At this point in time, the driver is assumed to initiate the ramp steering behavior for t_s seconds.

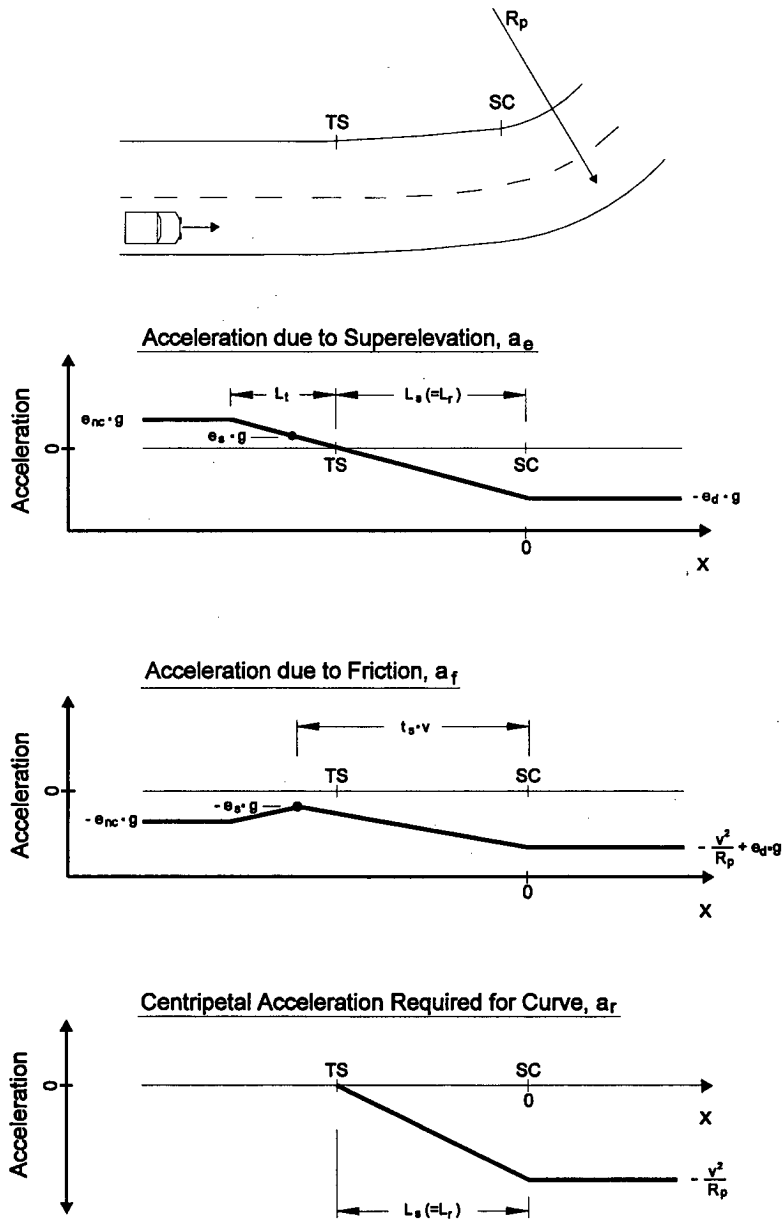

Figure D-9. Lateral accelerations during entry to a left-hand curve with a spiral curve transition design.

2. The spiral length is assumed to be equal to the minimum superelevation runoff length, as computed using Equation 2.

Lateral Acceleration As a Result of Superelevation

The acceleration as a result of superelevation can be computed as follows:

$$a_e(x) = g\, e(x)\, 0.01 \qquad (26)$$

with

$$e(x) = \begin{cases} e_{NC} & : x \le x_1 \\ (e_d - e_{NC})\dfrac{x - x_1}{x_{SC} - x_1} + e_{NC} & : x_1 < x < x_{SC} \\ e_d & : x \ge x_{SC} \end{cases} \qquad (27)$$

$$x_1 = x_{SC} - (L_s - L_t) \qquad (28)$$

where:

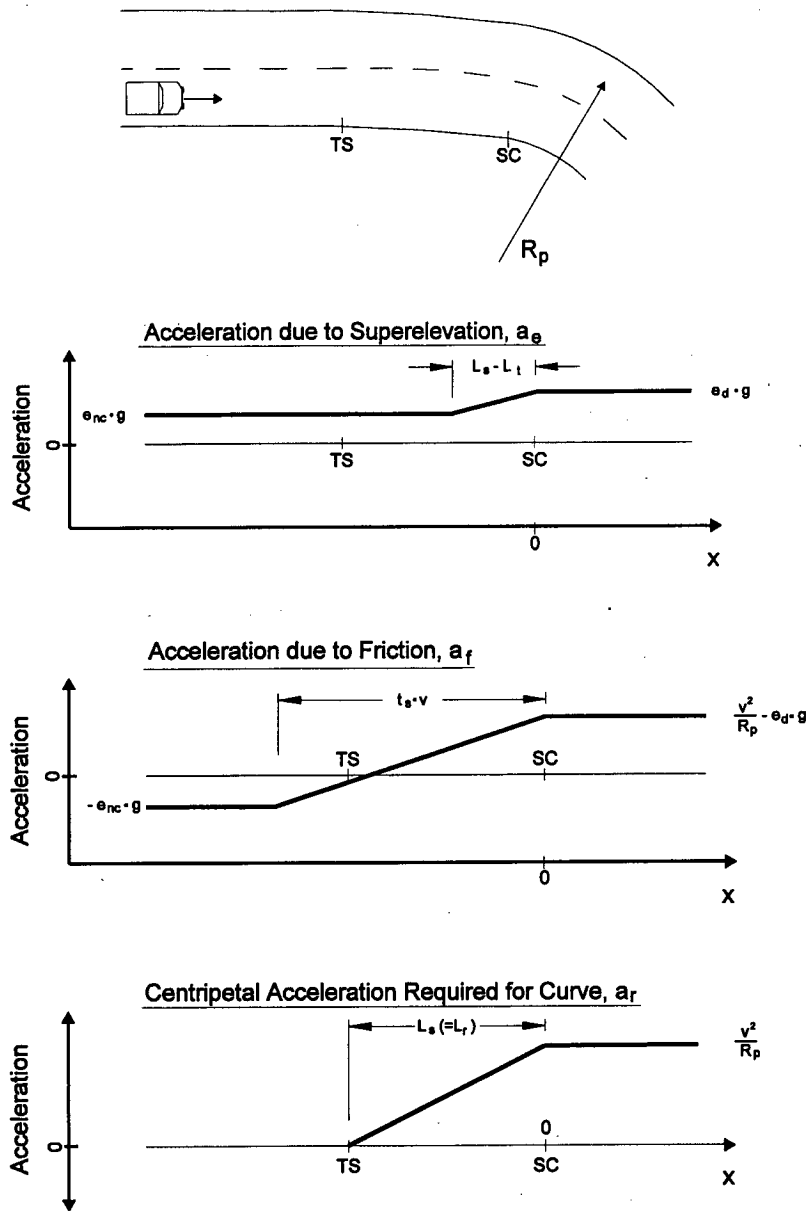

Figure D-10. Lateral accelerations during entry to a right-hand curve with a spiral curve transition design.

$a_e(x)$ = acceleration sustained by superelevation at a distance x along the transition, m/s²;
L_s = length of spiral (= L_r from Equation 2), m; and
x_1 = location where superelevation begins its change from e_{NC} to e_d relative to the SC.

Lateral Acceleration As a Result of Friction

The acceleration as a result of tire-pavement friction resulting from the ramp steering behavior can be computed as follows:

$$a_f(x) = \begin{cases} -e(x)g\,0.01 & : x \le x_a \\ \left(\dfrac{v^2}{R_p} - \dfrac{e_d}{100}g + \dfrac{e_s}{100}g\right)\dfrac{x - x_a}{x_{SC} - x_a} - \dfrac{e_s}{100}g & : x_a < x < x_{SC} \\ \dfrac{v^2}{R_p} - \dfrac{e_d}{100}g & : x \ge x_{SC} \end{cases} \quad (29)$$

with

$$e_s = \begin{cases} (e_d - e_{NC})\dfrac{x_a - x_1}{x_{SC} - x_1} + e_{NC} & : x_a > x_1 \\ e_{NC} & : x_a \le x_1 \end{cases} \quad (30)$$

$$x_a = x_{SC} - t_s v \quad (31)$$

The accelerations resulting from superelevation and steering must combine to provide the acceleration required to track the traffic lane. This acceleration is shown in the bottom portion of Figures D-9 and D-10. Any deviation from this requirement results in a lateral shift. This deviation between the applied lateral accelerations and the curve tracking acceleration represents the lateral acceleration that creates lateral motion. This resultant lateral acceleration can be computed as follows:

$$a_l(x) = a_e(x) + a_f(x) - a_r(x) \quad (32)$$

with

$$a_r(x) = \begin{cases} 0.0 & : x \le x_r \\ x\dfrac{v^2}{R_p L_s} & : x_r < x < x_{SC} \\ \dfrac{v^2}{R_p} & : x \ge x_{SC} \end{cases} \quad (33)$$

$$x_r = x_{SC} - L_s \quad (34)$$

Equations 26 through 34 were applied to a typical two-lane highway curve having a radius of 249 m and a superelevation rate of 8 percent. The average speed was assumed to be 61 km/h and the steering time was assumed to be 2.8 s. The resulting lateral acceleration, velocity, and shift are shown in Figure D-11. The latter two characteristics were obtained by integrating the acceleration and velocity functions over distance, respectively.

The trend line shown in Figure D-11a (i.e., the thick line) indicates that the resultant lateral acceleration is initially equal to zero because the acceleration from friction is equal and opposite to that required to maintain lane position on a normal cross slope. The driver initiates the ramp steering at 2.8 s (47 m) before the SC. At 38 m before the SC, the superelevation transition is encountered and additional acceleration from gravity is introduced. The resultant acceleration is maximum at this location and decreases thereafter until it reaches zero at the SC. As a result of these two accelerations, the vehicle drifts to the left (outward).

It should be noted that the peak lateral acceleration within the spiral curve transition is about one-third that of the tangent-

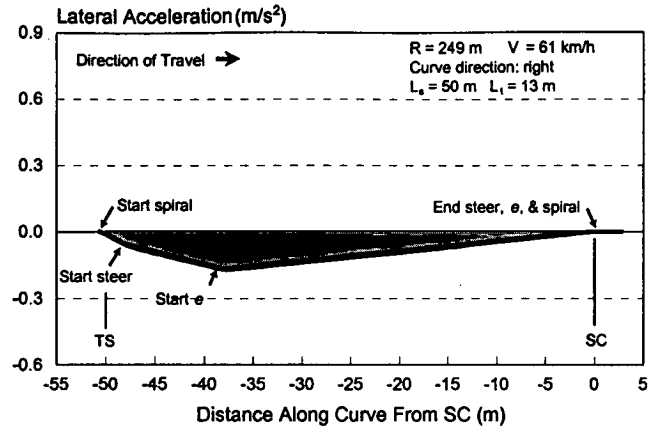

a. Lateral acceleration.

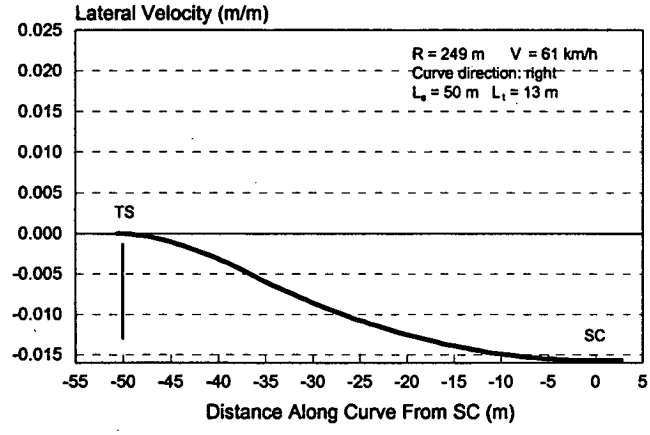

b. Lateral velocity.

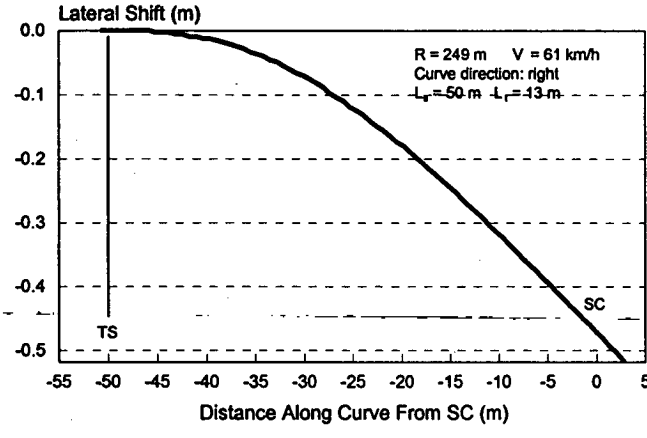

c. Lateral shift.

Figure D-11. Lateral motion during entry to a curve with spiral transition.

to-curve design. This trend is consistent with the observations of both Glennon et al. (*6*) and Segal et al (*7*) in separate simulation experiments comparing spiral and tangent-to-curve transitions.

Figure D-11b indicates that the lateral velocity reaches its maximum value at the SC. After this point, the driver will need to make a small steering correction to negate the associated drift. The negative (outward) direction of drift suggests that the correction required will be one of increased steering angle. This increase will create a critical path radius that is smaller than that of the highway curve. It should be noted that the lateral velocity at the end of the spiral curve is about three times larger than that found for the tangent-to-curve design.

Figure D-11c indicates the lateral shift reaches its maximum value at the SC. Additional outward shift is inevitable because the driver makes additional steering corrections to stop the lateral velocity. It should also be noted that the magnitude of the shift at the end of the spiral curve is approximately equal to that found for the tangent-to-curve design.

These results illustrate the tangent-to-curve and spiral curve transition design models. Different variable values will produce different results. It is shown in Chapter 3 that optimum design values can be selected for both transition design types such that their resulting lateral velocity and shift are about the same.

Lateral Velocity

The equations for lateral acceleration were integrated to yield the following equation for predicting lateral velocity at the end of the spiral curve transition section:

$$v_l = \begin{cases} \dfrac{t_s v - L_s}{2R_p} & : L_s > t_s v + L_t \\ \dfrac{t_s v - L_s}{2R_p} + \dfrac{g\Delta^* 0.01}{2v^2 w n_l}\left[(L_s - L_t)^2 - t_s v (L_s - L_t)\right] & : L_s \le t_s v + L_t \end{cases} \quad (35)$$

where:

v_l = lateral velocity at the end of the transition, m/m.

The two forms of the equation are necessitated by the independence of the two applied accelerations. The first equation is appropriate when the ramp steering is initiated after the superelevation rotation begins. The second equation applies when the ramp steering is initiated prior to the point where superelevation rotation begins. It should be noted that the resultant lateral velocity predicted by Equation 35 is applicable to either curve entry or exit due to the integration process.

Lateral Shift

The equations for lateral velocity were integrated to yield the following equation for predicting lateral shift at the end of the spiral curve transition section:

$$y_l = \begin{cases} \dfrac{(t_s v)^2 - L_s^2}{6R_p} & : L_s > t_s v + L_t \\ \dfrac{(t_s v)^2 - L_s^2}{6R_p} + \dfrac{g\Delta^* 0.01}{6v^2 w n_l}\left[(L_s - L_t)^3 - (t_s v)^2 (L_s - L_t)\right] & : L_s \le t_s v + L_t \end{cases} \quad (36)$$

where:

y_l = lateral shift at the end of the transition, m.

The resultant lateral shift predicted by Equation 36 is applicable to either curve entry or exit due to the integration process.

MODEL CALIBRATION

This section describes the calibration of the tangent-to-curve and spiral curve transition models. The calibration step consisted primarily of defining the value of steering time t_s that most accurately reproduced observed lateral shifts. Two sources were considered for the calibration data. The first source was the lateral shift data published by Segal et al. (*7*). The second data source considered was the HVOSM simulation model.

HVOSM Simulation Data

The HVOSM model was used to generate lateral shift data for passenger cars with different speeds traveling on transitions with different geometric properties. However, a stability problem was encountered during the use of the model. This problem relates to the model's generation of unsteady travel path data. Specifically, the simulated vehicle exhibited transient peaks (perhaps oscillatory in nature) in lateral shift that suggested a deficiency in some aspect of the model structure. Such transients have been noted by Glennon et al. (*6*), who used a modified, Roadside Design version of HVOSM to simulate vehicles entering and traveling along a curve. Glennon et al. (*6*) rationalized that the HVOSM steering control model (that they had incorporated from the Vehicle Dynamics version) was the source of the instability. As a result, they made several enhancements to the HVOSM control model source code to minimize this instability.

In contrast to the approach used by Glennon et al. (*6*), the Vehicle Dynamics version of HVOSM was used for this research. A steering control model is distributed with this version of HVOSM; although, it is not well documented in

the User's Manual (*11*). This model allows the "desired" travel path to be defined by a series of five line segments. A preprocessing software package was developed for this research to define the center of the traveled lane in terms of these five line segments.

HVOSM reads nine input parameters to describe the driver preview, reaction time, and speed-control processes. Default values are not explicitly described in the User's Manual; however, typical values were obtained from an example input file included in the manual.

The stability of the steering control model was initially evaluated for its ability to smoothly track the segmented travel path. This evaluation was based on an examination of the steer angle provided in the HVOSM output for each 0.5-s time step. The results of one such evaluation are provided in Figure D-12. The steering-wheel angles represented in this figure are based on a steering-wheel-angle-to-steer-angle ratio of 20:1. Steering-wheel angle is shown instead of steer angle because it is believed to be easier to interpret.

The trend line shown in Figure D-12 that is attributed to the HVOSM steering model has some characteristics that are similar to those of the ramp steering model. Specifically, the HVOSM model has a steering behavior that closely resembles ramp steering, although HVOSM "smooths" the transition to and from the slope of constant steering-wheel rotation. Another similarity is that the HVOSM steering model approximately centers the steering time on the curve PC.

The HVOSM and ramp steering models shown in Figure D-12 also have a major difference. Specifically, the steering time is only about 1.0 s for the HVOSM model whereas that for the ramp steering model is 2.8 s. The 1.0 s duration is shorter than any of the steering times reported in the literature. The literature review described in the Background section indicated that steering time typically varies from 2.2 to 3.5 s. It should also be noted that this tendency of HVOSM to produce a short steering time was observed by both Glennon et al. (*6*) and Segal et al. (*7*). In fact, Glennon et al. (*6*, p. 164) included a figure in their final report that is very similar to Figure D-12; even though, they used a modified version of HVOSM with an enhanced steering control model.

The relatively short steering time produced by HVOSM results in a much more rapid introduction of lateral acceleration. This "burst" of acceleration appears to introduce a dynamic response in the vehicle's sprung mass that causes some unsteady, oscillatory behavior in the vehicle's lateral motion.

Figure D-13 illustrates the lateral shift that corresponds to the steering behavior shown in Figure D-12. This shift data was obtained from the *x-y* coordinates of the sprung mass (obtained from the HVOSM output) and the corresponding coordinates for the roadway centerline (computed externally). These coordinate pairs were used to compute the lateral shift for each 0.5-s time step.

The trend line shown in Figure D-13 illustrates the unrealistic oscillatory response in the HVOSM output. This response is believed to be due to the short steering time associated with HVOSM's steering control model. The oscillations are inconsistent with the lateral shift trends reported in the literature (as shown in Figure D-3) and are believed to be aberrations of the HVOSM model logic rather than replication of true driver behavior.

Additional simulations were conducted for left- and right-hand curves with speeds ranging from 20 to 110 km/h and radii ranging from 30 to 1,300 m. Trends similar to those shown in Figures D-12 and D-13 were found in all cases. As a result, the HVOSM model was not used to calibrate the lateral motion models.

Published Lateral Shift Data

Segal et al. (*7*) measured the lateral shift of passenger cars and trucks on three curves. Two of these curves used the tangent-to-curve transition design. The third curve used the spiral curve transition design. The curves using the tangent-

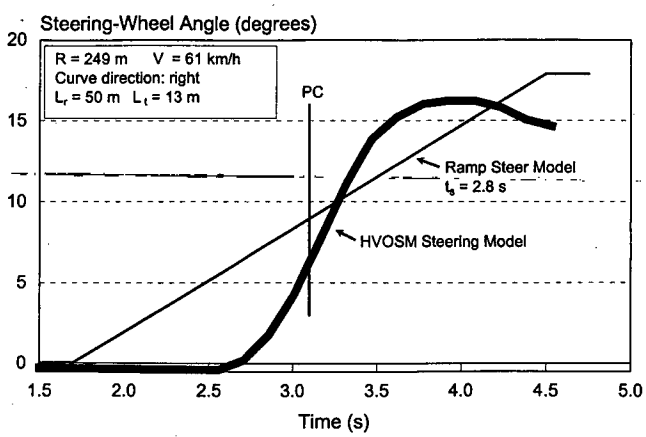

Figure D-12. Steering-wheel angle as a function of travel time based on HVOSM output.

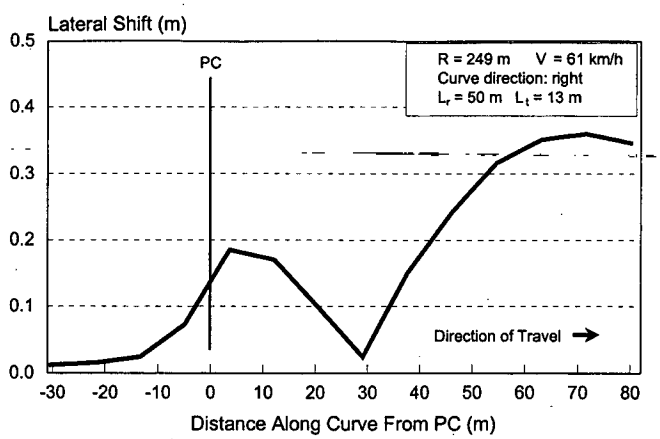

Figure D-13. Lateral shift based on HVOSM output.

to-curve design had 46- and 55-m radii and were located on interchange off-ramps. The curve with the spiral transition had a 46-m spiral length and a 218-m radius; it was located on an interchange on-ramp. With one exception, the lateral shifts of 30 passenger cars and 30 trucks were observed on each curve. The only exception was for the spiral curve where only 20 trucks were observed. Data describing the superelevation rate at 13 to 16 points along the transition section of each curve location were also reported by Segal et al. (*7*).

The model calibration consisted of obtaining a visual "best fit" between the predicted and the average of the observed lateral shifts. The model calibration parameter was steering time t_s. Once the speed, radius, and superelevation information were input to the model, the steering time parameter was varied until the best fit was obtained for the entire shift trace. This process was repeated for each of the two vehicle types and for each of the three curves studied by Segal et al. (*7*).

A comparison of the observed and predicted lateral shifts are shown in Figures D-14, D-15 and D-16. In general, the model fit to the observed data was believed to be quite good given the simplicity of the assumed ramp steering model. Steering time values for the passenger cars ranged from 2.40 to 3.04 s; those for the trucks were slightly higher, ranging from 2.70 to 3.70 s. Unfortunately, the limited number of sites does not allow for generalization about differences in steering time between the tangent-to-curve and spiral curve transition designs. However, the data shown in Figures D-14, D-15, and D-16 do not make a strong case for concluding that there is a difference in driver behavior between the two transition designs.

Based on this calibration process, it is concluded that the ramp steering model represents a reasonable, first-order approximation of driver steering behavior. Thus, it is concluded that the tangent-to-curve and spiral curve models are sufficiently accurate to define acceptable design control values. Finally, it is concluded that the model is most accurate

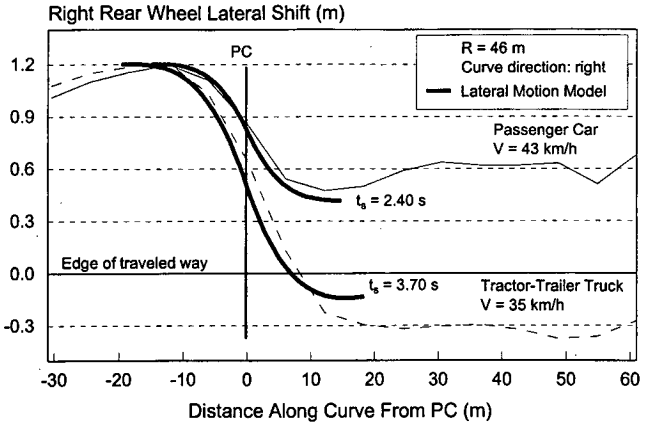

Figure D-14. Comparison of observed and predicted lateral shift on a curve with a 46-m radius and a tangent-to-curve transition design..

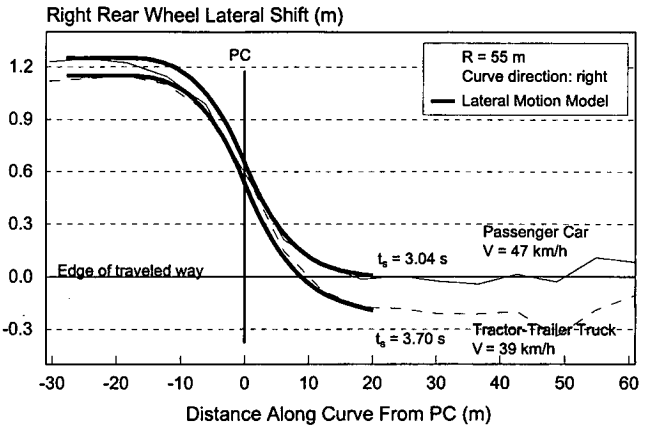

Figure D-15. Comparison of observed and predicted lateral shift on a curve with a 55-m radius and a tangent-to-curve transition design.

for a wide range of conditions when a steering time of 2.8 s is used. The choice of this value is based partly on the results of the calibration process and partly on the findings from the literature review.

SENSITIVITY ANALYSIS

This section describes an examination of the sensitivity of lateral motion to a wide range of transition design variables. In particular, the equations for predicting lateral velocity and lateral shift were used to make relative assessments of alternative control values. The evaluation focused on the effects of the following variables:

1. Superelevation rate (2.0 to 12 percent);
2. Width of rotated roadway (3.6 and 7.2 m);
3. Runoff length with and without imposition of the travel time control;

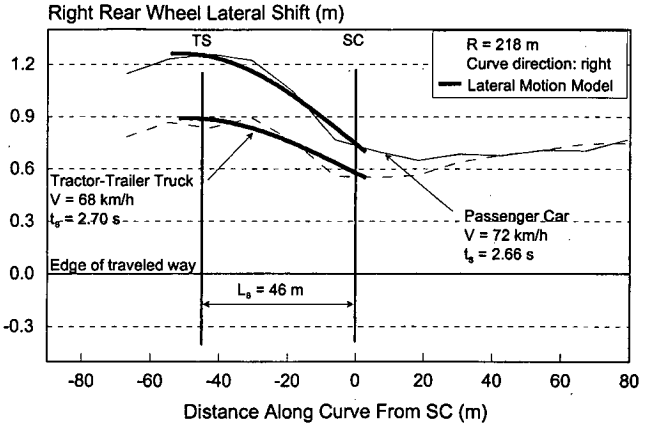

Figure D-16. Comparison of observed and predicted lateral shift on a curve with a 218-m radius and a spiral transition design.

4. 95th Percentile Curve Speed (30, 70, and 100 km/h), and;
5. Portion of runoff located prior to the PC (0.67 and 1.0).

Superelevation rate was considered a fundamental variable; hence, it was included in the evaluation of Variables 2 through 5. The underlined values for Variables 2 through 5 are defined as the "base" condition. The sensitivity analysis was based on changing one variable value at a time, relative to the base condition.

Equations 16, 18, 35, and 36 were used to compute the lateral velocity and shift for the tangent-to-curve and spiral curve transition designs for each of the five aforementioned variables. Lateral velocity and shift were computed for the inside (i.e., right-hand) and outside (left-hand) curve directions. The spiral length was set equal to the minimum superelevation runoff length, as obtained from Equation 2. Because of the mathematical relationship among superelevation rate, curve radius, and design speed implied by the superelevation distribution method, it was determined that radius would be computed from the superelevation rate and 95th percentile speed. The distribution method used is that recommended in Chapter 3 for application to RHS facilities.

Several points need to be made regarding the interpretation and assessment of lateral velocity and shift. These points are made here to provide some context for later statements about the effect of each variable considered. Many of these points have been discussed in previous sections; however, they will be restated here for convenience. First, the lateral velocity and shift for both curve directions (i.e., inside and outside) should be considered together because most roadways serve two-way traffic flows. Thus, acceptable values of velocity or shift are necessary for both directions when assessing the merits of a specific design element value.

Second, lateral velocities near zero at the end of the transition are most desirable; however, they are not achievable in both travel directions for most variable combinations. Hence, small lateral velocities should be considered acceptable provided that they are in an "inward" direction (i.e., positive for the inside direction and negative for the outside direction). A consequence of lateral velocity in an outward direction is that the driver will likely increase the steering angle and thereby, adopt a critical path radius (i.e., a travel path radius sharper than that of the roadway).

Specification of an upper limit of lateral velocity based on a corresponding critical radius was attempted; however, additional assumptions about driver steering behavior were required. One model relating this velocity and radius was considered but the resulting relation was unduly complex. As a result, this work is not reported herein. However, based on this analysis and an examination of predicted velocities for a range of typical design values, it was determined that inward lateral velocities up to 0.01 m/m were considered acceptable.

Finally, the lateral shift should not be excessively large. Large shift values will likely result in the vehicle encroaching on an adjacent lane or shoulder. Thus, predicted shift values of up to 1.0 m were considered acceptable for most conditions.

Effect of Superelevation Rate

The results of the evaluation of superelevation rate are shown in Figures D-17 and D-18. The base condition value for each of Variables 2 through 5 was used for this evaluation. The trends shown in Figures D-17 and D-18 indicate that the tangent-to-curve design produces an acceptable lateral velocity and shift over the range of superelevation rates. The lateral velocity for the spiral curve transition design is slightly larger than that of the tangent-to-curve design for superelevation rates of 7.0 percent or less. However, the velocity and shift for the spiral design increase significantly as the superelevation rate exceeds 7.0 percent. This increase is a consequence of the spiral length exceeding the steering time (represented in terms of travel distance, i.e., $t_s v$). The superelevation rate that corresponds to this length is referred to hereafter as the "critical" superelevation rate.

While it might be argued that the driver would adopt a ramp steering duration that matched the spiral (i.e., from TS to SC) to avoid lateral motion, this behavior is not likely to occur because drivers rely extensively on visual cues to initiate the steering maneuver (e.g., the PC). The beginning of a spiral (TS) is intentionally imperceptible; hence, drivers are more likely to initiate their steering response based on (1) their perception of sharp curvature ahead in the vicinity of the spiral end (SC), (2) a sensation of superelevation being introduced, (3) their perception of significant lateral shift, or (4) some combination of all of these stimuli. All stimuli considered, drivers are most likely to initiate their steering after the start of "long" spirals (i.e., spiral lengths that exceed the ramp steering time).

The extreme velocity and shift corresponding to large superelevation rates (and spiral lengths) are not likely to be realized in actual curve driving. This belief is based on the

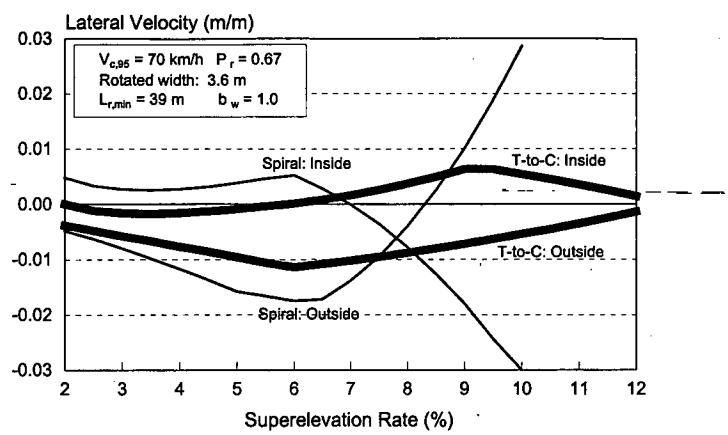

Figure D-17. Effect of superelevation rate and transition design on lateral velocity.

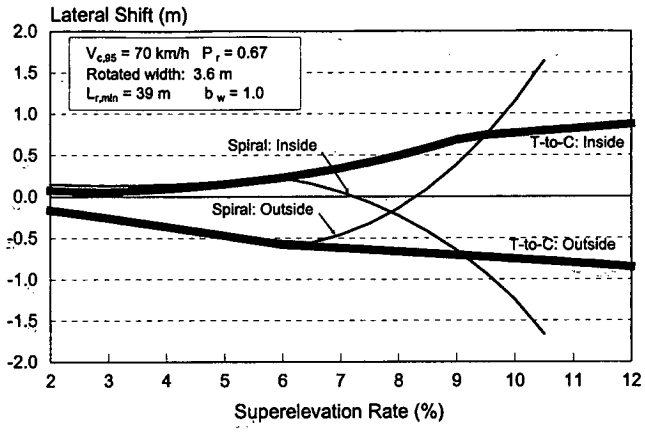

Figure D-18. Effect of superelevation rate and transition design on lateral shift.

likelihood that drivers would notice significant lateral shift and modify their steering behavior accordingly to minimize this shift. However, such steering modifications would likely be continuous and oscillatory in nature (because they would stem from the compensatory steering response mechanism). If they occur, these characteristics would be undesirable because they are likely to (1) require greater driving effort and (2) produce critical path radii.

Effect of Rotated Width

The effect of rotating a two-lane section of pavement (as opposed to one lane) in the superelevation transition section is shown in Figure D-19. This figure illustrates the effect of rotated width on lateral velocity for both the tangent-to-curve design (in Figure D-19a) and the spiral design (in Figure D-19b). The thick trend lines represent the expected lateral velocity for the two-lane condition. The thin trend lines represent one lane of rotated pavement and are equivalent to those in Figures D-17 or D-18 for the tangent-to-curve or spiral design, respectively. These thin lines are provided to clearly illustrate the effect of rotated width on velocity for a range of superelevation rates. The trends shown in Figure D-19 indicate that rotated width has an inconsistent effect on lateral velocity over the range of superelevation rates and transition design types shown. For the tangent-to-curve design, the effect varies from a slight decrease to a slight increase in lateral speed, depending on the superelevation rate. For superelevation rates larger than 8.5 percent, the resulting lateral velocity is in the undesirable outward direction for both curve directions. For the spiral design, the increased spiral length (resulting from the wider rotated width) reduces the critical superelevation rate to about 4.5 percent.

The effect of increasing the rotated width on lateral shift was also examined. For the tangent-to-curve design, the increase in rotated width reduced the lateral shift slightly for

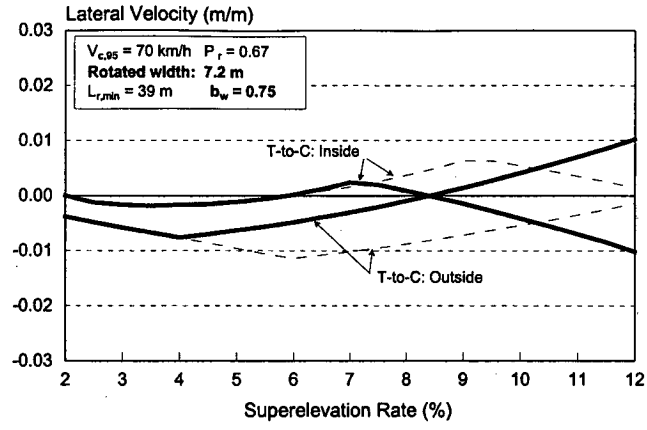

a. Tangent-to-curve transition design.

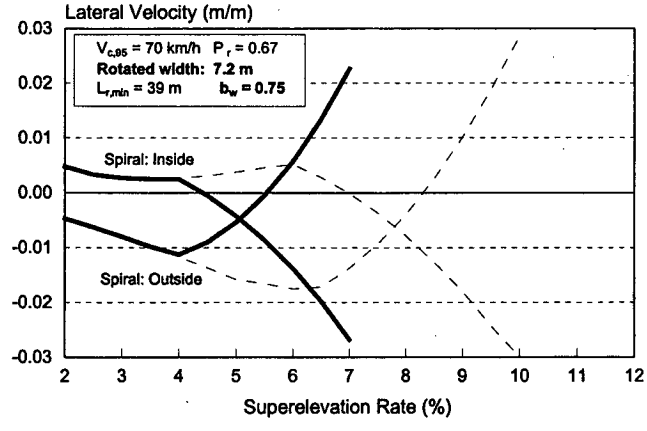

b. Spiral curve transition design.

Figure D-19. Effect of superelevation rate and rotated width on lateral velocity.

superelevation rates of 6.0 percent or more. For the spiral design, the lateral shift was found to be excessively large for rates of 7.0 percent or more.

Effect of the Travel Time Control

As indicated by Equation 2, runoff (and spiral) length is based on consideration of a travel time control and a maximum relative gradient control. As this equation was used for all previous evaluations, the effect of both controls has been reflected in Figures D-17 to D-19. Consideration of the travel time control ensures that the runoff length will exceed 2 s of travel time. Travel time typically controls runoff length when the rotated width is only one lane wide and the superelevation rate is small. For this evaluation, the travel time control was not used when computing the runoff length (i.e., runoff length was based on only the maximum relative gradient control). The results of this evaluation are shown in Figure D-20 as they relate to lateral velocity.

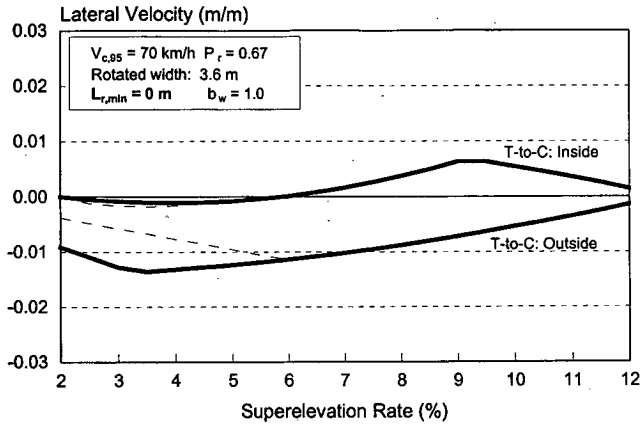

a. Tangent-to-curve transition design.

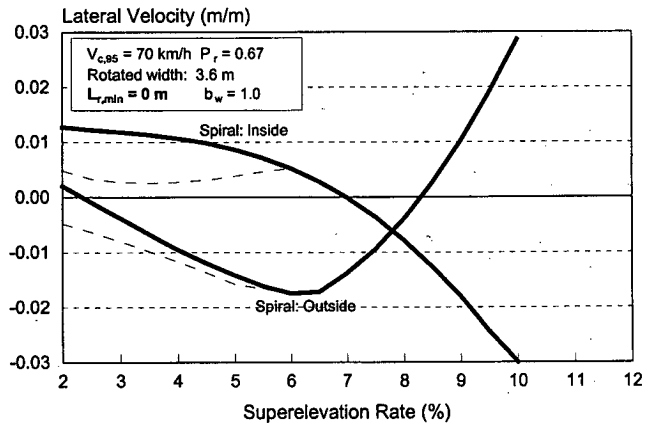

b. Spiral curve transition design.

Figure D-20. Effect of superelevation rate and travel time control on lateral velocity.

The trends shown in Figure D-20 indicate that the effect of excluding the travel time control is evident only for superelevation rates of 6.0 percent or less. Further examination of this trend indicates that runoff lengths corresponding to superelevation rates below 6.0 percent are based on the travel time control; lengths corresponding to rates above this value are based on the gradient control. As before, the thin dashed lines represent the lateral velocity expected for the base condition (which includes consideration of the travel time control).

The trends shown in Figure D-20 are not consistent between the tangent-to-curve and spiral designs. For the tangent-to-curve design, exclusion of the travel time control has negligible effect on the lateral velocity for the inside lane, but it increases this velocity for the outside direction. For the spiral design, elimination of the travel time control increases the lateral velocity for the inside lane and reduces it (in terms of absolute value) for the outside lane. Similar trends were observed for lateral shift.

In general, the travel time control reduces the combined lateral velocity slightly for both the tangent-to-curve and spiral designs over a range of small to moderate superelevation rates. It has no effect on the lateral velocity or shift associated with larger superelevation rates.

Effect of Speed

The effect of lower or higher travel speed through the superelevation transition section is shown in Figures D-21 and D-22, respectively. These figures illustrate the effect of speed on lateral velocity for both the tangent-to-curve and spiral designs. The thin lines replicate the trends in Figures D-17 and D-18 and are provided to clearly indicate the effect of speed on lateral velocity for a range of superelevation rates.

The trends shown in Figure D-21 indicate that low speed introduces a critical superelevation rate for the tangent-to-curve design (analogous to that noted for the spiral design). Superelevation rates larger than the critical rate produce large and undesirable outward lateral velocities. For the tangent-to-

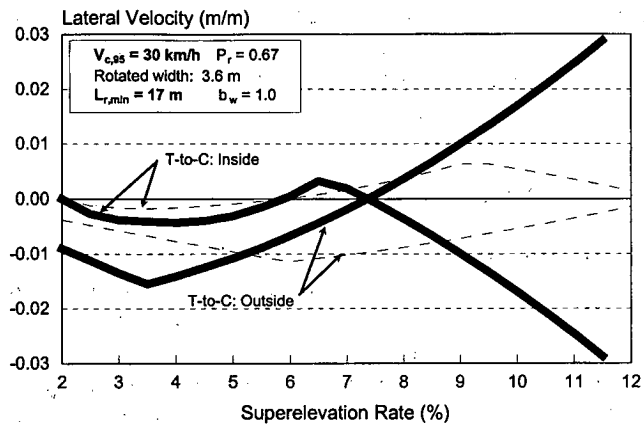

a. Tangent-to-curve transition design.

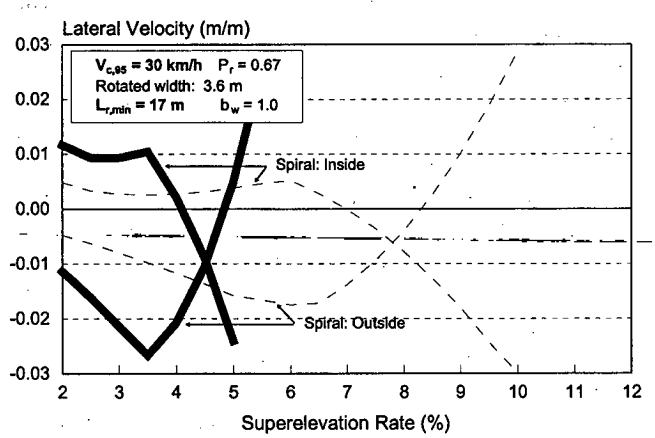

b. Spiral curve transition design.

Figure D-21. Effect of superelevation rate and low speed on lateral velocity.

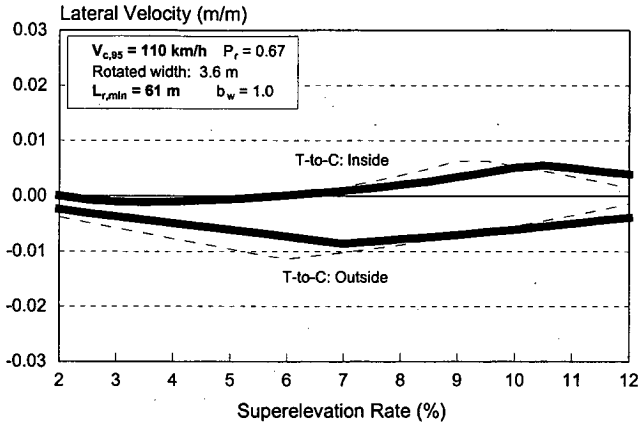

a. Tangent-to-curve transition design.

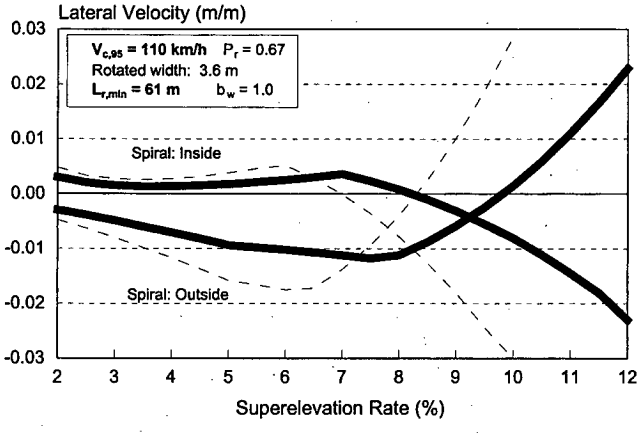

b. Spiral curve transition design.

Figure D-22. Effect of superelevation rate and high speed on lateral velocity.

curve design, the critical radius appears to be about 7.5 percent for the 30 km/h analysis speed. For the spiral design, the reduction in speed to 30 km/h lowers the critical rate to about 4.5 percent.

The effect of a decrease in speed on lateral shift was also examined. For the tangent-to-curve design, decreasing the speed from 70 to 30 km/h increased the lateral shift, significantly so for superelevation rates above the critical rate. For the spiral design, the lateral shift was also found to be excessive (i.e., in excess of 1.0 m) for rates above the critical rate.

As shown in Figure D-22, increasing the speed from 70 to 110 km/h had a negligible effect on lateral velocity for the tangent-to-curve design. A negligible effect on lateral shift was also noted for this design. For the spiral design, the increase in speed increased the critical superelevation rate to about 9.0 percent. In addition, the lateral velocity and shift for superelevation rates below the critical rate were reduced slightly by the increase in speed.

In general, it appears that low-speed transition designs may be more sensitive to design element values for the resulting lateral velocity and shift. Relatively low critical superelevation rates for both the tangent-to-curve and spiral curve transition designs emerge when their corresponding lengths exceed the steering time t_s (in terms of the corresponding travel distance t_a v).

Effect of Portion-of-Runoff-Prior-to-the-Curve Control

Equation 16 was used to examine the relationship between the portion of superelevation runoff located prior to the PC and lateral velocity. For this examination, a two-lane highway curve with a superelevation rate of 6.0 percent was considered, as was entry to the curve from both directions. The results of this analysis are shown in Figure D-23.

The trends shown in Figure D-23 indicate that "portion" does not have the same effect on lateral velocity in the two travel directions. For the outside direction, lateral velocity decreases with increasing portion. It reaches a desirable lateral velocity of zero when the portion is about 0.3. For the inside direction, lateral velocity increases with increasing portion. It reaches a desirable velocity of zero when the portion is about 0.67.

Two line thicknesses are used in Figure D-23 for each of the trend lines. The part of the line that is thin denotes an undesirable outward lateral velocity, relative to the travel direction. The thick part of the line denotes an acceptable inward lateral velocity. Based on this identification, a portion of 0.67 appears to offer the best compromise value for the conditions analyzed. This portion should have negligible drift in the inside direction and an inward drift in the outside direction that is very near the acceptable limit. Portions

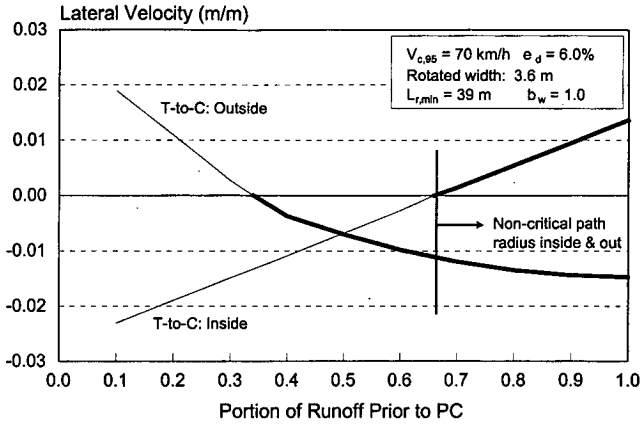

Figure D-23. Effect of portion-of-runoff-prior-to-curve on lateral velocity.

above or below the value of 0.67 produce either undesirable outward drift or undesirably large lateral velocities.

SUMMARY

Based on the results of the sensitivity analysis, some control values appear to be consistent with minimum lateral velocity and shift. Specifically, it appears that larger superelevation rates may be associated with larger lateral velocities and shifts; this is especially true for the spiral curve transition design. Increasing the rotated width (and corresponding spiral length) further increases the aforementioned effect of superelevation rate. Large lateral velocities and shifts are associated with moderate to large superelevation rates when the rotated width is increased.

The travel time control appears to have a small beneficial effect on the magnitude of lateral velocity. Specifically, the travel time control tends to make the combined lateral velocity from the two travel directions smaller for small to moderate superelevation rates.

Low speeds tend to make the transition operation more sensitive to control values, especially those transitions with moderate to large superelevation rates.

The portion of runoff located prior to the curve appears to have a significant effect on lateral velocity. More important, it appears that there may be a small range of values for this control that offer the best compromise in terms of an acceptable combination of lateral velocity for both travel directions.

Finally, it appears that lateral velocity and shift are most likely to be large when the length of the spiral curve transition differs significantly from the steering time (expressed as a travel distance, i.e., $t_s v$). Thus, spiral length should desirably be as consistent as possible with driver steering time.

REFERENCES

1. Donges, E., "A Two-Level Model of Driver Steering Behavior." *Human Factors*, Vol. 20(6) (1978) pp. 691–707.
2. Godthelp, H., "Vehicle Control During Curve Driving." *Human Factors*, Vol. 28(2) (1986) pp. 211–221.
3. McLean, J.R., "Driver Behavior on Curves—A Review." *ARRB Proceedings*, Vol. 7, Part 5, Australian Road Research Board (1974) pp. 129–143.
4. *A Policy on Geometric Design of Highways and Streets*. American Association of State Highway and Transportation Officials, Washington, D.C. (1994).
5. Stewart, D., "The Case of the Left-Hand Bend." *The Highway Engineer*, Vol. 24(6). Institution of Highway Engineers, (1977) pp. 12–17.
6. Glennon, J.C., T.R. Neuman, and J.E. Leisch, *Safety and Operational Considerations for Design of Rural Highway Curves*. Report No. FHWA/RD-86/035, Federal Highway Administration, U.S. Department of Transportation, Washington, D.C. (1985).
7. Segal, D.J. and T.A. Banney, *Evaluation of Horizontal Curve Design*. Report No. FHWA-RD-79-48, Federal Highway Administration, U.S. Department of Transportation, Washington, D.C. (1980).
8. Wong, Y. and A. Nicholson, "Speed and Lateral Placement on Horizontal Curves." *Road and Transport Research*, Vol. 2, No. 1 (March 1993) pp. 74–87.
9. Stewart, D. and C.J. Chudworth, "A Remedy for Accidents at Bends." *Traffic Engineering & Control*, Vol. 31, No. 2 (February 1990) pp. 88–93.
10. Emmerson, J., "Speeds of Cars on Sharp Horizontal Curves." *Traffic Engineering & Control* (July 1969) pp. 135–137.
11. Segal, D.J., *Highway-Vehicle-Object Simulation Model—1976 User's Manual*. Report No. FHWA-RD-76-162, Federal Highway Administration, U.S. Department of Transportation, Washington, D.C. (1976).

APPENDIX E

RECOMMENDED REVISIONS TO THE AASHTO *GREEN BOOK*

INTRODUCTION

This appendix presents the recommended revisions to the design guidelines in the 1994 AASHTO publication *A Policy on Geometric Design of Highways and Streets*, known as the *Green Book*. These recommendations are intended for consideration by the AASHTO Task Force on Geometric Design for possible incorporation in a future edition of the *Green Book*.

The recommended revisions are derived from the findings of this research. These revisions focus on design controls applicable to superelevation distribution methods and transition designs. However, the findings of this research also address design side friction factors because of their fundamental relationship to horizontal curve design.

The recommended revisions contain controls that are in general agreement with those provided in the *Green Book*. However, in many instances, the material has been reorganized, simplified, or modified to better promote design consistency and safe traffic operations. The more extensive modifications are based on the analysis of field data and a review of design guidelines used by numerous state and international transportation agencies.

The safety benefits associated with the recommended modifications are based on rational arguments regarding the effect of design consistency, driver behavior, and vehicle performance on motorist safety. More consistency in curve design corresponds to a reduced driver workload, which translates into a reduced crash potential. Design consistency relates to (1) the uniform application of design controls such that drivers can develop expectancies (i.e., a "library" of successful responses to driving situations) and (2) design controls that are based on observed driver behavior under "normal" operating conditions.

Sections of the *Green Book* affected by the recommended revisions are primarily located in Chapter III. However, some material in Chapters II, IX, and X is also affected. The remainder of this report presents the text of the *Green Book* that has been modified. It is believed that designers will find the revised material easy to understand and apply. The basic assumptions underlying most of the design controls are included in the recommended text; however, references to this final report are also included where appropriate for those readers who desire additional background information.

CHAPTER II—DESIGN CONTROLS AND CRITERIA

The text provided on the following pages represents the recommended modifications to selected paragraphs in *Green Book* Chapter II. These paragraphs are located in a section that addresses the relationship between design speed and running speed. Recommended deletions of text are shown as ~~strikeouts~~ and additions to the text are shown in **bold** typeface.

Chapter II

DESIGN CONTROLS AND CRITERIA

. . .

Running Speed

In design it is necessary to know actual vehicle speeds ~~for traffic en masse~~ to be expected on ~~highways~~ **roadways** of different design speeds and ~~various~~ volume conditions. Speed of operation is one measure of the service that a ~~highway~~ **roadway** renders, and it affords a means of evaluating road-user costs and benefits. **Of several speed measures available, running speed is the most appropriate for evaluating level of service and road-user costs.** The running speed is the speed of a vehicle over a specified section of ~~highway~~ **roadway**, being the distance traveled divided by the running time (the time the vehicle is in motion). **Similarly, the average running speed for all traffic or component of traffic is defined as the summation of distances traveled divided by the summation of running times.**

One means of obtaining an ~~equivalent~~ **estimate of the** average running speed on an existing facility where flow is reasonably continuous is to measure the spot speed. The average spot speed is the arithmetic mean of the speeds of all traffic **as measured** at a specified point. For short sections of ~~highway~~ **roadway** on which speed characteristics do not vary materially, the average spot speed may be considered as being ~~representative~~ **an approximation** of the average running speed. On longer stretches of ~~rural highway~~ **roadway**, spot speeds measured at several points, where each **point** represents the speed characteristics pertinent to a selected segment of ~~highway~~ **roadway**, may be averaged (taking relative lengths into account) to ~~represent~~ **provide a better approximation of** the average running speed.

~~Average spot speeds, which generally are indicative of average running speeds, have been measured over a period of years in many States on highway sections of favorable alinement. The average speed slowly increased over the years, then leveled out, and subsequently dropped with the advent of the 55-mph speed limit. Since then it has decreased very slightly on highways where the 55-mph speed limit is still in effect. On interstate highways with 105-km/h speed limits the increase has been greater.~~

~~Experience on horizontal curves shows that speeds are lower than those on tangent alinement and that the difference between average spot speed and calculated design speed on such curves becomes less as the radius of curvature decreases. In this regard, it is generally accepted that a greater proportion of drivers operate near or at the design speed on highways with low design speed than on highways with high design speed. It is also known that some sections of low-design-speed highways are frequently overdriven, with an appreciable number of drivers exceeding the design speed.~~

~~Observed speeds of free-moving vehicles on horizontal curves indicate that low-design-speed curves yield an average spot speed close to the design speed; on high-design-speed curves the average speed is substantially below the design speed and approaches the average spot speed found on long stretches of tangent alinement. Because horizontal curvature is the principal factor related to design speed on open sections of rural highways and average spot speed approximates the average running speed for such conditions, a useful relation between the highway design speed and the average running speed (for low volume conditions) may be established from these data. Comparing the observed average speeds with calculated design speeds, it is found that on sections having a 30-mph design speed, the average running speed is approximately 90 to 95 percent of the design speed.~~

~~The general relation between design speed and average running speed (the average for all traffic or component of traffic, being the summation of distances divided by the summation of running times; it is approximately equal to the average of the running speeds of all vehicles being considered) is illustrated in Figure II-19. The upper curve represents the conditions for low traffic volume as just described. As traffic volume increases on any highway, the average running speed decreases because of interference among vehicles. The curve labeled "Intermediate Volume" represents the relation between design speed and average running speed when the volume approximates the design service volume for rural highways. Should the volume exceed the intermediate level, the average running speed would be further lowered, and in the extreme case, where the volume is equal to the possible capacity of the highway, the speed of traffic is influenced more by congestion than by the design speed, especially where the design speed is above 50 mph. The relation between design speed and average running speed for very high traffic volumes is illustrated by the lower curve in Figure II-19. This curve is of academic interest only. It establishes a limiting condition for average running speeds but it is of little value in design. Highways should usually be designed to accommodate their traffic volumes without being subjected to the high degree of congestion represented by this curve.~~

It is desirable that the running speed of a large proportion of drivers be lower than the design speed. Experience indicates that deviations from this desired goal are most evident and problematic on sharper horizontal curves. In par-

ticular, curves with a low design speed (relative to driver expectation) are frequently overdriven and tend to have poor safety records. Therefore, it is important that the design speed used for horizontal curve design be a conservative reflection of the expected speed on the constructed facility.

For horizontal curve design, an appropriate design speed is considered equivalent to the expected (or anticipated) 95th percentile running speed of the passenger car traffic stream during low-volume conditions. Because the average spot speed is a more commonly measured speed statistic on curves than is running speed, it is useful to quantify the relationship between the 95th percentile and average spot speeds. The relationship between 95th percentile speed and average spot speed is illustrated in Figure II-19. This relationship is applicable to volumes ranging from low to intermediate because most speed-flow relationships indicate that speed is insensitive to volumes within this range.

~~A design that satisfies the requirements for average running speed at low volume is adequate for traffic using the highway when the volumes are higher and the speeds are lower. At low volumes, about 50 percent of all vehicles travel at speeds within 8 km/h of the average running speeds, as shown by the speed distribution curves in Figure II-18. For volumes in the intermediate range, about 90 percent of all vehicles travel at or less than the average running speed representative of low volumes. For this reason, low volumes control certain highway elements, such as lane and shoulder widths, treatment of intersection curves, and speed-change lanes.~~

Average running speed on a given ~~highway~~ **roadway** varies somewhat during the day, depending primarily on the volume of traffic. Therefore, when reference is made to running speed it should be clear whether this speed is for peak hours or off-peak hours or whether it is an average for the day. The first two are of concern in design and operation; the latter is of importance in economic analyses.

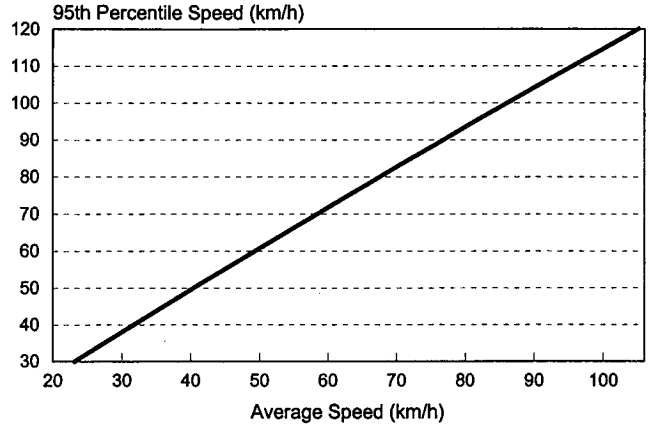

Figure II-19. Relationship between the average and 95th percentile speed for low- to intermediate-volume conditions.

. . .

CHAPTER III—ELEMENTS OF DESIGN

This section presents recommended revisions to the section in *Green Book* Chapter III that addresses horizontal alignment design. Specifically, the text presented in this section is a complete replacement for the section "Horizontal Alinement" in Chapter III. Some of the guidance provided in this section of the *Green Book* has been retained, but the recommended changes are sufficiently extensive that a complete rewriting of the text was considered the most efficient method of presenting the material.

In preparing the revised text, the presentation of topical material was reorganized. A new section emphasizing the concept of "curve design speed" was added, as were individual sections for each of the alternative transition design types (i.e., tangent-to-curve, spiral curve, and compound curve). A revised table of contents for this section and the revised text follow.

Chapter III

ELEMENTS OF DESIGN

. . .

Horizontal Alignment
- Theoretical Considerations
- General Considerations
  - Curve Design Speed
  - Facility Types
  - Superelevation
  - Side Friction Factor
  - Methods of Distributing Superelevation and Side Friction
- Curve Design Controls
  - Maximum Superelevation Rates
  - Maximum Design Side Friction Factors
  - Minimum Radius
  - Minimum Radius with Normal Cross Slope
- Design Superelevation Tables
  - Superelevation for Rural Highways and High-Speed Urban Streets
  - Superelevation for Low-Speed Urban Streets
  - Superelevation for Turning Roadways
  - Effects of Grade
- Expected Curve Speed
- Transition Design Controls
  - General Considerations
  - Tangent-to-Curve Transition
    - Minimum length of superelevation runoff
    - Minimum length of tangent runout
    - Location with respect to end of curve
    - Limiting superelevation rates
  - Spiral Curve Transition
    - Maximum radius for use of a spiral
    - Minimum length of spiral
    - Maximum length of spiral
    - Desirable length of spiral
    - Length of superelevation runoff
    - Limiting superelevation rates
    - Length of tangent runout
  - Compound Curve Transition
  - Methods of Attaining Superelevation
  - Design of Smooth Profiles for Traveled Way Edges
  - Axis of Rotation with a Median
  - Minimum Transition Grades
- Turning Roadway Design

. . .

Chapter III

ELEMENTS OF DESIGN

. . .

HORIZONTAL ALIGNMENT

Theoretical Considerations

For balance in roadway design all geometric elements should, as far as economically feasible, be determined to provide safe, continuous operation at a speed likely to be observed under the general conditions for that roadway. For the most part, this is done through the use of design speed as the overall control. In the design of roadway curves, it is necessary to establish the proper relation between design speed and curvature and also their joint relations with superelevation and side friction. Although these relations stem from the laws of mechanics, the actual values for use in design depend on practical limits and factors determined more or less empirically over the range of variables involved. These limits and factors are explained in the following paragraphs, as they would be used for the logical determination of controls for roadway curve design.

When a vehicle moves in a circular path, it undergoes a centripetal acceleration that acts toward the center of curvature. This acceleration is sustained by the vehicle mass component related to the roadway superelevation, the side friction developed between the tires and surface, or by a combination of the two. As a matter of conceptual convenience, centripetal acceleration is sometimes equated to centrifugal force. However, this force is an imaginary force that motorists believe is pushing them outward while cornering when, in fact, they are truly feeling the vehicle being accelerated in an inward direction. Centripetal acceleration is used hereafter because it is fundamentally correct.

From the laws of mechanics, the basic point mass (curve) formula for vehicle operation on a curve is the following:

$$\frac{0.01e+f}{1-0.01ef}=\frac{v^2}{gR}=\frac{0.0079V^2}{R}=\frac{V^2}{127R}$$

where:

e = rate of roadway superelevation, percent;
f = side friction (demand) factor;
v = vehicle speed, m/s;
g = gravitational constant, 9.807 m/s^2;
V = vehicle speed, km/h; and
R = radius of curve, m.

The value of the product "*ef*" in this equation is always small. As a result, the "*1 – 0.01 ef*" term is normally omitted in roadway design. Omission of this term yields the following basic side friction formula:

$$f=\frac{V^2}{127R}-0.001e$$

This equation yields slightly larger (and thus, more conservative) estimates of friction demand than would be obtained by the previous equation.

The side friction factor represents the driver's side friction need (or demand); it also represents the lateral acceleration a_f that acts on the vehicle. This acceleration can be computed as the product of the side friction demand factor f and the gravitational constant g (i.e., $a_f=fg$). It should be noted that the lateral acceleration experienced by the vehicle occupants tends to be slightly larger than that predicted by the product "*fg*" because of vehicle body roll.

From accumulated research and experience, maximum values of superelevation rate and side friction demand (i.e., e_{max} and f_{max}) have been established for curve design. Using these maximum values in the basic formula permits determination of a minimum curve radius. Use of curves with radii larger than this minimum calls for superelevation, side friction, or both to have values below their respective maximums. The amount that each factor is below its respective maximum is based on an equitable contribution of each toward sustaining the resultant centripetal acceleration. The methods used to achieve this equity for different design situations are discussed in the next section.

General Considerations

Curve Design Speed

Safe and efficient operations require harmony between the design speed and the observed distribution of traffic speeds. The design speed should equal or exceed the speed ultimately adopted by the large majority of drivers on the constructed facility.

Drivers tend to base their speed choice on the roadway environment as they perceive it. These environmental features are represented by the roadway's degree of access control, pavement surface roughness, urban or rural location, and the frequency of horizontal and vertical curves (especially those with sharper curvature). In general, drivers will adopt lower speeds on roadways with frequent access points, rough or uneven pavement surfaces, curbside parking, frequent curves, or hilly terrain. Selection of a design speed that is below that deemed appropriate by drivers should be avoided because it results in a significant percentage of vehicles exceeding the design speed **(18)**.

For horizontal curve design, an appropriate curve design speed is considered to be the expected 95th percentile speed of the passenger car traffic stream on the curve during low-volume conditions. Desirably, this curve design speed should equal the 95th percentile passenger car speed on the tangent approach to the curve. However, a recent study **(19)** indicates that a small speed reduction may be acceptable when conditions warrant the use of sharper curves. If a small speed reduction is allowed, then the curve design speed will be lower than the expected 95th percentile approach speed by the amount of the reduction.

Subsequent sections of this policy that address horizontal alignment design are based on the concept of "curve design speed." However, this speed may reflect an acceptable speed reduction on the curve. Therefore, to facilitate consistency with the controls for other design features, all curve design controls are referenced to the expected 95th percentile *approach* speed. The 95th percentile approach speed is assumed to closely represent the design speed used to size other elements of the roadway.

Unless explicitly noted otherwise, the expected 95th percentile approach speed is defined to represent a passenger car traffic stream during low-volume conditions. This speed is that expected (or anticipated) on the facility at any time during its design life. For major reconstruction projects, this speed may be measured directly. For new construction, it can be estimated using speed data for existing facilities in the vicinity of the proposed roadway that have a similar function and environment.

Facility Types

Horizontal curve design is influenced by the functional classification, movement type, and design speed of the associated roadway. For example, side friction demand is recognized to vary depending on whether the curve is on an open highway or an interchange ramp. Similar sensitivities to function and speed are recognized in the selection of a superelevation rate. In recognition of these influences, three facility types are defined to simplify the discussion of horizontal curve design controls:

1. All rural highways and high-speed urban streets,
2. Low-speed urban streets, and
3. Turning roadways.

The "speed" referred to in the facility-type names is the design speed. Facilities with a design speed of 70 km/h or less are referred to as low-speed facilities; those with a design speed of 80 km/h or greater are referred to as high-speed facilities.

Turning roadways are connecting roadways serving traffic turning between two intersecting through roadways. Turning roadways include exit terminals, central sections, and entrance terminals—all of which can include one or more curves. They can be further categorized as either interchange ramps or intersection curves. Interchange ramps have horizontal alignments that (1) have a loop or diamond configuration and (2) may include tangent sections, as needed, to minimize the right-of-way requirement. In contrast, intersection curves have alignments that have a diamond configuration and generally consist only of curves. Finally, turning roadways have design speeds of 20 km/h or greater and, at intersections, are associated with a channelizing island. In addition to this chapter, guidance related to these two categories of turning roadway is provided in Chapters IX and X.

Superelevation

There are practical upper limits to the rate of superelevation. These limits relate to considerations of climate, constructability, adjacent land use, and frequency of slow-moving vehicles. In recognition of these limits, all states have adopted one or more maximum superelevation rates. The maximum values used by most states include 4.0, 6.0, 8.0, 10, and 12 percent. A discussion of the aforementioned considerations and the rationale used to establish a particular rate as the maximum rate is provided in "Maximum Superelevation Rates."

Side Friction Factor

A primary objective in horizontal curve design is to have a curve design speed that equals or exceeds the expected speed of most motorists. This objective can be accomplished by providing a radius and superelevation rate that combine to yield a safe and comfortable lateral acceleration for a reasonably large percentage of drivers. The safety aspect is satisfied when the side friction factor used in design provides a significant margin of safety against slide or roll failure for both passenger cars and trucks. The comfort aspect is satisfied when lateral acceleration is less than a threshold value associated with motorist discomfort.

The comfort aspect is used herein to define the maximum side friction factors for design. This approach is conservative in that it inherently yields design side friction factors that also provide an adequate margin of safety against failure. "Margin of safety" is defined as the difference between side friction demand and side friction supply. Friction supply for slide failure is based on the tire-pavement friction properties. Friction supply for roll failure is a conceptual limit that reflects the friction coincident with vehicle rollover. This concept is useful for relative comparisons of the margin of safety for slide and roll failure. For design purposes, roll failure is considered only for trucks and other vehicles with a high center of gravity.

The maximum side friction factor for design represents an upper limit on the motorist's side friction demand. This limit coincides with the point at which the lateral acceleration is sufficient to cause the driver to experience a feeling of discomfort such that he or she reacts instinctively to avoid higher speed.

Two field study techniques have been used to determine maximum side friction factors for design based on comfort criteria. Both techniques measure curve speed and then use this speed in the basic side friction formula to compute a corresponding side friction demand. One study uses test subjects in controlled experiments. These subjects indicate when uncomfortable curve speeds are reached on a curve. A second study relies on the roadside observation of drivers traveling along a curve. For this study technique, the distribution of the observed speeds is used as a surrogate means of defining the side friction factor associated with discomfort. An upper percentile speed is assumed to represent the comfortable limit of lateral acceleration.

Both field study techniques have advantages and disadvantages. The first study type has the advantage of direct assessment of motorist comfort; however, its resource requirements can be significant. In contrast, the second study type has the advantages of minimal resource requirements and broad geometric coverage; however, there is less assurance that motorist comfort is being measured.

A modified form of the second study type was proposed by Haile (**20**). His modification was intended to improve the likelihood that the speeds recorded are representative of motorists at their comfort limits. He suggested that only those drivers who reduce speed during curve entry be recorded. He argued that those drivers who do not reduce speed are likely traveling below the speed they would consider to be the maximum comfortable or safe for the curve. Hence, these drivers would likely convey no information regarding the maximum side friction factor based on comfort criteria.

A recent NCHRP study (**19**) examined the relationship between side friction demand and speed for a wide range of curves located on streets, highways, and turning roadways. This study re-examined previously published findings on this topic and analyzed new data collected at numerous horizontal curves. The approach suggested by Haile (**20**) was adopted during the data reduction process. In addition, speeds of both cars and trucks were measured and analyzed separately to assess the side friction demands of both vehicle types. For each vehicle type and study site, the 95th percentile speed was used to compute a corresponding 95^{th} percentile side friction demand.

The study found that side friction demand is dependent on the speed to which the driver slowed when entering the curve. Those drivers slowing significantly experienced larger side friction demand. Figure III-4 illustrates the threshold friction factors below which no speed reduction was observed. This figure also illustrates the friction factors found when drivers slowed 5 km/h. Finally, the thick trend line represents the side friction factors recommended in the NCHRP study (**19**) for design applications.

The side friction demand factors associated with the thick line in Figure III-4 are generally consistent with the side friction factors reported in the literature and in previous editions of this policy. It should be noted that these factors are representative of both passenger cars and trucks.

Figure III-4 also illustrates conservative values of maximum side friction supply for both passenger cars and trucks. Slightly lower values may be realized for steep downgrades because some of the friction supply is used for deceleration purposes (**19**). The vertical distance between the friction demand and supply trend lines reflects the margin of safety for a given design speed. In general, the margin of safety for both cars and trucks is relatively constant over the range of speeds. Although, it should be noted that the margin of safety available to trucks is less than one-half that available to cars.

Methods of Distributing Superelevation and Side Friction

In general, a range of radii are available for use at each alignment deflection. The minimum radius available is based on the use of maximum values of superelevation rate and side friction demand (i.e., e_{max} and f_{max}). Radii larger than this minimum generally require a superelevation rate, side friction, or both that are below their respective maximums. This section describes

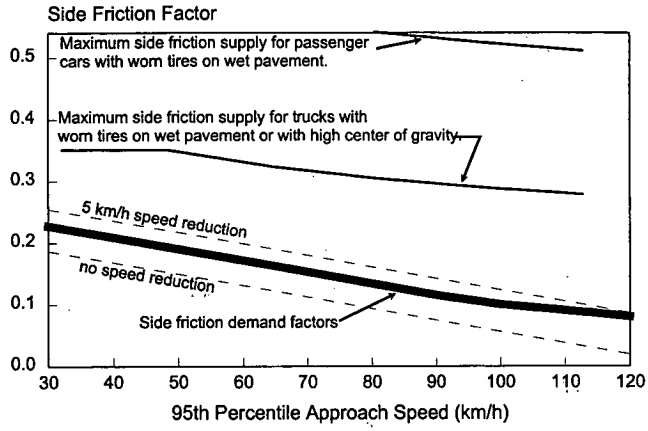

Figure III-4. Comparison of side friction supply and demand factors.

alternative methods for defining the proportion of superelevation and side friction appropriate for a given curve radius, curve speed, and facility type.

Historically, several methods have been used to define or distribute the proportions of superelevation and side friction over the range of curve radii. These methods are generally described using curvature (= $1/R$), as opposed to radius, for the independent variable. This approach stems from the simple, linear relationship that exists between superelevation rate (or side friction demand) and curvature, as indicated in the basic side friction formula.

Distribution methods used can be generally described as belonging to one of two basic categories. One category emphasizes the generous use of superelevation; the other emphasizes the conservative use of superelevation. Both of these fundamental distribution methods are shown in Figure III-5. They are described in more detail in the next few paragraphs.

The distribution method based on the generous use of superelevation is generally used for rural highways and high-speed urban streets. This method implies that superelevation will be used to counteract much of the centripetal acceleration. With this method, superelevation is provided over the full range of curvature at an amount sufficient to fully meet the centripetal acceleration needs of slower drivers and most of the needs of faster drivers. In this manner, faster drivers would only have to rely on a minimum amount of side friction. The advantage of this method is that it minimizes reliance on side friction and thereby, provides an added degree of safety against slide or roll failure. The emphasis on the needs of slower drivers reflects a desire to avoid negative side friction. Negative side friction requires the driver to steer against the direction of the curve which is unnatural and may lead to erratic driving.

The distribution method based on the conservative use of superelevation is generally used for low-speed urban streets. This method implies that side friction is used to counteract most, if not all, of the centripetal acceleration. With this method, superelevation is only provided on the sharpest curves when the side friction demand of the faster drivers equals the maximum level

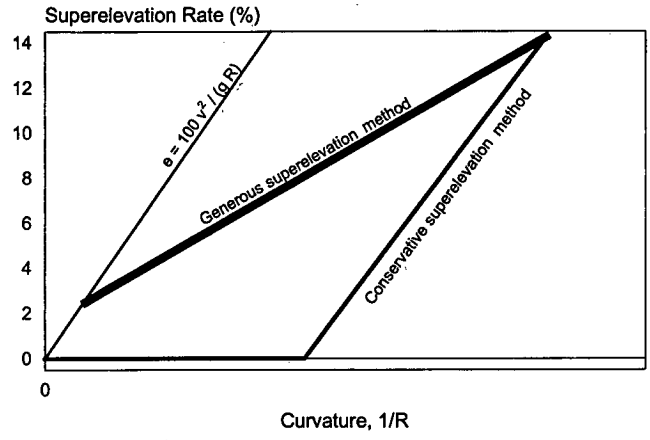

Figure III-5. Methods of distributing superelevation and side friction.

considered acceptable for design. In this manner, the side friction demand of slower drivers is lower than the design maximum. The advantage of this method is that it generally allows the designer to avoid superelevation when conditions justify its limited use.

The conditions that justify the conservative use of superelevation relate to (1) drainage, (2) access, (3) terminal transition, and (4) slow speed. Drainage conditions may limit the use of superelevation when the earthwork associated with the superelevated cross section creates some type of impediment to runoff from properties adjacent to the roadway. Access conditions may limit the use of superelevation when such superelevation results in large grade breaks when transitioning to or from the alignment of an intersecting road or driveway. Large grade breaks can be uncomfortable to side street drivers when crossed at moderate speed and can pose a safety risk if crossed at slow speeds. Terminal transition conditions may limit the use of superelevation at short turning roadway terminals when such superelevation makes it difficult to safely transition to or from the alignment of the through roadway without excessive pavement surface warping. This warping along the cross over crown line may compromise the stability of large trucks and make vehicle control difficult. Finally, exceptionally slow curve speed conditions may limit the use of superelevation when such speeds are so slow as to precipitate negative side friction. These slow speeds may be caused by traffic congestion, frequent access points, or traffic control devices (i.e., signals or signs).

By definition, the two distribution methods represent extreme applications of either superelevation or side friction. Superelevation rates between these extremes (as represented by the region between the thick trend lines in Figure III-5) are likely to provide acceptable levels of side friction for all drivers. On the other hand, these levels many not provide the advantages noted previously for the two methods.

Superelevation rates obtained from either distribution method (and values in between) have been used for turning roadways. In general, the first distribution method offers definite safety benefits because of its generous use of superelevation while maintaining a sensitivity to the friction demands of both slow and fast drivers. However, the second distribution method is more appropriate when any one of the four previously mentioned conditions justifying the conservative use superelevation apply. Thus, the first distribution method is considered preferable for application to turning roadways. However, the second method is acceptable for low-speed turning roadways when drainage, terminal transition, or slow-speed conditions are evident.

Curve Design Controls

This section describes several design controls that can be used to size selected curve design elements. These controls include the maximum superelevation rate, the maximum design side friction factor, minimum radius (with maximum superelevation), and the minimum radius with normal cross slope.

Maximum Superelevation Rates

The maximum rates of superelevation usable on horizontal curves are controlled by four factors: (1) climate conditions, (2) constructability; (3) adjacent land use (i.e., as they relate to drainage and access), and (4) frequency of very slow-moving vehicles. With regard to factors 1 and 3, the range of conditions likely to be encountered within the United States leads to the conclusion that no single maximum superelevation rate is applicable to all roadway curves on a nationwide basis. However, using only one maximum superelevation rate within a region of similar climate and land use should be considered desirable because such a practice would promote design consistency.

Design consistency relates to the uniformity of the highway alignment and its associated design element dimensions. This uniformity allows drivers to improve their perception-response skills by developing expectancies. Design elements that are not uniformly sized for similar types of roadways will be counter to a driver's expectancy and result in an increase in driver workload. Logically, there is an inherent relationship between design consistency, driver workload, and motorist safety with "consistent" designs being associated with lower workloads and safer roadways.

A superelevation rate of 12 percent represents a maximum practical value where snow and ice do not exist. Current practice indicates that rates in excess of 12 percent are beyond practical limits with regard to difficulties associated with construction and maintenance of steep cross slopes.

Where snow and ice are factors, experience indicates that a superelevation rate of 8 percent is a logical maximum. A rate of 8 percent or less will minimize the potential for a vehicle to slip across an ice-covered highway when stopped or attempting to slowly gain momentum from a stopped position. This conclusion is consistent with the findings from a study that reported friction values measured on roadways covered with ice, snow, or both **(21)**. It should also be noted that some agencies believe that 8 percent represents a logical maximum rate, regardless of snow or ice conditions. Such a limit tends to reduce the likelihood that slow drivers will experience negative side friction, which can result in excessive steering effort and erratic driving.

Conditions in urban areas often require the use of a low maximum rate of superelevation, usually 4 to 6 percent. In these areas, traffic congestion, traffic control, or extensive marginal development act to create slow speeds that can result in negative side friction. In addition, a low maximum rate of superelevation is desirable in urban areas because it minimizes the adverse impact of the roadway on adjacent property access and drainage.

A superelevation rate of 10 percent represents a practical maximum value for low-speed turning roadways when other factors do not dictate the use of a lower rate. This maximum recognizes the practical difficulty of attaining superelevation without creating an abrupt cross-slope change at the turning roadway terminal, primarily because of sharp curvature and short lengths of turning roadway.

In summary, it may be concluded that (1) several rates, rather than a single rate, of maximum superelevation should be recognized for design controls for highway curves, (2) one maximum rate should be used in areas of similar climate and land use, (3) a rate of 12 percent should not be exceeded, (4) a rate of 8 percent should not be exceeded in areas with frequent ice or snow, (5) a maximum rate of 4 to 6 percent is applicable to urban areas, and (6) a maximum rate of 10 percent is applicable to low-speed turning roadways. Accordingly, five maximum superelevation rates—4, 6, 8, 10, and 12 percent—are used herein.

Maximum Design Side Friction Factors

The maximum side friction demand factors recommended for design are listed in Table III-6. These factors are intended for use in the design of all facility types. Hereafter, these factors are referred to as the "maximum design side friction factors" to denote they represent maximum values for design applications.

Field observations indicate that the maximum design side friction factors listed in Table III-6 are associated with a small speed reduction (**19**). Observation of speeds on street and highway curves suggest the speed reductions range from 3 to 5 km/h. Similar levels of side friction demand were also observed on turning roadways; however, the observed speed reduction ranged from 6 to 10 km/h. This larger speed reduction is logical because drivers on turning roadways anticipate sharp curves and accept such reductions as they transition between intersecting roadways.

Minimum Radius

The minimum radius is a limiting value of curvature that is associated with a side friction demand equal to the design maximum when the curve has maximum superelevation and is traveled at the curve design speed. Use of sharper curvature would call for superelevation beyond the limit considered practical, side friction beyond what is considered comfortable by many drivers, or both. Thus, the minimum radius is a significant control in horizontal alignment design.

The minimum radius R_{min} can be calculated directly from the basic side friction formula described previously. In fact, this formula can be restructured to yield the following equation for calculating the minimum radius:

$$R_{min} = \frac{V_c^2}{127(0.01e_{max} + f_{max})}$$

Design Speed (km/h)	Maximum Design Side Friction Factor, f_{max}
30	0.227
40	0.209
50	0.190
60	0.171
70	0.153
80	0.134
90	0.115
100	0.100
110	0.090
120	0.080

Table III-6. Maximum design side friction factors.

where:

R_{min} = minimum radius, m;
V_c = curve design speed, km/h;
e_{max} = maximum superelevation rate, percent; and
f_{max} = maximum design side friction factor (from Table III-6).

Minimum radii for each combination of design speed, maximum design side friction factor, and maximum superelevation rate are listed in Table III-7.

The curve design speed listed in Table III-7 is equal to the roadway design speed less an acceptable speed reduction. The speed reductions listed in this table correspond to values observed on sharper curves (**19**). Larger reductions will likely result if curve radii smaller than those listed are used. Experience indicates that the speed reductions listed in Table III-7 represent a reasonable compromise between the designers' occasional need to use sharp radius curves and their desire to maintain a consistent design speed along the roadway.

It is useful to note that the radii referred to in this section have different reference locations, depending on the facility type. Curve radius is generally referenced to the centerline of a street or highway. On the other hand, the reference location is commonly moved to the inner edge of the traveled way for a turning roadway.

Minimum Radius for Section with Normal Cross Slope

In general, flat horizontal curves require no superelevation. Traffic entering a flat curve to the right has some superelevation because of the normal cross slope. As a result, the side friction demand is negligible. In contrast, traffic entering a flat curve to the left has an adverse or negative superelevation because of the normal cross slope. As a result, the side friction required to counteract both the centripetal acceleration and the negative superelevation is not necessarily negligible, but it is within an acceptable range.

For a given design speed, a minimum radius can be associated with a combined maximum desirable side friction demand and adverse cross slope. The radius associated with this limiting condition is defined as the minimum radius for which the normal cross slope yields an acceptable level of lateral acceleration. Hereafter, this radius is referred to as the "minimum radius with normal cross slope." Curves with radii sharper than this minimum value should use superelevation to counter some of the centripetal acceleration.

The basic side friction formula can be modified to develop an equation for computing the minimum radius with normal cross slope. The resulting equation is as follows:

$$R_{NC} = \frac{V_c^2}{127(0.01e_{NC} + f_{NC})}$$

where:

R_{NC} = minimum radius with normal cross slope, m;
e_{NC} = normal cross slope rate (−2.0 percent assumed), percent; and
f_{NC} = maximum side friction demand with adverse cross slope.

Design Speed (km/h)	Assumed Speed Reduction (km/h)	Curve Design Speed (km/h)	Minimum Radius (m), R_{min}				
			Max. Superelevation Rate, e_{max} (%)				
			4	6	8	10	12
30	3.00	27	21	20	19	18	17
40	3.00	37	43	40	37	35	33
50	3.00	47	76	70	64	60	56
60	3.00	57	121	111	102	94	88
70	3.00	67	183	166	152	140	129
80	3.00	77	268	241	218	200	184
90	3.00	87	385	341	306	277	254
100	3.25	96.75	526	461	409	369	335
110	3.90	106.10	682	591	521	467	422
120	4.55	115.45	875	750	656	583	525

Table III-7. Minimum radius with maximum superelevation and side friction.

As the terms in this equation indicate, the minimum radius with normal cross slope is dependent on the normal cross slope rate and the maximum friction with adverse cross slope. The normal cross slope rate is expressed as a negative value in this equation because it is in an adverse direction relative to the more critical, left-hand curve direction.

The normal cross slope is generally determined by drainage requirements. The usually accepted minimum values range from 1.5 to 2.0 percent. Additional information is available on this topic in Chapter IV. For the purpose of defining the minimum radius with normal cross slope, a value of 2.0 percent is used herein as a single representative value.

The maximum side friction to be used in the preceding equation is dependent on the method used to distribute superelevation and side friction. Specifically, a method which emphasizes the generous use of superelevation should limit the level of adverse side friction to a relatively small value. As noted in "Methods of Distributing Superelevation and Side Friction," this type of method is appropriate for rural highway and high-speed urban street design. A review of current practice indicates that a value of f_{NC} equal to 0.04 is consistent with the objectives of this distribution method.

In contrast to the conclusion reached in the preceding paragraph, a distribution method that emphasizes the conservative use of superelevation implies that a large amount of side friction is accepted by the driver. When this method is applied to low-speed urban streets, it is assumed that superelevation will only be provided when the side friction demand would otherwise exceed the maximum design side friction factor. Thus, for low-speed urban streets, the minimum radius with normal cross slope is based on f_{NC} being equal to the maximum design side friction factor f_{max} (shown in Table III-6).

Based on the preceding discussion, the minimum radii available for use with normal cross slope are listed in Table III-8. The speed reductions shown in this table are expected amounts based on the corresponding maximum side friction demand factor f_{NC}. For rural highways and high-speed urban streets, this factor is sufficiently small as to result in no speed reduction except for the highest approach speeds. In contrast, the large amount of side friction used to define minimum radii for low-speed urban streets will likely result in a 3.0 km/h speed reduction. In general, larger speed reductions will occur if smaller radii are used with a normal cross slope.

Design Superelevation Tables

This section describes the superelevation rates and corresponding radii recommended for horizontal curve design. These rates and radii are based on the distribution methods described in "Methods of Distributing Superelevation and Side Friction." Specifically, values for rural highways and high-speed urban streets are based on the generous use of superelevation. In contrast, values for low-speed urban streets are based on the conservative use of superelevation. The rates and radii for rural highways and high-speed urban streets are preferable for use on turning roadways; however, the values recommended for low-speed urban streets are acceptable for low-speed turning roadways when conditions justify their use (see "Methods of Distributing Superelevation and Side Friction").

Design Speed (km/h)	Rural Highways and High-Speed Urban Streets			Low-Speed Urban Streets		
	Assumed Speed Reduction[1] (km/h)	Curve Design Speed (km/h)	Minimum Radius[2] R_{NC} (m)	Assumed Speed Reduction[1] (km/h)	Curve Design Speed (km/h)	Minimum Radius[2] R_{NC} (m)
30	0.00	30	354	3.00	27	28
40	0.00	40	630	3.00	37	57
50	0.00	50	984	3.00	47	102
60	0.00	60	1,417	3.00	57	169
70	0.00	70	1,929	3.00	67	266
80	0.00	80	2,520	--	--	--
90	0.00	90	3,189	--	--	--
100	0.00	100	3,937	--	--	--
110	0.20	109.80	4,746	--	--	--
120	1.58	118.42	5,521	--	--	--

[1] Expected speed reduction for the associated maximum side friction demand factor f_{NC} based on the trends shown in Figure III-4.

[2] Normal cross slope is assumed to equal -2.0 percent.

Table III-8. Minimum radius for section with normal cross slope.

Superelevation for Rural Highways and High-Speed Urban Streets

The method used to define superelevation rates and corresponding radii for rural highways and high-speed urban streets is based on the generous use of superelevation. However, excessive superelevation can result in negative side friction for slower drivers. Thus, this method is developed to yield superelevation rates that are generous for the corresponding radius range but not so generous as to produce negative side friction for a large majority of drivers.

Consistent with the use of an upper percentile speed to define curve design speed, a lower percentile speed is appropriate for defining the side friction needs of slower drivers. The 5th percentile speed is a logical cutoff value because it is consistent in coverage with 95th percentile speed used for other curve design controls. The 5th percentile speed of the truck traffic stream is the most appropriate control in this instance because truck speeds tend to be slightly lower than those of passenger cars.

Previous editions of this policy used a distribution method that provided for the generous application of superelevation. However, this method provided separate distributions for each of the five possible maximum superelevation rates. As a consequence, as many as five different superelevation rates were available to the designer for a given design speed. A recent survey of 138 highway curves found that this flexibility has resulted in there being little correlation between radius, superelevation rate, and curve design speed (**18**). This lack of uniformity complicates the driving task and is contrary to the goal of design consistency.

Based on the preceding discussion, the superelevation distribution method described in this section was developed to provide a unique radius and superelevation rate combination for each curve design speed. The following equations were used in calculating the design superelevation rate for a given speed and radius:

$$e_d = e^*_{max}\left(\frac{R^*_{min}}{R}\right)^n \quad (1)$$

with

$$n_e = \frac{\ln(-0.01e_{NC}) - \ln(0.01e^*_{max})}{\ln(R^*_{min}) - \ln(R_{NC})} \quad (2)$$

where:

e_d = design superelevation rate, percent;
e^*_{max} = defining maximum superelevation rate, percent;
R^*_{min} = defining minimum radius, m;
n = shape factor;
R = radius of curve, m;
R_{NC} = minimum radius with normal cross slope, m;
$\ln(x)$ = natural log of x; and
e_{NC} = normal cross slope rate (–2.0 percent assumed), percent.

Two fundamental variables in Equations 1 and 2 are the "defining" maximum superelevation rate and the "defining" minimum radius. These two variables represent the one combination of rate and radius that is common to both distribution methods (i.e., it is the point of intersection of the dashed and thick trend lines in Figure III-5). Sharper radii are not feasible because they would require either friction demand in excess of f_{max} or superelevation sufficiently large as to cause slower drivers to incur a negative side friction. These two variables can be computed as follows:

$$e^*_{max} = 100\frac{r_v f_{max} + 0.015}{1 - r_v} \quad (3)$$

and

$$R^*_{min} = \frac{V_c^2}{127(0.01e^*_{max} + f_{max})} \quad (4)$$

with

$$r_v = \frac{(V_{5,tk} - dv_{5,tk})^2}{V_c^2} \quad (5)$$

$$V_{5,tk} = 0.3256V^{1.167} \quad (6)$$

$$dv_{5,tk} = 0.763dv \quad (7)$$

where:

f_{max} = maximum design side friction factor (from Table III-6);
V_c = curve design speed (= $V - dv$), km/h;
V = design speed, km/h;
dv = assumed speed reduction, km/h (from Table III-7);
$V_{5,tk}$ = 5th percentile truck approach speed, km/h;
$dv_{5,tk}$ = 5th percentile truck speed reduction, km/h; and
r_v = ratio of truck to passenger car curve speeds.

Equation 1 satisfies two logical boundary conditions. First, it predicts a design superelevation rate equal to e^*_{max} when the curve radius equals R^*_{min}. Second, it predicts a design superelevation rate equal to the normal cross slope rate when the curve radius equals R_{NC}. Equations 6 and 7 are regression relationships based on extensive measurements of car and truck speeds on horizontal curves (**19**).

Equations 3 through 7 were used to develop the defining maximum superelevation rate and minimum radius for a range of design speeds. These defining values are listed in Table III-9.

Because the defining maximum superelevation rates listed in Table III-9 are typically larger than 12 percent, an agency's maximum superelevation rate must be "imposed" on the distribution represented by Equation 1. If Equation 1 yields a superelevation rate larger than the agency's recognized maximum superelevation rate, then the recognized maximum rate should be used instead of that obtained from Equation 1.

The values of the shape factor n are also shown in Table III-9. This factor introduces curvature into the distribution function (i.e., Equation 1). The factor is computed using Equation 2. This equation is derived to yield the aforementioned boundary conditions. The factors obtained from Equation 2 range from 0.589 to 0.759 for design speeds ranging from 30 to 120 km/h. Because these values are all less than 1.0, the distribution curve has a concave shape that emphasizes superelevation over side friction.

The distribution of superelevation rates for a range of curvatures is shown in Figure III-6. The trend shown coincides with a design speed of 70 km/h; similar trends result for other speeds.

The distribution shown in Figure III-6 is "stair-stepped" to illustrate the range of feasible radii for integer superelevation rates. Experience indicates that superelevation rates based on integer values are acceptable from the standpoint of traffic operations and consistency with construction tolerances. With regard to traffic operations, superelevation rates differing by less than 1 percent are not likely to have a significant effect on driver speed.

The design superelevation rates presented later in this section are based on integer superelevation rates (e.g., 3, 4, 5 percent) and a corresponding range of radii. Values at each stair "corner" represent the application of Equation 1 to compute the radius R twice; once using $e_d - 0.5\%$ and then again using $e_d + 0.5\%$. This approach corresponds to a superelevation rate of precision of ±0.5 percent.

Design Speed (km/h)	Assumed Speed Reduction (km/h)	Curve Design Speed (km/h)	Defining Maximum e, e^*_{max} (%)	Defining Minimum R, R^*_{min} (m)	Shape Factor, n
30	3.00	27	12.2	16.4	0.589
40	3.00	37	13.5	31.4	0.635
50	3.00	47	14.1	52.5	0.667
60	3.00	57	14.3	81.4	0.689
70	3.00	67	14.3	119.5	0.707
80	3.00	77	13.9	171.2	0.720
90	3.00	87	13.2	241.6	0.730
100	3.25	96.75	12.6	326.4	0.739
110	3.90	106.10	12.3	416.2	0.746
120	4.55	115.45	11.9	527.7	0.759

Table III-9. Defining maximum superelevation rate and minimum radius.

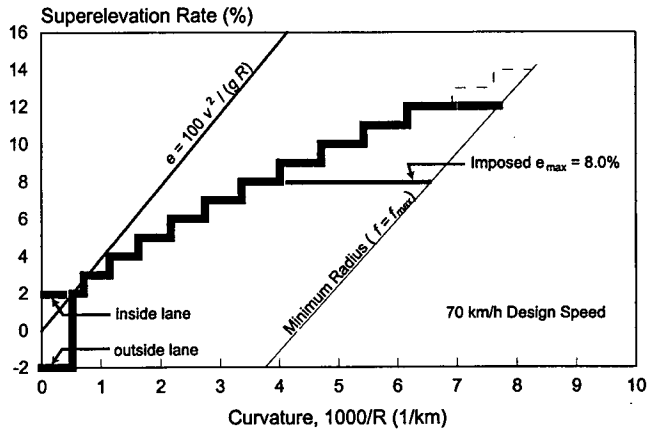

Figure III-6. Superelevation distribution method for rural highways and high-speed urban streets.

There is one exception to the general use of integer superelevation rates. For higher speeds, the precision is reduced to ±0.25 percent such that superelevation rates of 2.5, 3.5, 4.5, 5.5, and 6.5 percent may also be used. This modification ensures unique radius and superelevation combinations for these higher speeds. For example, if 2.5 percent were not used to define a range of radii for 90 km/h, the resulting radius ranges for integer rates of 2 and 3 percent would overlap with those for 80 and 100 km/h speeds. As discussed previously, unique combinations of rate and radius are desirable because they promote design consistency.

The maximum superelevation rate established by an agency (based on practical considerations) should be imposed on the distribution represented by Equation 1. Figure III-6 illustrates the imposition of an 8.0 percent agency-established maximum superelevation rate on the distribution for 70 km/h. By this imposition, the agency disregards superelevation rates predicted by Equation 1 that exceed 8.0 percent (i.e., it disregards the stair-steps in Figure III-6 greater than 8.0 percent). Instead, the agency uses 8.0 percent superelevation for radii in the range of 152 to 249 m (i.e., 6.6 to 4.0 km^{-1}). The two extreme values in this range correspond to the end points of the line labeled "Imposed e_{max} = 8.0%" in Figure III-6. It should be noted that radii in this range are associated with a small (i.e., less than 5 km/h) speed reduction.

In summary, the superelevation distribution is represented by the stair-stepped line for rates up to the recognized maximum rate (i.e., 4.0, 6.0, 8.0, 10, or 12 percent). Thereafter, the recognized maximum rate is used for a range of sharper radii, the sharpest of which is represented by the minimum radius R_{min}.

Tables III-10 and III-11 show the recommended range of radii associated with specific design superelevation rates. Table III-10 presents superelevation rate and radius combinations for high-speed streets and highways. Table III-11 presents similar combinations for low-speed rural highways. As indicated in the previous paragraphs, the radius ranges in each table are intended to yield the desired unique relationship between speed, radius, and rate. The only exception is for the lowest superelevation rates and highest speeds; however, the degree of range overlap for these conditions is minimal.

To illustrate the use of Table III-10, consider a highway with a design speed of 110 km/h and an agency-recognized, maximum superelevation rate of 6.0 percent. If a radius of 2,000 m is being used by the designer, Table III-10 indicates that the design radius lies in the range of 1,727 to 2,043 m, which corresponds to a superelevation rate of 4.0 percent. However, if a radius of 900 m is needed, then the design superelevation rate will be limited to the 6.0 percent maximum rate. Because this value is smaller than the desirable minimum radius of 1,030 m, a small speed reduction will likely be incurred by motorists. The minimum acceptable radius that could be considered for this design is 591 m; this radius would correspond to a speed reduction of 3.9 km/h (as indicated in Table III-7).

As mentioned previously, radii between the desirable minimum and minimum values are likely to result in a small speed reduction. In general, such speed reductions (and corresponding radii) should be avoided whenever possible to promote uniform traffic speeds. On downgrades, such avoidance is particularly important because the braking required for speed reduction consumes some of the available friction supply. While such braking consumes only a small portion of the friction supply for passenger cars, it can consume a significant portion of the supply for trucks. Therefore, on roadways with significant truck volume and a downgrade in excess of 5 percent, it is suggested that the curve radius be selected such that it equals or exceeds the desirable minimum value.

Super-elev. Rate e_d (%)	Design Speed (km/h)														
	80			90			100			110			120		
	Range of Design Radii (m)														
	Max. R	Des. Min.	Min. R	Max. R	Des. Min.	Min. R	Max. R	Des. Min.	Min. R	Max. R	Des. Min.	Min. R	Max. R	Des. Min.	Min. R
NC	tan.	2,520	--	tan.	3,189	--	tan.	3,937	--	tan.	4,746	--	tan.	5,521	--
2	2,520	2,139	--	3,189	2,714	--	3,937	3,356	--	4,746	4,053	--	5,521	4,727	--
2.5	2,139	1,619	--	2,714	2,062	--	3,356	2,557	--	4,053	3,097	--	4,727	3,628	--
3	1,619	1,283	--	2,062	1,640	--	2,557	2,039	--	3,097	2,475	--	3,628	2,911	--
3.5	1,283	1,052	--	1,640	1,348	--	2,039	1,680	--	2,475	2,043	--	2,911	2,411	--
4	1,052	884	268	1,348	1,136	385	1,680	1,418	526	2,043	1,727	682	2,411	2,044	875
4.5	884	757	--	1,136	975	--	1,418	1,219	--	1,727	1,488	--	2,044	1,765	--
5	757	618	--	975	798	--	1,219	1,065	--	1,488	1,301	--	1,765	1,547	--
5.5	--	--	--	--	--	--	1,065	941	--	1,301	1,151	--	1,547	1,372	--
6	618	490	241	798	635	341	941	797	461	1,151	1,030	591	1,372	1,230	750
6.5	--	--	--	--	--	--	--	--	--	1,030	929	--	1,230	1,111	--
7	490	402	--	635	522	--	797	657	--	929	806	--	1,111	967	--
8	402	337	218	522	440	306	657	554	409	806	682	521	967	820	656
9	337	289	--	440	377	--	554	477	--	682	587	--	820	708	--
10	289	251	200	377	329	277	477	416	369	587	513	467	708	620	583
11	251	222	--	329	290	--	416	368	--	513	454	--	620	550	--
12	222	197	184	290	259	254	368	335	335	454	422	422	550	525	525

Notes:
1. "Max. R": maximum radius, "Des. Min.": desirable minimum radius; "Min. R": minimum radius (with maximum superelevation); "NC": normal cross slope; "tan.": tangent section; " -- ": minimum radius not available.
2. Radii between the desirable minimum and the minimum should only be used with the maximum superelevation rate. It is preferable that this range be avoided when the alignment grade exceeds 5.0 percent and truck volumes are significant.
3. Design speeds for high-speed urban streets should be limited to 80, 90, or 100 km/h.
4. All superelevation rate and radii combinations in this table represent preferable values for turning roadways.

Table III-10. Superelevation distribution table for high-speed streets and highways.

Superelevation for Low-Speed Urban Streets

The method used to define superelevation rates for low-speed urban streets is based on the conservative use of superelevation. With this method, side friction is used to counter centripetal acceleration on all but the sharpest curves. On sharp curves, superelevation is provided in the amount needed to maintain side friction demand at the maximum acceptable level for design. The advantage of this method is that it minimizes the need for superelevation and the adverse impact it can have on adjacent property access and drainage.

As with high-speed urban streets, the 95th percentile passenger car speed is appropriate for defining the design speed for low-speed urban streets. The 95th percentile speed yields a conservative estimate of the superelevation needed by all but the fastest drivers. In addition, the passenger car is the controlling vehicle type because passenger car drivers tend to travel at higher speeds than truck drivers on moderate to sharp curves.

The following equation is used to calculate the recommended design superelevation rate for curves on low-speed urban streets:

$$e_d = 100\left(\frac{V_c^2}{127R} - f_{max}\right) \quad (8)$$

where:

e_d = design superelevation rate, percent;
R = radius of curve, m;

Super-elev. Rate e_d (%)	Design Speed (km/h)														
	30			40			50			60			70		
	Range of Design Radii (m)														
	Max. R	Des. Min.	Min. R	Max. R	Des. Min.	Min. R	Max. R	Des. Min.	Min. R	Max. R	Des. Min.	Min. R	Max. R	Des. Min.	Min. R
NC	tan.	354	--	tan.	630	--	tan.	984	--	tan.	1,417	--	tan.	1,929	--
2	354	243	--	630	443	--	984	704	--	1,417	1,025	--	1,929	1,406	--
3	234	137	--	443	261	--	704	425	--	1,025	629	--	1,406	873	--
4	137	89	21	261	176	43	425	291	76	629	437	121	873	612	183
5	89	64	--	176	128	--	291	216	--	437	326	--	612	460	--
6	64	48	20	128	98	40	216	168	70	326	256	111	460	363	166
7	48	37	--	98	79	--	168	135	--	256	208	--	363	297	--
8	37	30	19	79	64	37	135	112	64	208	173	102	297	249	152
9	30	25	--	64	54	--	112	95	--	173	148	--	249	212	--
10	25	21	18	54	46	35	95	82	60	148	128	94	212	184	140
11	21	18	--	46	40	--	82	71	--	128	112	--	184	162	--
12	18	17	17	40	35	33	71	63	56	112	99	88	162	144	129

Notes:
1. "Max. R": maximum radius, "Des. Min.": desirable minimum radius; "Min. R": minimum radius (with maximum superelevation); "NC": normal cross slope; "tan.": tangent section; " -- ": minimum radius not available.
2. Radii between the desirable minimum and the minimum should only be used with the maximum superelevation rate. It is preferable that this range be avoided when the alignment grade exceeds 5.0 percent and truck volume is significant.
3. When used with the tangent-to-curve transition design, the underlined radii and corresponding superelevation rates may cause turning vehicles to drift laterally to the extent that they may encroach into an adjacent lane or shoulder.
4. All superelevation rate and radii combinations in this table represent preferable values for turning roadways.
5. A rate of 4, 6, 8, or10 percent is considered to be the desirable maximum superelevation rate for low-speed turning roadways.

Table III-11. Superelevation distribution table for low-speed rural highways.

V_c = curve design speed, km/h; and
f_{max} = maximum design side friction factor (from Table III-6).

The distribution of superelevation rates for a range of curvatures is shown in Figure III-7. The trend shown coincides with a design speed of 70 km/h; similar trends result for other speeds.

The distribution is shown in Figure III-7 as being stair-stepped to illustrate the range of feasible radii for integer superelevation rates. As discussed in the preceding section, experience indicates that superelevation rates based on integer values are generally acceptable from the standpoint of traffic operations and consistency with construction tolerances. It should be noted that the stair-steps are positioned such that no one rate and radius combination yields a side friction demand that exceeds the maximum design side friction factor.

As with the distribution for rural highways and high-speed urban streets, the maximum superelevation rates recognized by an agency can be imposed on the distribution for low-speed urban streets. In this manner, the radius corresponding to the maximum superelevation rate represents the minimum radius; smaller radii or larger superelevation rates are not considered. It should be noted that superelevation rates obtained from this distribution are associated with a small (i.e., 3 km/h) speed reduction (see Table III-7).

Table III-12 shows the recommended range of radii associated with specific design superelevation rates. The use of this table follows that of Tables III-10 and III-11. In general, the radii in the columns labeled "Maximum" and "Desirable Minimum" define the range of desirable radii for a given design speed and superelevation rate. By definition, the desirable minimum and minimum radii are equal; however, both values are listed in the table for consistency with Tables III-10 and III-11.

Superelevation rates and radii shown in Table III-12 are applicable to facilities that require the conservative use of superelevation. As described previously in "Methods of Distributing Superelevation and Side Friction," there are several conditions that justify the conservative use of superelevation. These conditions include adjacent property drainage, adjacent property access, and frequent slow-moving vehicles. Because such considerations are frequently important in urban design, Table III-12

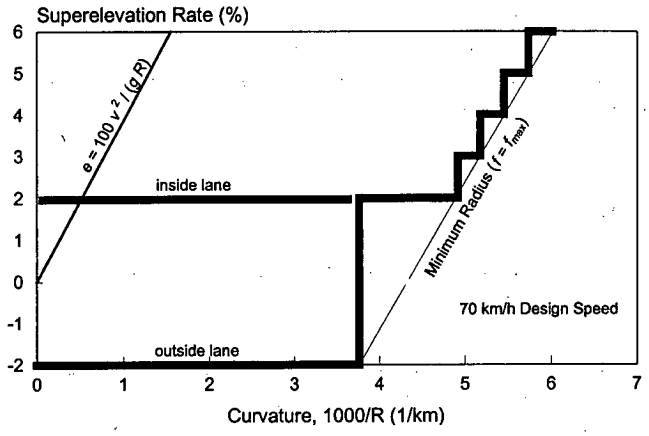

Figure III-7. Superelevation distribution method for low-speed urban streets.

should be used for all low-speed urban streets. When such considerations also control low-speed turning roadways, the values in Table III-12 represent acceptable design values. When conditions that require the conservative use of superelevation are not present, superelevation rate and radii combinations in Table III-11 are preferable to those in Table III-12.

Superelevation rates shown in Table III-12 range from 2 to 10 percent. This range is provided because the table is applicable to both urban streets and turning roadways. However, a rate of 4.0 or 6.0 percent is considered the desirable maximum superelevation rate for low-speed urban street conditions.

Super-elev. Rate e_d (%)	Design Speed (km/h)														
	30			40			50			60			70		
	Range of Design Radii (m)														
	Max. R	Des. Min.	Min. R	Max. R	Des. Min.	Min. R	Max. R	Des. Min.	Min. R	Max. R	Des. Min.	Min. R	Max. R	Des. Min.	Min. R
NC	tan.	28	--	tan.	57	--	tan.	102	--	tan.	169	--	tan.	266	--
2	28	23	--	57	47	--	102	83	--	169	134	--	266	205	--
3	23	22	--	47	45	--	83	79	--	134	127	--	205	193	--
4	22	21	21	45	43	43	79	76	76	127	121	121	193	183	183
5	21	21	--	43	42	--	76	72	--	121	116	--	183	174	--
6	21	20	20	42	40	40	72	70	70	116	111	111	174	166	166
7	20	19	--	40	39	--	70	67	--	111	106	--	166	159	--
8	19	19	19	39	37	37	67	64	64	106	102	102	159	152	152
9	19	18	--	37	36	--	64	62	--	102	98	--	152	146	--
10	18	18	18	36	35	35	62	60	60	98	94	94	146	140	140

Notes:

1. "Max. R": maximum radius, "Des. Min.": desirable minimum radius; "Min. R": minimum radius (with maximum superelevation); "NC": normal cross slope; "tan.": tangent section; " -- ": minimum radius not available.
2. When used with the tangent-to-curve transition design, the underlined radii and corresponding superelevation rates may cause turning vehicles to drift laterally to the extent that they may encroach into an adjacent lane or shoulder.
3. A rate of 4 or 6 percent is considered to be the desirable maximum superelevation rate for low-speed urban streets.
4. All superelevation rate and radii combinations shown in this table represent acceptable values for turning roadways. They should be considered when adverse impacts to adjacent property drainage or the frequency of slow-moving vehicles are important reasons to be conservative in the use of superelevation. It is also acceptable to consider the rates and radii in this table for the terminal sections of low-speed turning roadways, especially those with a significant number of trucks.

Table III-12. Superelevation distribution table for low-speed urban streets.

To illustrate the use of Table III-12, consider an urban street with a design speed of 60 km/h and a required maximum superelevation rate of 6.0 percent. If a radius of 120 m is being used by the designer, Table III-12 indicates that the design radius lies in the range of 116 to 121 m, which corresponds to a superelevation rate of 5.0 percent. A speed reduction of about 3.0 km/h will likely be incurred by motorists on this curve.

Superelevation for Turning Roadways

A wide range of superelevation rates have been used for turning roadway design. This flexibility indicates the wide range of conditions to which turning roadways must often be adapted. Tables III-10, III-11, and III-12 have been developed to provide this flexibility.

In general, the significant speed reductions often observed on turning roadways suggest a need for a sensitivity to safety. Therefore, the distribution method associated with the generous use of superelevation is considered preferable for application to turning roadways. Tables III-10 and III-11 define these preferable combinations of superelevation and radius for turning roadways.

In some situations, conditions will exist that justify the conservative use of superelevation. These conditions include drainage, frequent slow-moving vehicles, and terminal transition. With regard to terminal transition, relatively short turning roadway terminals may limit the use of superelevation when such superelevation makes it difficult to safely transition to or from the alignment of the through roadway without excessive pavement surface warping. This warping along the crossover crown line may compromise the stability of large trucks and make vehicle control difficult. In these situations, the distribution method associated with the conservative use of superelevation is considered acceptable for turning roadways. Table III-12 defines these acceptable combinations of superelevation and radius for low-speed turning roadways.

Effects of Grade

On long or fairly steep grades, drivers tend to travel somewhat faster in the downgrade than in the upgrade direction. In a refined design, this tendency should be recognized and some adjustment in superelevation rates would follow.

In the case of a divided roadway with both travel directions independently superelevated (or on a one-way ramp), adjustments in the superelevation rate can be made readily. In the simplest practical form, values from Tables III-10 and III-11 can be used directly by assuming a somewhat higher speed for the downgrade and a somewhat lower design speed for the upgrade. The variation of design speed necessarily would depend on the particular conditions, especially the rate and length of grade and the relative value of the radius of the curve as compared with other curves on the approach roadway section.

In the case of an undivided roadway, it is questionable whether any adjustment to superelevation rate should be made. In one respect, the two directions of traffic tend to balance each other and adjustment of superelevation is not needed. However, the downgrade speed is the most critical and adjustment for it may be desirable in some cases. One option for this adjustment is to select a superelevation rate suitable for the whole traveled way based on the downgrade speed. In this situation, the extra cross slope would not significantly affect upgrade travel (with the possible exception of heavy trucks on long upgrades). The disadvantage of this option is that it requires a change in design speed that is counter to the concept of design consistency. In general, superelevation adjustments on undivided roadways should be avoided.

Experience indicates that drivers reduce speed as they enter sharp curves. The braking required for this speed reduction consumes some of the available friction supply. On downgrades, braking for speed maintenance also consumes some of the friction supply. While such braking consumes only a small portion of the friction supply for passenger cars, it can consume a significant portion of the friction supply for trucks. Therefore, on roadways with significant truck volume and a downgrade in excess of 5 percent, it is suggested that the curve radius be selected such that it equals or exceeds the desirable minimum values (as listed in Tables III-10 and III-11).

Expected Curve Speed

The speed adopted by a driver when traveling along a curve is based on several factors. These factors include running speed on the approach to the curve, curve radius, and curve superelevation rate. In general, a driver's curve speed will equal the approach speed except when it is limited to lower values through the use of sharp curvature or minimal levels of superelevation. The controls described in previous sections have been developed such that any reduction in speed because of geometry will be small (i.e., less than 5 km/h) for street and highway curves.

The information presented in this section is intended to provide a means for the designer to estimate the expected 95th percentile curve speed. This estimate is based on the selected curve geometry and the 95th percentile approach speed. From the perspective of good design practice, the expected curve speed should coincide with a speed reduction of 10 km/h or less because large speed reductions are counter to the concept of design consistency and may increase accident potential.

A recent study (**19**) developed a relationship between curve speed, radius, and superelevation rate. This relationship was calibrated using data collected on numerous street and highway curves. These relationships are shown in Figures III-8 and III-9 for a range of approach speeds.

The relationships in Figure III-8 and III-9 are based on passenger car speeds. The trends for trucks were very similar; however, truck speeds tend to be slightly slower than those of passenger cars. The difference in speeds is dependent on curve radius with differences as large as 6 percent being found on sharper curves.

To illustrate the use of Figure III-8, consider a curve with a radius of 500 m and a superelevation rate of 2.0 percent. Figure III-8 indicates that such a curve on a roadway with a 95th percentile speed of 80 km/h would impose no speed reduction. However, if the 95th percentile approach speed was 100 km/h, the 95th percentile curve speed would be about 95 km/h. This 5-km/h speed reduction would be adopted by all drivers (not just the 95th percentile driver). Finally, if the 95th percentile approach speed was 120 km/h, the typical speed reduction would be approximately 11 km/h.

The trends shown in Figures III-10 and III-11 are applicable to horizontal curves on turning roadways. A comparison of these trends with their counterparts in Figures III-8 and III-9 indicates that the magnitude of the speed reduction is greater on turning roadway curves than on street or highway curves. This trend suggests that drivers on turning roadways accept larger speed reductions as they transition between intersecting facilities. In general, the speed reduction on a turning roadway curve, for a given radius and superelevation rate, is between 50 and 80 percent larger than on a street or highway curve.

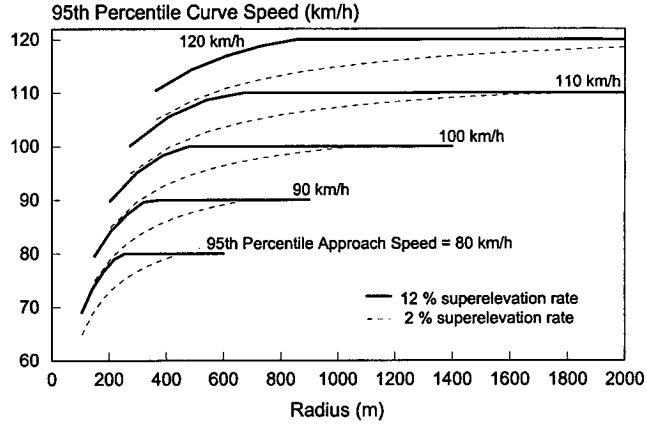

Figure III-8. Expected curve speeds for high-speed streets and highways.

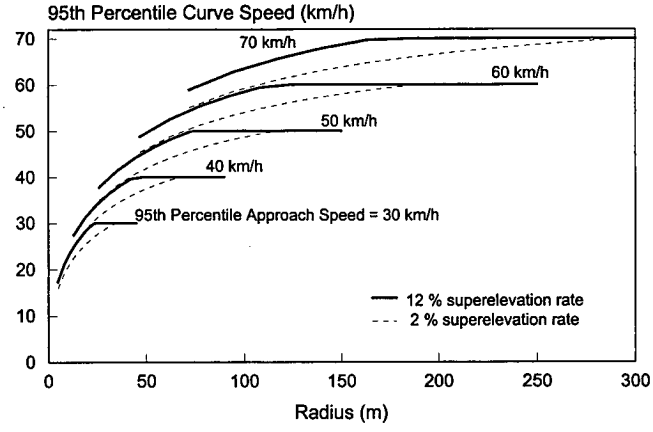

Figure III-9. Expected curve speeds for low-speed streets and highways.

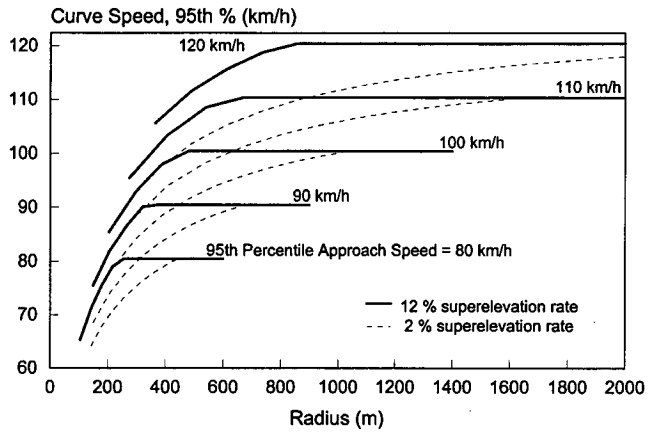

Figure III-10. Expected curve speeds for high-speed turning roadways.

Occasionally, the average speed is also needed during the highway design process. In these situations, the relationship between 95th percentile speed and average speed shown in Figure II-19 can be used in combination with Figures III-8, III-9, III-10, and III-11 to compute the average curve speed.

Transition Design Controls

General Considerations

This section describes the controls and criteria applicable to horizontal curve transition design. The design of the transition section includes consideration of the transition in roadway cross slope and a possible transition in horizontal alignment. The former consideration is referred to as superelevation transition and the latter is referred to as alignment transition. In most instances, both transition components occur over a common section of roadway at the beginning and end of the main circular curve.

The superelevation transition section consists of the superelevation runoff and tangent runout sections. The superelevation runoff section represents the length of roadway needed to accomplish a change in outside lane cross slope from zero (flat) to full superelevation, or vice versa. The tangent runout section represents the length of roadway needed to accomplish a change in outside lane cross slope from the normal cross slope rate to zero (flat), or vice versa. For purposes of safety and comfort, the pavement rotation in the superelevation transition section should be achieved over a length that is sufficient to make such rotation imperceptible to drivers. To be pleasing in appearance, the pavement edges should not be distorted as the driver views them.

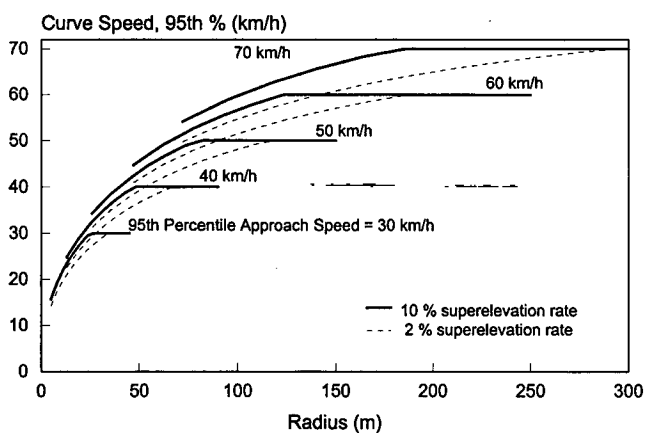

Figure III-11. Expected curve speeds for low-speed turning roadways.

With regard to alignment transition, a spiral or compound curve transition can be used to introduce the main circular curve in a natural manner (i.e., one that is consistent with the driver's steered path). Such transition curvature consists of one or more curves aligned and located to yield a gradual decrease in alignment radius. As a result, an alignment transition introduces the centripetal acceleration associated with the curve in a gentle manner. While this attribute is appealing, there is no definitive evidence that transition curves are essential to the safe operation of the roadway and, as a result, they are not used by many state highway agencies.

When a transition curve is not used, the roadway tangent directly intersects with the main circular curve. This type of transition design is referred to herein as the "tangent-to-curve" transition.

Tangent-to-Curve Transition

This section describes design controls applicable to the tangent-to-curve transition design. These controls include minimum transition length and location. Similar controls for the spiral and compound curve transition design are described in later sections.

Minimum length of superelevation runoff. For appearance and comfort, the length of superelevation runoff should be based on a maximum acceptable difference between the longitudinal grades of the axis of rotation and the edge of pavement. The axis of rotation is generally represented by the alignment centerline for undivided roadways; however, other pavement reference lines can be used. These lines and the rationale for their use are discussed in "Methods of Attaining Superelevation."

Current practice is to limit the grade difference, referred to as the maximum relative gradient, to a value of 0.50 percent at 80 km/h. This maximum is varied with design speed to yield longer runoff lengths at higher speeds and shorter lengths at lower speeds. Experience indicates that 0.75 and 0.38 percent yield acceptable lengths for design speeds of 30 and 120 km/h, respectively. Interpolation between these values yields the maximum relative gradients listed in Table III-13.

Previous editions of this policy have suggested that runoff lengths should be at least equal to the distance traveled in 2.0 s at the design speed. This control dictated the runoff lengths of curves with a small superelevation rate, high speed, or both. Experience with this control indicates that its appearance benefits are outweighed by its tendency to aggravate problems associated with pavement drainage in the transition section. In fact, some agencies do not use this control. From this evidence, it is concluded that a comfortable and aesthetically pleasing runoff design can be attained through the exclusive use of the maximum relative gradient control.

On the basis of the preceding discussion, the minimum length of runoff is as follows:

$$L_r = \frac{(w n_l) e_d}{\Delta} b_w$$

where:

L_r = minimum length of superelevation runoff, m;
Δ = maximum relative gradient, percent;
n_l = number of lanes rotated, lanes;
b_w = adjustment factor for number of lanes rotated;

Design Speed (km/h)	Maximum Relative Gradient (%)	Equivalent Maximum Relative Slope
30	0.75	1:133
40	0.70	1:143
50	0.65	1:150
60	0.60	1:167
70	0.55	1:182
80	0.50	1:200
90	0.47	1:213
100	0.44	1:227
110	0.41	1:244
120	0.38	1:263

Table III-13. Maximum relative gradients.

w = width of one traffic lane (typically 3.6 m), m; and
e_d = design superelevation rate, percent.

This equation can be used directly for undivided streets or highways where rotation is about the centerline and n_l equals one-half the number of lanes in the cross section. More generally, it can be used for rotation about any pavement reference line provided that the rotated width (= $w\ n_l$) has a common superelevation rate and is rotated as a plane.

A strict application of the maximum relative gradient yields runoff lengths for four-lane undivided roadways that are double those for two-lane roadways; those for six-lane roadways would be triple. While lengths of this order may be considered desirable, it is frequently not feasible to provide such lengths in design. On a purely empirical basis, it is concluded that minimum superelevation runoff lengths be adjusted downward to avoid excessive lengths for multilane roadways. The recommended adjustment factors are listed in Table III-14.

The adjustment factors listed in Table III-14 are directly applicable to undivided streets and highways. Runoff development for divided highways is discussed in more detail in the section "Axis of Rotation with a Median." The topic of runoff design for turning roadway terminals is discussed in Chapters IX and X.

Typical minimum superelevation runoff lengths are listed in Table III-15. The lengths shown represent cases where one and two lanes are rotated about a pavement edge. The former case can be found on two-lane roadways where the pavement is rotated about the centerline or on one-lane interchange ramps where rotation is about an edge line. The latter case can be found on undivided roadways where the pavement is rotated about the centerline or on four-lane divided roadways where each direction is separately rotated about an edge line.

Number of Lanes Rotated, n_l	Adjustment Factor, b_w[a]	Length increase relative to one-lane rotated (=$n_l\ b_w$)
1	1.00	1.0
1.5	0.83	1.25
2	0.75	1.5
2.5	0.70	1.75
3	0.67	2.0
3.5	0.64	2.25

[a] For other values of n_l, use the equation $b_w = (1 + 0.5\ (n_l - 1)) \div n_l$.

Table III-14. Adjustment factor for number of lanes rotated.

Design Element	Super-elevation Rate (%)	Minimum Runoff and Runout Length (m)									
		Design Speed (km/h)									
		30	40	50	60	70	80	90	100	110	120
		One Lane Rotated									
Runoff[1]	2	10	10	11	12	13	14	15	16	18	19
	4	19	21	22	24	26	29	31	33	35	38
	6	29	31	33	36	39	43	46	49	53	57
	8	38	41	44	48	52	58	61	65	70	76
	10	48	51	55	60	65	72	77	82	88	95
	12	58	62	66	72	79	86	92	98	105	114
Runout[2]	any	10	10	11	12	13	14	15	16	18	19
		Two Lanes Rotated									
Runoff[1]	2	14	15	17	18	20	22	23	25	26	28
	4	29	31	33	36	39	43	46	49	53	57
	6	43	46	50	54	59	65	69	74	79	85
	8	58	62	66	72	79	86	92	98	105	114
	10	72	77	83	90	98	108	115	123	132	142
	12	86	93	100	108	118	130	138	147	158	171
Runout[2]	any	14	15	17	18	20	22	23	25	26	28

[1] Based on 3.6-m lanes.
[2] Based on a 2.0 percent normal cross slope.

Table III-15. Minimum superelevation runoff and tangent runout lengths.

Elimination of the travel time control has resulted in shorter lengths for smaller superelevation rates and higher speeds. However, even the shortest lengths (corresponding to a superelevation rate of 2.0 percent) have travel times of 0.6 s which is sufficient to provide a smooth edge-of-pavement profile.

For high-type alignment, superelevation runoff lengths longer than those in Table III-15 may be desirable. The requirements of drainage or smoothness in the traveled way edge profiles may call for a small increase in runoff length.

The values given in Table III-15 are based on 3.6 m lanes. For other lane widths, the lengths of runoff vary in proportion to ratio of the actual lane width to 3.6 m. Shorter lengths could be applied for design with 3.0- and 3.3-m lanes, but considerations of consistency and practicality suggest that the values for 3.6-m lanes should be used in all cases.

Minimum length of tangent runout. The length of tangent runout is determined by the amount of adverse cross slope to be removed and the rate at which it is removed. To achieve a smooth edge of pavement profile, the rate of removal should equal the relative gradient used to define the superelevation runoff length. Based on this rationale, the following equation can be used to compute the minimum tangent runout length:

$$L_t = \frac{e_{NC}}{e_d} L_r$$

where:

L_t = minimum length of tangent runout, m; and
e_{NC} = normal cross slope rate, percent.

The tangent runout lengths obtained from this equation are listed in Table III-15.

Location with respect to end of curve. In the tangent-to-curve design, the location of the superelevation runoff length with respect to the point of curvature (PC) must also be addressed. The rationale for division of this length between the tangent and the circular curve is based on avoiding the extreme locations. With full superelevation attained at the PC, the runoff lies entirely on the approach tangent, where theoretically no superelevation is needed. At the other extreme, placement of the runoff entirely on the circular curve results in the initial portion of the curve having less than the desired amount of superelevation. Both of these extremes tend to be associated with a large peak lateral acceleration.

Experience indicates that locating a portion of the runoff on the tangent, in advance of the PC, is preferable because it minimizes the peak lateral acceleration and the resulting side friction demand. The magnitude of side friction demand incurred during travel through the runoff can vary with the actual vehicle travel path. Observation indicates that a spiral path results from the driver's natural steering behavior during curve entry or exit. This natural spiral usually begins on the tangent and ends beyond the beginning of the circular curve. Most evidence indicates that the length of this natural spiral ranges from 2 to 4 s travel time; however, its length may also be affected by lane width and the presence of other vehicles.

Based on the preceding discussion, locating a portion of the runoff on the tangent is consistent with the natural spiral path adopted by the driver during curve entry. In this manner, the gradual introduction of superelevation prior to the curve compensates for the gradual increase in centripetal acceleration associated with the spiral path. As a result of this harmony, theoretic considerations indicate that the peak lateral acceleration (incurred at the PC) is about equal to 50 percent of the centripetal acceleration associated with the circular curve.

In recognition of the aforementioned benefits, most agencies locate a portion of the runoff length on the tangent prior to the curve. The portions used vary from 0.6 to 0.8 (i.e., 60 to 80 percent) with a large majority of agencies using 0.67 (i.e., 67 percent). In addition, most agencies use one value for all street and highway curves.

Theoretical considerations confirm the desirability of placing a larger portion of the runoff length on the approach tangent rather than on the circular curve. Such considerations are based on analysis of the acceleration acting laterally on the vehicle while it travels through the transition section. This lateral acceleration can induce a lateral velocity and lane shift that could lead to operational problems. Specifically, a lateral velocity in an outward direction (relative to the curve) requires the driver to make a corrective steering maneuver that produces a path radius sharper than that of the roadway curve. Such a critical radius produces an undesirable increase in peak side friction demand. Moreover, a lateral velocity of sufficient magnitude to shift the vehicle into an adjacent lane (without corrective steering) is also undesirable for safety reasons.

Analysis of these theoretical considerations has led to the conclusion that desirable values of the "portion" control exist that minimize the operational problems (**19**). The values obtained from this analysis are listed in Table III-16.

If used in design, the values listed in Table III-16 should minimize lateral acceleration and the vehicle's lateral motion. Values smaller than those listed tend to have larger outward lateral velocities. Values larger than those listed tend to have larger lateral shifts.

Design Speed (km/h)	Portion of Runoff Located Prior to the Curve			
	No. of Lanes Rotated			
	1.0	1.5	2.0 - 2.5	3.0 - 3.5
30 - 70	0.80	0.85	0.90	0.90
80 - 120	0.70	0.75	0.80	0.85

Table III-16. Runoff locations that minimize the vehicle's lateral motion.

In summary, most agencies use one value of the portion control. The value used generally ranges from 0.6 to 0.8. Theoretical considerations indicate values in the range of 0.7 to 0.9 offer the best operating conditions; the specific value in this range being dependent on design speed and rotated width. Experience obtained from existing practice indicates that deviation from the values in Table III-16 by ±10% should not lead to measurable operational problems. Use of one value of the portion control in the range of 0.6 to 0.9 for all speeds and rotated widths is considered acceptable. However, refinement of this value, based on the trends shown in Table III-16, is desirable when conditions allow.

Limiting superelevation rates. Theoretic considerations of a vehicle's lateral motion when traveling through a tangent-to-curve transition indicate that large superelevation rates are associated with large lateral shifts. In general, such shifting is minimized by the proper location of the runoff section, as described in the preceding section. However, excessively large lateral shifts must be checked by the driver through corrective steering action.

In recognition of the adverse effect that an excessive lateral shift can have on safety, the threshold superelevation rates associated with a shift of 1.0 m are identified as 8, 10, 11, 11, and 12 percent for design speeds of 30, 40, 50, 60, and 70 km/h, respectively. Limiting rates do not apply for speeds of 80 km/h or greater when combined with superelevation rates of 12 percent or less.

Designs that incorporate superelevation in excess of the limiting rates may have excessive lateral shift. Therefore, it is recommended that these superelevation rates be avoided. However, if they are used, some consideration should be given to increasing the width of the traveled way along the curve to avoid encroachment into the adjacent lane.

Spiral Curve Transition

A recent study of transition design issues **(19)** found that spiral curve transitions provide some operational and safety benefits. However, this study also found that these benefits are realized only for certain conditions and only when the spiral is appropriately designed. Deviation from these conditions or the use of excessive spiral lengths has been correlated with an increased accident potential.

The main operational benefit from a spiral curve transition is that it produces a relatively low peak lateral acceleration in the transition section. Specifically, theoretic considerations indicate that drivers experience a peak lateral acceleration that is about equal to 30 percent of the centripetal acceleration of the circular curve. This peak is much lower than that experienced in transitions with the tangent-to-curve design (noted previously to be about 50 percent of the centripetal acceleration).

Research on spiral curve safety indicates that they have a small safety benefit when used on sharper horizontal curves **(22)**. However, there is also evidence that excessively long spirals can increase accident potential **(23)**. Also, spirals used in mountainous terrain have been found to increase accident potential. In recognition of these findings, guidance is offered in this section regarding (1) the conditions where spirals may be most beneficial and (2) the appropriate spiral curve length.

Maximum radius for use of a spiral. A review of guidance on the use of spiral curve transitions indicates a general lack of consistency among agencies. In general, much of this guidance suggests that an upper limit on curve radius can be established such that only radii below this maximum would likely exhibit some safety and operational benefit. Several agencies have established such a limiting radius in terms of a minimum centripetal acceleration rate. These rates have been found to vary from 0.4 to 1.3 m/s^2. Of these rates, the latter is consistent with the maximum radii for which some reduction in accident potential has also been noted. For these reasons, the maximum radius for use of a spiral is based on a minimum acceleration of 1.3 m/s^2. These radii are listed in Table III-17.

The radii listed in Table III-17 are intended for use by those agencies that desire to use spiral curve transitions. When combined with a spiral curve transition, horizontal curves with these radii may have slightly fewer accidents (relative to a transition-to-curve transition). Table III-17 is not intended to define radii that require the use of a spiral.

	Design Speed (km/h)									
	30	**40**	**50**	**60**	**70**	**80**	**90**	**100**	**110**	**120**
Maximum Radius (m)	53	95	148	214	291	380	481	594	718	855

[1] The safety benefits of spiral curve transitions are likely to be negligible for larger radii.

Table III-17. Maximum radius for use of a spiral curve transition.[1]

Minimum length of spiral. Several agencies define a minimum length of spiral based on consideration of motorist comfort and lateral shift. The comfort control produces a spiral length that allows for a comfortable increase in centripetal acceleration of the curve. The lateral shift control ensures that the spiral is long enough to provide a shift in the lane that is consistent with that produced by the vehicle's natural spiral path. It is recommended that these two controls be used together to determine the minimum length of spiral. Thus, the minimum spiral length can be computed as follows:

$$L_{s,\,\min} = Larger\ of: \left[\sqrt{24 p_{\min} R};\ \ 0.0214\frac{V^3}{RC}\right]$$

where:

$L_{s,\,\min}$ = minimum length of spiral, m;
$p_{\min}$ = minimum lateral offset between the tangent and circular curve (= 0.20 m);
R = radius of curve, m;
V = design speed, km/h; and
C = maximum rate of change in centripetal acceleration (= 1.2 m/s^3).

A value of 0.20 m is recommended for $p_{\min}$. This value is consistent with the minimum lateral shift that occurs as a result of the natural steering behavior of most drivers. A value of 1.2 m/s^3 is recommended for C. This value represents the maximum value that should be used, which is consistent with the intent of an upper limit control. The use of lower values will yield longer, more "comfortable" lengths; however, these lengths would not represent the minimum length associated with the comfort limit.

Maximum length of spiral. International experience indicates that there is a need to limit spiral length. This need stems from safety problems occurring on longer spirals (relative to the length of the curve). These problems occur when the spiral is so long that it misleads the driver about the sharpness of the impending curve. A conservative maximum length of spiral that avoids these problems can be computed as follows:

$$L_{s,\,\max} = \sqrt{24 p_{\max} R}$$

where:

$L_{s,\,\max}$ = maximum length of spiral, m; and
$p_{\max}$ = maximum lateral offset between the tangent and circular curve (= 1.0 m).

A value of 1.0 m is recommended for $p_{\max}$. This value is consistent with the maximum lateral shift that occurs as a result of the natural steering behavior of most drivers. It also provides a reasonable balance between spiral length and curve radius.

Desirable length of spiral. A recent study of the operational effects of spiral curve transitions **(19)** found that spiral length is an important design control. Specifically, the most desirable operating conditions were when the spiral curve length was approximately equal to the length of the natural spiral adopted by the driver. Deviations between these two lengths resulted in operational problems such as a large lateral velocity or shift at the end of the transition section. Specifically, a large lateral velocity in an outward direction (relative to the curve) requires the driver to make a corrective steering maneuver that produces a path radius sharper than that of the roadway curve. Such a critical radius produces an undesirable increase in peak side friction demand. Moreover, a lateral velocity of sufficient magnitude to shift the vehicle into an adjacent lane (without corrective steering) is also undesirable for safety reasons.

Based on these considerations, desirable lengths of spiral curve transition are listed in Table III-18. These lengths correspond to 2.0 s travel time at the design speed. This travel time has been found to be representative of the natural spiral path for most drivers (**19**).

The spiral lengths listed in Table III-18 are offered as desirable values for street and highway applications. Theoretical considerations suggest that significant deviations from these lengths increase the lateral shift in the lane, which may precipitate crowding of an adjacent lane or shoulder. The use of larger lengths (but less than $L_{s,\,max}$) is acceptable. However, if they are used, some consideration should be given to increasing the width of the traveled way along the curve to minimize encroachments into the adjacent lane.

Spiral lengths larger than those in Table III-18 may be needed at turning roadway terminals to adequately develop the desired superelevation. Specifically, spirals twice the length of those in Table III-18 may be necessary for such development. The lateral lane shift that results may exceed 1.0 m; however, such a shift is consistent with driver expectancy at a turning roadway terminal and can be accommodated by the additional lane width typically provided on these turning roadways.

Finally, the desirable spiral length should not supercede the minimum spiral length. In some instances, the minimum length equation will yield lengths that are slightly larger than the desirable length. In these instances, the minimum length should be used for spiral design.

Length of superelevation runoff. In transition design with a spiral curve, it is recommended that the superelevation runoff be achieved over the length of the spiral. In this manner, the length of runoff is set equal to the length of spiral, as determined using the spiral length controls described in the previous three sections. The change in cross slope begins by introducing a tangent runout section just in advance of the spiral. Full attainment of superelevation is then achieved over the length of spiral. By this design technique, the whole of the circular curve has full superelevation.

Limiting superelevation rates. One consequence of equating runoff length to spiral length is that the resulting relative gradient of the pavement edge may exceed the values listed in Table III-13. However, small increases in gradient have not been found to have an adverse effect on comfort or appearance. The adjustment factors listed in Table III-14 effectively allow for a 50 percent increase in the maximum relative gradient when three lanes are rotated.

The superelevation rates that are associated with a maximum relative gradient that is 50 percent larger than the values in Table III-13 are listed in Table III-19. If the superelevation rate used in design exceeds the rate listed in this table, the maximum relative gradient will be at least 50 percent larger than the maximum relative gradient allowed for a tangent-to-curve design. In this situation, special consideration should be given to the transition's appearance and the abruptness of its edge of pavement profile.

Length of tangent runout. The tangent runout length for a spiral curve transition design is based on the approach used for the tangent-to-curve design. Specifically, a smooth edge of pavement profile is desired such that a common edge slope gradi-

	Design Speed (km/h)									
	30	**40**	**50**	**60**	**70**	**80**	**90**	**100**	**110**	**120**
Spiral Length (m)	17	22	28	33	39	44	50	56	61	67

Table III-18. Desirable length of spiral curve transition.

No. of Lanes Rotated	Limiting Superelevation Rates (%)									
	Design Speed (km/h)									
	30	**40**	**50**	**60**	**70**	**80**	**90**	**100**	**110**	**120**
1	5.2	6.5	7.5	8.3	8.9	9.3	9.8	10.2	10.4	10.6
2	2.6	3.2	3.8	4.2	4.5	4.6	4.9	5.1	5.2	5.3
3	1.7	2.2	2.5	2.8	3.0	3.1	3.3	3.4	3.5	3.5

Note:
1. Based on the desirable length of spiral transition curve from Table III-18.

Table III-19. Superelevation rates associated with large relative gradients.

ent is maintained throughout the runout and runoff sections. Based on this rationale, the following equation can be used to compute the tangent runout length:

$$L_t = \frac{e_{NC}}{e_d} L_s$$

where:

L_t = length of tangent runout, m;
L_s = length of spiral, m;
e_d = design superelevation rate, percent; and
e_{NC} = normal cross slope rate, percent.

The tangent runout lengths obtained from this equation are listed in Table III-20. The lengths in this table tend to be long for combinations of low superelevation rate and high speed. Such lengths can present safety problems when there is insufficient profile grade to provide adequate pavement surface drainage. These problems can be avoided when the profile grade controls described in the section titled "Minimum Transition Grade" are applied to the spiral curve transition.

Compound Curve Transition

In general, the compound curve transition is most commonly considered for application to low-speed turning roadways at intersections. In contrast, tangent-to-curve or spiral curve transition designs are more commonly used on street and highway curves.

Guidance regarding compound curve transition design for turning roadways is provided in Chapters IX and X. The guidance in Chapter IX applies to low-speed turning roadway terminals at intersections whereas that in Chapter X applies to interchange ramp terminals.

Methods of Attaining Superelevation

Four methods are used to transition the pavement to a superelevated cross section. These methods include (1) revolving a traveled way with normal cross slopes about the centerline profile, (2) revolving a traveled way with normal cross slopes about the inside-edge profile, (3) revolving a traveled way with normal cross slopes about the outside-edge profile, and (4) revolving a straight cross-slope traveled way about the outside-edge profile. Figure III-12 illustrates these four methods diagrammatically.

The profile reference line provides control for the roadway's vertical alignment through the horizontal curve. Although shown as a horizontal line in Figure III-12, the profile reference line may correspond to a tangent, a vertical curve, or a combination of the two. In Figure III-12A, the profile reference line corresponds to the centerline profile. In Figures III-12B and III-12C, the profile reference line is represented as a "theoretical" centerline profile because it does not coincide with the axis of rotation. In Figure III-12D, the profile reference line corresponds to the outside edge of the traveled way. The cross sections at the bottom of each diagram in Figure III-12 indicate the traveled way cross slope condition at the lettered points.

The first method, as shown in Figure III-12A, revolves the traveled way about the centerline profile. This method is the most widely used because the required change in elevation of the edge of the traveled way is made with less distortion than with the other methods. Thus, one-half of the required change in elevation is made at each edge.

Superelevation Rate (%)	Tangent Runout Length (m)									
	Design Speed (km/h)									
	30	40	50	60	70	80	90	100	110	120
2	17	22	28	33	39	44	50	56	61	67
4	8	11	14	17	19	22	25	28	31	33
6	--	7	9	11	13	15	17	19	20	22
8	--	--	--	8	10	11	13	14	15	17
10	--	--	--	--	--	--	10	11	12	13

Notes:
1. Based on 2.0 percent normal cross slope.
2. Superelevation rates above 10 percent and cells with "–" coincide with a pavement edge grade that exceeds the maximum relative gradient in Table III-13 by 50 percent or more. These limits apply to roads where one lane is rotated; lower limits apply when more lanes are rotated (see Table III-19).

Table III-20. Tangent runout length for spiral curve transition design.

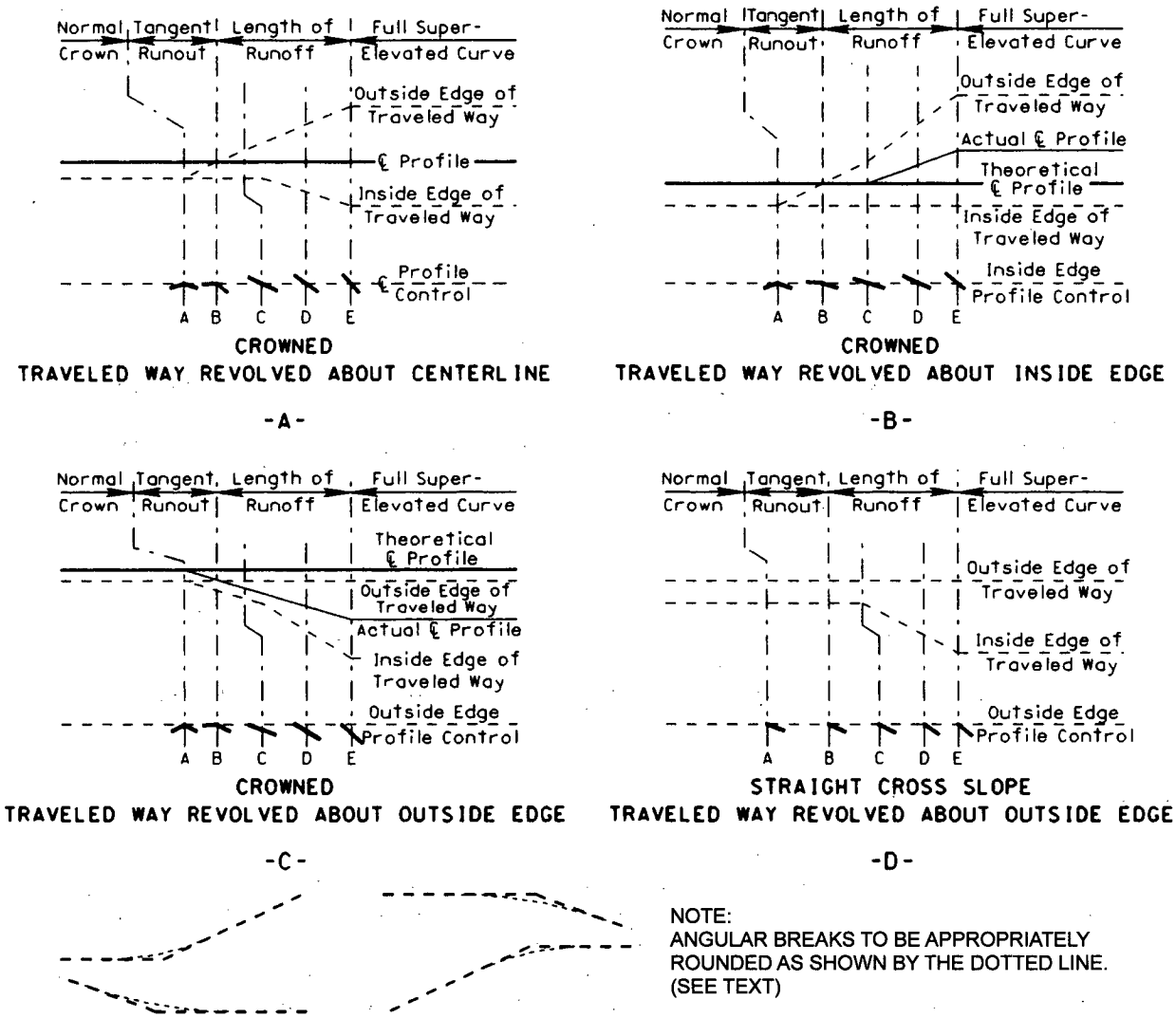

Figure III-12. Diagrammatic profiles showing methods of attaining superelevation for a curve to the right.

The second method, as shown in Figure III-12B, revolves the traveled way about the inside-edge profile. In this case, the inside-edge profile is determined as a line parallel to the profile reference line. One-half of the required change in elevation is made by raising the actual centerline profile with respect to the inside-edge profile and the other one-half by raising the outside-edge profile an equal amount with respect to the actual centerline profile.

The third method, as shown in Figure III-12C, revolves the traveled way about the outside-edge profile. This method is similar to that shown in Figure III-12B except that the elevation change is achieved below the outside-edge profile instead of above the inside-edge profile.

The fourth method, as shown in Figure III-12D, revolves the traveled way (having a straight cross-slope) about the outside-edge profile. This method is often used for two-lane one-way roadways where the axis of rotation coincides with the median edge of the traveled way.

The methods for attaining superelevation are nearly the same for all four of the methods. Cross section A at one end of the tangent runout is a normal (or straight) cross slope section. At cross section B, the other end of the tangent runout and the beginning of the superelevation runoff, the lane or lanes on the outside of the curve are made horizontal (or level) with the actual centerline profile for Figures III-12A, III-12B, and III-12C; there is no change in cross slope for Figure III-12D.

At cross section C, the traveled way is a plane, superelevated at the normal cross slope rate. Between cross sections B and C for Figures III-12A, III-12B and III-12C, the outside lane or lanes change from a level condition to one of superelevation at the normal cross slope rate and the normal cross slope is retained on the inner lanes. There is no change between cross sections B and C for Figure III-12D. Between cross sections C and E the pavement section is revolved to the full rate of super-

elevation. The rate of cross slope at any intermediate point (e.g., cross section D) is proportional to the distance from cross section C.

In an overall sense, the method of rotation about the centerline shown in Figure III-12A is usually the most adaptable. On the other hand, the method shown in Figure III-12B is preferable where the lower edge profile is a major control, as for drainage. With uniform profile conditions, its use results in the greatest distortion of the upper edge profile. Where the overall appearance is to be emphasized, the methods of Figures III-12C and III-12D are advantageous because the upper-edge profile—the edge most noticeable to drivers—retains the smoothness of the control profile. Thus, the shape and direction of the centerline profile may determine the preferred method for attaining superelevation.

Considering the infinite number of profile arrangements and in recognition of such specific problems as drainage, avoidance of critical grades, aesthetics, and fitting the roadway to the adjacent topography, the adoption of any specific axis of rotation cannot be recommended. To obtain the most pleasing and functional results, each superelevation transition section should be considered an individual problem. In practice, any pavement reference line used for the axis of rotation may be the most adaptable for the problem at hand.

Design of Smooth Profiles for Traveled Way Edges

In the diagrammatic profiles shown in Figure III-12, the tangent profile control lines result in angular breaks at cross sections A, C, and E. For general appearance and safety, these breaks should be rounded in final design by insertion of vertical curves. Even when the maximum relative gradient is used to define runoff length, the length of vertical curve required to conform to the break in grade need not be great.

Several methods are available for the development of smooth edge profiles in superelevation transition sections. One method defines the edge profiles on a straight-line basis, as shown in Figure III-12, and then develops the profile details based on inserting parabolic vertical curves at each edge break. In such cases, the minimum vertical curve length is often set equal to about 0.7 s travel time at the design speed.

A second method uses a graphical approach to define the edge profile. The method essentially is one of spline-line development. The natural bending of the spline almost always satisfies the requirements for minimum smoothing. Once the edge profiles are drawn in the proper relation to one another, elevations can be read at the appropriate intervals (as needed for construction control).

Divided highways warrant a greater refinement in design and greater attention to appearance than do two-lane highways because they serve much greater traffic volumes. Moreover, the cost of such refinements is insignificant compared with the construction cost of the divided highway. Accordingly, there should be greater emphasis on the development of smooth-flowing traveled way-edge profiles for divided highways.

Axis of Rotation with a Median

In the design of divided highways, streets, and parkways, the inclusion of a median in the cross section alters somewhat the superelevation transition design. This effect stems from the different possible locations for the axis of rotation. The most appropriate location for this axis is dependant on the width of the median and its cross section. Common combinations of these factors and a corresponding axis location are described in the following three cases:

Case I—The whole of the traveled way, including the median, is superelevated as a plane section.
Case II—The median is held in a horizontal plane and the two traveled ways are rotated separately around the median edges.
Case III—The two traveled ways are separately treated for runoff with a resultant variable difference in elevation at the median edges.

Case I necessarily is limited to narrow medians and moderate superelevation rates to avoid substantial differences in elevation of the extreme traveled way edges because of the median tilt. In this regard, a narrow median is a median having a width of 4 m or less. Superelevation can be attained using a method similar to that shown in Figure III-12A except for the two median edges, which will appear as profiles only slightly removed from the centerline.

Case II can apply to any width of median but has most application to those having a width between 4 and 12 m. By holding the median edges level, the difference in elevation of the extreme traveled way edges is limited to that needed to superelevate the roadway. Superelevation transition design for Case II usually has the median-edge profiles as the control. One traveled way is rotated about its lower edge and the other about its higher edge. Superelevation can be attained using any of the methods shown in Figures III-12B, III-12C, and III-12D, the profile reference line being the same for the two traveled ways.

Case III design can be used with wide medians (i.e., those having a width of 12 m or more). For this case, the differences in elevation of the extreme traveled way edges are minimized by a compensating slope across the median. With a wide median, it is possible to design separately the profiles and superelevation transition for the two roadways. Accordingly, superelevation can be attained by the method otherwise considered appropriate (i.e., any of the methods in Figure III-12 can be used).

Superelevation runoff lengths may vary for each of the three cases. For Case I designs, the length of runoff should be based on the total rotated width (including the median width). Runoff lengths for Case II designs should be the same as those for undivided highways with a similar number of lanes. Finally, runoff lengths for Case III designs are based on the needs of the separate one-way roadways, as defined by their superelevation rates and rotated widths.

Minimum Transition Grades

Two pavement surface drainage problems are of concern in the superelevation transition section. One problem relates to the potential lack of adequate longitudinal grade. This problem generally occurs when the grade of the axis of rotation is equal to the effective relative gradient but opposite in sign. It results in the edge of pavement having negligible longitudinal grade, which can lead to poor pavement surface drainage, especially on curbed cross sections.

The other drainage problem relates to inadequate lateral drainage because of negligible cross slope during pavement rotation. This problem occurs in the transition section where the cross slope of the outside lane varies from an adverse slope at the normal cross slope rate to a superelevated slope at the normal cross slope rate. This length of the transition section includes the tangent runout section and an equal length of the runoff section. Within this length, the pavement cross slope may not be sufficient to adequately drain the pavement laterally.

Two techniques can be used to alleviate these drainage problems. One technique is to provide a minimum profile grade in the transition section. The second technique is to provide a minimum edge of pavement grade in the transition section. Both techniques can be incorporated in the design by using the following grade controls:

1. A minimum profile grade of 0.5 percent maintained through the transition section.
2. A minimum edge of pavement grade of 0.2 percent (0.5 percent for curbed streets) maintained through the transition section.

The second grade control is equivalent to the following series of equations relating profile grade and effective maximum relative gradient:

$$\begin{aligned} G &\le -\Delta^* - 0.2 \\ G &\ge -\Delta^* + 0.2 \\ G &\le \Delta^* - 0.2 \\ G &\ge \Delta^* + 0.2 \end{aligned} \qquad (1)$$

with

$$\Delta^* = \frac{(w\, n_l)\, e_d}{L_r} \qquad (2)$$

where:

G = profile grade, percent;
Δ^* = effective maximum relative gradient, percent;
L_r = length of superelevation runoff, m;
n_l = number of lanes rotated, lanes;
w = width of one traffic lane (typically 3.6 m), m; and
e_d = design superelevation rate, percent.

The value of "0.2" in Equation 1 represents the minimum edge of pavement grade for uncurbed roadways (in percent). If this equation is applied to curbed streets, it is suggested that the value "0.2" be replaced with "0.5".

To illustrate the combined use of the two grade controls, consider an uncurbed roadway curve having an effective maximum relative gradient of 0.65 percent in the transition section. The first control would exclude profile grades between – 0.50 and + 0.50 percent. The second grade control would exclude grades in the range of – 0.85 to – 0.45 percent (via the first two

components of Equation 1) and those in the range of 0.45 to 0.85 percent (via the last two components of Equation 1). Given the overlap between the ranges for Controls 1 and 2, the profile grade within the transition would have to be outside the range of – 0.85 to + 0.85 percent to satisfy both controls and provide adequate pavement surface drainage.

Turning Roadway Design

Turning roadways can be categorized as interchange ramps or intersection curves. At interchanges, they have a loop or diamond configuration and consist of combinations of tangents and curves. At intersections, they have a diamond configuration and consist of curves (often compound curves). Turning roadways have design speeds of 20 km/h or more and, at intersections, are associated with a channelizing island. Turning roadway design does not apply to the case of minimum edge-of-traveled-way design for turns at intersections. Here it is a matter of closely fitting compound curves to the inside edge of the design vehicle's swept path (as described in Chapter IX).

When the design speed of the turning roadway is 70 km/h or less, compound curvature can be used to form the entire alignment of the turning roadway. When the design speed exceeds 70 km/h, the exclusive use of compound curves is often impractical because it requires a large amount of right-of-way. Thus, most high-speed turning roadways follow the interchange ramp design guidelines in Chapter X and include a mix of tangents and curves. By this approach, the design can be more sensitive to right-of-way impacts as well as driver comfort and safety.

For compound curves at intersections, it is preferable that the ratio of the flatter radius to the sharper radius not exceed 2:1. This ratio results in approximately a 10 km/h reduction in average running speeds for the two curves.

For compound curves at interchanges, it is preferable that the ratio of the flatter radius to the sharper radius not exceed 1.75:1. However, general observations on ramps having differences in radii with a ratio of 2:1 indicate that both operation and appearance are satisfactory.

Curves that are compounded should not be too short or their effect in enabling a change in speed from the tangent or flat curve to the sharp curve is lost. In a series of curves of decreasing radii, each curve should be long enough to enable the driver to decelerate at a reasonable rate. At intersections, the assumed maximum rate is 5 km/h/s (although 3 km/h/s is desirable). The desirable rate indicates very light braking, because deceleration in gear alone generally results in overall rates between 1.5 and 2.5 km/h/s. Minimum compound curve lengths on this basis are given in Table III-21.

The compound curve lengths in Table III-21 are developed on the premise that travel is in the direction of sharper curvature. For the acceleration condition, the 2:1 ratio is not as critical and may be exceeded.

Control Condition	Minimum Length of Circular Arc (m)						
	Radius (m)						
	30	50	60	75	100	125	150 or more
Acceptable	12	15	20	25	30	35	45
Desirable	20	20	30	35	45	55	60

Table III-21. Lengths of circular arc for different compound curve radii.

REFERENCES

. . .

18. Krammes, R., R. Brackett, M. Shafer, J. Ottesen, I. Anderson, K. Fink, K. Collins, O. Pendleton, and C. Messer. *Horizontal Alignment Design Consistency for Rural Two-Lane Highways.* Report FHWA-RD-94-034, Federal Highway Administration, Washington, D.C. (1995).
19. Bonneson, J.A. *NCHRP Report 439: Superelevation Distribution Methods and Transition Designs.* National Cooperative Highway Research Program, National Research Council, Washington, D.C., 2000.
20. Haile, E.R. "Discussion of Friction Factors and Superelevation." Discussion paper published with: Barnett, J. "Safe Side Friction Factors and Superelevation Design." *Proceedings of the HRB*, Vol. 16., Highway Research Board, National Research Council, Washington, D.C., 1936, p. 69–80.
21. Hajela, G.P. *Compiler, Resume of Tests on Passenger Cars on Winter Driving Surfaces,* 1939–1966. Chicago: National Safety Council, Committee on Winter Driving Hazards, 1968.
22. Council, F.M."Safety Benefits of Spiral Transitions on Horizontal Curves on Two-Lane Rural Roads." *Transportation Research Record 1635*, National Research Council, Washington, D.C., 1998, p. 10–17.
23. Stewart, D. and C.J. Chudworth. "A Remedy for Accidents at Bends." *Traffic Engineering & Control,* Vol. 31, No. 2, London, England, 1990, p. 88–93.

Delete references 22 to 27.

CHAPTER IX—INTERSECTIONS

The text provided on the following pages represents the recommended modifications to selected paragraphs in *Green Book* Chapter IX. These paragraphs are located in two sections. The first section addresses turning roadway terminal design (p. 690–695). The second section addresses superelevation at turning roadways (i.e., general considerations and superelevation runoff; p. 726–730). Both sections apply to low-speed turning roadways at intersections.

Some of the guidance provided in the *Green Book* has been retained but the recommended changes are sufficiently extensive that a complete rewriting of the text was considered the most efficient method of presenting the material.

Chapter IX

INTERSECTIONS
APPLICATION AT TURNING ROADWAY TERMINALS

An important part of intersection design is the design of the alignment where the turning roadway departs from or joins the through roadway. Ease and smoothness of operation result when the turning roadway terminal is designed with spiral or compound curves. The shape and length of these curves should be such that they (1) allow drivers to avoid abrupt deceleration before they leave the through roadway, (2) permit development of superelevation in advance of the maximum curvature, and (3) enable vehicles to follow natural turning paths.

The design speed of the turning roadway may vary between the terminal and the central section. The design speed of the turning roadway terminal should equal that of the through roadway, unless the terminal forms a stop-controlled intersection. The design speed of the central section of the turning roadway should be based on the values in Table X-1. Guidance associated with this table indicates that turning roadways at intersections should use the "upper-range" design speeds; although, the "middle-range" speeds are acceptable when practical considerations dictate.

Various degrees of turning roadway terminal design are illustrated in Figure IX-30. For this illustration, the through roadway is assumed to have a design speed of 40 km/h and a maximum superelevation rate of 10 percent. Right-of-way conditions are assumed to require the use of sharp curvature.

Based on the given information, the relevant design controls can be identified. First, the turning roadway terminal design speed is 40 km/h. Table III-11 indicates that a minimum radius of 35 m (and superelevation rate of 10 percent) is acceptable for a 40-km/h design speed. Because of right-of-way constraints, a radius of 35 m is used. An extrapolation of the trends in Table X-1 indicates that the desirable design speed of the central section of the turning roadway should be 30 km/h (i.e., based on the upper range); however, this information is not used for this illustration of terminal design.

Figure IX-30A illustrates the tangent-to-curve transition, as applied to a turning roadway terminal. This design has the advantage of simplicity; however, it does not provide adequate length for deceleration (from 40 to 30 km/h) off of the through-traffic lane. Moreover, the development of superelevation is problematic because there is no transition curve provided. As a result, the slope change at the crossover crown line may be undesirably abrupt. Hence, this design is not recommended.

Figure IX-30B illustrates the use of a spiral curve transition. Its length is 22 m based on the desirable lengths recommended in Table III-18. Operationally, this curve is a substantial improvement over the simple curve shown in Figure IX-30A. This design is acceptable when the design superelevation rate can be developed in a manner that provides an attractive and comfortable transition. Unfortunately, the spiral is too short for the development of the 10-percent superelevation rate used for this illustration.

Figure IX-30C illustrates the use of a long spiral curve transition. The length of the spiral is increased by an amount sufficient to develop the desired rate of superelevation. This length is estimated as 41 m, based on a change in cross slope of 8 percent (from 2 percent on the through roadway to 10 percent on the turning roadway) and a maximum relative gradient of 0.70 percent.

Figure IX-30D illustrates the use of a compound curve transition. The radius of the initial curve is 70 m, based on the 2 : 1 ratio established for turning roadway design. This design is similar to Figure IX-30B in that it yields acceptable operation provided that the length of the transition curve is sufficient to develop the design superelevation rate. Unfortunately, the 70-m transition curve is too short (i.e., 24 m) to develop the 10-percent superelevation rate used for this illustration.

Figure IX-30E illustrates the use of a three-step compound curve transition. In this case, the 35-m radius is preceded by 70 and 140-m radii curves of approximately the minimum lengths, as given in Table III-21. This arrangement requires more space as indicated by the 10-m lateral offset p to the 35-m radius curve; however, it is quite likely to have sufficient length to develop the design superelevation rate. This design is particularly useful when the turning volumes are relatively large or when large trucks need to be accommodated. Where this design is not feasible due to space limitations, arrangements similar to those shown in Figures IX-30B, IX-30C and IX-30D should be used.

Figure IX-30 illustrates turning roadway terminal design for exit points. However, similar arrangements are applicable to turning roadway terminal designs for entrance points. One exception is that the approach nose for the entrance becomes a merging end without offset from the edge of the traveled way.

The arrangements shown in Figure IX-30 are applicable when joining a parallel auxiliary or speed change lane. If the right-hand lane is a deceleration lane, the pavement taper beyond the nose would be that shown by the dashed line in Figure IX-30E, joining the edge of through traveled way at "e."

For an alternate method of designing turning roadway terminals, a straight taper to an offset circular curve may be used instead of a spiral or compound curve. This arrangement requires more paved area than a compound curve, but it provides a gradual turnout and some additional length for deceleration off the through traffic lanes.

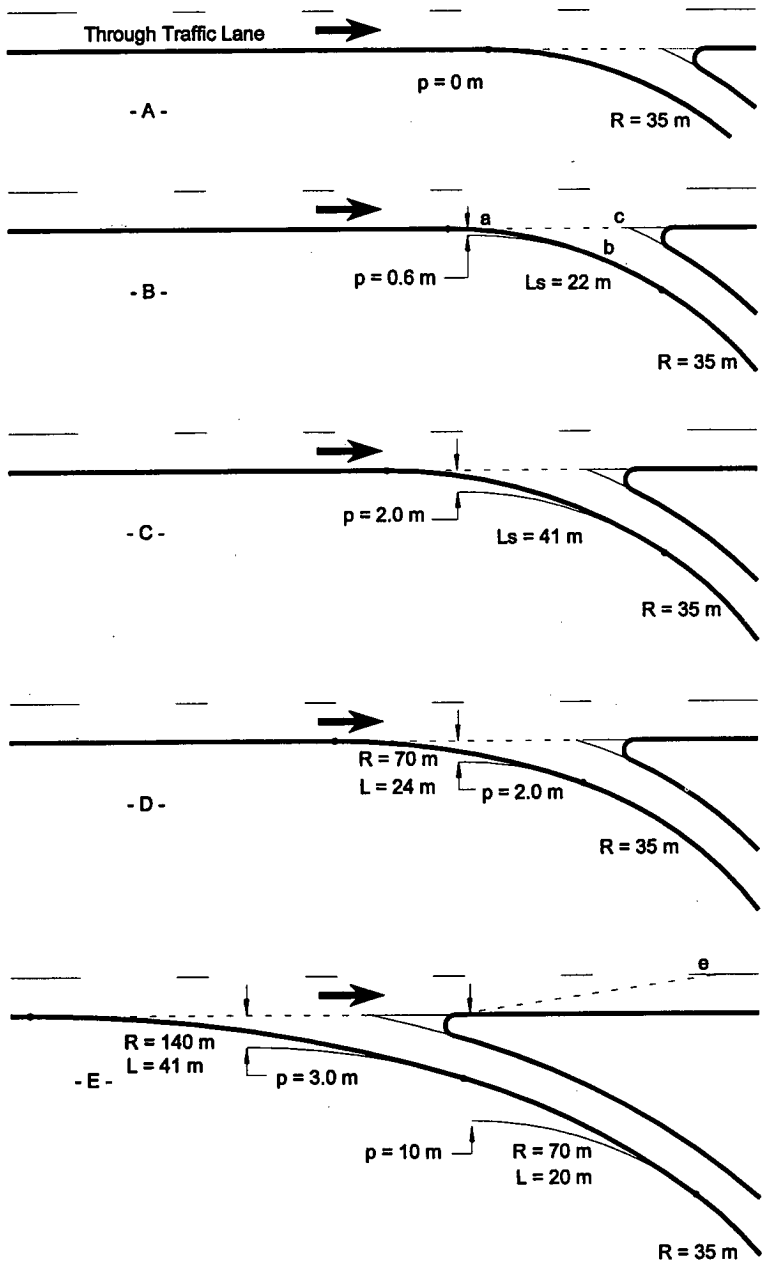

Figure IX-30. Use of spiral and compound curves at a turning roadway terminal.

SUPERELEVATION FOR TURNING ROADWAYS AT INTERSECTIONS

General Design Guidelines

The general factors that control the maximum rates of superelevation for open highway conditions as discussed in Chapter III also apply to turning roadways at intersections. Maximum superelevation rates up to 10 percent may be used where climatic conditions are favorable. However, maximum rates up to 8 percent generally should be used where snow and icing conditions prevail.

In intersection design, the feasible curves for turning roadways are often of limited radii and length. When speed is not affected by other vehicles, drivers on turning roadways anticipate the sharp curves and accept operation with higher side friction than they accept on open highway curves of the same radii. This behavior stems from their desire to maintain their speed through the curve, although some speed reduction typically occurs. When other traffic is present, drivers will travel slower on turning roadways than on open highway curves of the same radii because they must diverge from and merge with through traffic. Therefore, in designing for safe operation, periods of light traffic volumes and corresponding speeds generally will control.

It is desirable to provide as much superelevation as practical on turning roadways. Designs with gradually changing curvature, achieved by the use of compound curves, spirals, or both, permit desirable development of superelevation. For these designs, the design superelevation rates and corresponding radii listed in Table III-11 are desirable.

The practical difficulty of attaining superelevation without abrupt cross-slope change at turning roadway terminals, primarily because of sharp curvature and short lengths of turning roadway, sometimes can prevent the development of a generous rate of superelevation. Abrupt changes in cross slope can adversely affect the stability of trucks and other vehicles with high centers of gravity. The design superelevation rates and corresponding radii listed in Table III-12 can be used when conditions justify the conservative use of superelevation.

Superelevation Runoff

The principles of superelevation runoff design discussed in Chapter III generally apply to turning roadways at intersections. In general, the rate of change in cross slope in the runoff section should be based on the maximum relative gradients Δ listed in Table III-13. The values listed in this table are applicable to a single lane of rotation. The adjustment factors b_w listed in Table III-14 allow for slight increases in the effective gradient for wider rotated widths. The effective maximum relative gradients (equal to $\Delta \div b_w$) that can be used for a range of turning roadway widths are listed in Table IX-12.

Design Speed (km/h)	Effective Maximum Relative Gradient (%)		
	Rotated Width (m)		
	3.6	5.4	7.2
30	0.8	0.90	1.00
40	0.7	0.84	0.93
50	0.7	0.78	0.87
60	0.6	0.72	0.80
70	0.6	0.66	0.73
80	0.5	0.60	0.67
90	0.5	0.57	0.63
100	0.4	0.53	0.59
110	0.4	0.49	0.55
120	0.4	0.46	0.51

Note:
1. Based on maximum relative gradients listed in Table III-13 and the adjustment factors in Table III-14. One lane is assumed to equal 3.6 m.
2. Gradients for speeds of 80 km/h and above are applicable to turning roadways at interchanges (i.e., ramps).

Table IX-12. Effective maximum relative gradients.

[delete existing Table IX-12 and add Table IX-12 above]

Usually, the profile of one edge of the traveled way is established first, and the profile on the other edge is developed by stepping up or down from the first edge by the amount of desired superelevation at that location. This step is done by plotting a few control points on the second edge by using the maximum relative gradients in Table IX-12 and then plotting a smooth profile for the second edge of traveled way. Drainage may be an additional control, particularly for curbed roadways.

[delete existing Table IX-13]

CHAPTER X—GRADE SEPARATIONS AND INTERCHANGES

The text provided on the following pages represents the recommended modifications to selected paragraphs in *Green Book* Chapter X. These paragraphs are located in two sections. The first section addresses turning roadway curvature (p. 919). The second section addresses superelevation and cross slope at turning roadways (p. 923). Both sections apply to turning roadways at interchanges.

Some of the guidance provided in the *Green Book* has been retained but the recommended changes are sufficiently extensive that a complete rewriting of the text was considered the most efficient method of presenting the material.

Chapter X

GRADE SEPARATIONS AND INTERCHANGES

. . .

Ramps

. . .

General Ramp Design Considerations

. . .

Curvature. The design guidelines for turning roadways at interchanges are described in Chapter III. They apply directly to the design of ramp curves. Compound or spiral curve transitions are desirable to (1) achieve the desired shape of ramps, (2) provide a comfortable transition between the design speeds of the through and turning roadways, and (3) fit the natural paths of vehicles. Caution should be exercised in the use of compound curvature to prevent unexpected and abrupt speed adjustments. Additional design information on the use of compound curves is contained in Chapter III.

. . .

Superelevation and cross slope. The following guidance should be used for cross slope design on ramps:

1. Superelevation rates, as related to curvature and design speed on ramps, are given in Tables III-10 and III-11. Where drainage impacts to adjacent property or the frequency of slow-moving vehicles are important considerations, the superelevation rates and corresponding radii in Table III-12 can be used.
2. The cross slope on portions of ramps on tangent normally are sloped one way at a practical rate that may range from 1.5 percent to 2 percent for high-type pavements.
3. In general, the rate of change in cross slope in the superelevation runoff section should be based on the maximum relative gradients Δ listed in Table III-13. The values listed in this table are applicable to a single lane of rotation. The adjustment factors b_w listed in Table III-14 allow for slight increases in the effective gradient for wider rotated widths. The effective maximum relative gradients (equal to $\Delta \div b_w$) applicable to a range of roadway widths are listed in Table IX-12. The superelevation development is started or ended along the auxiliary lane of the ramp terminal. Alternate profile lines for both edges should be studied to determine that all profiles match the control points and that no unsightly bumps and dips are inadvertently developed. Spline profiles are very useful in developing smooth lane and shoulder edges.
4. Another important control in developing superelevation along the ramp terminal is that of the crossover crown line at the edge of the through traffic lane. The maximum algebraic difference in cross slope between the auxiliary lane and the adjacent through lane is shown in Table IX-14.
5. Three segments of a ramp should be analyzed to determine superelevation rates that would be compatible with the design speed and the configuration of the ramp. The exit terminal, the ramp proper, and the entrance terminal should be studied in combination to ascertain the appropriate design speed and superelevation rates.

With regard to Item 5, the guidance offered can vary depending on the type of ramp configuration. Three ramp configurations are described in the following paragraphs. The diamond ramp usually consists of a high-speed exit terminal, tangent or curved alignment on the ramp proper, and stop or yield conditions at the entrance terminal. Deceleration to the first controlling curve speed should occur on the auxiliary lane of the exit terminal and continued deceleration to stop or yield conditions would occur on the ramp proper. As a result, superelevation rate and radii used should reflect a decreasing sequence of design speeds for the exit terminal, ramp proper, and entrance terminal.

The loop ramp, as at a cloverleaf interchange, consists of a moderate-speed exit terminal connecting to a slow-speed ramp proper, which in turn connects to a moderate-speed acceleration lane. The curvature of the ramp proper could be a simple curve or combination of curves. The curvature of the ramp proper would be determined by the design speed and superelevation rate used. Superelevation would have to be gradually developed into and out of the curves for the ramp proper, as detailed later in this discussion.

Direct and semi-direct ramps generally are designed with a high-speed exit, a moderate or high-speed ramp proper, and a high-speed entrance. As a result, the design speed and superelevation rates used are comparable to open-road conditions.

The **Transportation Research Board** is a unit of the National Research Council, which serves the National Academy of Sciences and the National Academy of Engineering. The Board's mission is to promote innovation and progress in transportation by stimulating and conducting research, facilitating the dissemination of information, and encouraging the implementation of research results. The Board's varied activities annually draw on approximately 4,000 engineers, scientists, and other transportation researchers and practitioners from the public and private sectors and academia, all of whom contribute their expertise in the public interest. The program is supported by state transportation departments, federal agencies including the component administrations of the U.S. Department of Transportation, and other organizations and individuals interested in the development of transportation.

The National Academy of Sciences is a private, nonprofit, self-perpetuating society of distinguished scholars engaged in scientific and engineering research, dedicated to the furtherance of science and technology and to their use for the general welfare. Upon the authority of the charter granted to it by the Congress in 1863, the Academy has a mandate that requires it to advise the federal government on scientific and technical matters. Dr. Bruce M. Alberts is president of the National Academy of Sciences.

The National Academy of Engineering was established in 1964, under the charter of the National Academy of Sciences, as a parallel organization of outstanding engineers. It is autonomous in its administration and in the selection of its members, sharing with the National Academy of Sciences the responsibility for advising the federal government. The National Academy of Engineering also sponsors engineering programs aimed at meeting national needs, encourages education and research, and recognizes the superior achievements of engineers. Dr. William A. Wulf is president of the National Academy of Engineering.

The Institute of Medicine was established in 1970 by the National Academy of Sciences to secure the services of eminent members of appropriate professions in the examination of policy matters pertaining to the health of the public. The Institute acts under the responsibility given to the National Academy of Sciences by its congressional charter to be an adviser to the federal government and, upon its own initiative, to identify issues of medical care, research, and education. Dr. Kenneth I. Shine is president of the Institute of Medicine.

The National Research Council was organized by the National Academy of Sciences in 1916 to associate the broad community of science and technology with the Academy's purpose of furthering knowledge and advising the federal government. Functioning in accordance with general policies determined by the Academy, the Council has become the principal operating agency of both the National Academy of Sciences and the National Academy of Engineering in providing services to the government, the public, and the scientific and engineering communities. The Council is administered jointly by both the Academies and the Institute of Medicine. Dr. Bruce M. Alberts and Dr. William A. Wulf are chairman and vice chairman, respectively, of the National Research Council.

Abbreviations used without definitions in TRB publications:

AASHO	American Association of State Highway Officials
AASHTO	American Association of State Highway and Transportation Officials
ASCE	American Society of Civil Engineers
ASME	American Society of Mechanical Engineers
ASTM	American Society for Testing and Materials
FAA	Federal Aviation Administration
FHWA	Federal Highway Administration
FRA	Federal Railroad Administration
FTA	Federal Transit Administration
IEEE	Institute of Electrical and Electronics Engineers
ITE	Institute of Transportation Engineers
NCHRP	National Cooperative Highway Research Program
NCTRP	National Cooperative Transit Research and Development Program
NHTSA	National Highway Traffic Safety Administration
SAE	Society of Automotive Engineers
TCRP	Transit Cooperative Research Program
TRB	Transportation Research Board
U.S.DOT	United States Department of Transportation

THE NATIONAL ACADEMIES

Advisers to the Nation on Science, Engineering, and Medicine

National Academy of Sciences
National Academy of Engineering
Institute of Medicine
National Research Council

TRANSPORTATION RESEARCH BOARD
National Research Council
2101 Constitution Avenue, N.W.
Washington, D.C. 20418

ADDRESS CORRECTION REQUESTED

S36 P3
(000021-15)
IDAHO TRANSPORTATION DEPT
PO BOX 7129
BOISE ID 83707-1129